River Conveyance Analysis in a Data Sparse and a Data Rich Region: Case Studies in Kenya and Switzerland

Master's Thesis

Faculty of Science

University of Bern

presented by

Danielle Huser

2016

Supervisor:

Prof. Dr. Rolf Weingartner
Institute of Geography and Oeschger Centre for Climate Change Research

Co-Supervisor:

Dr. Andreas Zischg
Institute of Geography and Oeschger Centre for Climate Change Research

Advisor:

Dr. Hanspeter Liniger
Institute of Geography

Abstract

This master thesis addresses two cases studies with rather different initial condition. First, it aims to establish stage discharge relations in data-sparse regions in the lower Ewaso Ng'rio Basin in Kenya, and secondly, it proceeds to a weak point analysis along the main rivers of the Bernese Oberland in Switzerland. Regardless of their geographical distance, for both regions with their respective issues a hydrodynamic 1D simulations were conducted with the software Basement, providing simulations of river flow based on measured cross sections.

In arid regions water scarcity is becoming a threat to more and more people. The Ewaso Ng'rio Basin (64 000 km^2), located around the Mount Kenya is subjected to increasing pressure on water resources because of rising demands for irrigation, domestic purposes, and livestock in the upper basin. In the lower basin, users suffer from even more pronounced water scarcity, because they have secondary access to the rivers. Research on hydrological processes is limited since gauging stations (RGS) were missing up to this study. In order to overcome that limitation, this study aims to establish stage-discharge relations for four sites in the lower Ewaso Ng'iro Basin by relying on newly installed RGS providing water level data. The here developped methodological approach is adapted to the scarcely distributed measurement equipment. To establish stage-discharge relations, the river sites were surveyed with a dumpy level to collect the necessary input variable geometry, and Manning-Strickler values for the 1D simulations in Basement (Vetsch et al., 2015b). The hydrodynamic model is based on the Saint-Venant and Manning-Strickler equations. The stage-discharge relation was simulated with Basement without a calibration of the model. The curve fitting and analysis of the relation between stage and discharge was evaluated with the statistical program R, using a non-linear model based on a power function. For all four river sites, the survey method enabled simulations of river flows in Basement. The curve mirrored the relations rather well with some deviations at low flow. Despite of probably high and unquantifiable uncertainties of data collected in field surveys, this study nevertheless provides a first step to a more comprehensive understanding of the magnitude and timing of the river flow in the lower Ewaso Ng'rio Basin. Further research should focus on calibrating the stage discharge relation of the four sites.

In Switzerland, climate change is likely to increase the frequency of extreme flow events. Hydrology has extensively been studied in terms of frequency of flood events and of weak points along the rivers. The focus of these analyses lies on single river sections. Alternatively, this study proposes to evaluate weak points based on the bank-full discharge with associated return period at measured cross sections along the main rivers of the Bernese Oberland. This simple approach can be applied identically to all the rivers and allows for the first time a comparison on large scale. For each cross section along the rivers Hasliaare, Aare Thun-Bern, Simme, Kander and Lütschine, discharges of flood events with return periods of 10, 30, 50, 100, and 300 years (HQ_x) were identified. With the help of known HQ_{10}, HQ_{30}, HQ_{50}, HQ_{100} and HQ_{300}, discharge rates were calculated at the RGS stations. The discharge rates were then extrapolated or interpolated over the catchment size of all the cross sections along the entire river. HQ values for different return periods were compared at some reference points with estimations provided by the HQx_meso_CH tool (Barben, 2001) and the PREVAH_regHQ tool (Viviroli and Weingartner, 2012). The bank-full discharge, or

what discharge fills the channel to the top, was evaluated for each cross section by 1D simulations in Basement for each river. The models were calibrated on the basis of measured stage-discharge relations. The results of the estimations of HQ_{10}, HQ_{30}, HQ_{50}, HQ_{100} and HQ_{300} seemed to depend on the number and the position of the RGS: the more stations and the higher upstream, the better the estimation. Identifiable changes of the HQ_x along the river are caused by tributary inflow. Low bank-full discharge values could be identified at single or conglomerated cross sections, and they could be backtracked to the topographic situation. Identified weak points were mostly located along non-populated areas. Interestingly, some areas with extensive construction measures against floods still exhibited low return periods. The rather simple and time saving methodological approach of extrapolating HQ_x values at the site of the RGS and of running a 1D simulation in Basement produced results comparable with literature, though some deviations occurred. This is remarkable, as, compared to other studies, the covered area was large and the riverbed was reconstructed from measured cross sections. Because the model is simple and relies on available data, it could be extended countrywide. This would further favour a better comparison between different rivers, because results would be based on one identical methodological approach – something that is currently lacking in today's procedures in flood assessment. As the advantages of the model are promising, it is recommended to conduct further studies in order to reach more comprehensive calibrations and to conduct validations.

Acknowledgement

I would like to thank to.....

....Rolf Weingartner, who gave me the opportunity to write this thesis and the support to find a second topic to complete the thesis.

....Hanspeter Liniger for introducing us in Nanyuki Kenya during the 2 week excursion and the support by phone during the 3 month field work.

....the CETRAD water team, for their assisstence and encouragement during my fieldwork.

....Andras Zischg for the support by mail during the time in Kenya, for being as flexible to come up with a second topic, and for the encouragement, the helpful input, feedback, and the informative field trips in the Bernese Oberland.

....Julia Stefanovic and Jérôme Léchot to proof-reading my thesis

....My family and friends for their encouragement throughout the working process. Especially, to Noemi Imfeld and Fabienne Kaufmann for the positive energy, the confidence and motivation, the scientific and no-scientific discussions and the nice dinners during the time we shared in Nankyuki, Kenya

Contents

List of Figures

List of Tables

List of Abbreviations

A	Cross Section Area
Basement	Basic Simulation Environment
CDE	Centre for Development and Environment
CETRAD	Centre for Training and Integrated Research in ASAL Development
DEM	Digital Elevation Model
ETHZ	Swiss Federal Institute of Technology in Zurich
FOEN	Federal Office for the Environment
HQ$_x$	Flood with a Certain Return Period
IPCC	Intergovernmental Panel on Climate Change
ITCZ	Intertropical Convergence Zone
M-Aare	Model Chain Atmosphere-Hydrology-Flood-Losses in the Aare Catchment
HQx_meso_CH	Flood with a Certain Return Period, Meso Scale Catchment, Catchment of Switzerland
kst-coefficient	Manning-Strickler Coefficient
MSE	Manning-Strickler Equation
m.a.s.l	Meter Above Sea Level
PREVAH_regHQ	Precipitation-Runoff-Evapotranspiration HRU Model, Regionalization, Flood
Q	Discharge
RGS	River Gauging Station
SVE	Saint-Venant Equation
W	Water level or Stage
WLRC	Water and Land Resource Centre
WMO	World Meteorological Organisation

Dedicated to my parents and my tupperware group

Chapter 1

Introduction

1.1 Background

This master thesis looks at river conveyances in data sparse and data rich regions. One case study is located in Kenya (lower Ewaso Ng'iro Basin), and the other in Switzerland (Bernese Oberland). They strongly differ in terms of climatic and hydrological conditions, but also in terms of data availability. Nevertheless, one hydrodynamic model was applied to both case study sites in order to gain a better understanding of the respective conveyances of the rivers (Fig 1.1). The key tool is a 1D hydrodynamic model implemented in the software Basement. 'Basement' is an acronym for 'Basic Simulation Environment for Computation of Environmental Flow' (Vetsch et al., 2015b). It enables the simulation of river flow based on cross section information. Basement was adapted to the peculiarities of the two case studies.

Figure 1.1: Kenya vs. Switzerland: Merille (left), Weisse Lütschine (right)

The first case study deals with the evaluation of the procedure necessary to establish stage-discharge relations and enables a first estimation of the channel capacities in a data and research sparse region in the lower Ewaso Ng'iro Basin in Kenya. The project was part of the Water and Land Resource Centre (WLRC) program of the Centre for Development and Environment (CDE) of the University of Bern in collaboration with Centre for Training and Integrated Research in ASAL Development (CETRAD) in Nanyuki, Kenya. The 1D model provided by Basement was applied to short river sections to evaluate the water

level-discharge relation next to newly installed river gauging stations, thereby enabling the conversion of measured water levels to the associated discharge value. The cross section input data had first to be collected in a field campaign. The results can be considered as a first approach of how to simulate river flow by establishing rating curves with a minimum of data. In other words, this approach not only provides better knowledge about the river conveyance in the lower Ewaso Ng'iro Basin, but it also proposes a method that enables further investigations. However, only predictive values without calibration could be provided so far.
The second case study is concerned with developing a weak point analysis along the main rivers in the Bernese Oberland and the Aare upstream of Bern. The better availability of data allowed modelling of a more data-demanding question. The aim here was to evaluate the channel capacity of all measured cross section along the rivers of interest and to attribute channel capacities to the associated return periods of a flood. This second case study is associated to the 'Model chain atmosphere-hydrology-flood-losses in the Aare catchment' (M-AARE) project, which aims at improving estimations of extreme floods in a high spatial resolution (MobiliarLab, 2015). Here, the hydrodynamic 1D simulation was applied along entire rivers to evaluate the discharge capacity of the channel based on single measured cross sections. Put in other terms, getting a grasp at the conveyance of these rivers enables an analysis of weak points of a river. The high resolution of the cross section data and the availability of measured water levels permitted for a calibration of the models.
Even if the two case studies differ in levels of complexity, the here joint studies could provide answers that both in a first step satisfy their respective needs. For the drought-threatened Kenya, the question of how much water flows through the lower Ewaso Ng'iro Basin is crucial. Even if a calibration of the model could not be conducted, this case study provides a first answer that may be further refined. For Switzerland, in contrast, floods are the more pressing threat at least for the moment. If in Kenya droughts are of essentially interest, here the risk of flood events needs handling. The here presented second case study aims at providing knowledge of the weak points of the rivers in the Bernese Oberland. In order to enhance the predictive quality of the model, a validation may be conducted in the future.

1.2 Outline

First, an introduction to the functioning of Basement will be given. In chapter 2 and chapter 3, the two case studies and their peculiarities starting from the problem description to the conclusion will be depicted. Finally, the gained knowledge from the two case studies will be integrated in a final conclusion.

1.3 Software Basement: Basechain 1D

The Basement software serves as a basic-simulation-environment. It was developed by the Laboratory of Hydraulics, Hydrology and Glaciology of the Swiss Federal Institute of Technology in Zurich (ETH). In the words of the developer: 'Unlike currently used programs for the simulation of a specific flow behaviour, BASEMENT intends the arrangement of many different problem types with one single tool to gain an integrated understanding for the

initial position, the solution process and its results' (Vetsch et al., 2015b). It is intended to provide numerical simulations of alpine rivers including sediment transport. The software provides two models: Basechain for 1D hydrodynamic simulations, and Baseplain for 2D hydrodynamic simulations with adaptable boundaries. Bed load and suspending load can be included in the model. For this study, the relevant model is Basechain, more specifically: 1D simulations excluding sediment transport (Vetsch et al., 2015b). For more information, a large Manual is provided by Vetsch et al. (2015b).
The Basechain models are useful for the simulation of long time periods. The topography of the river is reproduced based on cross section profiles. The output for each time step and cross section of the simulation is the water level, the riverbed position as well as the average discharge flow velocity (Rousselot, Vetsch, and Faeh, 2012). It is calculated with the Saint-Venant equation (SVE), where the streamed cross section area (A) and the associated discharge (Q) are the conservative variables (Unsinn, 2008).

1.3.1 Hydraulic Background

As mentioned, Basechain provides simulations of river reaches based on cross section information. The computational grid is illustrated in Figure 1.2 left. The orange lines are the cross sections and the violet points with crosses are nodes. An element for the centred discretization consists of two nodes with a known cross section, and the midpoint of the line between two nodes defines the edge of two elements (see the violet points lines, Fig 1.2 left). At the location of the nodes, the variables flow velocity, flow depth and the cross section geometry are defined. The more nodes are known, the better the river is represented (Vetsch et al., 2015b).

1.3.1.1 Flow Equation

The hydraulic calculation in Basechain is based on the SVE for unsteady one dimensional flow:

$$c\frac{dQ}{dt} + \frac{d(u \cdot Q)}{dx} = -g \cdot A \cdot \frac{dz_s}{dx} - g \cdot A \cdot I_E$$

$$\begin{aligned} \text{with } Q &= \text{Discharge } [m^3/s] \\ t &= \text{Time } [s] \\ u &= \text{Flow velocity x-direction } [m/s] \\ A &= \text{Cross section area } [m^2] \\ g &= \text{Acceleration of gravity } [m/s^2] \\ I_E &= \text{Energy gradient, slope [-]} \end{aligned} \tag{1.1}$$

Equation 1.1 comprises the conservation of momentum (right side) and conservation of mass (left side). The SVE one dimensional equation is the simplified Navier-Stock flow equation which considers flow in 3 dimensions. In the SVE, the flow is depth- and width averaged to describe a simplified channel flow, and thereby, only the flow velocity in x-direction is

considered (Unsinn, 2008). The use of the SVE implies the following assumptions to be valid:

- hydrostatic pressure; fulfilled if the vertical acceleration is negligible
- uniform velocity over the whole cross-section
- small slope of the channel bottom (Vetsch et al., 2015b; Unsinn, 2008)

Formula 1.1 shows that the flow velocity has to be determined to apply the SVE. The equation for the flow velocity implemented in Basement is the MSE:

$$u = k_{st} \cdot R^{\frac{2}{3}} \cdot \sqrt{I_E}$$
$$\text{with } u = \text{Flow velocity } [m/s]$$
$$k_{st} = \text{roughness coefficient by Strickler } [m^{\frac{1}{3}}/s]$$
$$R = \text{Hydraulic radius } [m]$$
$$I_E = \text{Energy gradient [-]} \tag{1.2}$$

(Unsinn, 2008)

The friction is defined with the Manning-Strickler coefficient (kst-coefficient). It represents not only the roughness of the channel but also the inner roughness due to turbulence. That is, all sources of roughness (inner roughness, bottom roughness and bank roughness) are combined in one parameter (Unsinn, 2008).

1.3.1.2 Numerical Solution of the SVE

The SVE is a nonlinear, coupled partial differential (PDG) equation system. A unique analytical solution is only available for idealised and simplified conditions (**reference**). In practice, numerical solutions are required. Such a numerical solution is obtained by discretization. The idea behind the discretization is to divide the area in many small sub-areas, where the PDG can be solved approximately. The smaller the discretizing elements are, the smaller is the numerical dispersion (Unsinn, 2008).
The equation has to be discretized temporally and spatially. The spatial disrectization may be obtained in different grids such as Cartesian, non-orthogonal, structured or unstructured ones. The temporal discretization is normally obtained by a Finite difference scheme. It can be explicitly or implicitly. For the SVE, the value of the next time step only considers the value from the last time step: the explicit Euler schema is applied to solve for prospective time steps. The spatial discretization is based on the finite volume method and the integration of the equation takes place over one single element (for the definition of an element, see section 1.3.1) (Vetsch et al., 2015a).

1.3.2 Modelling Procedure

The main variable of interest depends upon the aim of the simulation and will thereby differ from case to case. Figure 1.2 right shows an overview of the work procedure from pre-processing to model output.

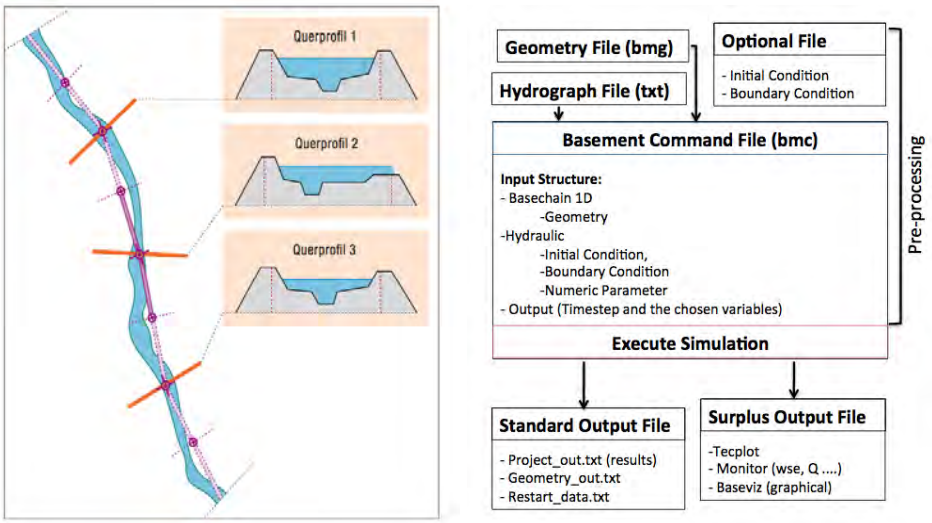

Figure 1.2: Basechain: topographic representation of a river (left), composition of Basechain adapted from Unsinn (2008)(right)

The pre-processing process is required to determine parameters for the geometry file and for the Basement command file. The Basement command file has the task to operate and run the simulation. The geometry (bmg) file contains every cross section of the river sections, and each cross section requires the following information, which has to be determined:

- Distance from the first cross section upstream
- Orientation angle
- Left point coordinate
- Bottom range
- Active range
- Friction coefficients (kst-coefficients)
- Friction range
- Coordinate of the points along the cross section
- Default friction coefficient

The geometry file has to be added to the geometry section of the command file and serves as the basis for the calculation, as the hydrograph determines the inflow condition at the upper boundary. The second part of the command file, the hydraulic part which includes the initial condition and the upper and lower boundary condition, has to be determined.

For the initial condition, the input can be predefined, either with a restart file, where the riverbed is always filled with a certain amount of water at the start of the simulation, or the option of a dry riverbed is chosen. Then the simulation can be run and calibrated if possible. The generated outputs files of the simulation are shown in Figure 1.2. Additional output files provide a visualization the river section with Basevize or enable to generate a file with one variable for a chosen cross sections.

1.3.2.1 Boundary Condition

The hydraulic conditions at the upper and lower boundary of the river section one intends to simulate have to be accurately defined. It is important to know how the adjacent area influences the chosen river section. The influence from system boundaries is taken into account by the propagation velocity of a perturbation. A perturbation can propagate in two directions, upstream and downstream. This velocity term has then to be added to the flow velocity in the studied channel. In case of supercritical flow, the information of the perturbation cannot spread upstream to a given point because the velocity of the perturbation is too low as compared to the flow velocity in the channel. There, no propagation from downstream is possible, i.e. the conditions are not influenced from downstream at the boundary. The sub-critical flow shows the opposite phenomena: the flow (information) can be spread in both directions. These two possibilities determine the number of boundary conditions which have to be considered in the simulations. For the case of sub-critical flow, one boundary condition is given by the influence from downstream, while the other has to be fixed. For supercritical flow, two boundary conditions need to be defined.
The input value at the upstream boundary normally is Q (Vetsch et al., 2015b). It can be defined at the upstream boundary with a hydrograph that describes a course of a flood or a steady state flow. Then the flow velocity at the first cross section is calculated using the continuity equation based on the water level at the antecedent time step. In the case of supercritical flow, no information on the water level at the antecedent time step is available. It will be calculated iteratively with a given slope and a normal discharge value. There are multiple possibilities to describe the discharge condition at the downstream boundary of a section. For this study, the upper boundary condition was set by a steady state hydrograph, and for the lower boundary, a hq-relation (water level-discharge relation) was considered. This means the water surface elevation is specified as a function of the discharge with the help of the local slope (Brechtold, 2015).

1.3.2.2 Calibration

As explained in section 1.3.1, the calculations of the river flow are based on the MSE. The kst-coefficients are unknown and have to be determined by the user. It is the tuning variable, i.e. this variable should be calibrated. This is done at cross sections where a stage-discharge relation based on river flow measurements exists. One discharge of the stage-discharge relation is used as input to the simulation, and the associated water level to this discharge is the target output of the simulation. In that procedure, the kst-coefficients are changed until the simulation reaches the target water level. The kst-coefficient is then used for the different runs.

Chapter 2

Determination of the Stage-Discharge Relations in a Data Sparse Region in Lower Ewaso Ng'iro Basin Kenya

2.1 Introduction

2.1.1 Problem Description

Water is the most important and valuable resource on earth. Today, a lot of countries suffer not only from insufficient quality of water but also from water scarcity due to human activities. The Ewaso Ng'iro Basin, located around Mount Kenya, covers an area of about 64.000 km^2 and is confronted with the problem of water scarcity. Mountains like Mount Kenya, Aberdares, Mathew ranges and Mount Marsabit are water towers feeding many perennial and seasonal rivers in the Ewaso Ng'iro Basin. In the dry season, the water in the lowlands is mainly coming from the upper and middle part of Mount Kenya, from the Aberdares, from spring water in the area between Buffalo Springs (Archers Post) and Ngotu as well as from stored flood water in the Merti and Lorrian Swamps (Kiteme et al., 2008; Liniger, 2015). The problem of water availability concerns the whole Ewaso Ng'iro Basin and become more acute in the past few years. For the upper Ewaso Ng'rio Basin, hydrology and water problems have been well researched. The Water and Land Resource Centre (WRLC) project, based on a cooperation between the University of Bern and the Centre for Training and Integrated Research in ASAL Development (CERTRAD) conducted a number of studies on a broad range of topics including water abstraction (Aeschbacher, 2003), run-off modelling of certain rivers (Notter, 2003; Sutter, 2012), socio-economic impacts (Wiesmann et al., 2000) and long term precipitation in the area (Schmocker, 2013). They stated that the upper Ewaso Ng'iro Basin has experienced expansive and rapid changes since the 1980ties. Population increased tenfold between 1960 and 2000, at the same time, agricultural practice shifted from subsistence farming to intensified irrigated agriculture (Kiteme et al., 2008; Notter et al., 2012). Thereby, the abstraction of water for irrigation, domestic purposes, and livestock in mountain regions increased dramatically. These changes exert increasing pressure on natural resources, primarily water, and lead to conflicts between up- and downstream users (Aeschbacher, Linger, and Weingartner, 2005; Kiteme et al., 2007; MacMillan and Liniger, 2005; Liniger et al., 2005).

Especially people located in the lowland are in an disadvantageous position. As downstream users, they only have secondary access to river water and are therefore more strongly affected by water scarcity.
Changes in the upper basin lead to a faster drying up of rivers in the lower basin, which forces pastoral groups to shift westwards, what in turn leads to conflict with other pastoral groups (IUCN, 2015). Therefore, the water problem in the lowland is at least as serious as in the upper basin in addition to that, there is only limited knowledge regarding watershed hydrology. Research on detailed hydrological processes is limited because river gauging stations (RGS) are still largely missing. The same is reported by the Intergovernmental Panel on Climate Change (IPCC), stating that the hydrological response remains one of the major uncertainties of climate predictions, mainly for dry regions and their ephemeral streams. One reason for these uncertainties, is the lack of monitoring systems (Benito et al., 2011). We nevertheless are able to find out how much and how many days per year the water reaches the Lorrian Swamp, which is an important water reservoir for the farmers, by consulting the analysis of satellite images by De Leeuw et al. (2012). During most of the year, rivers are dry in the lowlands, but during the wet season the rivers are flooded and thereby the region is recharged with water (Liniger et al., 2014). For water recharge in the lowland, local rain events do not play a key role. The major contribution comes from the rain in the mountains (Liniger et al., 2014).
Particular hydrological setting plus the rising potential for social conflicts both indicate how urgent it is to arrive at a better and reliable understanding of the hydrology of the lower Basin.
To meet the aforementioned challenges at least to some extent, this study aims to establish a measurement system at the chosen sites, and, in a second step, to evaluate the available methods on-site and develop stage-discharge relations. With the stage-discharge relation the maximum discharge of the rivers at the different sites can be estimated. Discharge is the most basic variable for understanding watershed hydrology. In order to conduct hydrological analysis and calculate discharges, stage-discharge relations alongside with riverbed measurements are necessary. In order to achieve the aforementioned aims, riverbeds are surveyed with the dumpy level for each region of interest, and stage discharge relations are calculated with Basement for the four sites in the lower Ewas Ng'iro Basin, where the RGS are installed.

2.1.2 Objectives and Research Questions

The overall aim of this part of the study is to establish reliable stage-discharge relations for the four study sites. They may serve as a cornerstones for future analysis of measured water level data. In order to achieve that objective the following specific objectives and related research questions are formulated:

a) **Establish the optimal stage-discharge relations for the four sites by conducting fieldwork and considering scarce measurement equipment**
   - Which variables are essential to obtain a valid stage-discharge relation?
   - Is the dumpy level method sufficiently precise?

b) **To develop stage-discharge relations and make first estimations of the channel capacity for the sites with the measured parameters and with an appropriate program/method**

- Is data quality sufficient to derive the stage-discharge relation with Basement?
- How to reasonable cope with large uncertainties due to the chosen method?
- How to best fit a curve in the simulated data?

This study was conducted within the framework of the WLRC project and intends to contribute to the purpose of its overarching project. It states: 'In these river basins, the transboundary negotiations and decision-making on water management are extremely challenging, and talks frequently falter because of poor information as well as political and economic power imbalances between the parties involved. The project aims that the ultimate beneficiaries of the WLRCs will be those living in the Eastern Nile and the Ewaso Ng'iro Basins - especially land users, smallholders, and the rural poor. They should directly profit from better water and land governance/management and more secure environmental services' (CDE, 2014). The study contribution to the project shall be a manual of the work process of establish stage-discharge relation to support the local water team in Nanyuki, and to assess further river sites in the region.

2.1.3 Study Area

The four sites, Sereolevi, Merille, Melgis and Habaswein and their watersheds are situated, in the lower Ewaso Ng'rio Basin, of central Kenya. The catchments are located between 2°51.275280' N and 0°19.3279' S, with the western extreme at 36°22.7586' E and the most eastern point at 39°29.603220' E (Fig. 2.1).
The Ewaso Ng'iro Basin draining at Habaswein is 64'000 km^2 large, one and a half time the size of Switzerland. The basin covers a diversity of ecological zones, ranging from the semi-humid mountain zones (see Figure 2.2, right side) at the boundary of the basin to semi-arid and vast arid areas (Fig. 2.2, left side) in the lowland (Gichuki et al., 1998). Figure 2.3 shows the course of the Ewaso Ngiro river. It originates in the Central Kenyan Highland, drains at the slope of Mount Kenya and the Aberdares Mountains and runs through the Laikipia plateau (De Leeuw et al., 2012). This part of the basin, called the upper Ewaso Ng'iro Basin, is characterized by tertiary volcano rocks of Mount Kenya (Gichuki, Linger, and Schwilch, 1998). Further downstream the river passes by Arches Post and flows over a large plateau, where it is transformed into an ephemeral stream and discharged into Lorrian Swamp near Merti. On its way through the lowland, the Ewaso Ngiro is fed by the three ephemeral rivers, Sereolevi, Merille and Melgis, where the three study sites are located (Fig. 2.1.3). Sereolevi and Merille originate in the Mathew ranges and Melgis is fed by the Mathews and the mountain ridge of Maralal. Probably, it terminates in Habaswein, where the fourth study site is located, after passing the Lorrian Swamp, a huge wetland located in the arid zone of north eastern Kenya (De Leeuw et al., 2012).

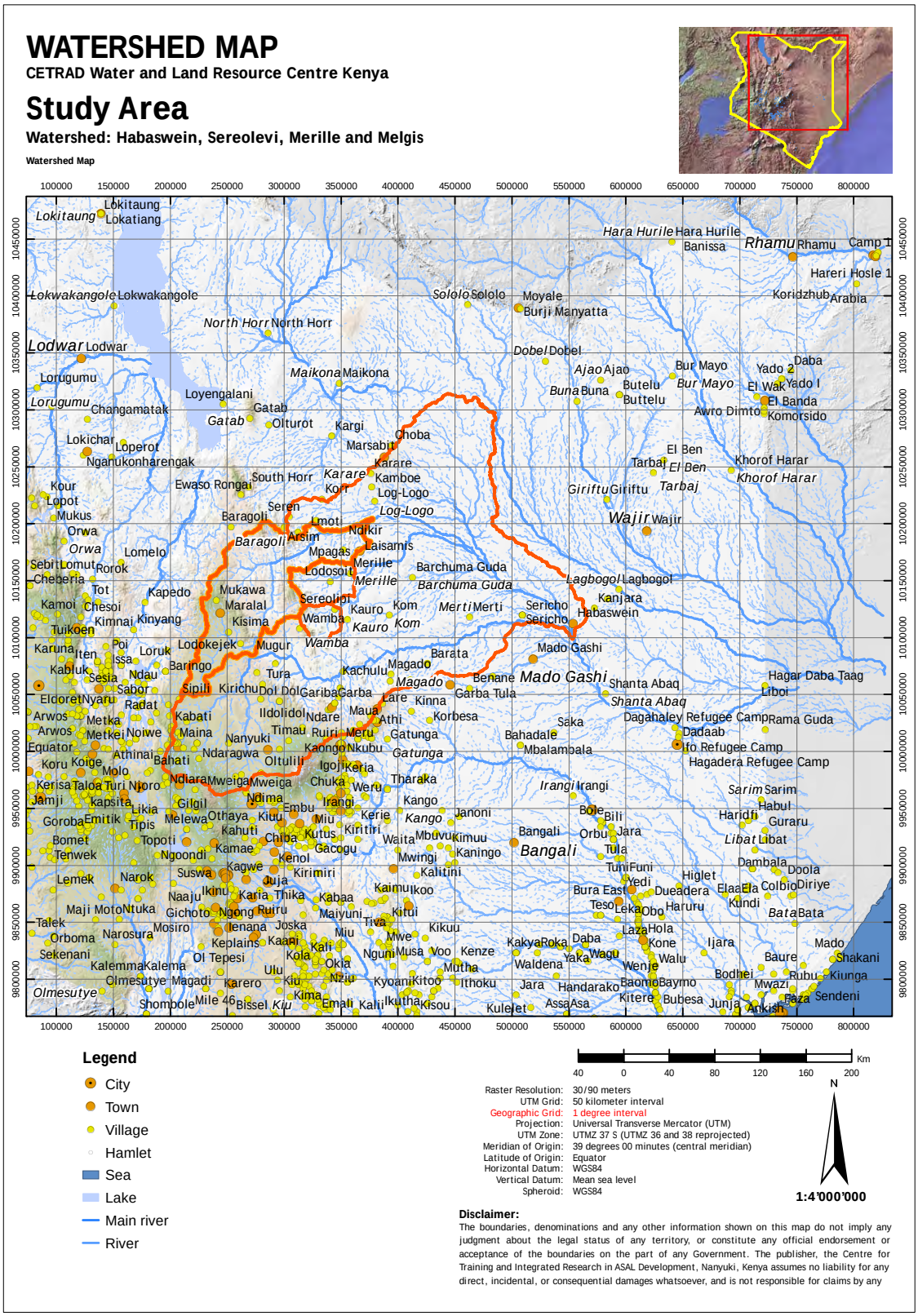

Figure 2.1: Watershed Ewaso Ng'iro river

Figure 2.2: Ecological zones: arid zone (left), semi humid mountain zone (right)

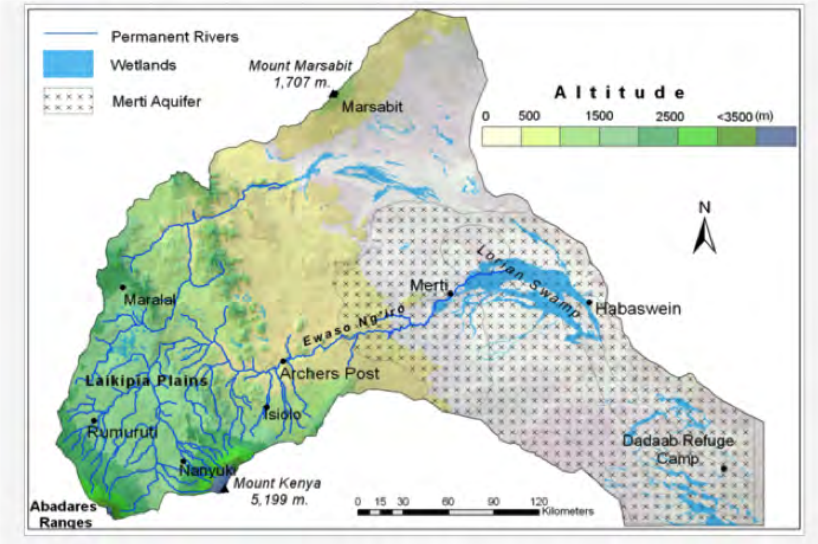

Figure 2.3: The perennial river parts of the Ewaso Ng'iro Basin

The climate is mostly driven by the movement of the intertropical convergence zone (ITCZ). The ITCZ is a band of strong convection, where huge cumulus clouds are formed caused by the strong solar radiation. The position of the ITCZ depends on the zenith of the sun, meaning that it moves from 20° N to 20° S and back in one year (Schmocker, 2013) This leads to a bimodal rain pattern, with two dry and two wet seasons alternating in the course of the year. In the Ewaso Ng'iro Basin the long rains occur from March to May and the short rains from October to December. However, rain pattern can also be overturned by large scale phenomena, mainly the El Nino. Additionally, the distribution of the rain depends on the topography and exposition. I.e. the amount of rain increases with height, ranging to 3200 m.a.s.l. Further, there is more rain on the south east side of Mount Kenya, because the air comes from the ocean there (Liniger, Weingartner, and Grosjean, 1998).
The Ewaso Ng'iro Basin is a typical high-lowland system and is further illustrative of the

interaction between highland-lowland systems. The water-rich upper part with its lush vegetation serves as a donator, while the scarcely vegetated lower part, acts as a consumer (Kiteme et al., 1998).

2.1.3.1 Characteristics of the Survey Sites

The characteristics of the four watersheds, Habaswein, Melgsi, Merille and Sereolevi are summarized in the Table 2.1 below. The table describes basic watershed characteristics and land cover characteristics. As mentioned before, the sites are all located in the lower basin downriver of Archers Post. The Watershed of Habaswein includes the whole Ewaso Ng'iro Basin, meaning also the three other sites. This dimensional difference is illustrated in Figure 2.1.

River	Sereolevi	Merille	Melgis	Habaswein
Basic Watershed Characteristics				
Area $[km^2]$	974.5	1727.2	9628.7	64087.4
Average Altitude $[m]$	980.4	837.5	1354.3	954.3
Lowest Point $[m]$	708	582	459	191
Highest Point $[m]$	2655	2272	2620	5030
Average Slope [%]	11.7	8.1	11.4	5
Landcover Characteristics				
Evergreen Boradleaf Forest [%]	0.7	1.5	2.6	1
Deciduous Broadleaf Forest [%]	0.3	0	0.2	0.1
Mixed Forest [%]	1.5	1.7	1.9	0.5
Closed Shrublands [%]	0	0	0.2	0.1
Opend Shrublands [%]	45.3	57.3	38.9	52.3
Woody savannas [%]	6.1	2.2	6.4	4
Savanna [%]	0	0	0	2.2
Grassland [%]	29.4	22.4	30	28.7
Croplands [%]	2.7	4.1	3.3	2.1
Cropland/ Natural Vegetation Mosaic [%]	12.6	9.7	13.3	8
Barren Sparsely Vegetated [%]	0	0	0.1	0.8

Table 2.1: Watershed characteristics generated with the Kenya watershed tool

The RGS at the four sites are each fixed on a bridge pillar which facilitates installation and the determination of a well defined profile. The measuring device for the three ephemeral river (Sereolevi, Merille and Melgis) is a solinist. It only measures the water pressure. Additionally, at the Merille site also a measuring device for the air pressure was installed. At the site of Habaswein an ecolog was installed, thus a measurement device for the air pressure was superfluous. All the measuring tools are equipped with an antenna and transfer the data automatically.

2.2 Methods

As outlined already, to gain an understanding of the hydrology of a certain site and it's catchment, it is necessary to obtain information about the discharge. The discharge is the amount of water, which flows trough a cross section, expressed as volume per unit of time. Stream discharge cannot be measured directly, but must be computed from other measured variables such as gauge height, stream depth, stream width, and stream velocity, as the discharge formula 2.1 shows (Adrien, 2004):

$$\begin{aligned} Q &= v \cdot A \\ \text{with } Q &= \text{Discharge } [m^3/s] \\ v &= \text{Flow velocityl } [m/s] \\ A &= \text{Cross section area } [m] \end{aligned} \tag{2.1}$$

For this study, application of the method was restricted both because the available measurement equipment was limited and because the streams considered are ephemeral. As mentioned in the section 2.1.3, this means that it is hard to predict whether there will be high or low flow. Therefore it was not possible to measure the stream velocity and calculate the discharge with the measured variables. The result should thereby be seen as a first assessment but cannot replace discharge measurement. Nevertheless, this study provides a first assessment of stream geometry and velocity by applying the empirical MSE (section 1.3.1). These results can serve as a basis for further river hydrological investigations in a region where such data is largely missing.
These basic variables had to be collected on site during the field survey. Afterwards, the software Basement was used to simulate the discharge belonging to a certain water level. The software Basement has the MSE implemented, showing up in the SVE . Based on the survey and with the software Basement stage-discharge relations were calculated and have to be explained with a convenient function. The stage-discharge relation is necessary to translate a measured stage by the RGS directly into the related discharge value. Establishing a stage-discharge relation (rating curve) is the most simple and common method for monitoring stream flow at a hydro-metric station (Le Coz, 2012).

2.2.1 Field Survey

In order to assess the relevant variables during fieldwork, a number of instructions by the World Meteorological Organisation (WMO) were conducted. They will be described in more detail in the following subsections and include:

- Define channel geometry of the area which controls the cross section by the RGS
- Measure width and depth of channel cross section
- Note down the factors influencing channel roughness
- Identify channel roughness
- Document the site with photographs (WMO, 2009)

These listed points correspond to the components of MSE and SVE: Channel characteristics, profile of cross sections, and slope and roughness coefficient.
The fieldwork was conducted during the months of February, March and April 2015.

2.2.1.1 Channel Geometry

At the time of fieldwork the only measurement equipment that was available for the survey (measuring channel geometry and cross section) was the dumpy level, which is a common instrument employed in tachometry. Tachometry is a survey method of optical distance measurement, which have been used for a long time in different disciplines. A staff is used to determine surface elevation. In order to read the values from staff a sighting instrument is used. The surface elevation and the location of points in relation to the others can be derived from the horizontal distance to the staff and the staff readings (Gorden et al., 2004). For every site a reference point has to be determined because the dumpy level can just indicate the height of the staff. To connect two cross sections in one river the height of cross section in relation to the other is needed. Then, the reference point is measured after each position change of the dumpy level. Since at least one person has to hold the staff vertically at the surveying point and another has to read the values with a sighting instrument, at least two people are necessary in order to conduct a measurement of this type (Gorden et al., 2004). A training was completed with the local staff of CETRAD that then participated in the measurements for this study. A field sheet was prepared to note all relevant variables required for the calculation (collimeter method) (Appendix A) and to enable a handier data collection. For the sites Habaswein and Melgis we measured four cross sections and for the sites Sereolevi and Merille we measured only three cross sections with the dumpy level (Fig. 2.4).

Figure 2.4: Fieldwork impressions: person holding staff (left), measuring elevation (middle) and sighting instrument (right)

That is, the height of a point in the cross sections in relation to the reference point and the distance between the cross sections by taking the measure between the lowest points of each cross section. For each RGS, in order to include the flow controlling part, three cross section were measured: one above, one at and one below the RGS. All the RGS were installed at bridge piers to ensure a more stable cross section over time, as the bridge has a pre-define cross section at least at the bank. In addition to that, the installation of RGS is easier at bridge piers. The distance between the surveying points along one cross section (perpendicular to

the river flow) was controlled with a tap. The measurements are only usable if the relation of one cross section to the other is known. With the help of a GPS device it was possible to measure the orientation of each cross section and the orientation of the line between the lowest points of each cross section. During further data processing, the distance and height of the points in the cross section and its slope were calculated. The measured orientation and the pythagorean theorem were used to represent the riverbed and calculate the slope. Put it in a coordinate system, all the necessary information is available in order to start the simulation in Basement.

2.2.1.2 Roughness Coefficient

The roughness coefficient can be either determined by look-up a table or by dividing a proportionality constant by the determined grain size of the channel material (Brechtold, 2015). In this study, the value was determined by consulting a look-up table ('Strickler Beiwert nach Naudscher, 1992' (Uni Karlsruhe, 2016)) (Appendix A). Since all the study sites are located in an arid region (savanna) the riverbeds are similar, mainly filled with sand and some shrubs at the bank.
The collected data are summarized in an excel sheet and documented with photos. This compilation served as input data set for the software Basement.

2.2.2 Water level-Discharge Simulation

Depending on the available amount of time, there are different possibilities to calculate the discharge without measuring the velocity. Often, cross section geometries of one site are merged together by taking the average geometry out of the three or four cross sections. Afterwards, the calculation of the discharge is only done for this cross section. In this study the discharge is calculated with the 1D simulation in Basement. The advantage is, first, that it is possible to simulate the discharge over these three or four cross sections and thereby have the changes of the geometry and the slopes in it. Secondly, more than one kst-coefficient can be considered, one for the riverbed and one for the bank sides.
As mentioned in section 1.3.2, the required input data are the following for each cross sections of the river: the x,z coordinate for each point in the cross section, the x,y,z coordinates of the left point of the cross section, the kst-coefficients, the angle of the cross section and the distance to the first cross section upstream. This information is contained in the Basechain geometry file (Fig. 2.5) and serves as basis for the simulation. Figure 2.5 shows one cross section on the left side and the evaluated information: the range of the bottom, the range of the main channel and the kst-coefficients. In the Basement Edit Commando, decisions about simulated output, the way of simulation and the hydraulic conditions like the start and boundary conditions were taken. The initial condition was set to dry condition, the upper boundary condition to steady state inflow and the downstream boundary condition as a hq-relation. For each simulation run of one site, an output file was generated with an associated discharge value. In the end a stage-discharge relation was established. The kst-coefficients were assumed to be constant.

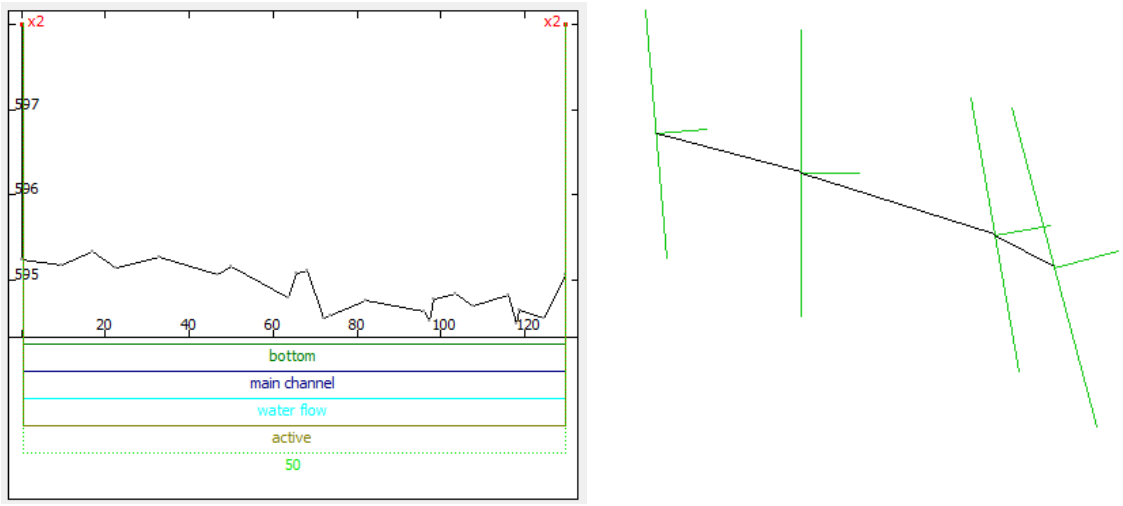

Figure 2.5: Merille: cross section with width and height (left), cross sections in relation to one another (right)

2.2.3 Establishing Rating Curves

'Stage-discharge relations are hydraulic relations that can be defined according to the type of control that exists and it is the best fit between the stage and the discharge at a certain site' (Suter, 2014). The control is responsible for the shape of the curve, mainly defined by the geometry of elements downstream of the RGS. The equation can be expressed in a basic and general form as following (WMO, 2010):

$$Q = C \cdot (h - e)^{\beta}$$

$$\begin{aligned} \text{with } Q &= \text{Discharge } [m^3/s] \\ h &= \text{Waterlevel } [m] \\ e &= \text{Waterlevel of zero flow } [m] \\ \beta &= \text{Exponent } [-] \\ C &= \text{Coefficient } [-] \end{aligned} \tag{2.2}$$

Rating equations describe the relationship between stage and discharge. The stage-discharge relation for most RGS is defined by plotting the two variables against each other (Bosshart, 1997).

2.2.4 Curve Fitting

In order to model the stage-discharge relation, it is recommended to use a non linear model and to fit the model to the data with the least squares method in order to obtain a statistical and objective relation. In hydrology, a power function as equation 2.2 is commonly used to

establish a relationship between stage and discharge (Bosshart, 1997). The curve fitting and analysis of the relation between stage and discharge was obtained with help of the statistical program R. This software provides basic tools needed here like non linear models (nls) and the calculation of confidence bands. The non linear model was applied and a power function was chosen to fit the model. The non linear model function calculates a best fit for the curve. The accuracy of the fit can by analysed by looking at the residuals standard error. Parameter estimation is based on an iterative procedure that involves a linearization approximation leading to a least squares problem at each step. Further, the stage-discharge relation enables to get a first impression of the the channel capacity at the four sites. It should be noted, that the river beds are sandy, the geometry of the cross section would continuously change with flow, thereby invalidating more sophisticated models (WMO, 2010). Considering the fact that this analysis aims at completing a first assessment of the discharge in these channels, the applied method is satisfactory to reach the aim.

2.2.5 Uncertainties and Sensitivity Analysis

Potential sources of uncertainties are natural uncertainties, knowledge uncertainties and data uncertainties during the establishment of the rating curve. The evaluation of the amplitude of the different sources of uncertainty is beyond the scope of this study, but it is important to keep the differentiation in mind. In addition to that, there are uncertainties due to the fitting of a curve to the stage-discharge relation, namely imperfect matching (Braca, 2008). Again, for this study, it was not possible to do the respective control to quantify the uncertainties.
The main task would consist of calibrating the kst-coefficients with velocity measurements, but this was not possible as no water was flowing during the period of data collection. The range of uncertainties was reported for the processes of establishing a rating curve the fitting of curves. To elaborate the sensitivity of the kst-coefficient pair, it was changed by +/-10% and the stage-discharge relation was simulated again for both cases. Additionally, the evaluated error range of +/- 20%, by applying the MSE to calculate the discharge, was considered (Bosshart, 1997). To arrive at a final assessment of errors, the sources of error were summed up. The summation was not quadratic because it is was uncertain if the two error sources are correlated (Drosg, 2006).
It is still an open issue which methodology assesses the uncertainties associated with a given stage-discharge relation (Le Coz, 2012). In order to nevertheless get a grasp at the uncertainties of the stage-discharge relationship, a 95% confidence band based on the 2.5% and the 97.5% quantiles was automatically calculated for the fitted curve. This confidence band tells that with a probability of 95%, the best fit lies in between the two lines.

2.3 Results

The results are presented individually for each study site following the structure of the aims of this study: the output of the fieldwork (Tab. 2.2, 2.3, 2.4 and 2.5), the simulation of the stage-discharge relation in Basement (Fig. 2.8, 2.12, 2.16 and 2.20) and the established rating curve to convert the measured water level (Fig. 2.9, 2.13, 2.17 and 2.21).
Some general information which is valid for every site will be shortly introduced here. The geometry of the river section was visualised with the software Basement. For the simulation, the input discharge was always increased by 2 m^2/s for every run to obtain the stage-discharge relations. Concerning the output Figures (Fig. 2.9, 2.13, 2.17 and 2.21), it is noteworthy that the points are mostly in a line already because they were simulated, that is not necessarily representative of a 'natural' setup.
The uncertainties of the elaborated error sources, the variation of the kst-coefficients and the use of the MSE to elaborate the flow velocity, are high (Fig. 2.8, 2.12, 2.16 and 2.20). Errors, due to the field measurement could not be quantified but should be kept in mind. In all cases, the band of uncertainty is large.
The simulated relation for all the four sites are best modelled by a power function. This can be confirmed by plotting the two logged variables against each other. Therefore, it was not necessary to compare different models. The parameter were fitted in R, applying the nls model (non-linear model). The residual sum of squares for the model and every site was judged to be acceptable.

2.3.1 Sereolevi

As shown in Table 2.2 this site it is a very flat and straight river and with no backwater effect. In the field, four cross sections have been measured, but for the analysis, only three were valid. The roughness coefficients (kst-coefficients) were determined for every cross section separately. The channel was found to be homogeneous, sandy, and hardly no vegetation or stones in the channel except for some shrubs at the bank (Fig. 2.6). Since there is an old and a new bridge which both have a importantly influence on river flow, we measured cross sections for both bridges separately with each having a different orientation (Fig. 2.7).

2.3.1.1 Overview Sereolevi

Geometry	Width [m]	Orientation angle [°]	kst-coefficients $[m^{\frac{1}{3}}/s]$	Lowest point $[m.a.s.l.]$	Distance	Slope [‰]
Cross section UPS	89	300	50	737.65		
Cross section RGS	90.2	255	40	737.61	45.78	
Cross section DWS	90	280	25, 50, 35	737.315	99.48	3.3

Table 2.2: Fieldwork output Sereolevi

Figure 2.6: Estimation of kst-coefficients

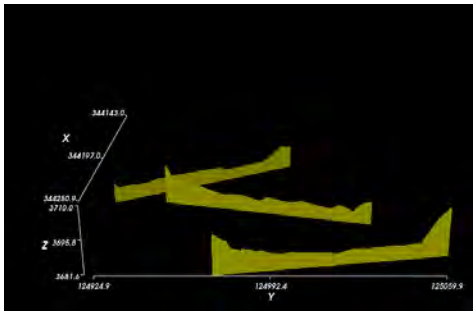

Figure 2.7: Geometry of the cross sections

2.3.1.2 Stage-Discharge Relation and Error Sources

Figure 2.8 top left shows the stage-discharge relation established for the Sereolevi study site. It illustrates that for low flow conditions, the discharge increases slowly with an increasing water level. On a water level above 0.5 m it increases continuously. Figure 2.8 bottom left indicates that changing the kst-coefficients does not greatly influence the discharge. For example, for a discharge of 100 m^3/s the water level varies between 1.096 m to 1.174 m as Figure 2.8 top left depicts. The error range of the MSE of +/- 20% on the other hand greatly influences the result. For a discharge of 100 m^3/s the water level ranges between 0.9044441 to 1.3566661 m. These two calculations are related to the simulated point and not to the rating curve.

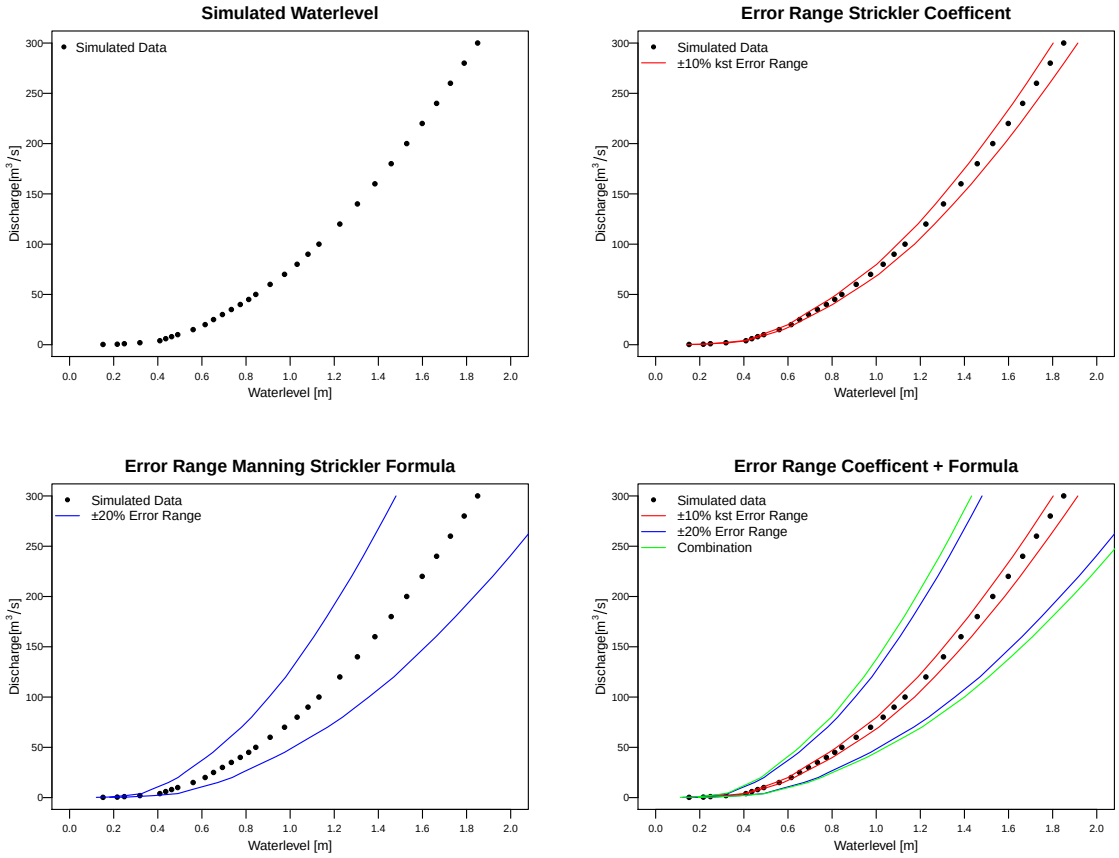

Figure 2.8: Simulated stage-discharge relation for Sereolevi: simulated stage-discharge relation (top left), with uncertainty range of kst-coefficient (top right), with uncertainty range applying MSE (bottom left) and combination of the uncertainties (bottom right)

2.3.1.3 Rating Curve and Power Function

The calculated rating curve (equation 2.3) reflects the simulated stage-discharge relation rather well. For low flow conditions the rating curve slightly overestimates the discharge as shown in Figure 2.9. The residual standard error for the rating curve in relation to the simulated point is 2.982 m^3/s and 29 points have been calculated. The channel capacity can be calculated with equation 2.3 and the measured bank site height. It is approximately 670 m^3/s and overflows first at the right side. It is an estimation depending on the accuracy of the rating curve and the measured bank site height.

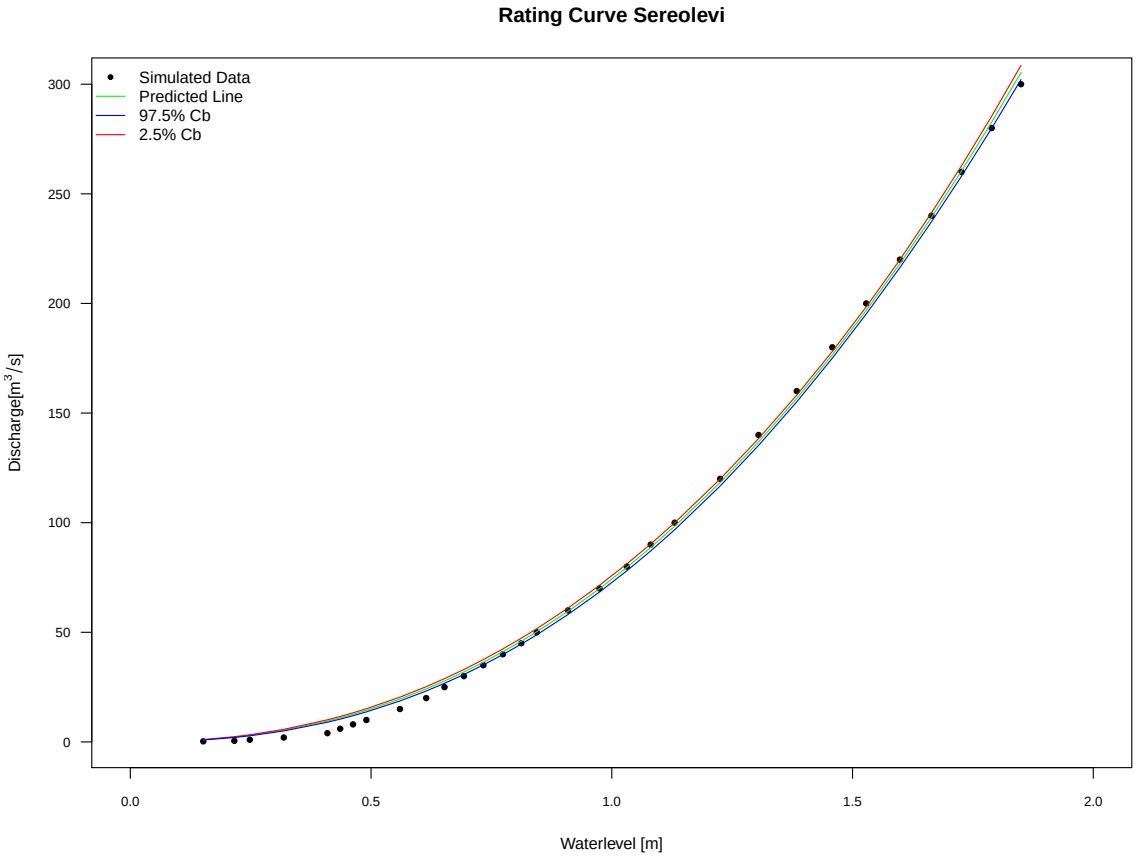

Figure 2.9: Fitted rating curve to the simulated stage-discharge relation

$$Q = 74.17506 \cdot (h)^{2.30022}$$
$$\text{with } Q = \text{Discharge } [m^3/s] \qquad (2.3)$$
$$h = \text{Waterlevel } [m]$$

2.3.2 Merille

The conditions at Merille site are similar to Sereolevi, which only lies 50 km away. The river at Merille is also very flat, wide (max. 154 m), sandy and has only little vegetation (Fig. 2.10). All four measured CS were valid and could be used (Tab. 2.3). One cross section was taken 165 m away from the RGS, because in that location, the riverbed is narrower due to a cliff on the right side facing upstream, potentially exerting a strong influence on the river. The simulated section consists of the four cross sections. The surveyed section is 200 m long. Figure 2.10 again shows, how flat and wide the river is.

2.3.2.1 Overview Merille

Geometry	Width [m]	Orientation angle [°]	kst-coefficients $[m^{\frac{1}{3}}/s]$	Lowest point $[m.a.s.l]$	Distance	Slope [‰]
Cross section UPS2	116.5	300	50	594.93	0	
Cross section UPS1	133.5	270	50	594.81	70.7	
Cross section RGS	129.5	280	50	594.47	165.4	
Cross section DWS	154	285	25,50	594.4	197.18	2.47

Table 2.3: Fieldwork output Merille

Figure 2.10: Estimation of kst-coefficients

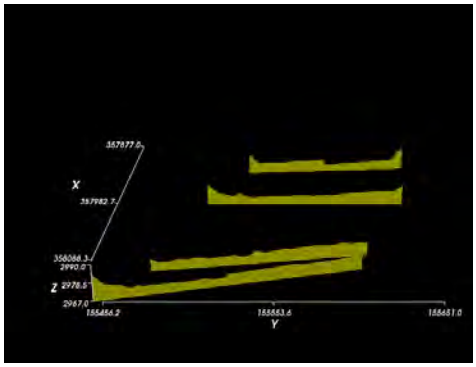

Figure 2.11: Geometry of the cross sections

2.3.2.2 Stage-Discharge Relation and Error Sources

In the case of the Merille river the simulated relation was similar to the Sereolevi site, but the discharge increased already at a lower stage of the water level. The simulation shows three segments, separated by two kinks (Fig. 2.12). The Figure 2.12 bottom left indicates that the sensitivity of the kst-coefficients is rather low. For example, at a discharge of 100 m^3/s, the water level varies from 0.9352238 m to 0.9739810 m (Fig. 2.12 top left). The error range of the MSE of +/- 20% however again exerts grater influence on the results. For a discharge of 100 m^3/s the water level ranges from 0.7141414 m to 1.0712120 m, i.e. the level rises by 40 cm (Fig. 2.12 bottom left).

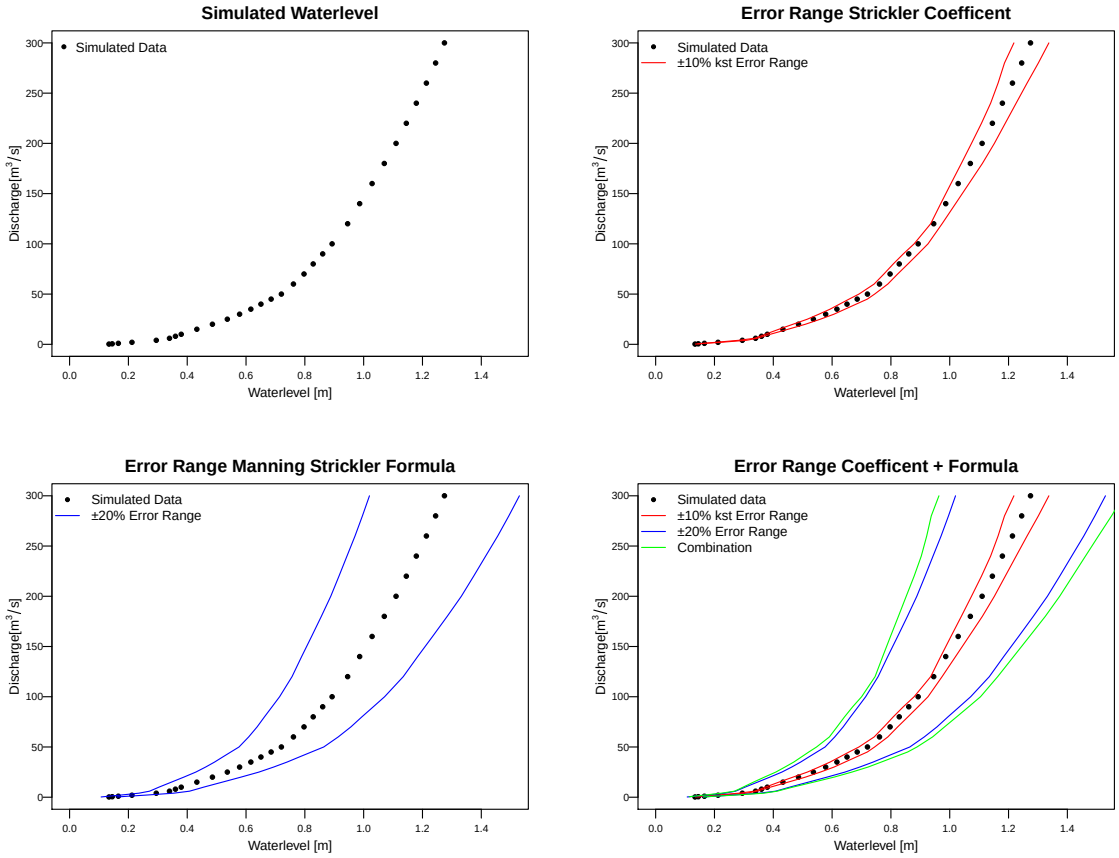

Figure 2.12: Simulated stage-discharge relation for Merille: simulated stage-discharge relation (top left), with uncertainty range of kst-coefficient (top right), with uncertainty range applying MSE (bottom left) and combination of the uncertainties (bottom right)

2.3.2.3 Rating Curve and Power Function

The simulated data points and the fitted curve exhibit the strongest difference at a water level between 0.4 and 0.6 m , where the discharge is underestimated. The residual standard error for the rating curve in relation to the simulated points is 2.11 m^3/s with 29 calculated points. The channel capacity for the Merille site is very high with approximately 2800 m^3/s and is overflowing first at the right side.

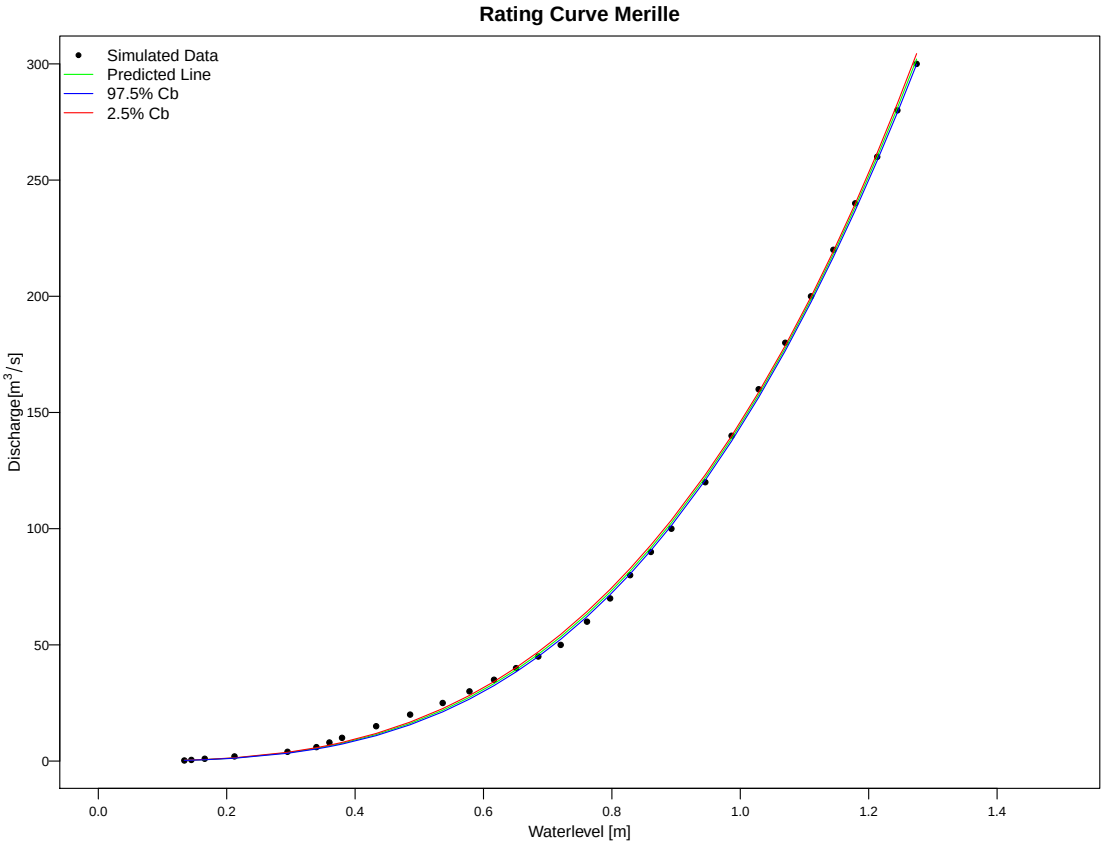

Figure 2.13: Fitted rating curve to the simulated stage-discharge relation

$$Q = 144.65579 \cdot (h)^{3.03393}$$
$$\text{with } Q = \text{Discharge } [m^3/s] \qquad (2.4)$$
$$h = \text{Waterlevel } [m]$$

2.3.3 Melgis

Melgis is the third river going northwards in direction of Marsabit, with a distance of 50 km to Merille. The Melgis river was different from the two other sites, as the fieldwork result (Tab. 2.4) and Figure 2.15 show. The riverbed is less flat, the bottom varied in height, some stones at the bottom of the river, the riverbed was deeper and narrower, and the bank was completely covered with shrumbs (Fig. 2.14). Furthermore, Melgis river had a constant water flow in the rainy season during one measurement campaign. It is noteworthy that there was a road construction right next to the river and that a dam was build upstream of the RGS to collect water. However, the dam was demolished during the rainy season, which led to the accumulation of large stones in the riverbed. Three cross sections were valid and used for the calculations. Downstream of the RGS the Melgis river exhibits a backwater effect as the slope increases again.

2.3.3.1 Overview Melgis

Geometry	Width[m]	Orientation angle [°]	kst-coefficients $[m^{\frac{1}{3}}/s]$	Lowest point $[m.a.s.l.]$	Distance	Slope [‰]
Cross section UPS	48.5	295	25, 45, 25	467.89	0	
Cross section RGS	63.4	280	35	467.32	59.2	
Cross section DWS	48.9	280	30	467.64	151.94	1.73

Table 2.4: Fieldwork output Melgis

Figure 2.14: Estimation of kst-coefficients

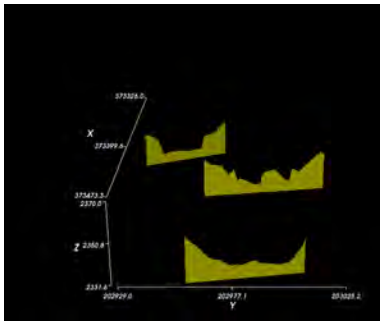

Figure 2.15: Geometry of the cross sections

2.3.3.2 Stage-Discharge Relation and Error Sources

The simulated relation is flatter compared to the other study sites, probably due to the fact that the river bed is narrower (Fig. 2.16). Figure 2.16 upper right indicates that the influence of changing kst-coefficients is small. For a discharge of 100 m^3/s the water level ranges from 2.3456130 m to 2.5338169 m as Figure 2.16 top right shows. The error range of the MSE of +/- 20% has a large influence on the result. For a discharge of 100 m^3/s, the water level ranges from 1.9459770 m to 2.9189656 m, i.e. it varies by almost 1 m (Fig. 2.16 bottom left).

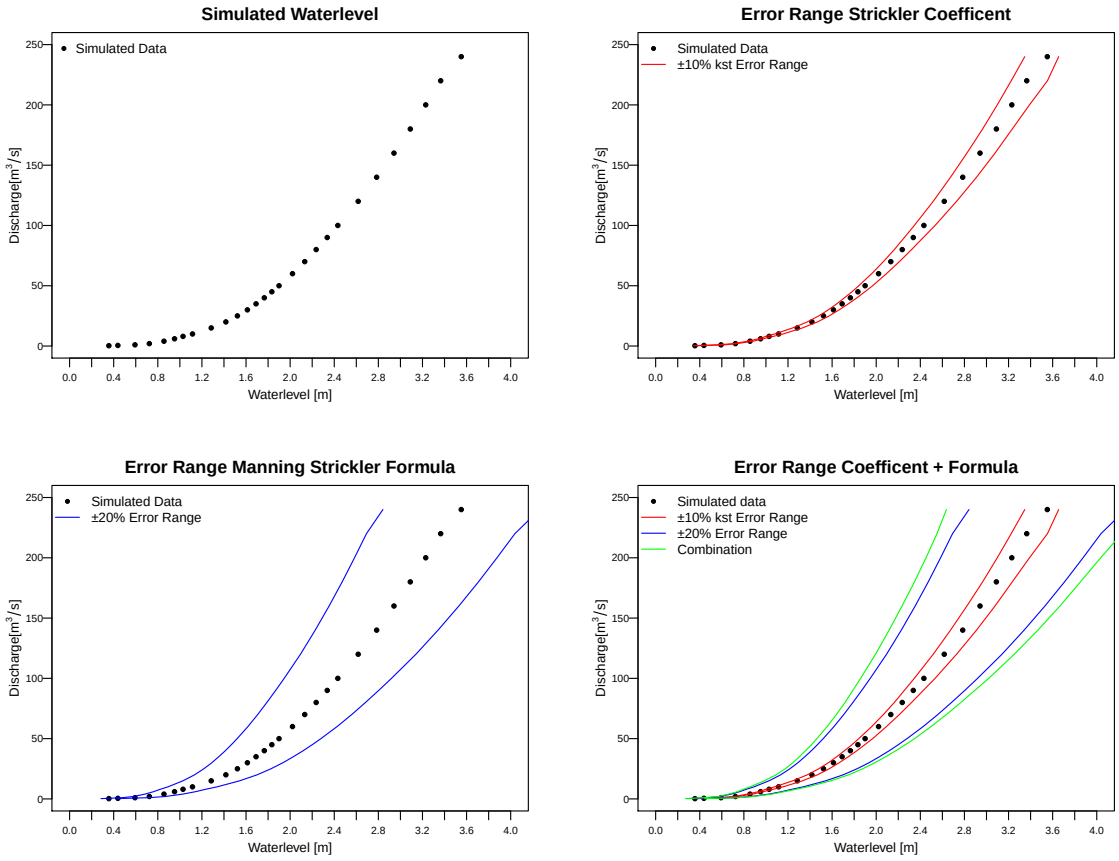

Figure 2.16: Simulated stage-discharge relation for Melgis: simulated stage-discharge relation (top left), with uncertainty range of kst-coefficient (top right), with uncertainty range applying MSE (bottom left) and combination of the uncertainties (bottom right)

2.3.3.3 Rating Curve and Power Function

Figure 2.17 shows that the fitted function 2.5 does not perfectly cover the points along the whole range of the water level. For low flow conditions it overestimates the discharge, while for high flow it underestimates it. This gets further confirmed by a high residual standard error of 3.772 m^3/s with 26 degree of freedom. The channel capacity for Melgis site is smaller compared to the two previous rivers with approximately 302 m^3/s and the right side is the weak side.

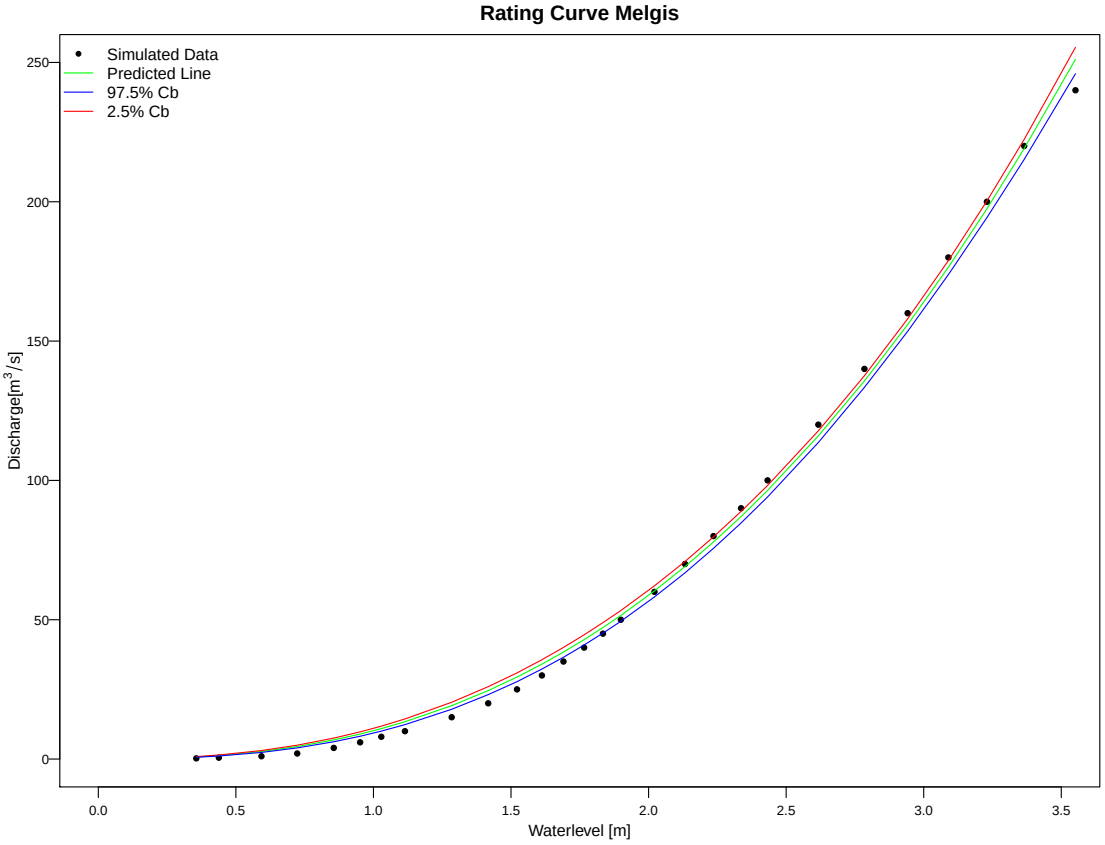

Figure 2.17: Fitted rating curve to the simulated stage-discharge relation

$$Q = 10.17219 \cdot (h)^{2.52978}$$
$$\text{with } Q = \text{Discharge } [m^3/s] \qquad (2.5)$$
$$h = \text{Waterlevel } [m]$$

2.3.4 Habaswein

As mentioned in the study area section, Habaswein lies on the other side of the catchment, after the swamps at the end of the Ewaso Ng'rio river. It is not a tributary of the Ewaso Ng'iro but the Ewaso N'giro main river itself. The riverbed is varying a lot in the short section where we conducted the measurements of the cross sections. This made it difficult to even define a riverbed. The bridge served as an indicator of periodical river flow. The riverbed was sandy with some stones, upstream of the bridge, a distinct riverbed could not be ascertained. Downstream of the bridge there was a pond-like structure generating a back water effect (Fig. 2.18 and Tab. 2.5). Because of the unsteady riverbed and the ponding, it was difficult to simulate the riverbed in the software Basement. The solution was to generate in Basement two additional cross sections between the bridge and the measured cross section downstream to simulate the lower flow (Fig. 2.19). A point was inserted into the cross section downstream to clarify the shape. Therefore, these results have to be interpreted with some care.

2.3.4.1 Overview Habaswein

Geometry	Width [m]	Orientation angle [°]	kst-coefficients $[m^{\frac{1}{3}}/s]$	Lowest point $[m.a.s.l]$	Distance	Slope [‰]
Cross section UPS	17.9	270	45	208.55,	0	
Cross section RGS	24.5	225	30,20,45, 30	208.061	21.18	
Cross section DWS	37.5	260	35	208.45	44.34	2.66

Table 2.5: Fieldwork output Habaswein

Figure 2.18: Estimation of kst-coefficients

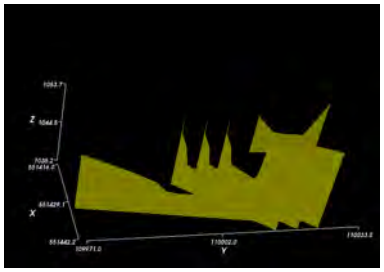

Figure 2.19: Geometry of the cross sections

2.3.4.2 Stage-Discharge Relation and Error Sources

As shown in Figure 2.20 top right, minimal flow could not be simulated. The river bed is narrow in comparison to the three other study sites and therefore, the simulation ends at 30 m^3/s. Figure 2.20 bottom left depicts that the influence of a change in the kst-coefficients is much smaller compared to other uncertainty sources. For a discharge of 20 m^3/s the water level ranges between 1.3591829 m and 1.4511102 m (Fig. 2.20 top left). In contrast the error range of the MSE of +/-20% has a larger influence on the result. For a discharge of 20 m^3/s the water level varies between 1.1198091 m and 1.6797137 m (Fig. 2.20 bottom left).

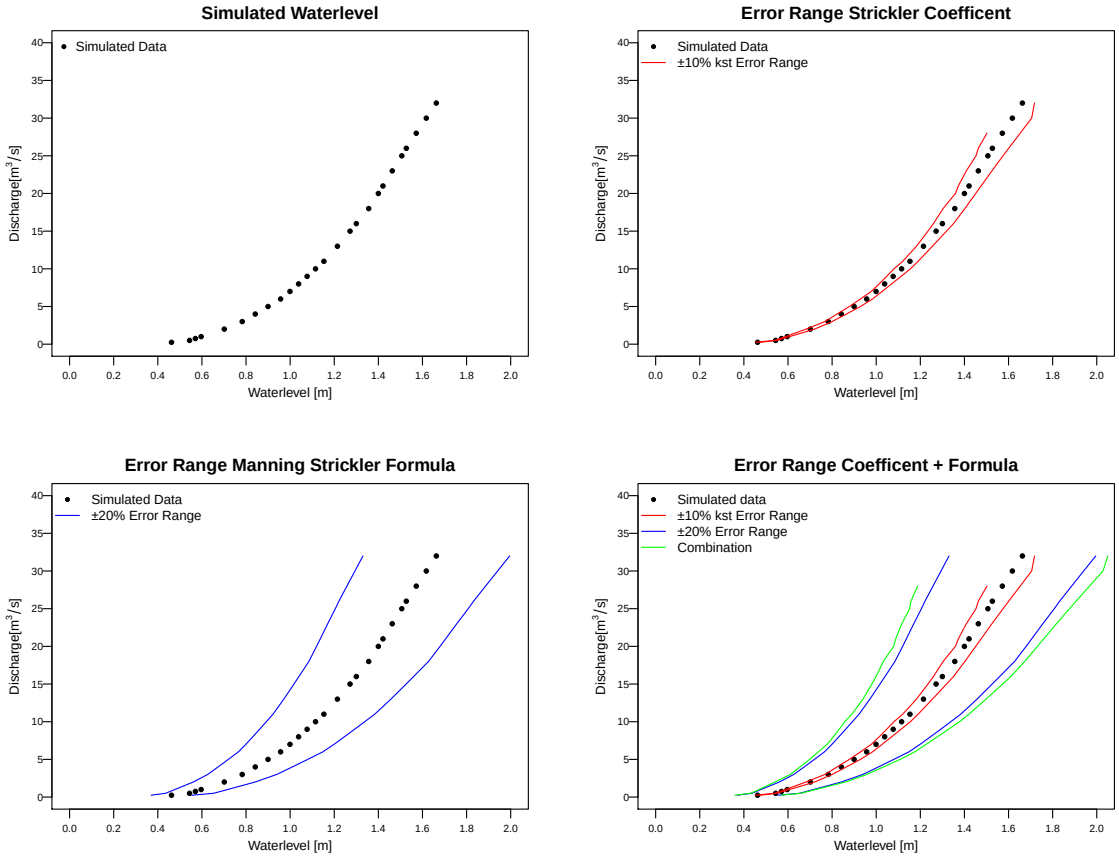

Figure 2.20: Simulated stage-discharge relation for Habaswein: simulated stage-discharge relation (top left), with uncertainty range of kst-coefficient (top right), with uncertainty range applying MSE (bottom left) and combination of the uncertainties (bottom right)

2.3.4.3 Rating Curve and Power Function

The function 2.6 overestimates the discharge value for low flow condition. In comparison to the fits of the other rivers it is much worse, but still acceptable. This is also reflected in the rather high residual standard error for the rating curve of 0.4169 m^3/s. In total, 24 points were simulated and integrated in the calculations. As the river next to Habaswein is much smaller than the others the channel capacity is also much smaller with approximately 23 m^3/s and the right side is the weak side.

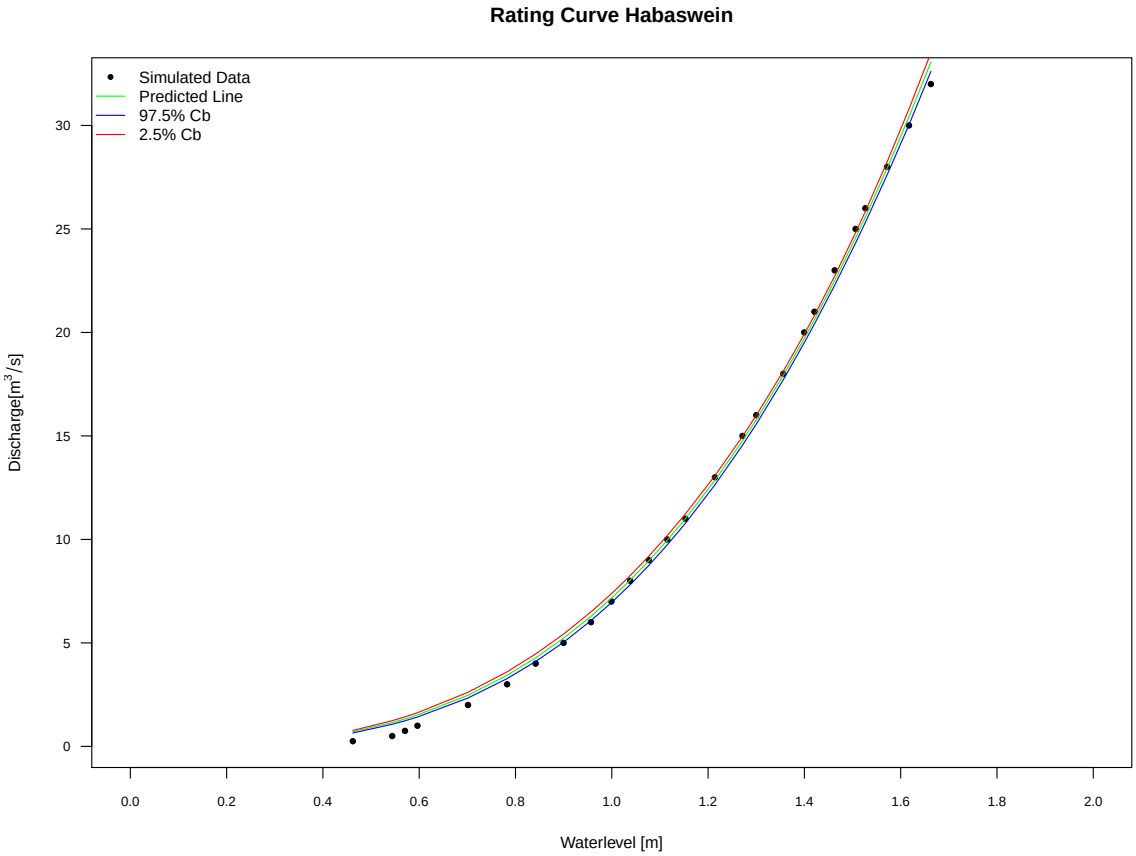

Figure 2.21: Fitted rating curve to the simulated stage-discharge relation

$$Q = 7.17677 \cdot (h)^{3.00431}$$
$$\text{with } Q = \text{Discharge } [m^3/s] \qquad (2.6)$$
$$h = \text{Waterlevel } [m]$$

2.4 Discussion

The here above obtained results indicate that it is possible to establish a function and the corresponding rating curve for each site with the here applied method, regardless of the scarcely available resource and input data. For the field survey, measurement with the dumpy level seems to be a good solution in such areas. The most important information could be collected, and the whole water team of CETRAD could be instructed for participating in this and potential future measurement campaigns.

However, two issues should be kept in mind: First, it was not possible to evaluate the errors occurring during the work steps. Secondly, the results do heavily depend up on the choice of the location of the cross section to be measured. All sites have sandy channels, i.e. the bottom channel geometry is not constant and will change with the water flowing through. Thus, results in this study related to geometry are restricted in their validity until next rainy season. However, for a rough estimate of the flow timing and intensity of the flow, the here established channel geometry may be used for several years.

Considering the 1D simulation in Basement, most of the basic physical variables are defined by the software and the user is not required to set or modify many parameters, which makes the procedure easier to handle. The output of the simulation depends on the kst-coefficients and the number of measured cross sections. In the Habaswein case, the influence of the number of cross sections was observed. At first, a simulation was not possible because the slope difference between two cross sections was too big. The implementation of two additional cross sections with the same geometry as the first one, enables the simulation to be run. Concerning influence of the kst-coefficient, the model proved to be sensitive, as the results for each river show (Fig. 2.8, 2.12, 2.16 and 2.20). However, as all of the rivers have sandy ground it is easier to define the kst-coefficient compared to other regions. Another advantage of the software Basement is that numerous possibilities of visualisation are being provided.

Regarding the establishment of the rating curve, the chosen method is simple and thereby is limited by the mentioned uncertainties occurring during the whole process. However, it seems that the rating curve mirrors the simulated relation rather well. The example of Merille (Fig. 2.10) suggests that a segmentation of the relation may, under certain circumstances, be a good option. Here, individual rating curves for the different segments, would permit a finer-grained resolution. But, before going into further details, first a calibration should be conducted in another measurement campaign. The uncertainty of the established rating curves also applies for the estimation of the channel capacity at the sites. In addition, the measurement of the bank site height is difficult because in can vary from rainy season to rainy season. The location of the RGS and its cross section is next to a bridge for all four sites. There, the bank sides are constructed and do not represent the situation up-and downstream. Therefore, it serves as a first idea of the channel capacity and it shows that in Sereolevi, Merille and Melgis the capacity is high.

The major limitation of this study is caused by the numerous and unquantified uncertainties indebted to approach here chosen, as illustrated in Figure 2.8, 2.12, 2.16 and 2.20. However, this study did not aim at any calibration, so that the latter limitation was included into the

very procedure. The errors occurring during the field work could not be quantified. The calculated ranges of uncertainties rather serves as first estimates. As mentioned in section 2.1.1, there was no other RGS in the region and no possibility to do any kind of more advanced hydrological analysis. With the available data, it was not possible to draw a conclusion about the accuracy of the elaborated functions, nor was it possible to discuss them in light of the broader geographical context.

2.5 Conclusion

This study aimed at establishing a rating curve and enables a first estimation of the channel capacity for the four chosen sites in the lower Ewaso Ng'iro Basin in Kenya with resource at hand, as the available measurement tools and workforce at the period of study. The work process included the collection of the required data on site, simulation of the stage-discharge relations in Basement and fitting curves to the simulated points. These investigations were intended to improve understanding of the hydrology of the lower Ewaso Ng'iro Basin and shall serve as a first estimation and assessment of the amount and timing of water, which flows trough these ephemeral rivers. This study proposes a first step of a hydrological analysis to gain a better understanding of the flow intensity and timing, channel capacity and basic hydrological process of those rivers. Further, the chosen methods are rather simple and can therefore be used by the water team of CETRAD in Nanyuki for other rivers, where the installation of RGS is projected.

To sum up, the chosen methods and the gained results allow for a first assessment about the discharge and the channel capacity at the RGS of these rivers and can thereby contribute a piece of puzzle mentioned in the IPCC report Benito et al. (2011), that is, to enhance knowledge of water flow in dry region with ephemeral rivers. This study can further be regarded as complementing the satellite study of De Leeuw et al. (2012), providing information about the water flow in the Ewaso Ng'rio river next to the swamps. Still, a number of issues should be addressed in future research. Above all, more research is required to develop a method that can calibrate and validate the here proposed results. For example, one promising method would be that of video recording the river flow to evaluate the flow velocity (Boursicaud et al., 2015).
All in all, it is remarkable to see what one can do even with a low budget and a rather straightforward approach. In terms of financial resources, the here proposed work flow may offer an attractive alternative to more extensive and thereby expensive methods. It does not require a lot of equipment, and the employed programs are all open source. If one keeps in mind its limitation, this is a viable approach for studies with similar interests in comparable areas.

Chapter 3

Weak Point Analysis along the Main Rivers of Bernese Oberland Switzerland

3.1 Introduction

3.1.1 Problem Description

Consequences and dangers of flood events have been of concern for major parts of Switzerland for a long time. In order to gain better insight into flood events and eventually enhance protection measures, the run-off of rivers their interaction with their surrounding has to be studied.
In Switzerland, the research related to flood event can be backtracked to the 19th century (Spreafico et al., 2003). Estimating the occurrence of flood events without direct measurements has been done since the 80ies and with climate change research related to flood events has become more and more relevant. In the 80ies, assessing flood risk was challenging because of low availability of hydrological data, poor spatially resolved information and the low computational capacity (Viviroli and Weingartner, 2012).
To this day, many investigations were conducted to improve understanding in this field. Main efforts were done in the areas of extending measurement systems, using extreme value statistics and establishing regionalization methods (Viviroli and Weingartner, 2012). Two helpful innovations to do estimations of floods with certain return periods in Switzerland were launched. First, the tool HQx_ meso_ CH created by Barben (2001) (HQ_x stays for flood with a certain return period, meso for meso scale catchment and CH for catchments in Switerland). It includes 10 different regionalization methods to estimate the flood events of a catchment. The second innovation includes the PREcipitation-Runoff-EVApotranspiration HRU model (PREVAH) build by Viviroli et al. (2009). It is a continuous precipitation-run off approach aiming to derive discharge hydrographs for meso scale catchment in Switzerland.
This brief overview on the field indicates that flood events and their occurrence have been well researched. The efforts of the hydrological group of the University of Bern triggered a broad range of studies around this topic including information search on flood events. A documentation of the largest over regional flood catastrophes of the last 200 years was established (Brunner, 2014) and the estimation of floods of small catchments in Switzerland to improve interpretation and practical application was studied (Dobmann, 2009). Further the

HQx_meso_CH-visual was developed to have a flood relevant representation of meso scale catchments in Switzerland (Klauser, 2004) and the flood situations of small sub catchments of the river Kander was analysed (Zgraggen, 2009). The influence of spatial and temporal precipitation variability on the peak discharge of the Simme basin in the Bernese Oberland was modelled (Brunner, 2014) and hydrology of the Kander-yesterday-today-tomorrow and analysis and modelling of floods and its space-time dynamic was studied (Wehren, 2010).
They mainly concluded that it is important to apply more than one method and results should be critically examined. These studies were based on the analysis on the catchment scale, examining the magnitude, source and development of river discharges, where it comes from and how it does develop.
Regarding flood protection in a holistic view, two main issues have to be considered, one being the discharge value of a flood and its return period and the second being the channel capacity (bank-full discharge) along the rivers. The later statement is mostly analysed on past flood events with the support of hydrodynamic models to calculate the bank-full discharge and the flooded areas. The bank-full discharge is of interest for the researchers, engineers and planners because it represent the water flow which fills the channel to the top of the bank (Wiliams, 1978). That is relevant in terms of floods. In Switzerland, many different engineering offices apply this type of analysis by order of the cantons or communities, and different models are used. The results are combined with the information on the probability of flood events and are implemented in natural hazard maps for floods showing the expected magnitudes of events in different areas and with technical reports provided. These evaluated points are considered the weak points along a river, the channel capacity is low and the associated return period high. There is a report for each community based on the approaches of the commissioned engineers offices. Example of such reports are EB AG (2008) and Aarewasser AG (2009) for the Simme next to Boltigen and the Aare Thun-Bern. Because of the different responsibilities for all the analysis of each river section, the methodological approach varies from case to case. These assessments are mostly done with hydraulic models, and the scope of the practice is rather broad. Mostly a 2D simulation is applied because the spatial resolution is better than in the 1D simulation, and the sections are shorter, however, at the price of higher computational power because of more detailed topographic resolution constraining the analysis to a small river section. For the spatially more comprehensive analysis, the 1D simulation is to be preferred (Rousselot, Vetsch, and Faeh, 2012; Vetsch et al., 2015b).
Due to all this research, a good survey on the flood situation in Switzerland already exists. However, the increasing frequency of flood events in the last few years in Switzerland (2007, 2014, 2015), the prospected climate change and the growth of the population results in increasing potential for damages. All points to the importance of doing further research to gain an even better understanding of the rivers and their interaction with environmental conditions. In Switzerland, all regions are affected by floods; mountain regions are concerned as densely populated areas are. The Bernese Oberland is of high importance because mountains serve as water towers for the lowlands. The water is transported via the rivers to the whole country. Mountains have an intense and very rapid run-off reaction, and they are highly vulnerable to climate change. Despite the high flood risk in the Bernese Oberland, only few studies have tried to analyse and model channel capacity on a large perimeter. As described above, most studies have focussed on single rivers, applying different methods and making thereby a comparison between studies difficult.

This study aims at contributing to fill this gap by conducting a weak point analysis along the major river of Bernese Oberland. In order to gain a holistic view, the purpose of this work is to combine hydrological and hydrodynamic approaches. The channel capacity and its associated return period shall be determined for each measured cross section along the main rivers Hasliaare, the Aare (Thun-Bern), the Simme, the Kander and the Lütschine. The idea of this procedure is to evaluate the possibility of gaining plausible values with rather simple approaches, which could ideally be applied identically on every river, and that at each cross section.
In summary, the diversity of research concerning floods is immense. Many institutional players are engaged in it but primarily, they pay focused on a small scales, on single river sections. Complementing this widespread practice, this study focuses to establish plausible estimations of flood return periods and the channel capacity for each cross section over large perimeter.

3.1.2 Objectives and Research Questions

Given the situation, the main aim of this part of the thesis is to develop a map of the Bernese Oberland up to Bern, with identification of weak points attributed with the associated return period along the main rivers. To achieve this, the following specific objectives and related research question are formulated:

a) **Identification of the discharge for floods with return periods in the range of 10 to 300 years ($\mathbf{HQ_{10}}$ to $\mathbf{HQ_{300}}$) for all available cross sections**
   - What is a reasonable method to extrapolate the flood with a certain return period (HQ_x) from the sites with discharge measurements?
   - Are the produced results comparable with other results of the region?
   - How to quantify the uncertainties of the method?

b) **Determination of the bank-full discharge, i.e. the maximum capacity of the channel for all the measured cross sections**
   - What is a straightforward method to identify the bank-full discharge for every cross section in the simulations?
   - How can iteration steps be automatized?
   - Can similar results of the ongoing research be achieved with the calibration of the model?

c) **Attribution of the bank-full discharge with the calculated and associated return period to identify the weak points along the rivers**
   - Where are the weak point in this river system?

– Are the results comparable with existing studies, and if there are, what are the differences?

3.1.3 Study Area

The rivers Aare, Simme, Kander and the Lütschine are situated on the northern flank of the Alps, belong to the Aare Watershed (Fig. 3.1). The upper part of the watershed upstream of Thun belongs to a biogeographical region called 'Alpennordflanke', while downstream of Thun, the 'Mittelland' region starts. The Aare watershed to Bern has a size of 2945 km^2 (RGS Schönau). The average height of the catchment is 1610 m, and 8% of the area is glaciated (FOEN, 2015b).

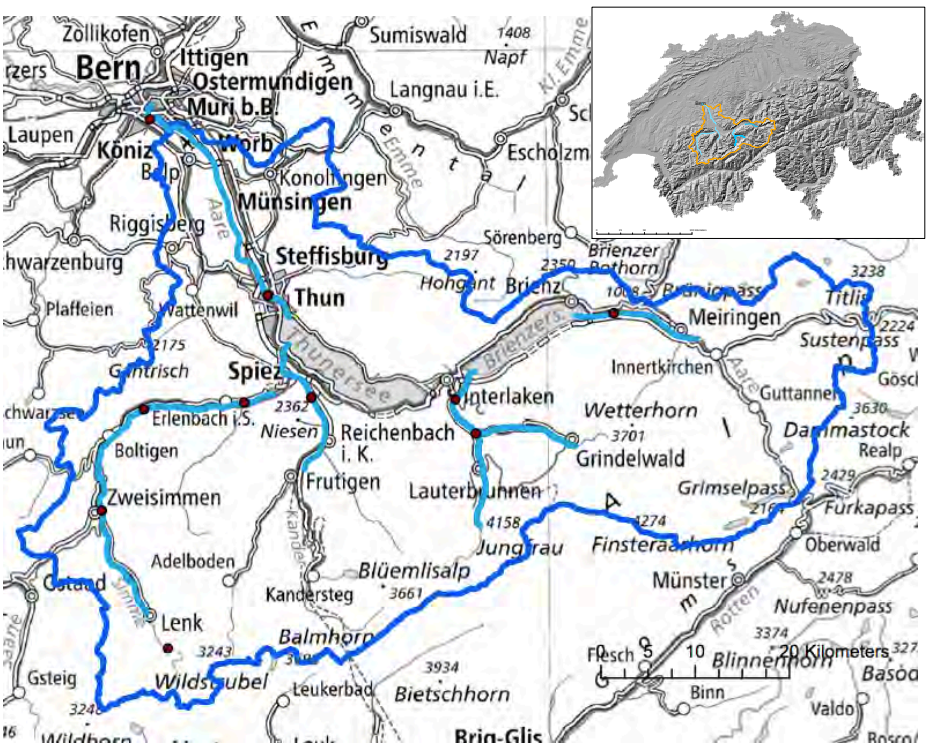

Figure 3.1: The Aare watershed up to Bern (blue), the major rivers (light blue) and the RGS along these rivers

The river Aare originates in the Alps, at the Aaregletscher. It drains at a steep slope from the mountains and runs trough the Aareschlucht as a b-glacial discharge regime. Further downstream, it passes Meiringen in highly straighten riverbed, discharges in the lake of Brienz and afterwards in the lake of Thun. From there on, it follows take its way in a corrected riverbed to Bern (Hunzinger, Zarn, and Bezzola, 2008; Aarewasser AG, 2009).

3.1.3.1 Survey Site

The survey sections are allocated along the main river belonging to the Aare Watershed: Simme, Kander, Lütschine Hasliaare and Aare Thun-Bern. The length of the sections depends on data availability. The riverbed of the Hasliaare (Meiringen-Brienz) has a shape of a double trapeze consisting of a main channel with a floodplain, bordered by flood controlling dams. The riverflow is affected by hydropower (Hunzinger, Zarn, and Bezzola, 2008) (Fig. 3.2).

Figure 3.2: Hasliaare: channel with floodplain

The channel of the Aare Thun-Bern is mainly characterized by straightening which took place between 1824 and 1892 (Aarewasser AG, 2009). To this day, a lot of work is done to renaturate some parts, and consequently, the sections vary strongly in terms of width, type of border and border vegetation. Figure 3.3 illustrates these differences.

Figure 3.3: Aare Thun-Bern: straightened (left) and renaturated (right)

The Simme (Lenk-Latterbach) is highly straightened until Weissenburg. Further downstream, it is widening up. Downriver, the Simme is meandering in an floodplain like region,

and partly, the riverbed is, deep in the valley, like a gorge. It ends in a barrier lake in Erlenbach. From Erlenbach to Latterbach, it is corrected again (Fig. 3.4).

Figure 3.4: Simme: upstream to downstream

The river course of the Kander (Frutigen-Lake of Thun) is characterized by straightening and corrections, which were started 100 years ago (Kander correction) (Mueller, 2009). The section Frutigen to Lattigen bei Spiez is corrected and exhibits a lot of swells. Just shortly above the confluence with the Simme, the course of the river has been left in its natural state (protected landscape). It has a gorge character. Figure 3.5 illustrates the explained situation.

Figure 3.5: Kander: straightening (left) versus protected landscape (right)

The Lütschine is divided into 3 subsections, the Schwarze, the Weisse and the Vereinte Lütschine. The Schwarze Lütschine (Grindelwald-junction) flows in a steep-like region nearly naturally but in the valley plains, the riverbed is restricted by the channelling and the flood controlling dams. In Burglauen, it passes a barrier lake, and afterwards, it flows to Hüslimatte, where the riverbed is deep in the valley. The same schema is observed for the river Weisse Lütschine (Stechelberg-Junction). An exception to that is in the region of Lauterbrunnen: a gorge section with huge stones. Also the Vereinte Lütschine (junction-lake of Brienz) is hardly corrected, apart from the first kilometres belonging to protected area. (Fischerei BE, 2016). The three parts of the river Lütschine are shown in Figure 3.6.

Figure 3.6: Lütschine: Weisse (left), Schwarze (middle) and Vereinte (right)

The rivers Simme, Kander, Lütschine are the major tributaries of the Aare and serve as water supplier. They are classified as montane, huge and middle-steep rivers. The characteristics of the river sections and their watershed are summarized in Table 3.1. Further, length, number of cross section and the average resolution is listed. The number of cross section number and the length depend on the available data. The resolution is ration between the length and the number of cross sections. The idea is to have an overview and to compare the rivers at a glance. The information in the table was collected from the Federal Office for the Environment (FOEN)-hompage (FOEN, 2015b) and the Geomap (Geomap, 2016) homepage.

Characteristics/River section	Hasliaare	Aare	Simme	Kander	Lütschine	weisse Lütschine	schwarze Lütschine
Basic Watershed Characteristics							
Area $[km^2]$	557.9	2962	583.6	1098.6	388.8	165	179.1
average height	2150	1610	1598	1900	2050	2170	2050
run off regime	-	-	n.-glacial - n. de transition	b-glacial- n.	a-glacial n.	b- to a- glacial n.	b- to a- glacial n.
Slope [%]	0.32	0.19	0.98	1.15	0.93	2.46	2.6
Basic river section Characteristics							
Length $[km]$	13	27.48	43.74	16.93	8.66	11.05	12.12
Number of Cross sections	59	180	403	234	89	121	114
Average Resolution [m]	220	115	108	72	97	91	106
Number of large tributary	3	6	4	2	1	4	3
Water exploitation	Yes	No	Yes		Yes	Yes	No
Obstruction/ straightening	high	high	middle	high	high	high	middle
Number of Gauging Station	1	2	3	1	1	1	0

Table 3.1: Hydrological characteristics of the river and basic characteristics of the river sections

3.2 Methodology

The concept of a weak point analysis is to attribute the associate return period of a flood event to each evaluated bank-full discharge and to thereby discover the weak points of a river. A weak point in this study is defined as following:
The evaluated channel capacity (bank-full discharge) of a cross section is associated with return period below 100 years, i.e. with a high frequency of occurrence. For this purpose, the results of the two specific objectives have to be combined to reach the third one. The methodology section is subdivided into two parts according to the first two objective, formulated in section 3.1.2. The flood estimation is based on the extrapolation or interpolation of data of RGS along the rivers. The bank-full discharge will be evaluated by 1D simulations in Basement (section 1.3). The analysis is done for every measured cross section, and for each river section, the same methodological procedure is applied. The software for the analysis include Basement, Arc Gis and R. The epistemic quality of the procedure is limited by many compromises. The representation of the rivers depend on the number of cross section which were measured during the campaigns. The output is valid for the year at the places where the measurement campaign was conducted. Table 3.1 shows the different numbers of cross sections and the related resolution for each river. For high quality modelling, it is recommended to keep the distance of the measured cross section below 100 m (WMO, 2013). In this study, the distance varies from cross section to cross section, but the average distance is mostly around 100 m with one exception (Hasliaare with 220 m). Table 3.2 depicts the year of measurement.

3.2.1 Data

The data can be grouped according to its purpose. First, basic data is used to establish the different overview maps. Secondly, the simulation in Basement requires certain input data, and at last, data is needed to extrapolate the flood values. Table 3.2 summarizes the grouping of the data. The first group is called geodata, the second hydraulic data (mainly geometry data), and the third group refers to the hydrology data.

Data Set	Source	Resolution	Date	Comment
Geodata				
Orthofotos (SWISSIMAGE 25)	Swisstopo (2016)	25 m	-	map and visual estimation of channel boundary
Digital elevation model(DEM25)	Swisstopo (2016)	25 m	-	basis for catchment size calculation
country map (LK25)	Swisstopo (2016)	1:25000 m	-	for maps
Stream network (Vector25)	Swisstopo (2016)	1:25000 m	2008	for map and comparison
Geometric basics				
QPlines	FOEN	-	1953-2011	compiled by A. Zischg, shape file of the cross section
QPpoints	FOEN	-	1953-2011	compiled by A. Zischg, shape file of all points along cross sections
QPFlowline	FOEN	-	1953-2011	compiled by A. Zischg, shape file of the flow line of the rivers
Hydrological data				
Discharge data	FOEN	0.1 m^3/s	2014	RGS along the river sections
Stage-discharge relation	FOEN	0.1 m^3/s	2014	RGS along the river sections
HQ_x Data	FOEN	0.1 m^3/s	2014	based on the discharge data and conducted extreme value statistics

Table 3.2: Data source, Resolution and date for the maps, the simulation in Basement and the flood assessment

The geometric data of the cross section specific to a river are integrated in the three mentioned datasets (QPlines, QPpoints and QPFlowline). The profiles geometric data were measured by the FOEN, section risk prevention. Andreas Zischg proceeded the division into these three files and completed the data. The QP_lines involves the information about the length of the cross section, the coordinates of the right and left end, the orientation angle and the distance between the cross sections. The QP_point contains information about each point in the cross section, namely the x-,y- and z coordinate and the kst-coefficients. The mentioned variables of the two datasets were used for the analysis.

3.2.2 Flood Assessment

As mentioned in section 3.1.1, there is no established single method of how to estimate a flood with a certain return period. The appropriate approach always depends on the data situation, the survey sites and the purposed aim. In order to reach the objectives of this study, a method, which is applicable on every river section and allows for comparison between them is developed. The encountered conditions, such as the size of study area and the number of RGS, suggest that the method should be applied on a large scale, should rather be simple to apply and should no heavily depending on expert knowledge.
Accordingly, the idea of the flood assessment in this study is to use the information of floods of a certain return period of the nine RGS situated along the studied river sections and to extrapolate or interpolate the information over the catchment size of each cross section along one river to determine a HQ_{10}, HQ_{30}, HQ_{50}, HQ_{100} and HQ_{300} for each cross section. The approach is a statistical approach and integrates only information about the catchment size. Other possible approaches are to use the program HQx_meso_CH, which is based on regionalization methods or the PREVAHregHQ tool, which is predicted on hydrological model data. Following the first approach, the problem is that the catchment size boundary is limited to 200-500 km^2 for a reliable result, which is too low for the study sites of interest

here. The later is based on modelled data. Here, there are inaccuracies due to the modelling process, and the lapse of time of the input data is only 20 years (Viviroli and Weingartner, 2012). Thereby an extrapolation of a HQ_{100} is not reasonably feasible. However, those two methods will serve as a reference for the result, meaning as a comparison.
The attribution of cross sections with a flood of a certain return period can be subdivided into different steps. This will be outlined in the next three sections.

3.2.2.1 Catchment Size

The determination of the size of the catchments is the basis for the extrapolation. The calculations were implemented in the ArcHydro tool in ArcGis. The necessary input data is provided by the digital elevation model (DEM) and the coordinates of one point at each cross section. First, the tools of ArcHydro are used to correct the DEM, and and in a second step, the watershed can be drained according to the height information in space with the remaining six tools of the Terrain processing. Finally, one obtains a watershed which comprises every stream and their catchments.

1) Terrain Processing
   - Fill in the DEM: The program was not able to correctly represent the boundary of the Aare Watershed. Therefore, the produced DEM was clipped with the watershed of the Aare, which is an open source data set of the 'Gewaesserinformationssystem der Schweiz (GEWISS)' (FOEN, 2015a) to end up with the correct drained watershed.
   - Flow Direction
   - Flow Accumulation
   - Stream Segmentation
   - Catchment grid Delination
   - Catchment Polygon Processing
   - Drainage line Processing
   - Adjoint Catchment Processing

   Based on the the Terrain Processing and the determined drainage point the watershed specific for the cross section was calculated.

2) Drainage Point
   - Batch point: A shape file was created with point features that can be used as input. The batch point were generated based on the cross section. The left point coordinates were taken for all of the cross sections.

3) Watershed Processing
   - Batch Watershed delineation: The watershed calculation is based on the batch point. At some point, the batch points were too far away from the flow line (drainage line processing), and corrections by hand had to be introduced in order

to calculated the correct watershed. If a calculation of the catchment size based on this point was still not possible, an interpolation between the catchment size of the one above and the one below was conducted.

Figure 3.7 shows the calculated watersheds and the batch point for the Lütschine.

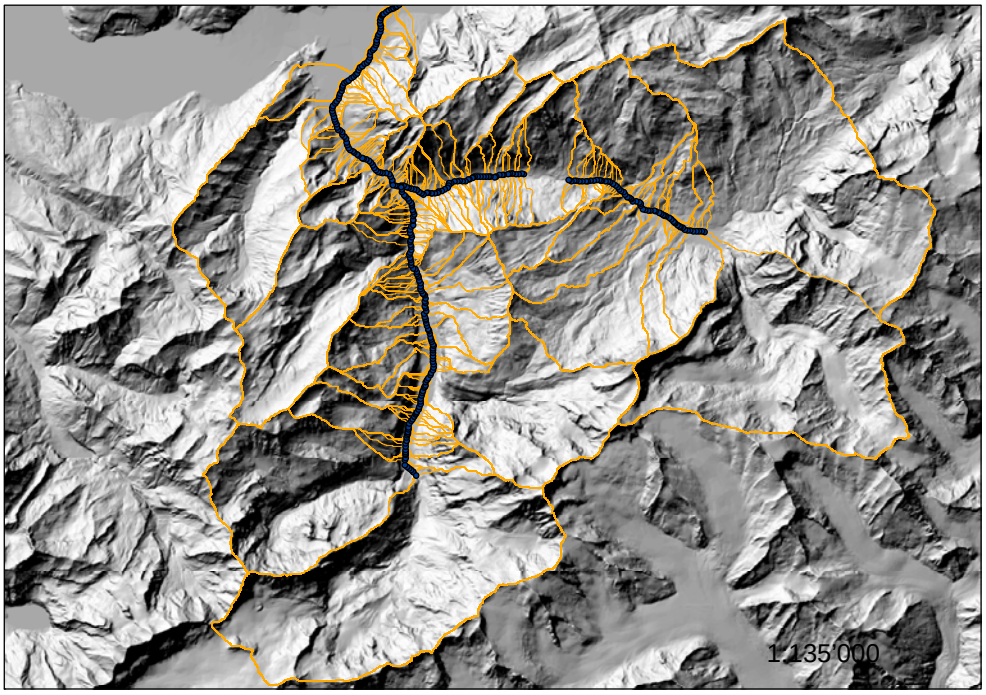

Figure 3.7: Processed Watersheds for the batch points of the each cross sections along the Lütschine

3.2.2.2 Calculation of the HQ_x along the Rivers

The attribution of the flood event with return periods of 10, 30, 50, 100 and 300 years is based on the data of the nine RGS along the studied river sections and on the calculated catchment size for each cross section. No analysis of the quality of the RGS data was made, i.e. all data was used and was processed the same way. The HQ_{10}, HQ_{30}, HQ_{50}, HQ_{100} and HQ_{300} at the cross section of the RGS were calculated based on extreme value statistics and are provided by the FOEN, as mentioned. During the evaluation of the HQ_x, two different cases were possible depending on the number of available RGS along a river section. If only one RGS was available, an extrapolation was conducted, the discharge rate (proportion between the discharge and the catchment size) at this location was calculated and the result was multiplied with the catchment sizes of all other cross sections along this river section. This

procedure was applied to the river sections Kander, Weisse Lütschine, Vereinte Lütschine and Hasliaare (compare section 3.2.1 in table 3.2). In the case of multiple RGS for a river section an interpolation based on the following equation was conducted:

$$\frac{HQup}{HQd} = (\frac{Aup}{Ad})^{y(t)}$$

$$\begin{aligned} \text{with } HQup &= \text{flood discharge RGS upstream } [m^3/s] \\ HQd &= \text{flood discharge RGS downstream } [m^3/s] \\ Aup &= \text{catchmentsize RGS upstream } [km^2] \\ Ad &= \text{catchmentsize RGS downstream } [km^2] \\ y(t) &= \text{exponent depending on the return period} \end{aligned} \tag{3.1}$$

(Walther et al., 2012)

Formula 3.1 has to be reformulated for the exponent y(t). It establish a relationship between the fraction of the discharge up- and downstream and the fraction of the catchment size up- and downstream. In a second step equation 3.1 has to be reformulated to assess the discharge value, while all the other parameters are known. This is calculated for a discharge of 10, 30, 50, 100 and 300 annual return period. This procedure was applied for the Simme, where three RGS are available and to the Aare Bern-Thun with two RGS (section 3.2.1, Tab.3.2). For the river Simme, it was not possible to do an interpolation over the three stations since in Erlenbach, there is a barrier lake. There, an interpolation was calculated between the upper two RGS, and these values were extrapolated further downstream to the barrier lake. Downriver of the barrier lake, the values were extrapolated in upstream direction from the third RGS in Latterbach. The river section of the Schwarze Lütschine is an exception here, as no RGS data exists. This lack of data was compensated extrapolating the data of the RGS along the Vereinte Lütschine further upstream.
In order to simplify terminology, the used approach will be referred to as 'extrapolation method' and the HQ_x for all cross section as 'extrapolated values'. But one should keep in mind the here mentioned specifications.

3.2.2.3 Plausibility

HQx_meso_CH tool

For catchments without measurement stations, methods of regional transfer were used for the determination of floods. The purpose of the HQx_meso_CH software is to provide a tool, which does estimations of floods with a certain return period of one catchment, relying on different methods by doing so. The different procedures are based on the rational equation, envelope or simple conceptual models (Wehren, 2010). The basic idea of regional transformation is to mathematically formulate the variability of hydrological variables in space. It aims to estimate the discharge without discharge measurement. The derivation of the formula is based on catchments with discharge measurements (Spreafico et al., 2003). The methods that here used were Momente, Giub'96, Kölla, BaD7. Those methods will not be explained in detail here (more information can be found in the Manual of Barben (2001)). The output variables of the tool are the HQ_{100} for the methods Momenta, Giub'96, Kölla and

BaD7. Additionally, for BaD7 and Momenta, the HQ_{30} can be estimated. For estimations of HQ_{300} the approach is based on a study of Dobmann (2009). She proposed to multiply the HQ_{100} with a factor of 1.3, which was here applied.
The necessary input data for the program are the respective sizes of the catchments. For this, the generated catchment shape file was used. The necessary files were compiled with the R-code of Schwanbeck (2016). It is important to emphasize that only a few points that are reference points (catchments) along the rivers were used to do the comparison with this tool. The selection is based on significant changes in the discharge value due to inflowing water of a tributary.
The developer of the HQx_meso_CH tool Barben (2001) recommends to analyse all the outputs, to delete very implausible values, and then to take the mean value, while the highest and lowest value can be seen as the lower and upper confidence boundary (Spreafico et al., 2003). The results can be considered plausible if the five estimations are close to each other and all are lower than the estimated value of the estimated maximal discharge. As mentioned, this tool is restricted to meso scale catchment, that is, to a size of 200/500 km^2. For this reason, it is only used as a reference, because most catchments in this study are larger.

PREVAH_regHQ

The concept of PREVAH_regHQ is based on the PREVAH model. It is a deterministic, conceptual and process oriented hydrological model and it simulates continuous discharge hydrographs for the time period of 1984-2003 (20 years). Those discharges are evaluated statistically in terms of the flood events. The estimation is based on meso scale catchments in the Rhein region. The estimation of the parameter is mostly based on regionalization because most of the catchments have no RGS. PREVAH stands for the name of the model, while "reg" stands for regionalization and "HQ" for floods (Viviroli and Weingartner, 2012). The simulation output and the flood statistics for the whole country are based on the 'Basiseinzugsgebiete' of the HADES. Only a few comparison sites could be chosen because they had to fit to the perimeter of the study site.

3.2.3 Determination of the Bank-full Discharge

The bank-full discharge is equal to the discharge when the water flow is at bank-full and overflows the active flood plain (Fig. 3.8)

The assignment of the bank-full discharges is describable by four common approaches, either by means of a rating curve, by hydraulic geometry, by flow recurrence frequencies or by flow equation such as the MSE. The method of the flow equation is the only approach, which can be used for cross sections without a RGS (Wiliams, 1978). Therefore, the chosen approach for this study was the MSE. The purpose is not to solve the equation for every cross section individually, but rather to run a simulation in Basement and to simulate the whole river section at the time. The advantage of using Basement instead of calculating the capacity of the channel for each cross section individually is that potential backwater effects can be considered. Additionally, it is possible to consider more than one M-coefficient and to calibrate the model. For the 1D simulation as opposed to the 2D simulation, the water is kept in the system and do not overflow. Therefore the channel capacity of each cross section

can be evaluated individually. This better fits with the aims of that study. Further, it could be applied to a larger region because of a lower computational time, which is also in a better accordance with the aim of this study. According to Rousselot, Vetsch, and Faeh (2012) the 1D simulation are adequate to large scale streams and limited level of detail. Therefore, the 1D model was chosen.

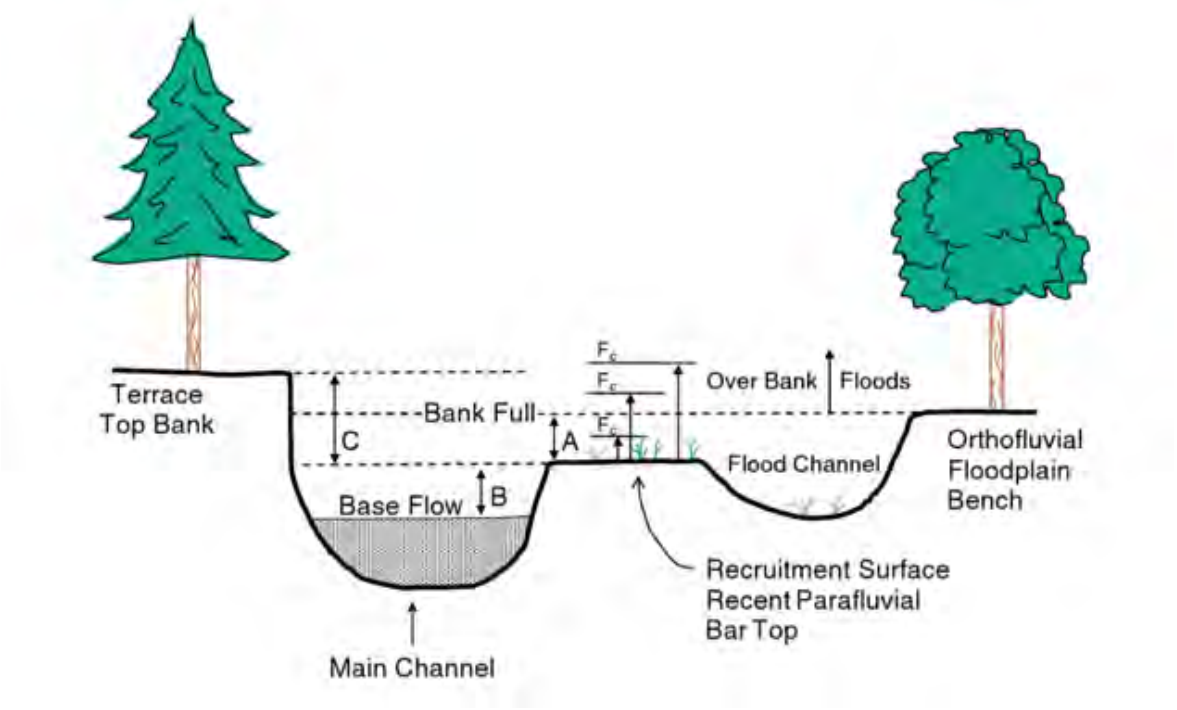

Figure 3.8: Definition of bank-full discharge (Hauer and Lamberti, 2006)

3.2.3.1 Pre-Processing

According to section 1.3.2, the geometry file, the boundary conditions and the initial condition have to be set in order to run the operational command file. The missing input for the geometry file, the active range of the channel, namely the boundary of the channel or bank-full height had to be determined. In this study the active range is defined as the highest point along the bank left side and right side (Fig. 3.8). The determination of the bank-full height was done manually for every cross section. The R code of Mosimann (2015b) was used to manually determine the bank-full height. The disadvantage of a that manual procedure is that for every cross section, the same question is open to judgement: where does the riverbed with bank end? It is an important decision because it determines the bank-full height and consequently the bank-full discharge.
For the definition of the boundary conditions, the type and slope at the boundaries had to be fixed. The boundary condition type was the same for every river section. Upstream, the input is a steady state inflow (hydrograph), and downstream it is a hq-relation (section 1.3.2.1). The slope at the upstream boundary is calculated based on the first and second profile, and the downstream boundary is defined based on the lowest and second lowest profile.

Regarding initial condition, the conclusion was to use a continuous inflow and not dry condition as in the case of the case study in Kenya. An R-code was written to constantly increase the inflow according to the increasing input discharge. The constant base flow is in that case constantly 2 m^2/s lower than the steady state input discharge.
The output file of interest, is the one which directly for every run indicates the water level for every cross section. Because it can be used directly in the R-code to evaluate the bank-full discharge.

3.2.3.2 Calibration

The discharge in the model is calculate with the help of the SME, while the kst-coefficients have to be set and optimized, as mentioned in section 1.3.2.2. As a first estimate kst-coefficients are evaluated during a field survey. However, this first estimate may not lead to the targeted results. Therefore, the kst-coefficients have to be calibrated based on known stage-discharge relation. The kst-coefficient is changed until the water level output reaches the water level associated with input discharge (Rousselot, Vetsch, and Faeh, 2012). The kst-coefficient can be calibrated at every cross section of a RGS. The simulation runs over the whole river section and the kst-coefficient is changed in every cross section for every run. The kst-coefficient depends, amongst other factors, on the magnitude of the discharge. The interest of this study is the channel capacity. Therefore, the input discharge should be as high as the calibrating cross section bank-full height allows for. Two kst-coefficients were fitted, one for the channel bed and one for the bank. The two kst-coefficients were changed iteratively and all reasonable combinations were plotted against each other in order to compare them with the FOEN stage-discharge relation. A reasonable kst-coefficient combination was defined as: the simulated water level does not deviate more than +/-5 cm of the anticipated FOEN water level. Figure 3.9 shows the calibration of the Zweilütschine site along the Weisse Lütschine. The grey and the blue lines indicate the simulated stage-discharge relation for a reasonable kst-coefficient combination. The black line is the FOEN target curve. All three lines reach the anticipated water level of 572.8 m.a.s.l associated with the discharge of 250 m^3/s, but the course of the curves below and above is not the same. The determination of the kst-coefficients is based on the kst-coefficient pair curve in those plots, which fits best for a longer part the FOEN curve in region of high discharge.
As mentioned, the calibration includes all cross sections of one studied river section and not only on a few cross sections, nearby the RGS. The reason for this is that the resulting kst-coefficients heavily depend on the number of cross sections. If more than one RGS stage-discharge relation of a river is available, the river section is divided into parts according to the hydraulic conditions.

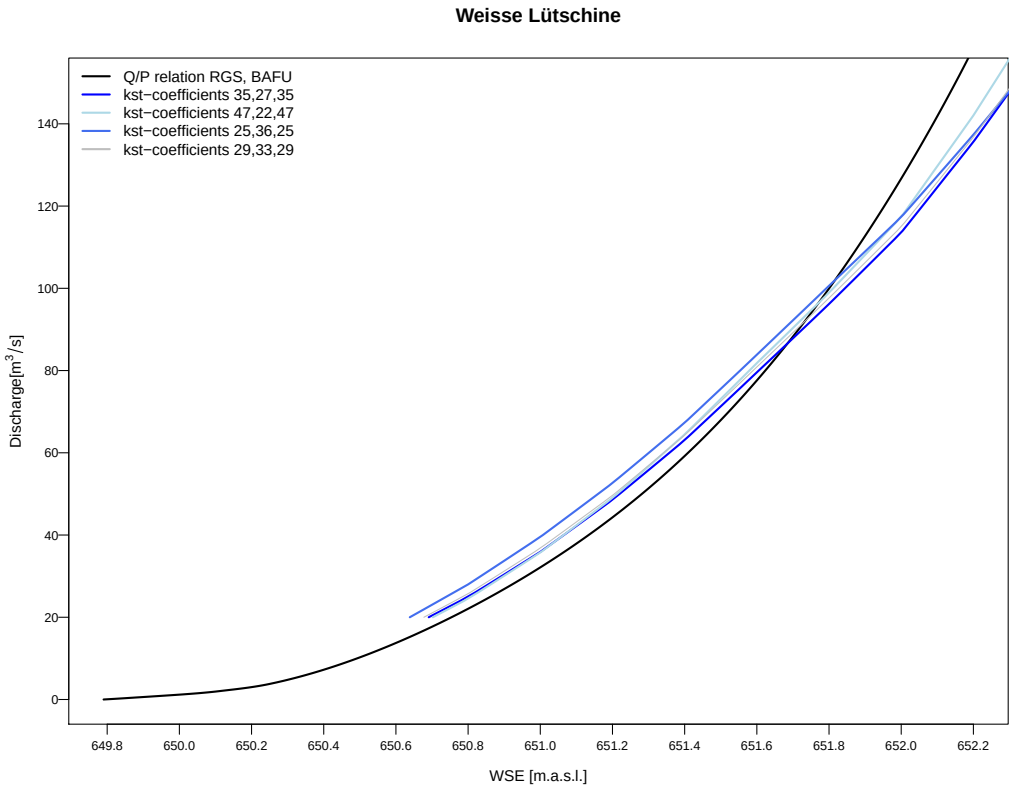

Figure 3.9: Comparison of the FOEN stage-discharge relation with the simulated stage-discharge relation based on the calibrated kst-coefficients

3.2.3.3 Simulations and Determination of the Bank-full Discharge

The bank-full discharge was identified with written R-code. It automates the simulations for a number of defined runs and increases the input discharge about 2 m^3/s for every run. The simulated water level and the input discharge are collected in a table for every run. In a second step, the left dam height and the right dam height (active range) were compared with all the simulated water levels. If there was a match, the corresponding discharge was taken as the channel capacity. The output was written in a table including the cross sections and the evaluated parameters: the bank-full discharge, the related water level and the related bank side of overflow.

3.2.3.4 Plausibility

A validation of running a scenario with the chosen parameters and comparing it with the high flood marks is beyond the scope of this study. However, the plausibility of the calculated values was evaluated. All rivers sections were visited by bike to judge the plausibility of the evaluate weak points and the calibrated kst-coefficients and, if necessary, slightly adjusted in the model.

3.3 Results

In this section, the results of the weak point analysis are presented. The results follow the structure of the three topics reviewed 3.1.2: Estimation of HQ_{30} to HQ_{300}, calculation of bank-full discharge, and identification of the weak points. The identified weak points results from a combination of the two first results. The exact values corresponding to the graphical values can be viewed in the tables of Appendix B for each river section.

3.3.1 Floods with Return Periods of 10, 30, 50, 100 and 300 Years

For each river section the estimated floods with return periods of 10, 30, 50, 100 and 300 are specified in a figure (Fig. 3.10 until 3.16), each including four different plots. The plot (a) gives an overview of the HQ_{10}, HQ_{30}, HQ_{50}, HQ_{100} and HQ_{300} along the river section based on each cross section. The plots (b), (c) and (d) separately depict the HQ_{30}, HQ_{100} and HQ_{300} and their confidence band at the respective RGS with additional information. These include the HQx_meso_CH estimation for the evaluated reference points, and, if available the output of the PREVAH_regHQ model. Besides these figures, the Tables 3.3 to 3.8 enable the comparison of the evaluated HQ_{30}, HQ_{100}, HQ_{300} of the reference methods with the applied method at the reference points. The values of the reference method are relative to the extrapolated values. The study sites can be compared because reference points were calculated relative to the extrapolated values. The reference points are set at the site of the RGS and next to the tributary inflow. The number of reference points is different from river section to river section. It depend on the number of larger tributaries. For the attribution of the calculated bank-full discharge with a flood recurrence period, only the results of plot (a) in Figure 3.10 until 3.16 are considered.

3.3.1.1 Hasliaare

The extrapolated values in Figure 3.10 (a) are based on the evaluated HQ_{10} ,HQ_{30}, HQ_{50}, HQ_{100} and HQ_{300} at the RGS Brienzwiler. Based on the location of the Brienzwiler RGS, the value had to be extrapolated mainly in upstream direction. The HQ_{10} ,HQ_{30}, HQ_{50}, HQ_{100} and HQ_{300} along the Hasliaare section increased slightly and constantly over the 13 km as Figure 3.10 (a) shows. The increase in comparison with the other river sections was rather small due to the small increase in the catchment size (Tab.3.3). The sudden leaps in the extrapolated lines can be backtracked to tributary inflow. From upstream to downstream, these are the Geissholzlowenen combined with the Alpbach and the Milibach, and further downstream, the Reichenbachfall with the largest increase, and the Hüslibach. These locations and the RGS correspond to the reference points. It is noteworthy that for the HQ_{30}, HQ_{100} and HQ_{300} at the RGS, the magnitude of the confidence band was large (200 m^3/s).
The estimation of the HQ_{30} with the Momenta and BaD7 method were both well above the extrapolated values, and the difference decreased with increasing distance (Fig. 3.10 (a)). For the reference point 1, the BaD7 value is 1.98 times higher compared to the extrapolated value and for the reference point 4, it is only 1.37 units higher (Tab. 3.3).
The results of the HQ_{100} showed an even larger spread. Again, the BaD7 method produced large values in the same range as for HQ_{30} (Tab. 3.3), and low values were obtained with

the Kölla Method. The lowest values exhibit with Kölla was only 0.37 for reference point 1 and 0.41 for reference point 4. The extrapolated values amounted to 442 m^3/s and 542 m^3/s. The mean values (Fig. 3.10 (b)-(d)) are in the range of 0.78 to 0.92 and thereby slightly below the extrapolated values (Tab. 3.3).
The pattern for the HQ_{300} was similar, but the range of the estimated values was smaller (Tab. 3.3). The Kölla method differed more importantly from the others and the Momenta method values changed from a positive relative deviation to an negative relative deviation when comparing the extrapolated values of the HQ_{100} to the HQ_{300} values.
In the case of PREVAHreg_HQ, an estimation fitted to the study site (reference point 3), the values were lower compared to the mean of the other reference estimates for each HQ_x. The difference increased with an increasing return period.
In summary, the range of the HQ_{30}, HQ_{100} and HQ_{300} estimations for the Hasliaare covers a broad range, but the extrapolated points were more or less in the middle of the different estimates and the mean values of the HQx_meso_CH method only differed slightly from the extrapolated values. They are in the range of 0.76 to 0.99 relative to the extrapolated values (Tab. 3.3). The HQ discharge along the river increased only slightly.

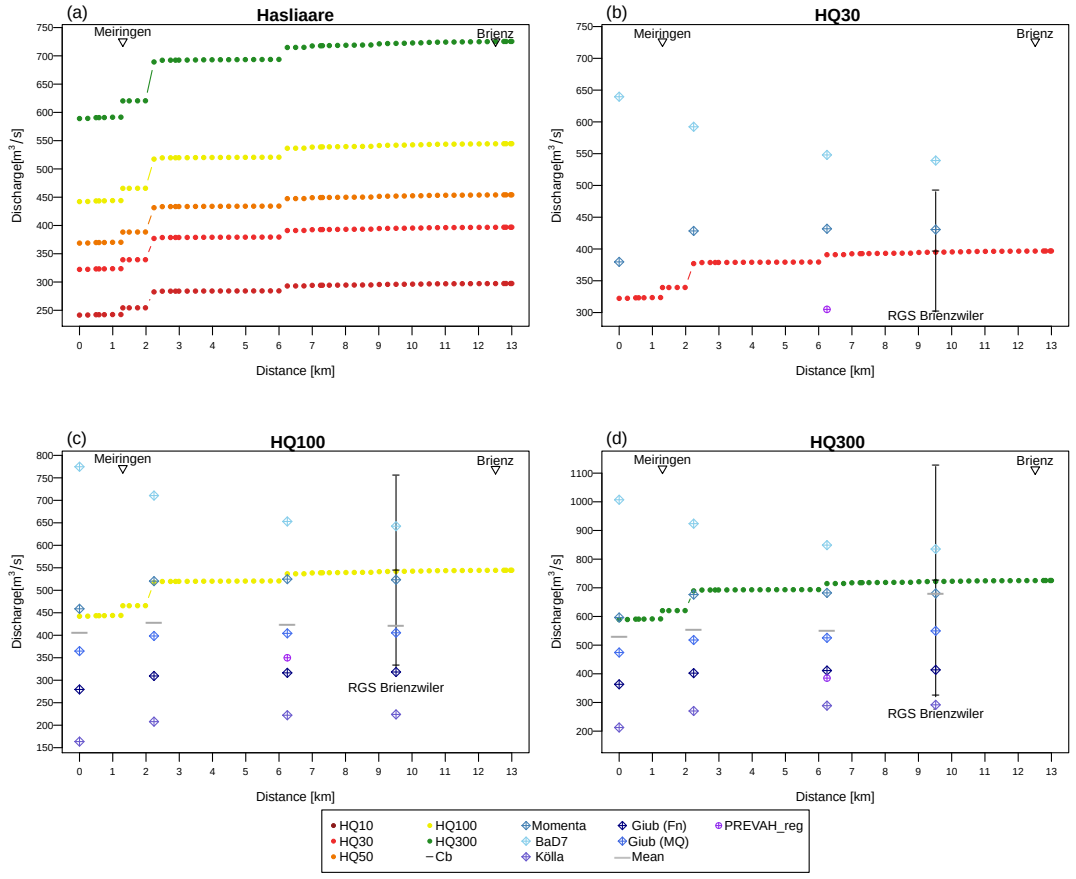

Figure 3.10: HQ_x extrapolation for the Hasliaare based on every single cross section with the estimations of the HQx_meso_CH and PREVAH_regHQ: (a) HQ_{10}, HQ_{30}, HQ_{50}, HQ_{100} and HQ_{300}, (b) HQ_{30}, (c) HQ_{100} and (d) HQ_{300}. River distance measured from Meiringen to Lake Brienz.

		Reference 1	Reference 2	Reference 3	Reference 4
	Catchment size (km^2)	453	530	549.6	555.2
HQ30	Extrapolation (m^3/s)	322.3	377.04	391.04	395
	Momenta	1.18	1.14	1.1	1.09
	BaD7	1.98	1.57	1.4	1.37
	PREVAH	-	-	0.78	-
HQ100	Extrapolation (E)	442.24	517.36	536.57	542
	Momenta	1.04	1.01	0.98	0.97
	BaD7	1.75	1.37	1.22	1.19
	Kölla	0.37	0.4	0.41	0.41
	Giub (Fn)	0.63	0.6	0.59	0.59
	Giub (MQ)	0.82	0.77	0.75	0.75
	Mean -	0.92	0.83	0.79	0.78
	PREVAH	-	-	0.65	-
HQ300	Extrapolation (m^3/s)	589	689.7	714.8	722
	Momenta	0.87	0.95	0.94	0.99
	BaD7	1.46	1.29	1.18	1.21
	Kölla	0.31	0.38	0.4	0.42
	Giub (Fn)	0.53	0.56	0.57	0.6
	Giub (MQ)	0.69	0.72	0.73	0.8
	Mean	0.77	0.78	0.76	0.99
	PREVAH	-	-	0.53	-

Table 3.3: Comparison of the HQx_meso_CH methods and the PREVAH_regHQ the extrapolated values for the HQ_{30}, HQ_{100} and HQ_{300} for the 4 reference points along the Hasliaare. The values of the comparisons are relative to the extrapolation. The catchment size and the extrapolated values are in absolute values

3.3.1.2 Aare Thun-Bern

For the river Aare, data of two RGS were available, and an interpolation between the RGS was possible. The confidence band seemed to be narrower for the different HQ_x and at the two RGS compared to the Hasliaare. The HQ_{10} ,HQ_{30}, HQ_{50}, HQ_{100} and HQ_{300} along the river is again only slightly increasing, and the influence of the tributaries from upstream to downstream (Zulg, Amletebach, Rotach, Kiesen, Giesen and Gürbe) were nicely visible. From the tributaries, the Gürbe has the largest catchment and consequently the highest impact (Fig. 3.11 (a)).
The river section Aare Thun-Bern is a special case, because it was not possible to proceed the reference approaches. First, the catchment size is high above the threshold for the other methods and secondly, the water flows through two lakes before flowing trough the Aare. There, the water flow is interrupted.
The evaluated HQ_{30}, HQ_{100} and HQ_{300} for Thun are 425 m^3/s, 471 m^3/s and 511 m^3/s and for Bern 492 m^3/s, 545 m^3/s and 590 m^3/s.

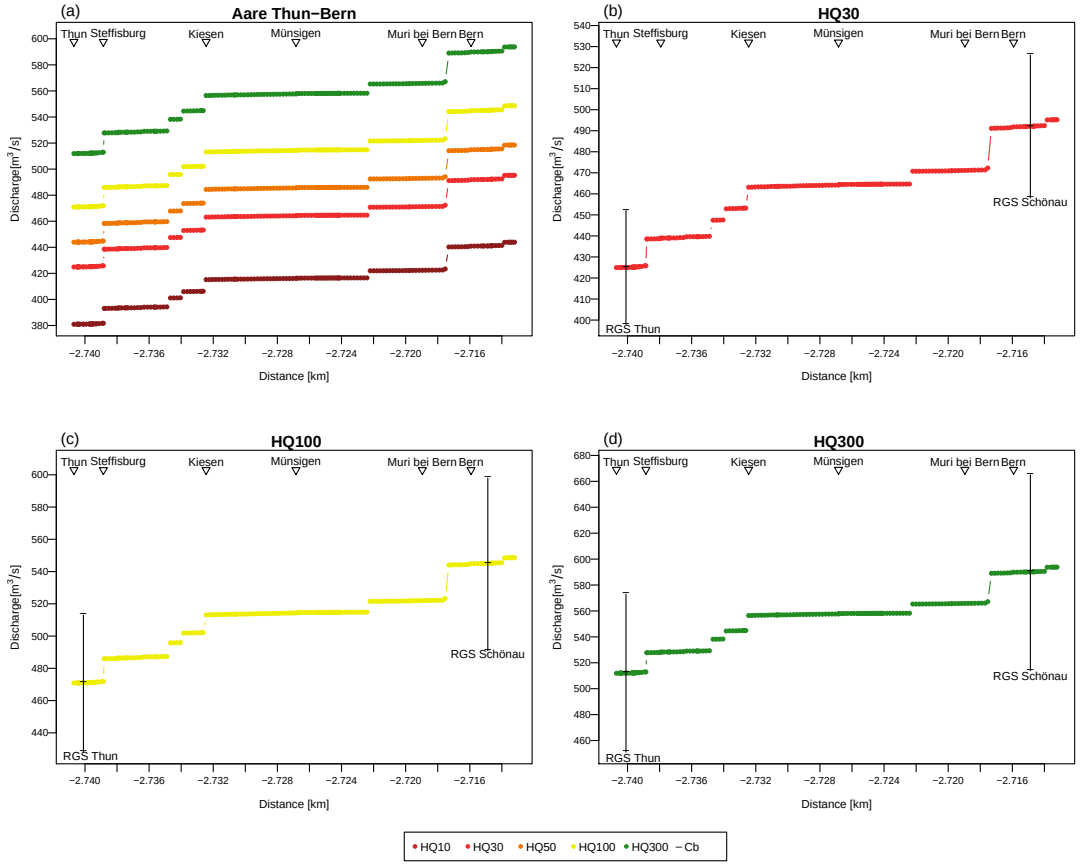

Figure 3.11: HQ_x extrapolation for the Aare Thun-Bern based on every single cross section: (a) HQ_{10}, HQ_{30}, HQ_{50}, HQ_{100} and HQ_{300}, (b) HQ_{30}, (c) HQ_{100} and (d) HQ_{300}

3.3.1.3 Simme

Again, the extrapolated lines showed a constant increase with sudden leaps that could be explained by the influence of the various tributaries (Fig. 3.12a). The main tributary from upstream to downstream are: Wallbach and Sitebach, Zelgbach and Cheeselbach, kleine Simme, Ruersgraben, Schwandgraben and Chrachigraben, Wuestbach, Buuschebach and Eygrabe, Steinibach and Chirel. The Chirel, the last tributary inflow, has the largest influence, pointing to its large catchment size. The reference point 1 is the RGS Oberried (Fig. 3.12), since the data of the RGS was used. The estimation with HQx_meso_CH were also calculated for this location even though no cross section data was available.
Figure 3.12 (a) illustrate the differences between the extrapolated values and the values of BaD7 and Momenta at the reference points (1-12) for HQ_{30}. For the reference points 1 to 3, the difference between BaD7 and Momenta as compared to the extrapolated values was small, and the extrapolated values are larger (Tab. 3.4). But for the next reference point, the magnitude of values scatters more strongly, especially in case of the BaD7, the values are 1.5 to 2.06 times higher than the extrapolated values.
The HQ_{100} shows a similar pattern for BaD7 (Fig. 3.12 (c) and Tab. 3.4). It is noteworthy that

for the course of the Kölla estimations for reference points 1 to 10, the estimations were above the extrapolated value, and afterwards, they were below (first, 1.11 to 1.54 times higher, and then 0.74 to 0.99 of the extrapolated values). The values of the three other methods, Giub (Fn), Giub (MQ) and Momenta were in the range of 0.74 to 1.34 relative to the extrapolated values for all the reference points. The mean values (including all methods) were larger than the extrapolated values (in the range of 0.92 to 1.43 relative to the extrapolated values for all the reference points).
For the HQ_{300}, the range of HQx_meso_CH method values was the largest, and the values were mostly higher than the extrapolated values (Tab. 3.4). The pattern of the estimations was similar to the HQ_{100}. The mean values were a factor of 1.21 to 1.59 higher than the extrapolated values (Fig. 3.12 (d)). Interestingly, the HQx_meso_CH estimates for HQ_{100} and HQ_{300} were lower at reference point 9 than at reference point 8, but exception doesn't count for the mean values of the methods.
The PREVAH_regHQ values at the reference points 2, 3 and 4 showed the same pattern for HQ_{30}, HQ_{100} and HQ_{300}, where the values were lower compared to the extrapolated values. For the points 7 and 11 the values are above: higher increase of the discharge between Zweisimmen and Latterbach compared than in extrapolated values. In general, the estimation at the RGS sites were not always lying in the range of the confidence band.
Overall, the values of the methods of HQx_meso_CH were higher than the extrapolated values. The extrapolated values were in the range of the reference methods. The mean values for the reference points 1 to 3 were very close to the extrapolated values.

		R 1	**R 2**	**R 3**	**R 4**	**R 5**	**R 6**	**R 7**	**R 8**	**R 9**	**R 10**	**R 11**	**R 12**
	Catchment size (km^2)	34.81	90.1	156.8	240.7	310.2	324.5	343.2	380.7	390.5	401.3	562.9	579.2
HQ30	Extrapolation (m^3/s)	31	82.26	105.21	127.28	142.46	145.33	149	156.01	157.79	159.72	250	257.26
	Momenta	0.77	0.65	0.87	1.1	1.27	1.28	1.31	1.36	1.38	1.68	1.14	1.13
	BaD7	0.93	0.62	0.88	1.53	2.04	2.11	2.18	2.14	2.17	2.6	1.83	1.81
	PREVAH	-	0.55	0.67	0.64	-	-	1.14	-	-	1.44	-	-
HQ100	Extrapolation (m^3/s)	39.3	90.64	121.53	152.49	174.42	178.61	184	194.36	197	199.89	298	306.65
	Momenta	0.74	0.72	0.92	1.12	1.26	1.27	1.29	1.32	1.34	1.11	1.15	1.14
	BaD7	0.88	0.69	0.92	1.52	1.98	2.05	2.11	2.04	2.07	1.75	1.83	1.81
	Kölla	1.11	1.51	1.51	1.54	1.43	1.4	1.35	1.29	1.31	1.31	0.76	0.76
	Giub (Fn)	1.08	0.86	0.91	0.96	0.98	0.99	0.99	1.31	1.01	1.31	0.84	0.83
	Giub (MQ)	1.08	0.82	0.87	0.92	0.96	0.96	0.97	1.21	0.99	1.21	0.84	0.83
	Mean	0.98	0.92	1.03	1.21	1.32	1.33	1.34	1.43	1.34	1.34	1.08	1.07
	PREVAH	-	0.61	0.72	0.69	-	-	1.2	-	-	1.35	-	-
HQ300	Extrapolation (m^3/s)	39.3	96.94	135.86	176.42	205.92	211.63	219	233.26	236.91	240.9	343	352.96
	Momenta	0.96	0.88	1.07	1.26	1.39	1.39	1.41	1.43	1.44	1.2	1.3	1.29
	BaD7	1.14	0.84	1.07	1.71	2.18	2.25	2.3	2.21	2.23	1.89	2.07	2.04
	Kölla	1.45	1.84	1.76	1.73	1.57	1.53	1.48	1.4	1.41	1.42	0.86	0.86
	Giub (Fn)	1.4	1.04	1.06	1.07	1.08	1.08	1.09	1.41	1.09	1.41	0.95	0.94
	Giub (MQ)	1.4	0.99	1.02	1.03	1.06	1.06	1.06	1.31	1.07	1.31	0.95	0.94
	Mean	1.27	1.12	1.2	1.36	1.46	1.46	1.47	1.39	1.45	1.44	1.22	1.21
	PREVAH	-	0.62	0.7	0.67	-	-	1.14	-	-	1.33	-	-

Table 3.4: Comparison of the HQx_meso_CH methods and the PREVAH_regHQ with extrapolated values for the HQ_{30}, HQ_{100} and HQ_{300} for the 13 reference points along the Simme. The values of the comparison are relative to the extrapolation. The catchment size and the extrapolated values are in absolute values

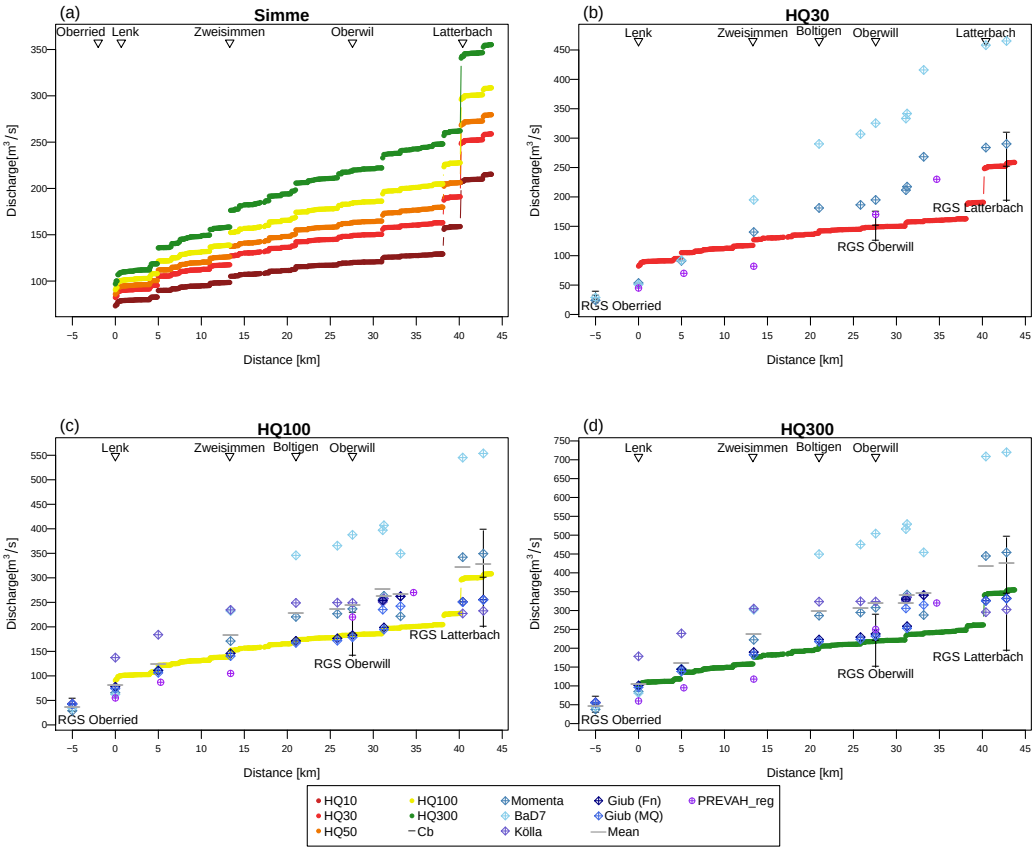

Figure 3.12: HQ_x extrapolation for the Simme based on every single cross section with the estimations of the HQx_meso_CH and PREVAH_regHQ: (a) HQ_{10}, HQ_{30}, HQ_{50}, HQ_{100} and HQ_{300}, (b) HQ_{30}, (c) HQ_{100} and (d) HQ_{300}

3.3.1.4 Kander

For the extrapolation of the HQ_{10}, HQ_{30}, HQ_{50}, HQ_{100} and HQ_{300} values, only the Hondrich data was available. The extrapolation is based on this data in up- and downstream direction. Figure 3.13 (a) illustrates the course of the HQ_{10}, HQ_{30}, HQ_{50}, HQ_{100} along the Kander from Frutigen to Spiez. The rise of the extrapolated line is rather slow. The tributaries which cause the sudden leaps include the Chiene, the Suld and the Simme. The increase due to the Simme is strong. No HQx_meso_CH estimation was reasonably at the junction and below because of the large size at the confluence point of the rivers. Overall, no PREVAH_regHQ calculations could fit this study site.
The estimated HQ_{30} values of the HQx_meso_CH were similar to the extrapolated points and were in the range of the confidence band of the RGS values (Fig. 3.13 (b)). The differences to the extrapolated values were constant along the river. The BaD7 values are around 1.09 times higher than the extrapolated values, and the Momenta values reached around 0.94 of extrapolated value.
The mean values for the estimated HQ_{100} values for each reference point were close to the extrapolated values and always smaller (Fig. 3.13 (b)-(d) and Tab. 3.5). The confidence band

of the RGS included all the estimated values. Especially the Giub (Fn) method exhibited low values.
For the HQ_{300} the pattern of distribution and deviation was similar to the HQ_{100}. Only for the reference point 1 the difference between the extrapolated value and the mean was higher. The confidence band at the RGS has a very large interval.
To sum up, the values for the HQ_{30} are similar for all estimation and for the HQ_{100} and HQ_{300}, the values of the Giub methods are the lowest for the first three reference point compared to the extrapolated values and thereby responsible for the deviation of the mean compared to the extrapolated values.

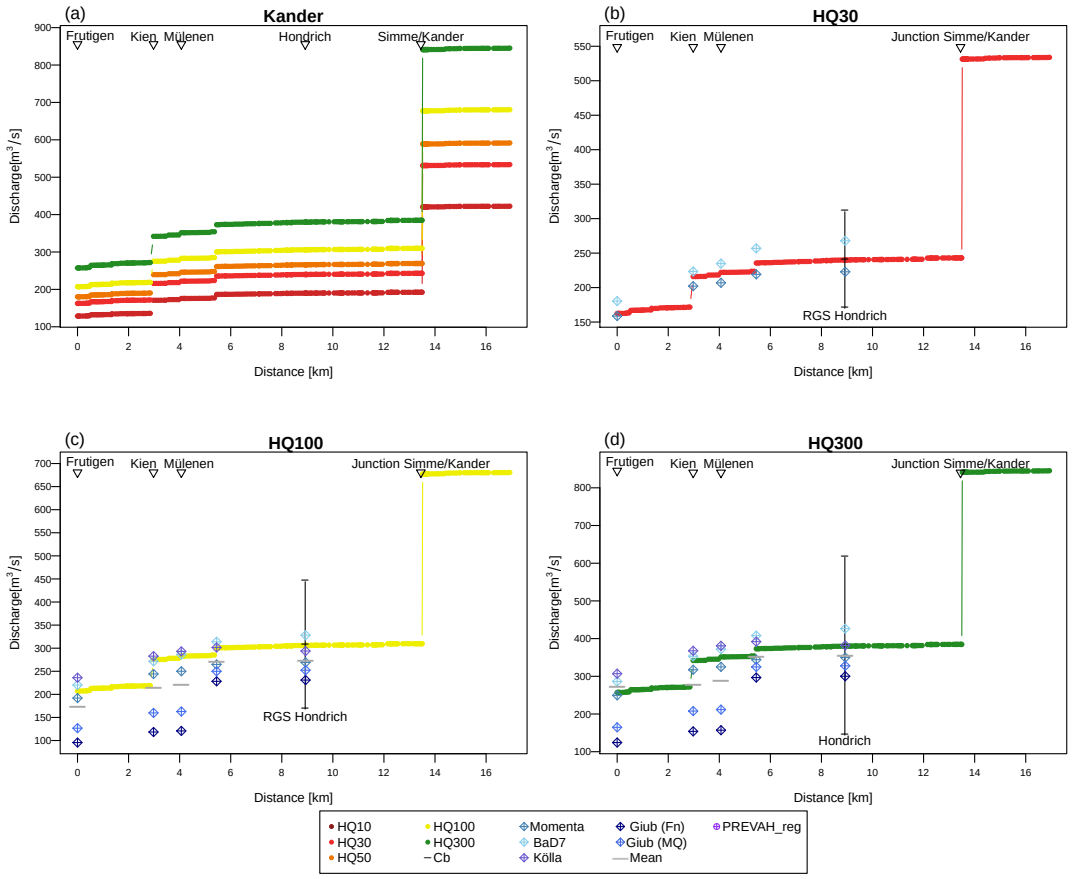

Figure 3.13: HQ_x extrapolation for the Kander based on every single cross section with the estimations of the HQx_meso_CH and PREVAH_regHQ: (a) HQ_{10}, HQ_{30}, HQ_{50}, HQ_{100} and HQ_{300}, (b) HQ_{30}, (c) HQ_{100} and (d) HQ_{300}

		Reference 1	Reference 2	Reference 3	Reference 4	Reference 5
	Catchment size (km^2)	334.2	444.2	456.7	484.7	493.63
HQ30	Extrapolation (m^3/s)	162.51	215.99	222.05	235.65	240
	Momenta	0.98	0.94	0.93	0.93	0.93
	BaD7	1.11	1.03	1.06	1.09	1.12
	PREVAH	-	-	-	-	-
HQ100	Extrapolation (m^3/s)	207.2	275.38	283.12	300.45	306
	Momenta	0.93	0.89	0.88	0.88	0.88
	BaD7	1.06	0.99	1.01	1.04	1.07
	Kölla	1.14	1.03	1.03	1	0.96
	Giub (Fn)	0.46	0.43	0.43	0.76	0.75
	Giub (MQ)	0.61	0.58	0.58	0.83	0.82
	Mean	0.84	0.78	0.79	0.9	0.9
	PREVAH	-	-	-	-	-
HQ300	Extrapolation (m^3/s)	257.3	341.98	351.59	373.11	380
	Momenta	0.97	0.93	0.92	0.92	0.92
	BaD7	1.11	1.03	1.06	1.09	1.12
	Kölla	1.19	1.08	1.08	1.05	1.01
	Giub (Fn)	0.48	0.45	0.45	0.8	0.79
	Giub (MQ)	0.64	0.61	0.6	0.87	0.86
	Mean	1.07	0.82	0.82	0.95	0.94
	PREVAH	-	-	-	-	-

Table 3.5: Comparison of the HQx_meso_CH methods and the PREVAH_regHQ with extrapolated values for the HQ_{30}, HQ_{100} and HQ_{300} for the 5 reference points along the Kander. The values of the comparison are relative to the extrapolation. The catchment size and the extrapolated value are in absolute values

3.3.1.5 Schwarze Lütschine

Along the schwarze Lütschine, no RGS is installed. Therefore, the values were extrapolated based on the RGS situated in Gsteig along the Vereinte Lütschine. The increase of the discharge along the river was larger than for the other rivers (Fig. 3.14 (a)). The main tributaries of the Schwarze Lütschine are the Schwendibach, Fallbach and Chienbach. It is noteworthy that HQ_{30}, HQ_{100} and HQ_{300} largely spread with the method of HQx_meso_CH. All these estimated values were large than the extrapolated ones.
In the case of the HQ_{30} calculated with BaD7 and Momenta, the values reached 2 to 2.23, and 1.95 to 2.39 respectively relative to the extrapolated values for the 4 reference points.
As mentioned, also to the HQ_{100} all the HQx_meso_CH estimations were above the extrapolated values (the mean values were 1.67 to 2.26 times higher, the mean was double of the extrapolated value).
The HQ_{300} estimations indicate the same picture and the difference were even more distinct. Interestingly, the PREVAH_regHQ estimations at reference point 4 for the HQ_{30}, HQ_{100} and HQ_{300} were higher compared to the extrapolated values.
Overall, the difference between the extrapolated values and the estimation of the reference method is the largest for the Schwarze Lütschine compared with the other rivers. The extrapolated values are even smaller than the PREVAH_regHQ estimations.

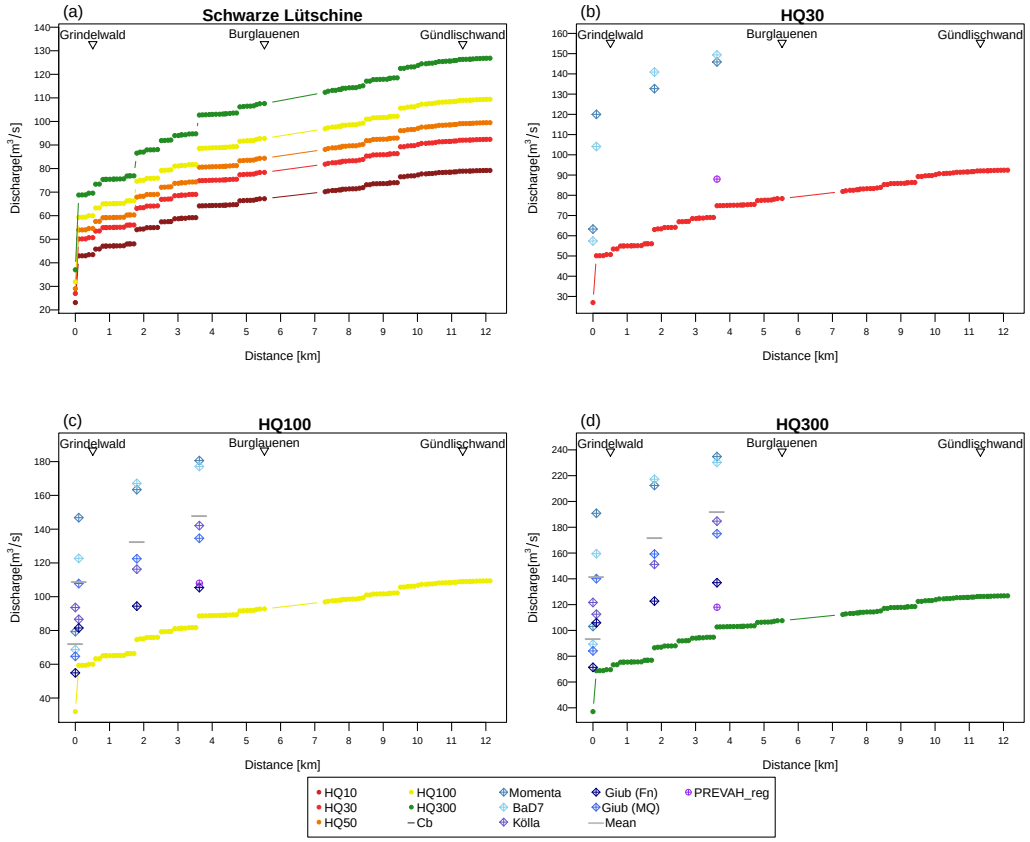

Figure 3.14: HQ_x extrapolation for the Schwarze Lütschine based on every single cross section with the estimations of the HQx_meso_CH and PREVAH_regHQ: (a) HQ_{10}, HQ_{30}, HQ_{50}, HQ_{100} and HQ_{300}, (b) HQ_{30}, (c) HQ_{100} and (d) HQ_{300}

		Reference 1	Reference 2	Reference 3	Reference 4
	Catchment size (km^2)	52.29	97.1	122.2	145.02
HQ30	Extrapolation (m^3/s)	26.98	50.11	63.06	74.84
	Momenta	2.35	2.39	2.1	1.95
	BaD7	2.13	2.08	2.23	2
	PREVAH	-	-	-	1.18
HQ100	Extrapolation (m^3/s)	31.94	59.31	74.64	88.58
	Momenta	2.48	2.48	2.19	2.04
	BaD7	2.15	2.07	2.24	2
	Kölla	2.93	1.46	1.56	1.6
	Giub (Fn)	1.72	1.37	1.26	1.19
	Giub (MQ)	2.03	1.82	1.64	1.52
	Mean	2.26	1.84	1.78	1.67
	PREVAH	-	-	-	1.22
HQ300	Extrapolation (m^3/s)	37.03	68.77	86.55	102.71
	Momenta	2.78	2.78	2.45	2.29
	BaD7	2.41	2.32	2.51	2.24
	Kölla	3.29	1.64	1.75	1.8
	Giub (Fn)	1.93	1.54	1.42	1.33
	Giub (MQ)	2.27	2.04	1.84	1.7
	Mean	2.54	2.06	1.99	1.87
	PREVAH	-	-	-	1.15

Table 3.6: Comparison of the HQx_meso_CH methods and the PREVAH_regHQ with the extrapolated values for the HQ_{30}, HQ_{100} and HQ_{300} for the 4 reference points along the Schwarze Lütschine. The values of the comparison are relative to the extrapolation. The catchment size and the extrapolated value are denoted as absolute values

3.3.1.6 Weisse Lütschine

The extrapolation of the HQ_{10}, HQ_{30}, HQ_{50}, HQ_{100} and HQ_{300} had to be done in upstream direction because the RGS of Zweilütschinen is at the end of the Weisse Lütschine. The main tributaries of the Weisse Lütschine are the Selfine Lütschine, Trümmelbach, (Suls- and Sousbach), all of which caused sudden leaps in the downstream increasing discharge (Fig. 3.15 (a)).
The deviations of the HQ_{30}, HQ_{100} and HQ_{300} estimations from the HQx_meso_CH methods were much smaller compared to the one in the Schwarze Lütschine case, but overall these still painted in a positive direction (Tab. 3.7).
The HQ_{30} Momenta estimations were always higher than the extrapolated values. The BaD7 was twice below and twice above the extrapolated values, but still rather close (Figure 3.15 (b)).
In the case of HQ_{100}, the order of the values of HQx_meso_CH method is interesting, since it changed from reference point 1 to reference point 2. First, the BaD7 showed the lowest value and the Momenta the highest. Afterwards, this changed to Giub (Fn) being the lowest and Kölla the highest. The majority of the values were above the extrapolated values. The mean values were 1.19 to 1.26 times higher than the extrapolated values. The Kölla estimation produced the highest values.
The differences between the methods of HQx_meso_CH and the extrapolated values for the HQ_{300} were even higher. The estimated value with the Kölla method was outside the confidence band for the reference point 4 (RGS).
In opposition to that, the difference between the PREVAH_regHQ estimation and the extrapolated values increased with increasing distance from reference point 1 to 2. The estimations reached 0.65 to 0.8 of the extrapolated values.
Overall, the extrapolated values are smaller than the estimations with the HQx_meso_CH methods in the case of the Weisse Lütschine.

		Reference 1	Reference 2	Reference 3	Reference 4
	Catchment size (km^2)	59.6	82.8	110.2	144
HQ30	Extrapolation (m^3/s)	40.55	57.21	77.14	102
	Momenta	1.28	1.18	1.27	1.19
	BaD7	0.96	1.12	1.29	0.97
	PREVAH -	0.67	-	0.71	0.8
HQ100	Extrapolation (m^3/s)	50.2	70.14	93.76	123
	Momenta -	1.26	1.18	1.28	1.21
	BaD7 -	0.9	1.08	1.27	0.93
	Kölla -	1.31	1.58	1.53	1.69
	Giub (Fn)	1.07	1.02	0.97	0.93
	Giub (MQ)	1.38	1.29	1.25	1.16
	Mean	1.19	1.23	1.26	1.19
	PREVAH	0.68	-	0.68	0.73
HQ300	Extrapolation (m^3/s)	59.57	82.82	110.22	144
	Momenta	1.38	1.3	1.41	1.35
	BaD7	0.99	1.19	1.4	1.03
	Kölla	1.43	1.74	1.7	1.88
	Giub (Fn)	1.17	1.12	1.07	1.03
	Giub (MQ)	1.51	1.42	1.39	1.29
	Mean	1.3	1.35	1.39	1.32
	PREVAH	0.64	-	0.65	0.73

Table 3.7: Comparison of the HQx_meso_CH methods and the PREVAH_regHQ with the extrapolated values for the HQ_{30}, HQ_{100} and HQ_{300} for the 4 reference points along the Weisse Lütschine. The values of the comparison are relative to the extrapolation. The catchment size and the extrapolated value are denoted as absolute values

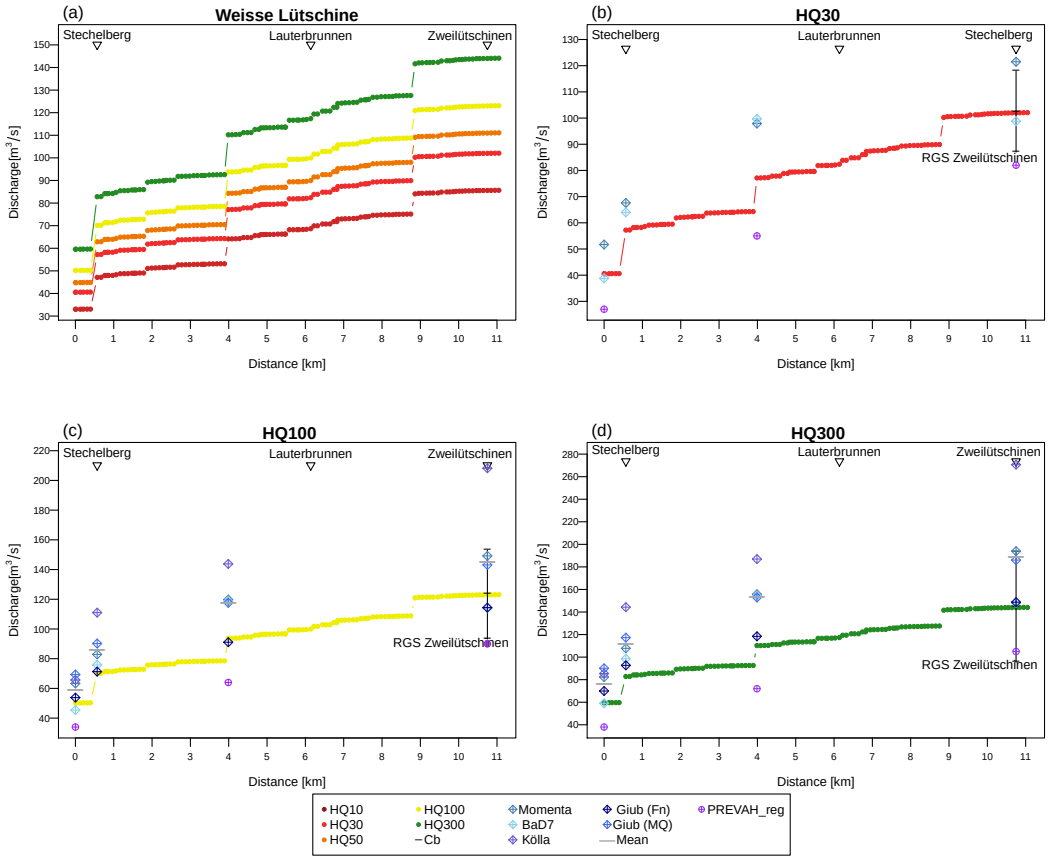

Figure 3.15: HQ_x extrapolation for the Weisse Lütschine based on every single cross section with the estimations of the HQx_meso_CH and PREVAH_regHQ: (a) HQ_{10}, HQ_{30}, HQ_{50}, HQ_{100} and HQ_{300}, (b) HQ_{30}, (c) HQ_{100} and (d) HQ_{300}

3.3.1.7 Vereinte Lütschine

The extrapolated values for each cross section are based on the evaluated HQ_{10}, HQ_{30}, HQ_{50}, HQ_{100} and HQ_{300} at the RGS in Gsteig. The extrapolation was conducted in down- and upstream direction. The Vereinte Lütschine had a smaller increase than the Weisse and Schwarze Lütschine due to the smaller catchment of the tributary (Fig. 3.16 (a)). The only notable tributary is the Saxetbach.
In the case of the HQ_{30} the BaD7 and Momenta estimations were higher than the extrapolated values (far outside the confidence band even though the values were only 1.3 to 1.37 higher than the extrapolated values).
The HQx_meso_CH estimations of the HQ_{100} for all reference points were scattered around the extrapolated values from 0.84 to 1.34 relative to the extrapolated values. Only the Giub (Fn) method produced a result below the extrapolated values. The Momenta estimations had the highest difference for the reference point 1, and further downstream, the values of the Kölla method were highest (Tab. 3.8).
The differences in the case of the HQ_{300} were higher compared to the HQ_{100} estimations but

the Giub (Fn) estimation was closer to the extrapolated values.
The PREVAH_regHQ estimations at the site of the RGS were similar for the HQ_{30}, HQ_{100} and HQ_{300} and reached 0.93 to 0.97 of the extrapolated values, which is close.
To sum up, the extrapolated values are lower compared to the values of the HQx_meso_CH method which are outside of the confidence band for the reference point next to the RGS.

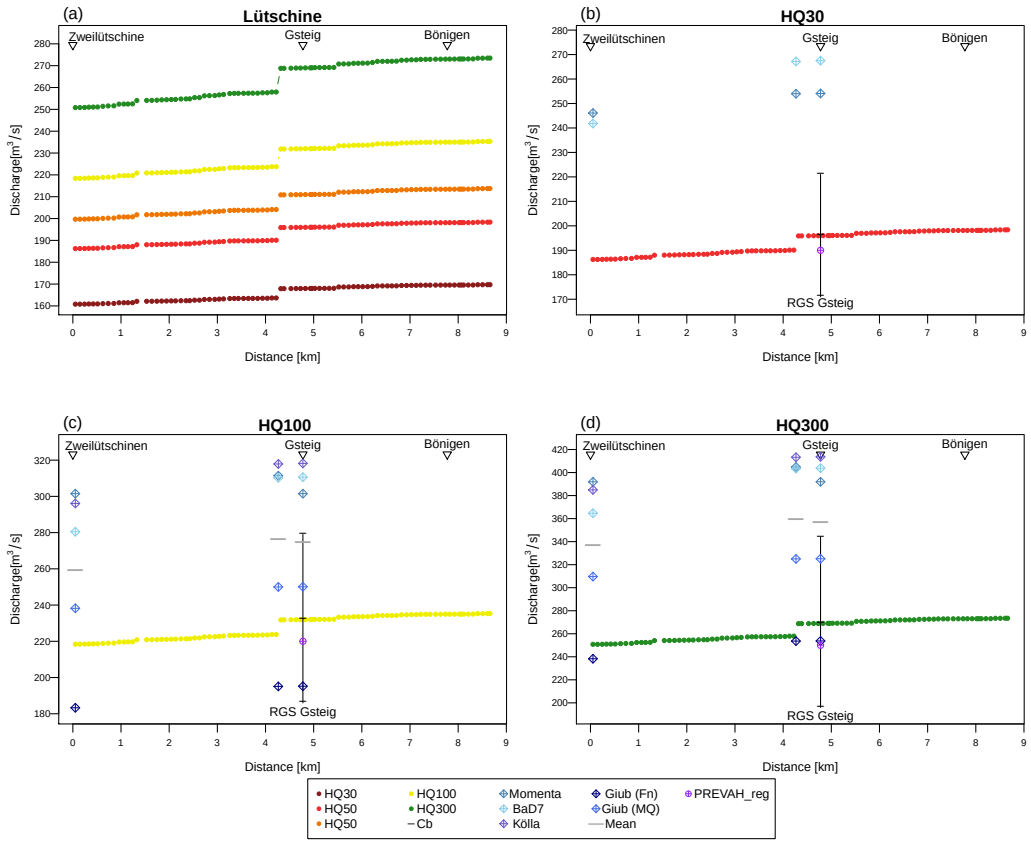

Figure 3.16: HQ_x extrapolation for the Vereinte Lütschine based on every single cross section with the estimations of the HQx_meso_CH and PREVAH_regHQ: (a) HQ_{10}, HQ_{30}, HQ_{50}, HQ_{100} and HQ_{300}, (b) HQ_{30}, (c) HQ_{100} and (d) HQ_{300}

		Reference 1	Reference 2	Reference 3
	Catchment size (km^2)	344	379.4	379.6
HQ30	Extrapolation (m^3/s)	186.25	195.89	195.96
	Momenta	1.32	1.3	1.3
	BaD7	1.3	1.36	1.37
	PREVAH	-	-	0.97
HQ100	Extrapolation (E)	218.41	231.84	231.94
	Momenta	1.38	1.34	1.3
	BaD7	1.28	1.34	1.34
	Kölla	1.36	1.37	1.37
	Giub (Fn)	0.84	0.84	0.84
	Giub (MQ)	1.09	1.08	1.08
	Mean	1.19	1.19	1.19
	PREVAH	-	-	0.95
HQ300	Extrapolation (m^3/s)	250.81	268.78	268.92
	Momenta	1.56	1.51	1.46
	BaD7	1.45	1.5	1.5
	Kölla	1.53	1.54	1.54
	Giub (Fn)	0.95	0.94	0.94
	Giub (MQ)	1.23	1.21	1.21
	Mean	1.35	1.34	1.33
	PREVAH	-	-	0.93

Table 3.8: Comparison of the HQx_meso_CH methods and the PREVAH_regHQ with the extrapolated values for the HQ_{30}, HQ_{100} and HQ_{300} for the 3 reference points along the Weisse Lütschine. The values of the comparison are relative to the extrapolation. The catchment size and the extrapolated value are denoted as absolute values

3.3.2 Bank-full Discharge of the Cross Sections

The results of the channel capacity based on every single cross section for every river section are integrated in a plot. The simulated bank-full discharge importantly depended on the choice of the kst-coefficients. This was determined in the calibration. First, the result of the calibration will be shown, followed by the results of the bank-full discharge for each river section.

3.3.2.1 Calibration

The results of the calibration are summarized in Table 3.9. The main output are the M - coefficients for the different river sections and the subsections of the river section. The creation of the subsections is based on hydraulic and hydrological considerations. For example the Simme, is much wider and less straightened in the second section than in the first and the third is influence by the barrier lake (Fig. 3.17).

Figure 3.17: The three kst-coefficient sections of the Simme River from upstream to downstream

River	Numbers of RGS	Sections	kst-coefficients	Data	P/Q relation
Hasliaare	1	1-59	45,30,45	Calibration campaign FOEN	572.8 m-250 m^3/s
Aare Thun-Bern	2	1-64	42,22,42	Calibration campaign FOEN	550 m-291 m^3/s
		65-180	56,59,56	Calibration campaign FOEN	504 m-445 m^3/s
Simme	3	1-236	25,35,25	Risk prevention campaign FOEN	930.7 m-88.5 m^3/s
		236-340	19,25,19	Calibration campaign FOEN	779 m-167.5 m^3/s
		341-403	21,24,21	Calibration campaign FOEN	665 m-211.5 m^3/s
Kander	1	1-203	35,46,35	Risk prevention campaign 2015 FOEN	648.66 m-172.5 m^3/s
Weisse Lütschine	1	1-121	47,22,47	Risk prevention campaign FOEN	651.8 m-100 m^3/s
Schwarze Lütschine	0	1-114	23,27,23	Values Vereinte Lütschine	-
Vereinte Lütschine	1	1-89	23,27,23	Risk prevention campaign FOEN	587 m-153.3 m^3/s

Table 3.9: The kst-coefficients for the different river sections, their subsections and the parameters on which the calibration is based upon

The Data column depicts which cross section could be used for the calibration. It was not always possible to use the cross section next to the RGS (calibration campaign of the FOEN) because the water level at the time of measurement was so low that the measured profile was not enough wide to calibrate the bank-full discharge. In these cases, the data of the risk prevention campaign of the FOEN (section 3.2.1) were used, but those are most of the time not precisely located next to the RGS but rather close. An exception is the Kander, where the data of the actual risk prevention campaign 2015 of the FOEN could be obtained. In this campaign measurements at the RGS were conducted. The column Q/P relation indicates for which stage discharge relation the kst-coefficient was calibrated. This was not always an easy decision because it depends on the surrounding conditions and on the cross section data availability. But the result varied just slightly for a water level 10 cm higher or lower.

To provide a framework about the influence of the magnitude of the calibrated kst-coefficients on the simulation output, two plots are shown, the Aare in Thun (Fig. 3.18 top) as an example of a constructed and wider river, and the Weisse Lütschine (Fig. 3.18, bottom) as an example for a smaller alpine river. The plots show the deviation of the discharge and the deviation of the water level as a function of changing kst-coefficients of the channel. The change in the water level or the discharge by scaling down the kst-coefficient by one is very different for the two cases. The Aare has an increase of the water level of 8 cm, and, in the opposite case, the discharge would decrease 15 m^3/s, which corresponds to a relative decrease of 5.2 %. Under the same variation of the kst-coefficient, the weisse Lütschine shows increase in the water level of 2 cm, and, in the opposite case, the discharge would decrease 4 m^3/s, which corresponds to a relative decrease of 4 %. It further shows also that the influence on the discharge or water level is not constant for an increase of the kst-coefficient by 1 (it differ from value to value).

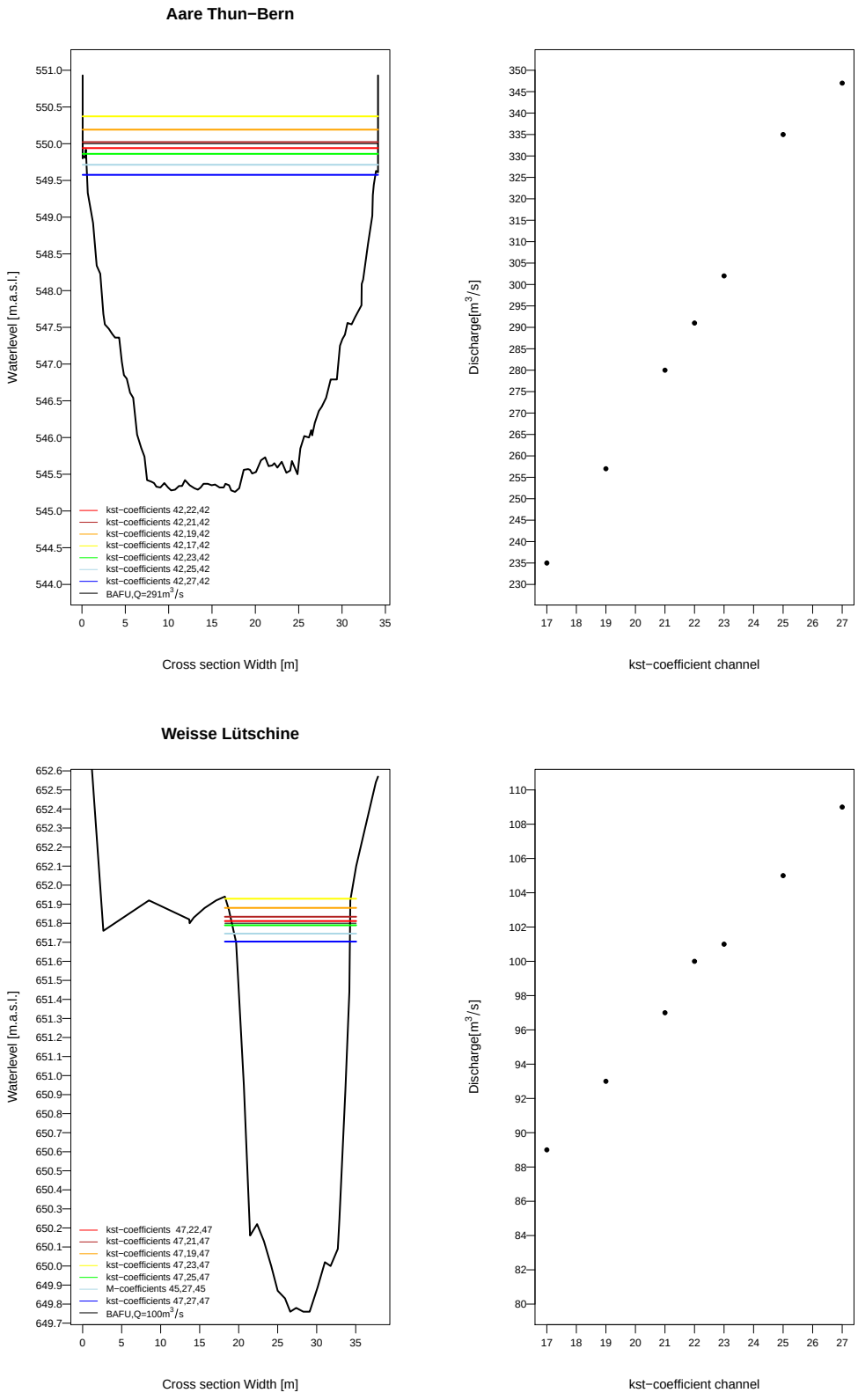

Figure 3.18: Influence of the kst-coefficient on the discharge and the water level: RGS Aare Thun (top), RGS Weisse Lütschine (bottom)

3.3.2.2 Hasliaare

Figure 3.19 illustrates that the river bed of the Hasliaare was homogeneous. The left bank and right bank site did not show large changes in the course and both sides were on a similar height. The only difference was observed at the beginning, where the right side was higher than the left side, and at kilometre 10 near the RGS, where the right side was again higher. I.e if it overflows on one side, the other side follows quickly. However, there are some section with a tendency of overflow for a side. Along the first kilometre, the weak side it changed from right to left quickly, but further downstream, at kilometre 7 to 9, the lower height of the right side will cause overflow. The opposite again is the case from kilometre 9 to 12.
There was a general increase of discharge from upstream to downstream. It was in a range of 300 m^3/s to 650 m^3/s, excluding the outliers in Meiringen and Brienz. There, the bank of the cross section was higher than before and after. Even though the fluctuations in the bank height were small, the difference of the channel capacity from cross section to cross section can amount up to 100 m^3/s. This occurred in the first kilometres and from kilometre 11 to 12 possibly because the Hasliaare has an average width of 20 m but still some narrow spots. The section around the RGS had also larger variations, but differences in the height of the bank site were visible. The lowest capacity of the channel was found between kilometre 9 to 10, where the discharge was only 304 m^3/s and 276 m^3/s. The other patch of low capacity was located between kilometre 4 and 7.
Overall, the Hasliaare seems to be homogeneous and the range of the bank-full discharge is rather small.

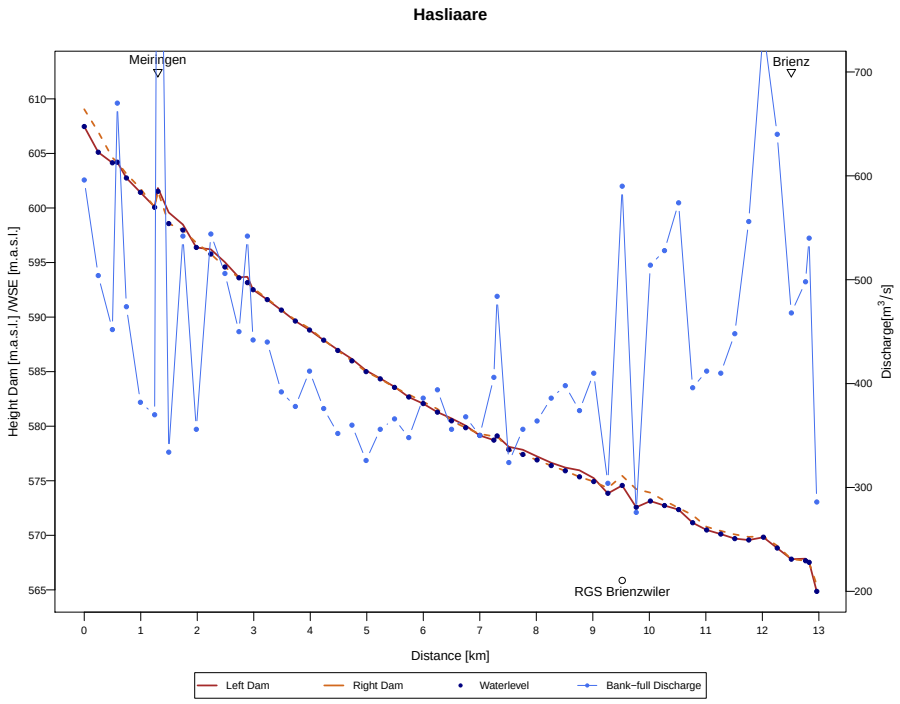

Figure 3.19: Bank-full discharge of each cross section with the associated water level and the left and right bank side height along the Hasliaare

3.3.2.3 Aare Thun-Bern

The section of Thun-Bern of the Aare was subdivided into two parts to gain a better overview (Fig. 3.20 (a) and (b)). The kst-coefficient pair changes next to the Chiesen inflow as mentioned in section 3.3.2.1. Figure 3.20 (a) shows four parts of the bank-full discharge. During the first kilometre of the first section, the channel capacity was around 550 m^3/s and varied in the range of approximately 100 m^3/s with one exception, where it reached 1112 m^3/s. The low bank-full discharge values with a channel capacity of 444 m^3/s to 534 m^3/s occurred in a location where the right bank side was higher. The bank side along this part ranges between high and low. The second section started with a heavy increase of all variables, and the channel capacity reached a level of 1420 m^3/s. Also the bank side height on the left and on right side are on a comparable level. It stayed at the level and increased even more before a low value, showed a capacity of 518 m^3/s only and which reflects a depression of the waterside.
Subsequently, the bank-full discharge decreased constantly to the distance of kilometre 8 to 470 m^3/s. This third section was first homogeneous even though the bank-full discharge varied from cross section to cross section up to 200 m^3/s. Afterwards, the left bank was much higher and the fluctuation was similar. At kilometre 8, next to Kiesen, the bank-full discharge increased to an extreme value of 1400 m^3/s. Downwards from these, both the variation in the bank-full discharge and in the bank-full height of one side was remarkable. Overall the values of this fourth section were high.
Figure 3.20 (b) shows the course from Münsigen to Bern (kilometre 13 to 28). It look as if the left dam side was higher most of the distance. At kilometre 16, a depression of the right dam side lead to a very low bank-full discharge of 322 m^3/s. There were two river segments in terms of the variability of the channel capacity. First, it decreased slowly with increasing distance until kilometre 8 and then it shortly increased until Muri, where the variation was abundant. At kilometre 19, the lowest value with a discharge of 522 m^3/s was calculated.
In the second section after Muri, the bank-full discharge decreased overall and the fluctuation between the cross sections was smaller. It was quite homogeneous and it looked as if all cross sections have a comparable capacity. The channel capacity decreased constantly with the exception of Schönau, where the bank sides were much higher.

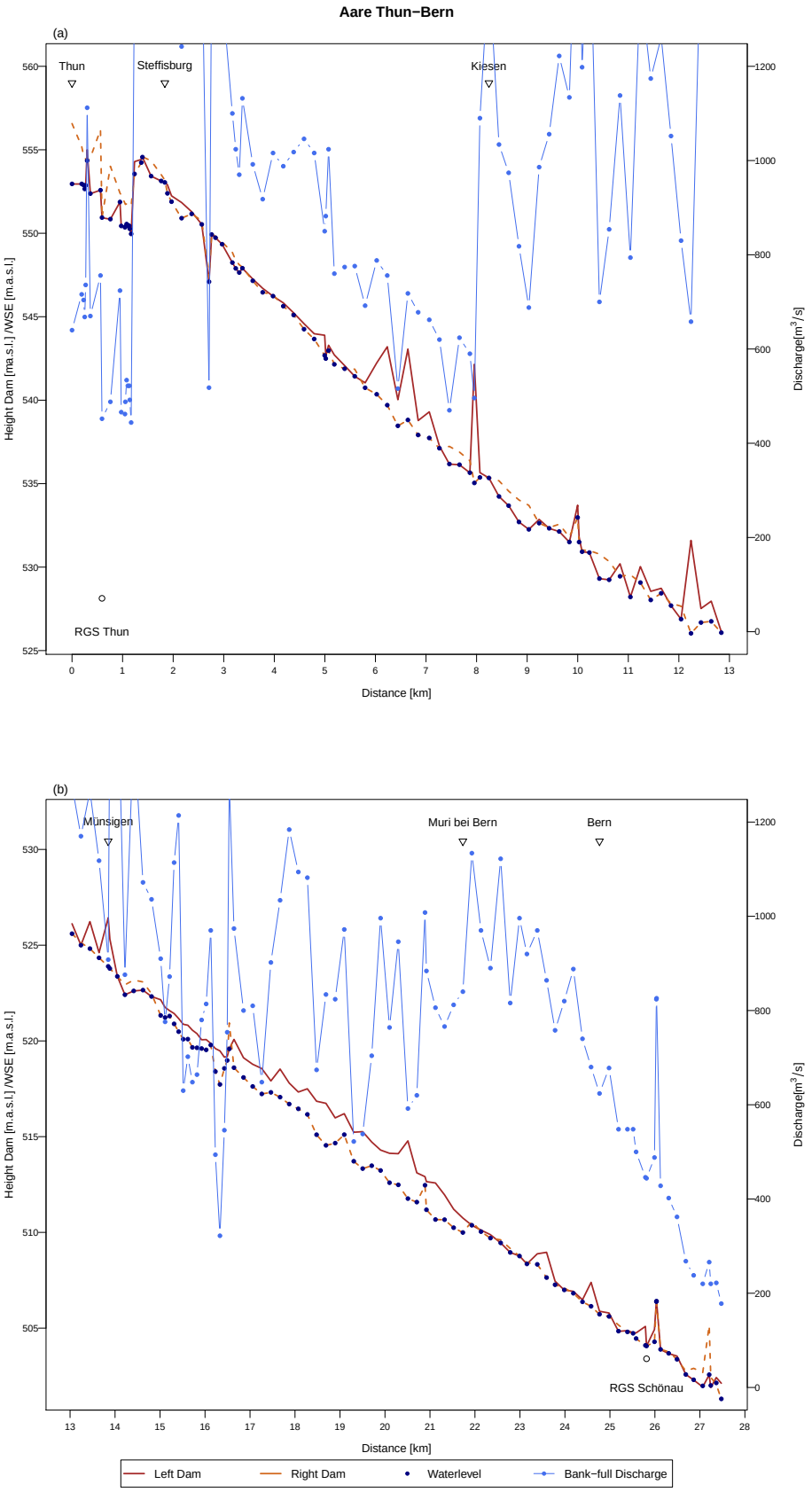

Figure 3.20: Bank-full discharge of each cross section with the associated water level and the left and right bank side height along the Aare Thun-Bern: (a) Thun-Münsigen, (b) Münsigen-Bern

3.3.2.4 Simme

The Simme was subdivided into three sections due to its length. Figure 3.21 (a) depicts the first 14 kilometres. Along this section, the river bed was more or less homogeneous with some exceptions where the left bank side was higher. Overall, no trend was visible for one side. The bank-full discharge increased with increasing distance and showed some strong fluctuations in the direction of high capacity (however, they are not in the focus of this analysis). The lower level of the bank-full discharge was in the range of 50 m^3/s to 150 m^3/s where most of the cross section of this section belong to. The bank-full discharge had the tendency to slightly increase in direction of Zweisimmen. The lowest value in St. Stephan was of 78 m^3/s, and between Lenk and St. Stephan, the capacity was even lower (50 m^3/s). At kilometre 24, the kst-coefficients in the model change as indicated in Table 3.9. For the section from Zweisimmen to Oberwil, the bank-full discharge was on a higher level of 150 m^3/s to 250 m^3/s with a lowest value of 120 m^3/s at kilometre 13.5 (Fig. 3.21 (b)). But the changes of the bank-full discharge from one cross section to the next were very high in some cases, as around kilometre 16. Along this part, the slope of the riverbed seemed to be very steep. Constant high values were found in the region of Boltigen, where the left bank side is the critical side. The level of the low points were of a similar value over the whole section. At kilometre 24, the bank-full discharge started to fluctuate again.
The third section showed unequal bank sides and heavy fluctuations in the bank-full discharge, changing from cross section to cross section (Fig. 3.21 (c)). Between kilometre 30 and 36, values were low in the range 50 m^3/s to 150 m^3/s along multiple cross sections. They were lower than the values of the enclosed cross sections apart from some exceptions. The third section with associated kst-coefficients starts in Erlenbach after the barrier lake at approximately kilometre 38. Upstream of Latterbach, the values were again rather low: in the scale of 76 m^3/s to 170 m^3/s. The last section showed an increase again with high fluctuations towards kilometre 42, before it started to decrease again.

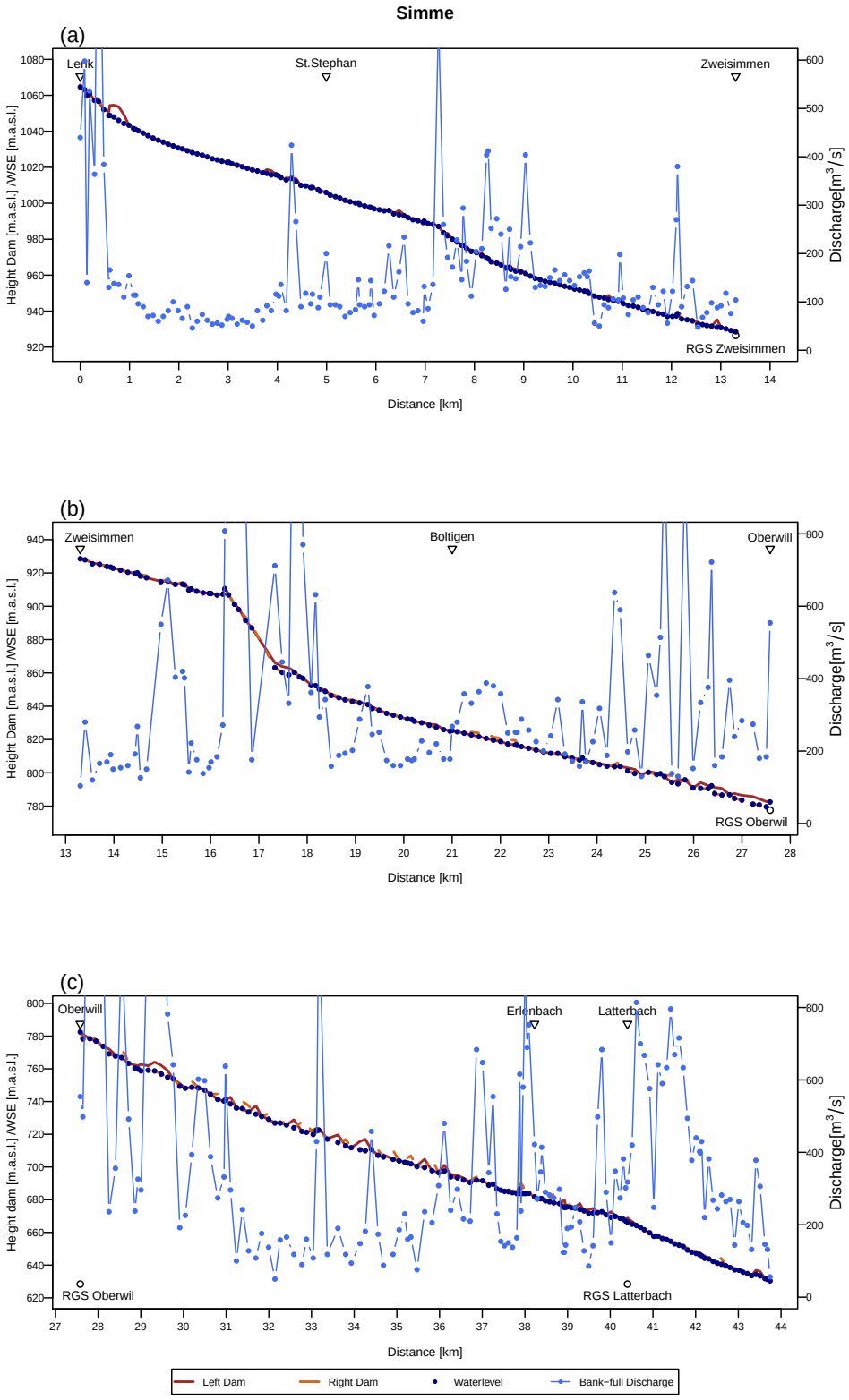

Figure 3.21: Bank-full discharge of each cross section with the associated water level and the left and right bank side height along the Simme: (a) Lenk-Zweisimmen, (b) Zweisimmen-Oberwil, (c) Oberwil-Latterbach

3.3.2.5 Kander

The Kander river in general showed high values for the bank-full discharge, mainly for the second part. The variation of the bank-full discharge between the cross sections in the second part were large. They in some cases reached more than 1000 m^3/s (Fig. 3.22 (b)). The first section had a more homogeneous river bed even tough the height of the bank side is varying. A weak side could not be determined, but a tendency for the left side being deeper in the upper part was detected. The variation in the bank-full height is probably the cause for the changes in bank-full discharges. Along the river, three very low values appeared, with discharge values of 60 m^3/s, 84 m^3/s and 60 m^3/s going downstream. A pattern of low values was detected in the region between Mülenen and Hondrich (Fig. 3.22 (a)), ranging between 200 m^3/s and 400 m^3/s, however with section with much higher values. Downstream of Hondrich, the capacity increased, with an exception to two outlier with lower discharges of 250 m^3/s and 236 m^3/s respectively. The fluctuation of the channel capacity was extreme and the height of the banks varies strongly.

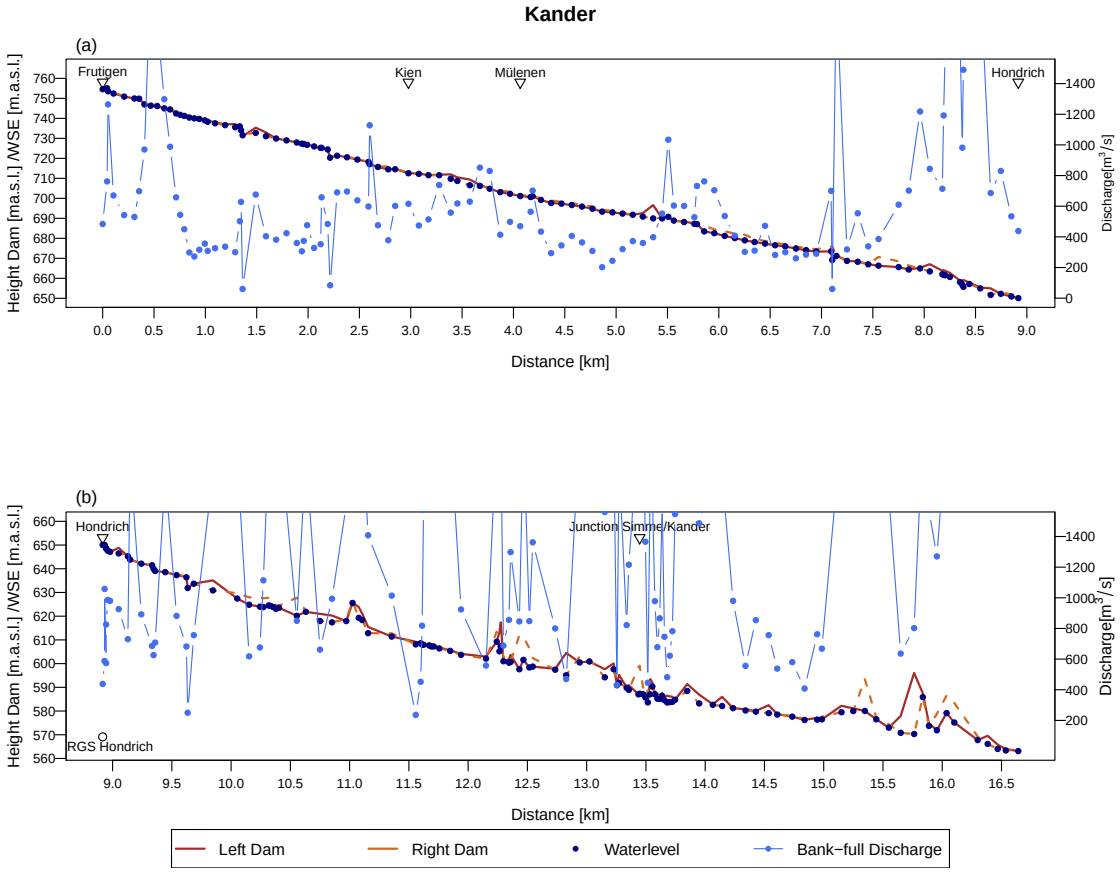

Figure 3.22: Bank-full discharge of each cross section with the associated water level and the left and right bank side height along the Kander

3.3.2.6 Schwarze Lütschine

In the case of the Schwarze Lütschine, the river was subdivided into two parts: Grindelwald-Burglauen and Burglauenen-Gündelischwand. In the first part, the channel capacity of the river tended to decrease with increasing distance. The lowest values of the fluctuating bank-full discharge were in the range of 60 m^3/s to maximally 130 m^3/s (Fig. 3.23). In terms of inundation risk, no tendency towards a bank side was detected. Few exceptions with very high values were mostly along a cross section where the bank side is higher. This result showed also that the capacity is different for every cross section. The curve rises and sink in the range of 200 m^3/s. This is a rather large difference for a river of such a small size.
The second part showed a similar picture. The bank-full discharge tended to decrease with increasing distance, and the bank-full discharge varied highly from cross section to cross section. The lowest values were located downstream of Gündlischwand, lying between 58 m^3/s and 88 m^3/s. For both parts, the bank sides seemed to be rather homogeneous. Only downstream of the river, the left side was higher.

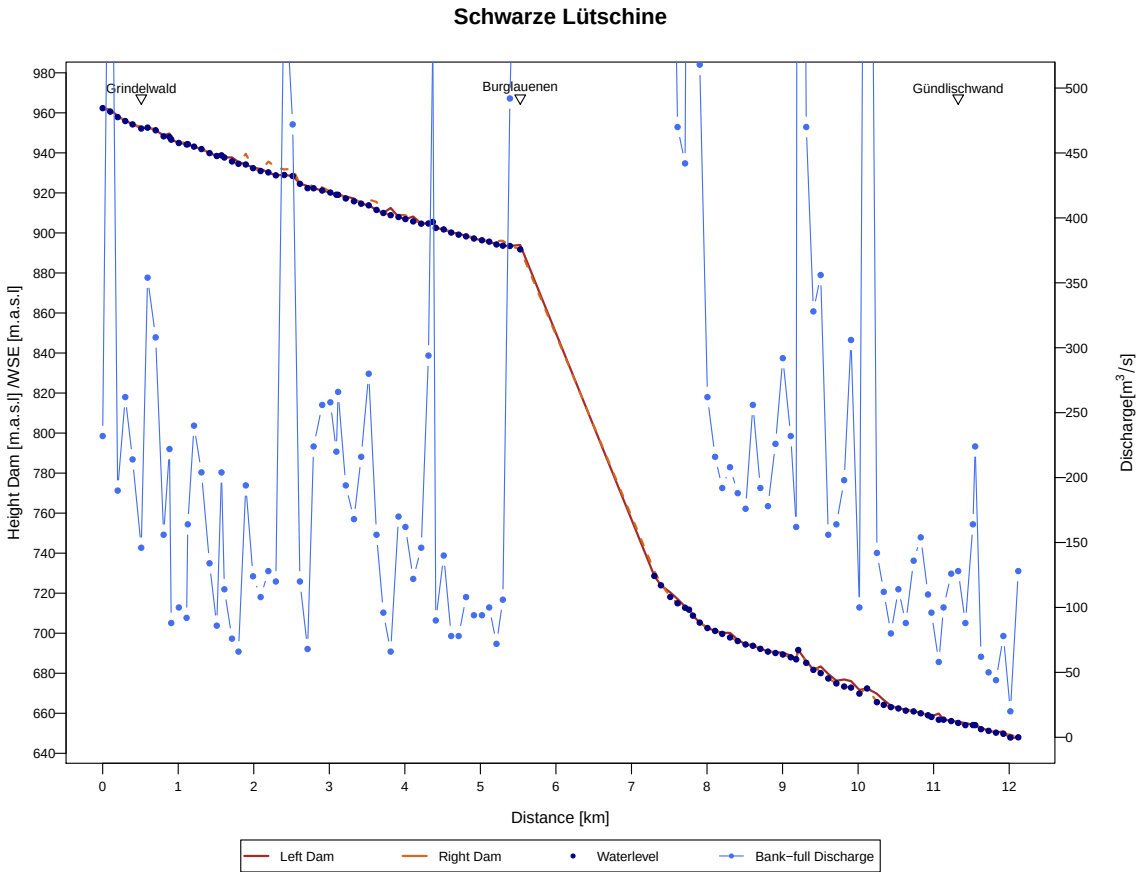

Figure 3.23: Bank-full discharge of each cross section with the associated water level and the left and right bank side height along the Schwarze Lütschine

3.3.2.7 Weisse Lütschine

The weisse Lütschine exhibited segments of low channel capacity in the range of 40 m^3/s to 120 m^3/s (Fig. 3.24). These segments were between kilometre 2 and 3, between kilometre 4 and 5, between kilometre 7.5 and 8.5, and between kilometre 10 and 11. There, most of the cross sections yielded low values, and there was less internal variation than in the case of the other rivers. In average, the bank-full discharge tended to increase from up- to downstream. However, two regions with a very high bank-full discharge were identified after Lauterbrunnen and next to Zweilütschinen, where the bank-full discharge was even higher than 2000 m^3/s. Up to and including kilometre 13, a tendency for weak left bank side was observed. All in all, the bank sides were rather homogeneous along the whole course.

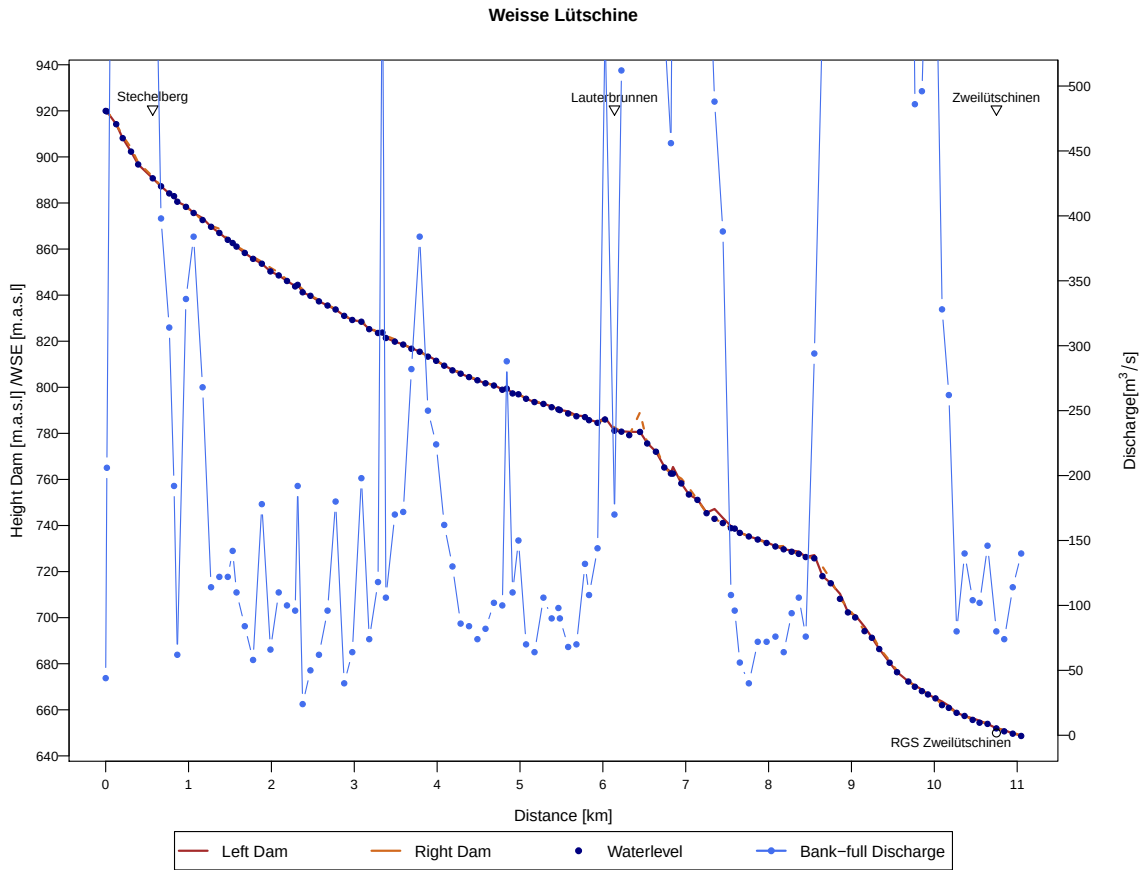

Figure 3.24: Bank-full discharge of each cross section with the associated water level and the left and right bank side height along the Weisse Lütschine

3.3.2.8 Vereinte Lütschine

The Vereinte Lütschine was subdivided in two sections with similar characteristics (Fig. 3.25). In the upper part up to kilometre 6, the bank sides height strongly varied and thereby caused a large variation in the bank-full discharge. The channel capacity was rather low in Zweilütschine, with a lowest bank-full discharge of approximately 150 m^3/s. Also, upstream of Gsteig, values between 140 m^3/s and 220 m^3/s were observed. The second section downstream exhibited less variability in the height of bank side and bank-full discharge, some exceptions set aside.

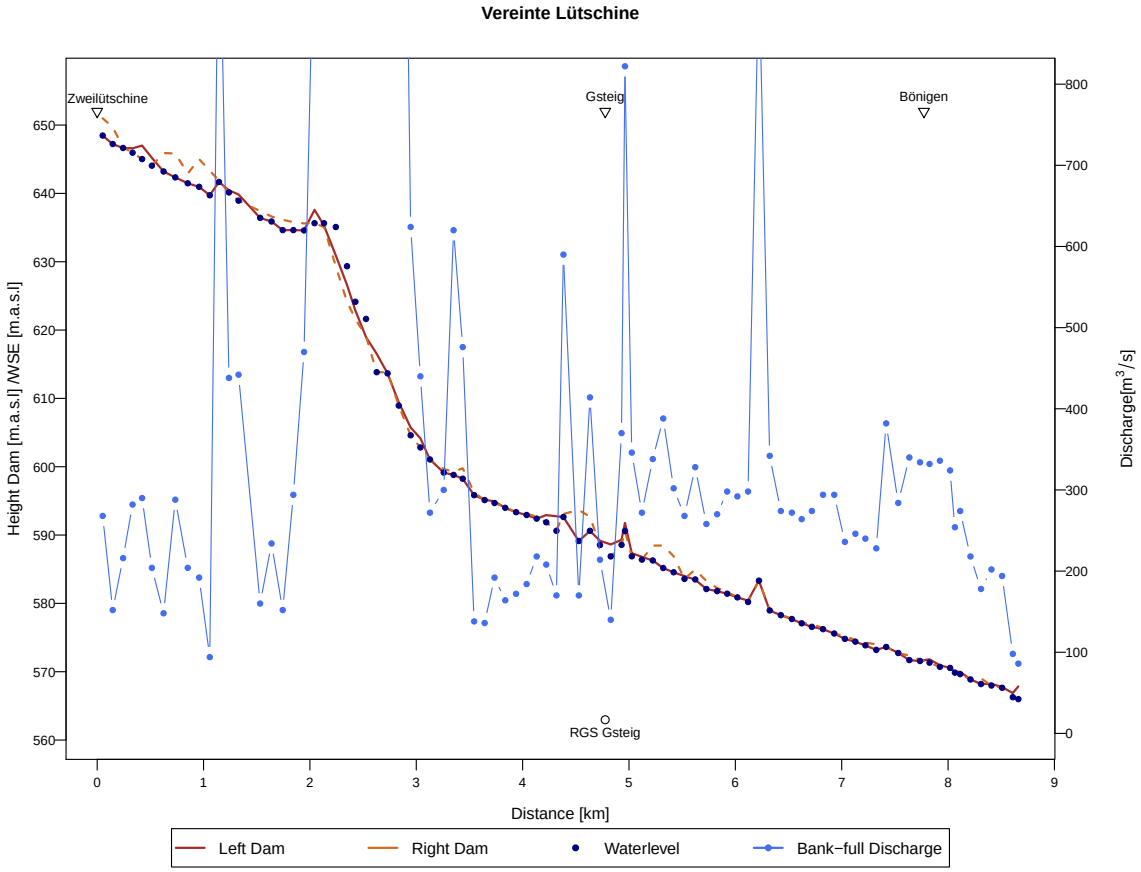

Figure 3.25: Bank-full discharge of each cross section with the associated water level and the left and right bank side height along the Vereinte Lütschine

3.3.3 Identification of the Weak Points

Weak points along a river are here defined as the cross sections whose bank-full discharge is attributed with a HQ between 10 and 100, meaning that the channel capacity exceedance has a high occurrence frequency. This part unites the results of section 3.3.1 and 3.3.1 section. First, the results are shown as a bar plot, where each bar indicates the return periods associated with one cross section. One bar includes the HQ_{10} to HQ_{300} and is subdivided according to this classification. The bank-full discharge is depicted as black dashed lines connected over a black line. Secondly, the results are represented on a map in order to have the geographical context. The background maps are provided by the Federal Office of Topography. The maps show a cutting of the river section and the corresponding cross sections. The cross section lines are coloured according to the associated return period of the bank-full discharge of the cross section. Above the cross section lines, the magnitude of bank-full discharge and the side of overflow is written. Additionally, the channel boundaries are circumscribed referred to as black points. Thirdly, the results are merge into a map where all river sections are showed.

3.3.3.1 Hasliaare

The results of the weak point analysis of Hasliaare showed a uniform appearance (Fig. 3.26). All cross sections, except for two, were attributed with an HQ_x in the range of 10 to 300. The major part thus was in the range of HQ_{30} to HQ_{100}. The cross sections with the lowest capacity (described in section 3.3.2) were mostly belonged to HQ_{30}. Those with the lowest capacity next to the RGS were even attributed with an HQ_{10}. This result shows that the described variation of the low channel capacity between the cross sections can already change the attributed HQ_x. The village Meiringen is not protected on the level of an HQ_{100} at some points (Fig. 3.27). Downstream of Meiringen, next to Balm, channel capacity was still low but a HQ_{100} can flow off. In Brienzwiler, the capacity was a HQ_{50} maximally with one exception. As explained the HQ_x was higher along the village than in their surroundings.

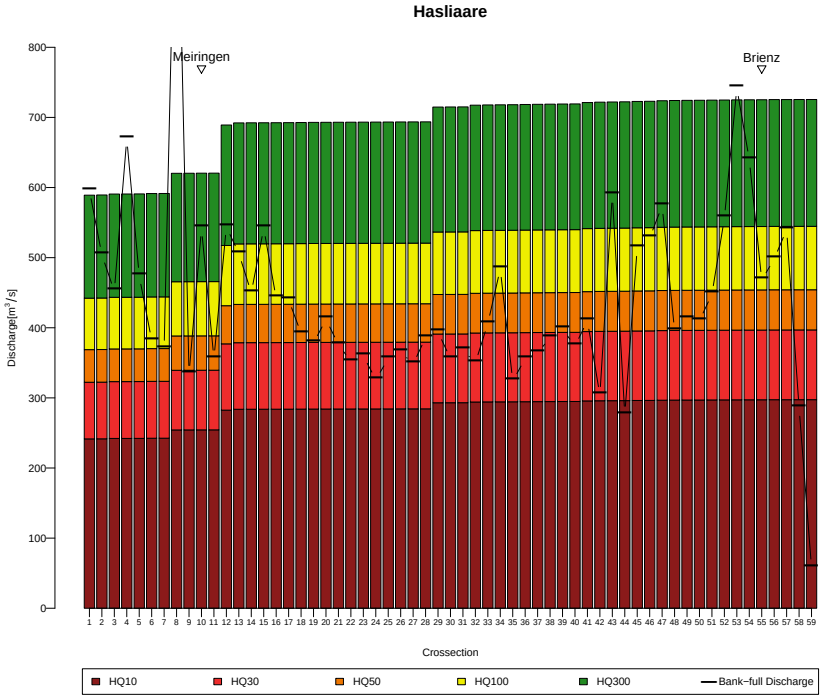

Figure 3.26: The HQ_{10} to HQ_{300} and the bank-full discharge for each cross section along the Hasliaare

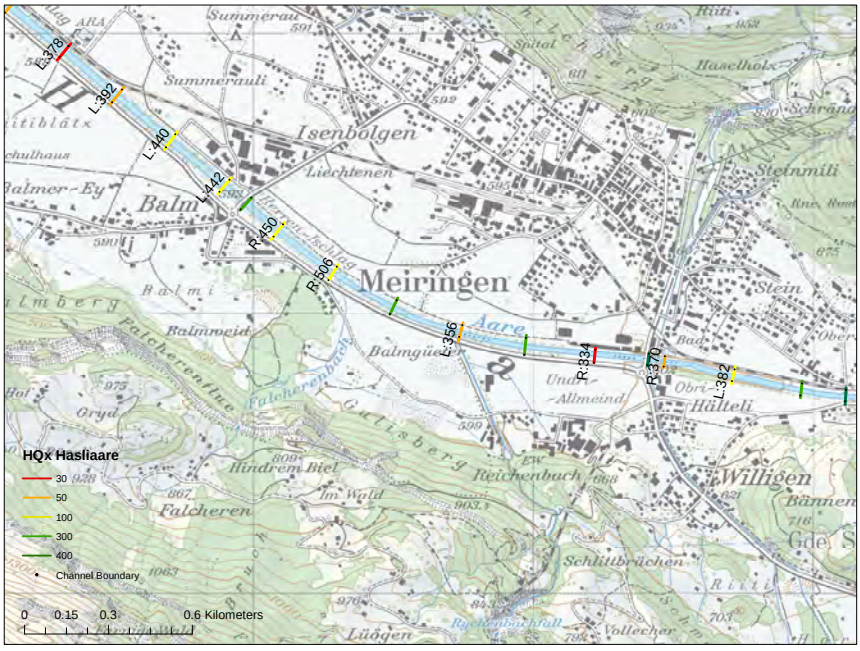

Figure 3.27: Weak points along the Hasliaare next to Meiringen

3.3.4 Aare Thun-Bern

The HQ_x attribution of the channel capacity along the Aare showed an inverted picture to the Hasliaare, as only few cross sections were associated with a low return period (Fig. 3.28). The overall capacity was rather high and consequently, most areas can be regarded as low risk. The areas with low capacities (potential weak points) include a zone next to Thun (RGS Thun). The cross sections were classified with HQ_{100}, and a single weak point was even attributed with a HQ_{50}. For the section in Jaberg, one cross section was attributed with a HQ_{100} and one with a HQ_{50}; the cross section in front of the Hunzigerbrücke showed the same. In the last section from Dählhölzli to Marzili, the associated HQ_x ranged from HQ_{10} to HQ_{50}. Figure 3.29 shows that the weak points are located in the city itself of Berne. The last 9 cross sections were deleted in Figure 3.29 because the values are very low and therefore implausible.

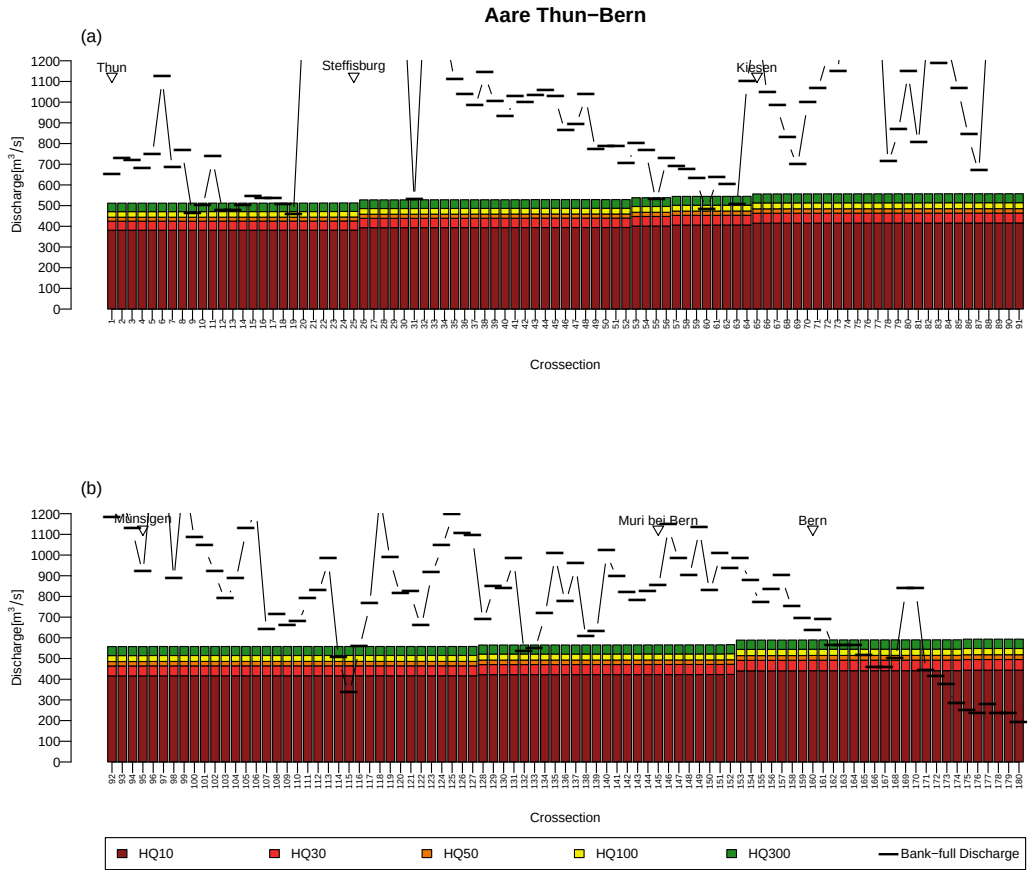

Figure 3.28: The HQ_{10} to HQ_{300} and the bank-full discharge for each cross section along the Aare Thun-Bern

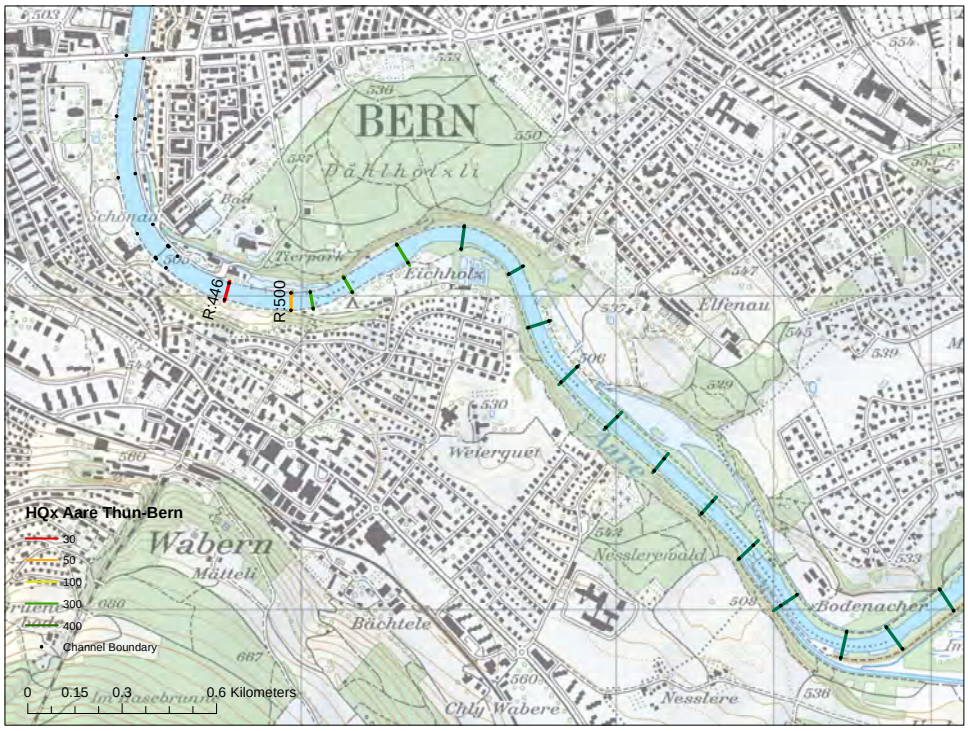

Figure 3.29: Weak points along the Aare Thun-Bern next to Bern

3.3.5 Simme

The Simme river was very heterogeneous in terms of the attributed return periods. Overall, it revealed a lot of weak points, mainly in the region between Lenk and Zweisimmen and close to Erlenbach (Fig. 3.30 (a) and (c) and Fig. 3.31). Between Lenk (outside the village) and St. Stephan, most of the cross sections were associated with return periods below 100 years. A majority even belongs to a HQ_{30} or lower. The region is not densely populated, but is still used for agricultural production. In the villages the Simme had higher return periods; some cross section did not show potential for danger. The S-curve in front of Zweisimmen constantly showed a HQ_{30} or lower, and next to Zweisimmen the HQ_x values were still low. As the results of the bank-full discharge already indicated, the section from Zweisimmen to Oberwil had less weak points and only a few were below a HQ_{100} (Fig. 3.34 (b)). The weak points were not aggregated nor close to populated areas. After Weissenburg, the channel capacity decreased again heavily and a zone of weak points showed up until Ringoldingen. With some exceptions, the return period varied from cross section to cross section. In this zone the Simme flows through a valley and is far from human settlements. In front of the barrier Lake in Erlenbach, the bank-full discharge again exhibited a HQ_{30} for four cross sections and for the cross section at the train bridge. Due to the inflow of the Chirel tributary, the discharge of the HQ_x increases. The channel showed a slightly higher capacity here but the bank-full discharge remained in the range of an HQ_{30} to HQ_{100} close to Burgholz.

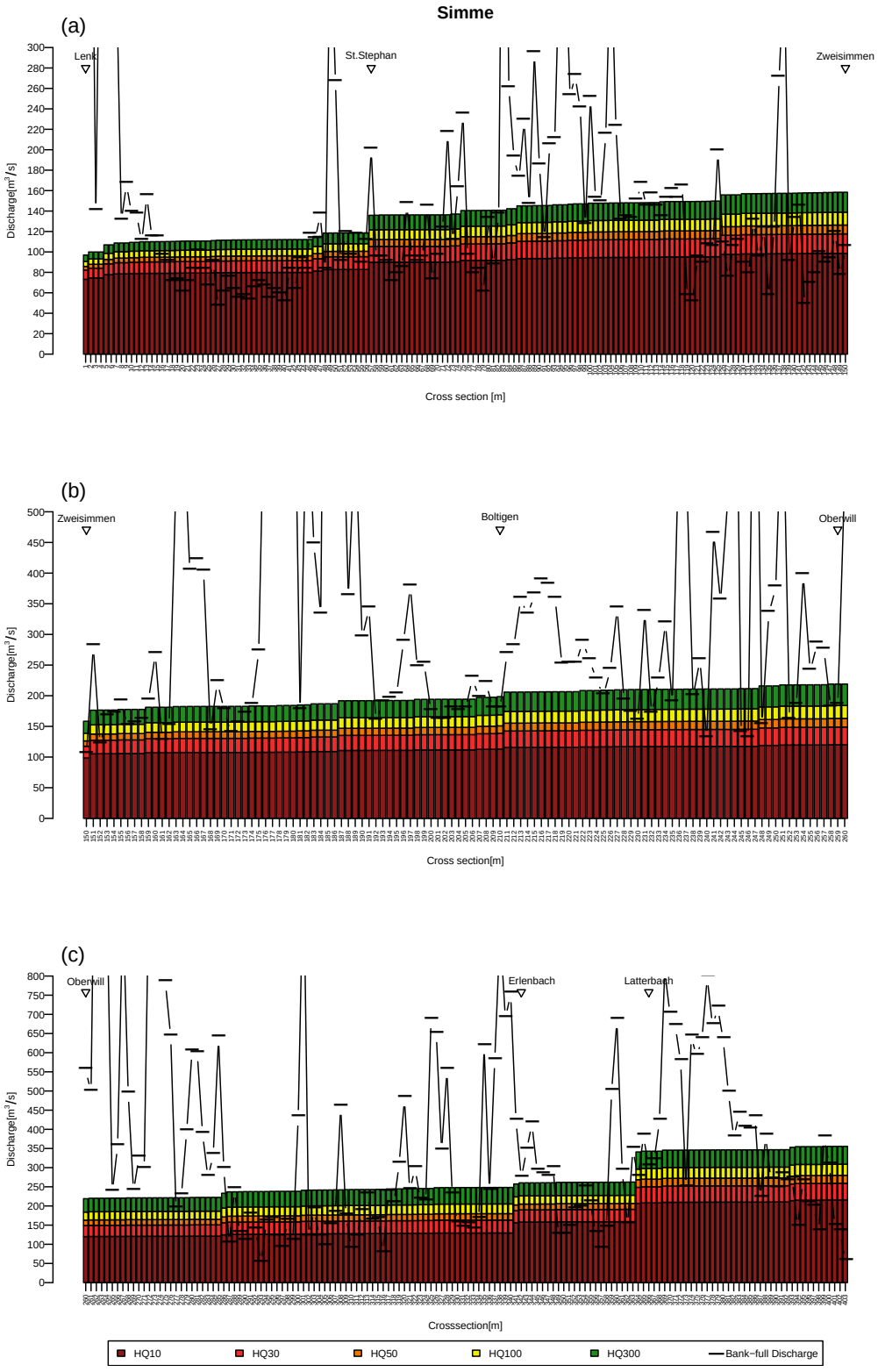

Figure 3.30: The HQ_{10} to HQ_{300} and the bank-full discharge for each cross section along the Simme

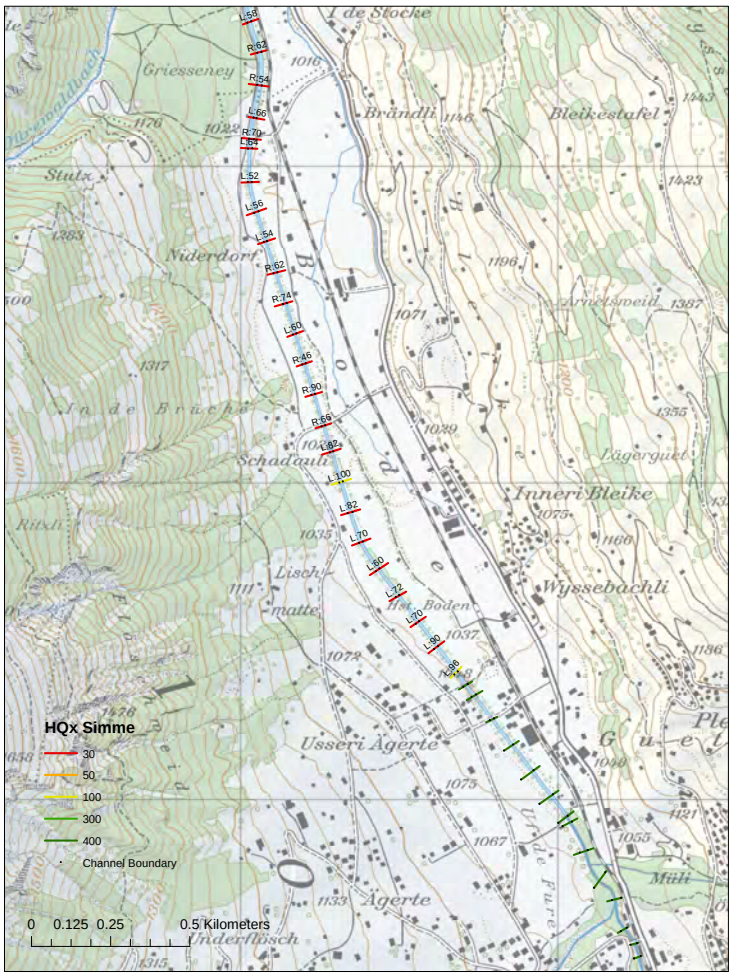

Figure 3.31: Weak points along the Simme downstream of the Lenk

3.3.6 Kander

In comparison to the Simme, the Kander river showed a inverted pattern. Along the river, most of the cross sections exhibited a low recurrence frequency (Fig. 3.32 (a) and (b)). As mentioned, two of the very low values are caused by the definition of the channel boundary and have to be ignored. The low capacity of the cross sections after Mülenen were attributed with the return periods of HQ_{50} and HQ_{30}. They are not located along the populated are and therefore have a low risk potential (Fig. 3.33). The side of overflow is the left side, i.e. the side opposite to the railway tracks. The section next to Bad Heustrich is attributed with a range of HQ_{30} to HQ_{100}. Further downstream, there were only two more weak points, and a few more after the joining with the Simme. Those weak points are not located in populated areas.

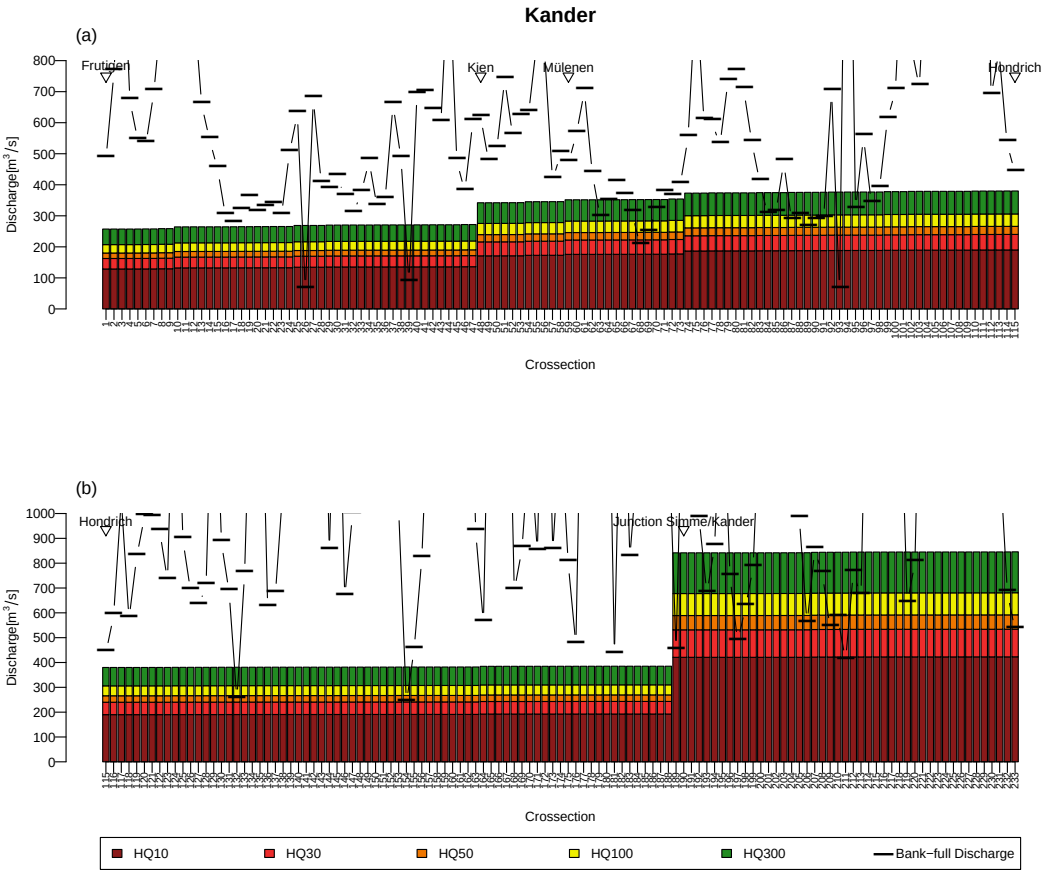

Figure 3.32: The HQ_{10} to HQ_{300} and the bank-full discharge for each cross section along the Kander

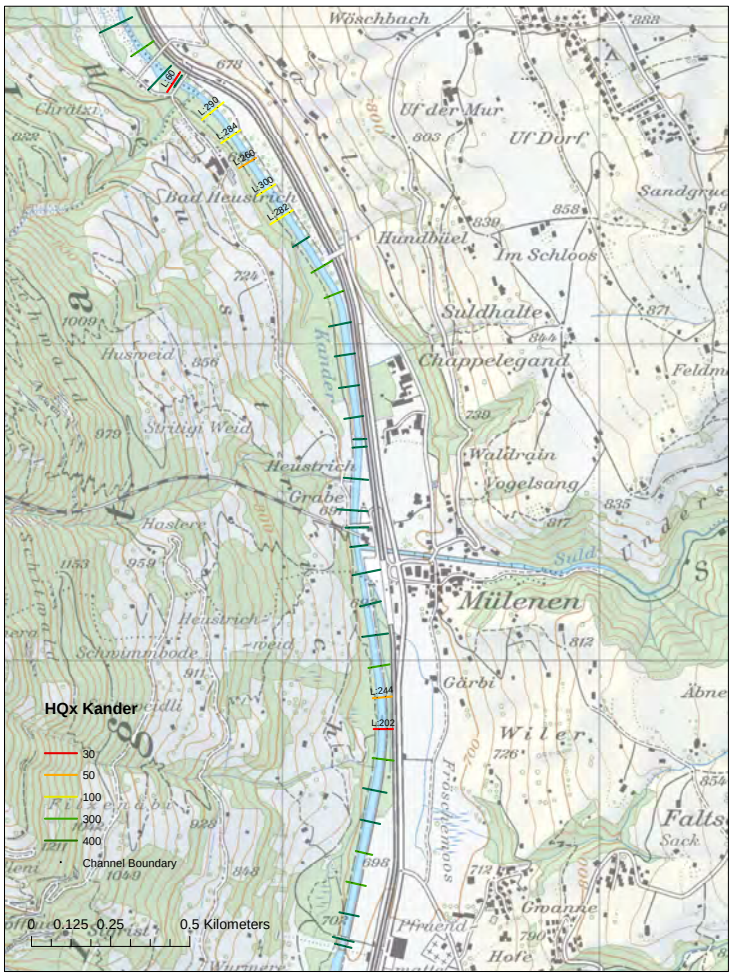

Figure 3.33: Weak points along the Kander next to Mülenen

3.3.7 Schwarze Lütschine

According to the showed Figure 3.34 the low capacity of the Schwarze Lütschine in Grund was not attributed with high recurrence frequency. In other words there are no weak points in Grund. Only six weak points with a return period below 100 years appeared downstream of Grund. Figure 3.34 shows the results based on the cross section number. The gap by the gorge part on Figure 3.35 is not included in the bar plot. Next to Rüdli, the Schwarze Lütschine gets narrower. In this section, a pattern of weak points appeared. Close to the junction, the weak points were attributed with a high frequency period, a HQ_{30}.

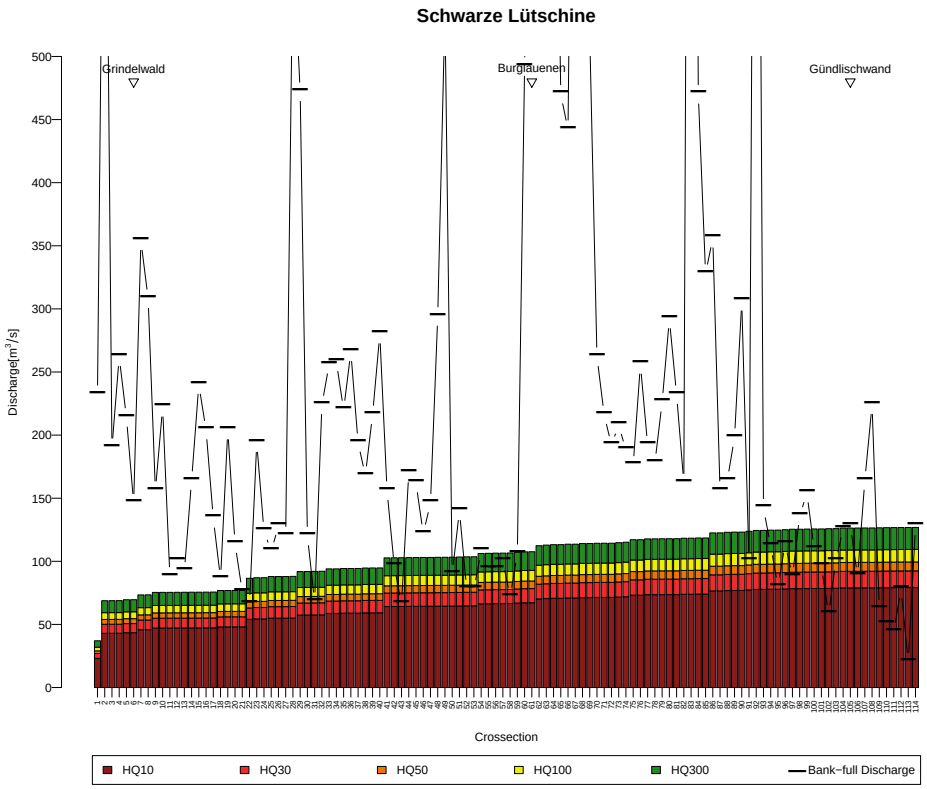

Figure 3.34: The HQ_{10} to HQ_{300} and the bank-full discharge for each cross section along the Schwarze Lütschine

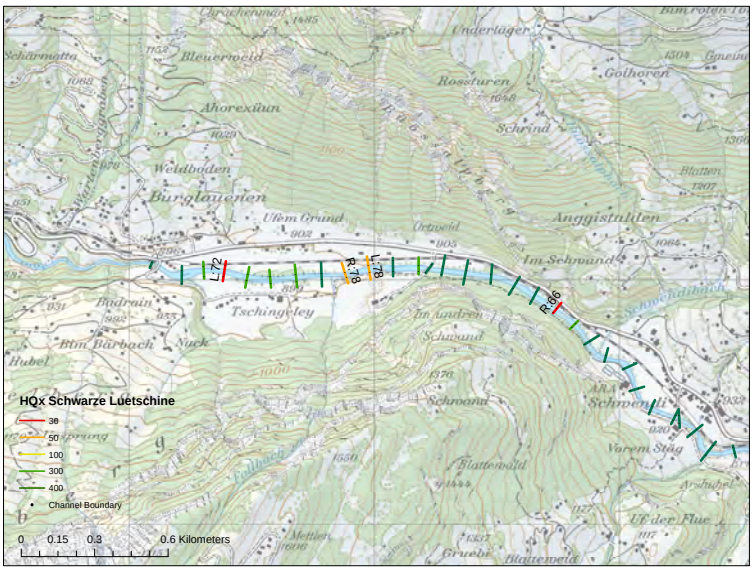

Figure 3.35: Weak points along the Schwarze Lütschine downstream of Grund

3.3.8 Weisse Lütschine

The four zones of low channel capacity along the Weisse Lütschine were attributed with high recurrence periods. As in the case of the other rivers, the magnitude of the return period varied from cross section to cross section (Fig. 3.36). The area which will be mostly overflowed is the surrounding of Brüggmatte and the area along the river course from Spiss to the cemetery in Lauterbrunnen (Fig. 3.37). For the first zone, the weak side was the left side, and for the second zone close to Lauterbrunnen, it was the right side. Both are populated areas. Most of the natural zones were not in danger. In the village of Lauterbrunnen, no risk potential was detected. Two further zones downstream of Lauterbrunnen were delineated. In the zones the frequency of flood events calculated for bank-full discharge is high. Most of the bank-full discharge values of these cross sections were below a HQ_{30} with no tendency for a weak side. Only a short part of that section is populated (Sandweidli). The last zone next to the RGS in Zweilütschinen showed a range of HQ_{30} to HQ_{50}. Next to the four zones the capacities were high and were not connected to a high frequency period.

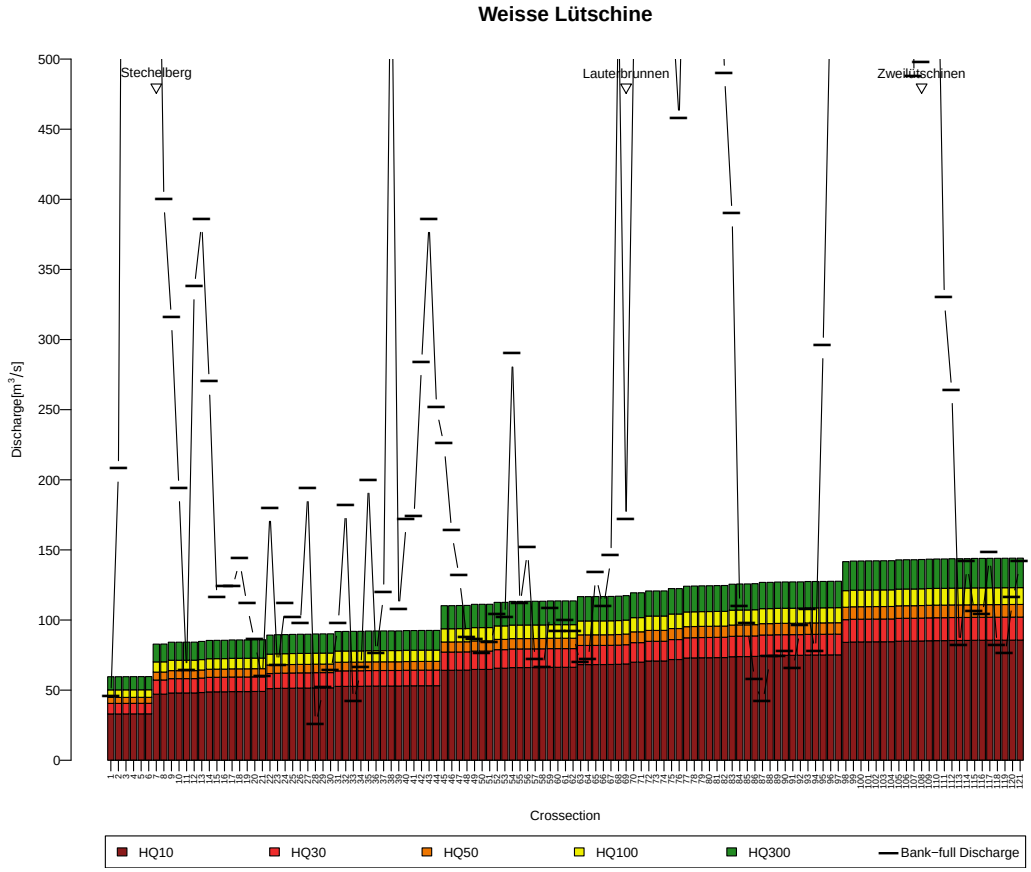

Figure 3.36: The HQ_{10} to HQ_{300} and the bank-full discharge for each cross section along the Weisse Lütschine

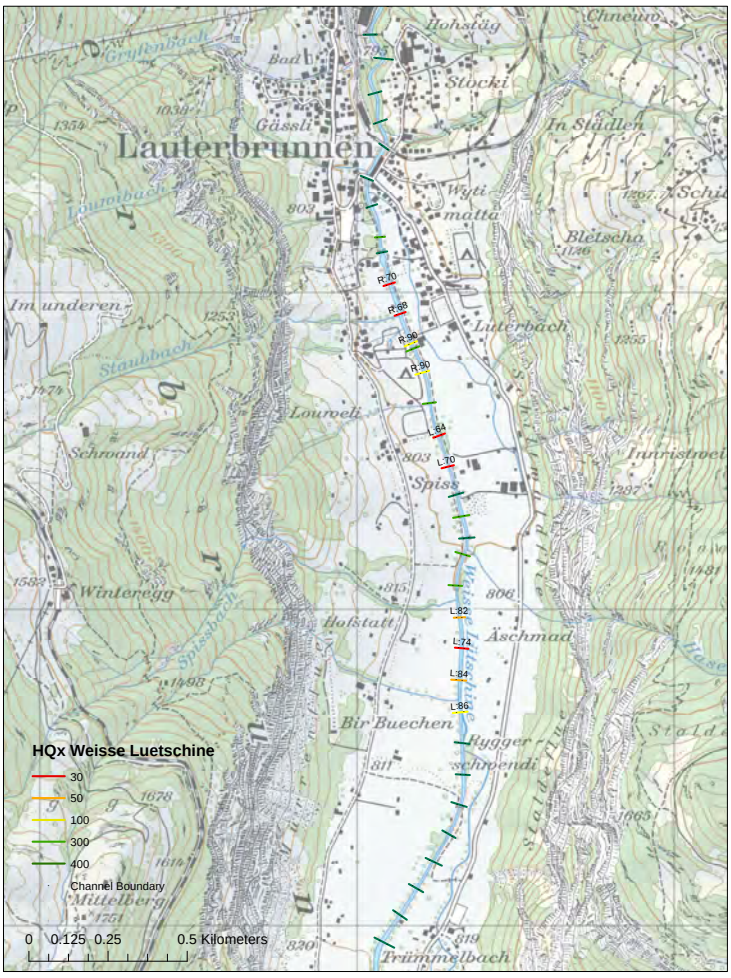

Figure 3.37: Weak points along the Weisse Lütschine next to Lauterbrunnen

3.3.9 Vereinte Lütschine

The Vereinte Lütschine exhibited weak points in the region downstream of Zweilütschinen, where the return period varied from HQ_{30} to HQ_{100}. The left bank side would be inundated (Fig. 3.38). The area where most of the inundation happens was located along the agriculture zone in front of Wilderswil and in Wilderswil itself (Fig. 3.39). Next to Böningen, the last zone of weak points was observed.

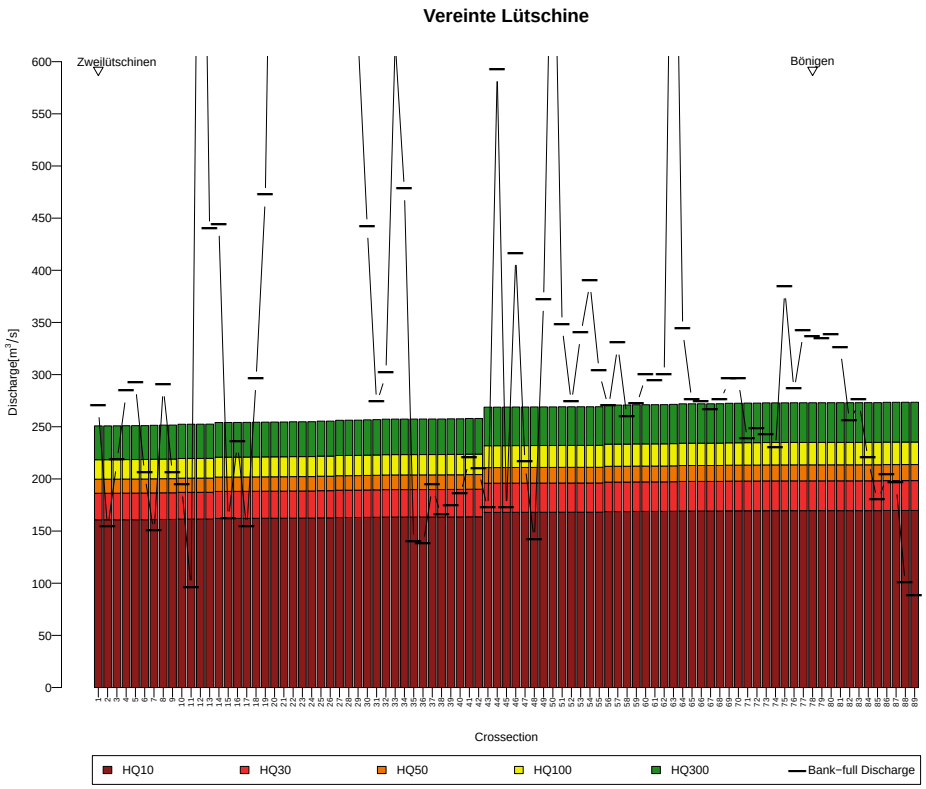

Figure 3.38: The HQ_{10} to HQ_{300} and the bank-full discharge for each cross section along the Vereinte Lütschine

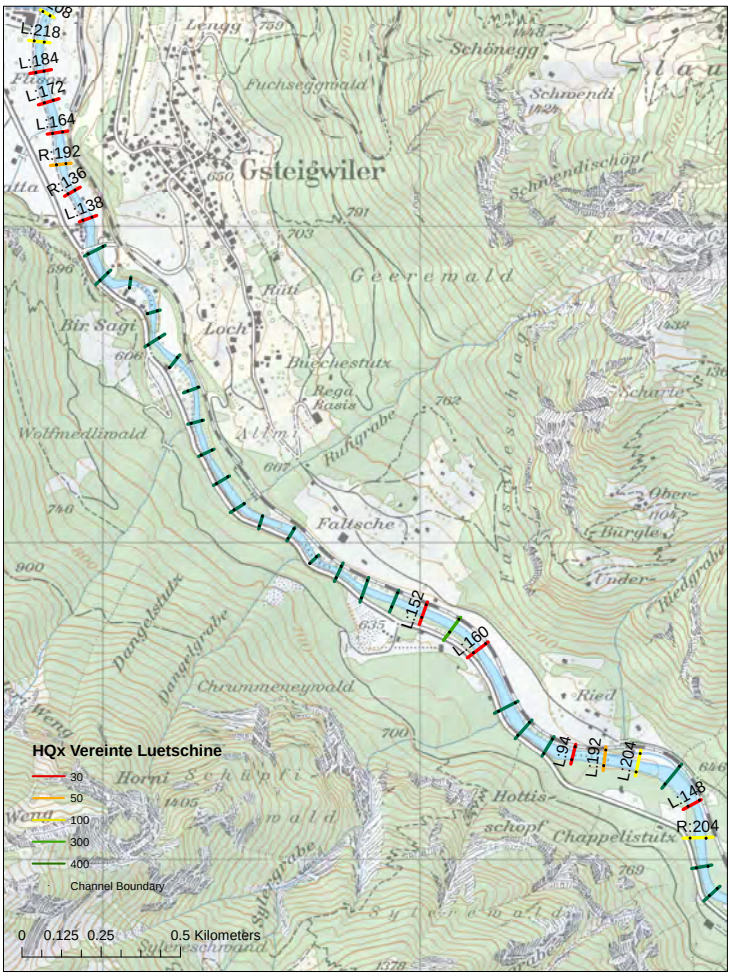

Figure 3.39: Weak points along the Vereinte Lütschine from Zweilütschinen to Wilderswil

3.3.10 Synthesis Map of the Main Rivers of the Bernese Oberland

Figure 3.40 shows the weak points of all rivers. The focus lies on small sections between all the cross sections. The sections are coloured according to the return period of the bank-full discharge of the cross sections. The main rivers are visible at a glance as also their weak points. It shows that the number of weak points along the rivers is very different. In the Simme, the Weisse Lütschine and the Hasliaare, the highest number of weak points relative to the number of cross sections was calculated. The very low value along the Aare in Bern are not considered in this map.

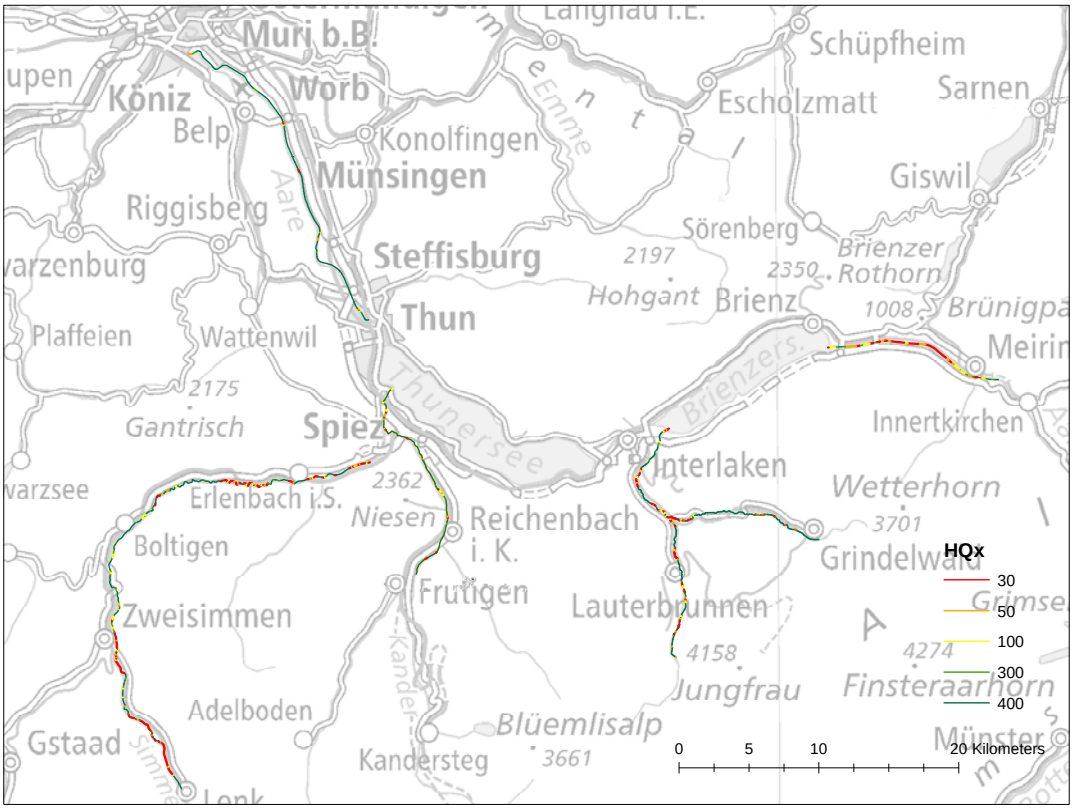

Figure 3.40: Weak points along the main rivers of the Bernese Oberland

3.4 Discussion

3.4.1 Floods with Return Periods of 10, 30, 100 and 300 Years

The results of the river sections showed that the estimated discharge values were different from river to river. The results drew a sketch of the individual characters of the rivers. It became evident that in all the river sections, the discharge increased from up- to downstream along the river. Differences in the magnitude of the increase can be explained with differences in the increase of the catchment sizes along the river a factor that is mainly determined by the catchment size of the tributaries. In comparison of the HQx_meso_CH method and the extrapolation method show that the mean values of HQx_meso_CH estimations were smaller than the extrapolated values at the reference points for the river Kander and Hasliaare, and larger for the Simme, the Vereinte Lütschine, Schwarze Lütschine and the Weisse Lütschine. The largest deviation was observed for the Schwarze Lütschine. There the extrapolated values were lower than all the values of all other methods. As mentioned, the values with a large deviation should not be considered to calculate the mean of the HQx_meso_CH results. However, in this study all values were considered in order to provide an overview over the differences. For this study area the Giub methods showed the smallest deviation from the reference values (RGS data) according to (Spreafico et al., 2003). For all river sections, it revealed a similar and constant pattern. The values were always rather low in comparison with the other methods.

The lower values of the extrapolation method compared to HQx_meso_CH estimations close to the origin of the Hasliaare, the Schwarze Lütschine, Weisse Lütschine could may be explained this way: First, the extrapolation method considers only the catchment size. Secondly, the extrapolation was conducted from RGS located downstream. Further, the water that inundated surrounding areas on the way down left the system border (river) and could not be considered even if in reality, it is likely to reappear further downstream. There is no data evidence for the amount of water flowing in the upper part of these rivers. Additionally, these three rivers are characterized by a very high percentage of glacial area leading to a greater amount of water flowing from the origin of the rivers. This was neither considered here, because in this analysis, the discharge value increase/ decrease according to the catchment size. The study site of the Simme also indicates that if more RGS were available, the interpolation would produce a more satisfying result closer to the HQx_meso_CH result in the origin.

The high deviation of some estimations of the HQx_meso_CH methods were caused by both limitations of the HQx_meso_CH tool and the employed method. The Hasliaare with a catchment size of 530 km^2 at reference point 2 is already out of the valid part for all methods. Therefore, the results of HQx_meso_CH tool for the Hasliaare should be interpreted carefully. Probably, decreasing values with increasing catchment sizes in the BaD7 method and the low values of the Kölla method may be due to too large catchment size.
This may also explain the extreme increase from reference point 4 to 5 along the river Simme of the BaD7 estimations because at this point, the catchment size exceeds 200 km^2. For further analyses it would be better to eliminate these values and recalculate the mean of the HQx_meso_CH methods.
Also, for the Vereinte Lütschine, the deviating values in the BaD7 and the Momenta method

is probably caused by the large catchment size, which is already 344 km^2 at the first reference point.

The intrinsic limitations within the estimation methods of the HQx_meso_CH tool may be responsible for some artefacts by the Kölla method at Hasliaare and at Weisse Lütschine. According to Spreafico et al. (2003), the method should not be applied to catchments with controversial parameter combinations like high percentage of glaciation or high percentage of urbanisation. The catchment of the Hasliaare shows 21% of glaciation (catchment Brienzwiler), and the Weisse Lütschine 17.4% (catchment Zweilütschine). The same weakness holds for the Momenta and the BaD7 method, thereby explaining the very high values along the Schwarze Lütschine. No satisfactory explanation could be found for the very low values of the Giub (Fn) method for the first three reference points in the case of the Kander and the lower values of the reference point 10 in comparison with reference point 9 along the Simme for the HQ_{100} and HQ_{300}.

To sum up, differences in the outcomes were related mainly to the limitations of each single method or to the implementation restrictions of HQx_meso_CH tool. Therefore, recalculating the mean with excluded outliers would most probably reproduce more similar HQx_meso_CH estimations and extrapolated values. However, if we consider the confidence band of the values at the RGS most of the estimated values lie inside of the range.

The estimations of the PREVAH_regHQ were always smaller than the extrapolated values. An exception to that are the higher values for the Schwarze Lütschine, which supports the hypothesis that the extrapolation based on the RGS in Gsteig alone is not sufficient to estimated the values along the Schwarze Lütschine. Comparing to the HQx_meso_CH methods and the PREVAH_regHQ method, the extrapolation method produced satisfactory results. The only river where the results should be questioned is the Schwarze Lütschine.

In the following, the results of this study are related to findings from other studies and technical reports.
For the Hasliaare, the determined discharge values of Hunzinger, Zarn, and Bezzola (2008) are slightly higher. They assessed HQ_{100} of 530 m^3/s next to Meiringen. The difference may be explained by their consideration of the barrier lake further upstream.

In the case of the Aare, the Aarewasser AG (2009) accounted for a HQ_{100} of 550 m^3/s before the Gürbe tributary, and 600 m^3/s afterwards. They raised the value due to the higher frequency of floods in the last years. In this thesis, values were interpolated between two FOEN RGS. This data basis is the same even though our discharge values were lower.

Along the Simme, the comparison of the attributed return period is difficult and complex since the technical reports based their calculation on heterogeneous approaches. The extrapolated HQ_{30} of this thesis for all possible points of comparison (Lenk, St. Stephan, Boltigen, Latterbach) are in a comparable range with the results of the technical reports by GEOTEST AG (2012), KH AG and KZ AG (2008) and EB AG (2008). However, the steps between the HQ_{30} and HQ_{100} as well as between HQ_{100} and HQ_{300} showed a larger spread in the technical reports. Next to Lenk, the values of GEOTEST AG (2012) are 70 m^3/s, 90 m^3/s and 115 m^3/s, and next to St. Stephan the HQ_{30}, HQ_{100} and HQ_{300} of KH AG and KZ AG (2008) amount to 103 m^3/s, 124 m^3/s and 145 m^3/s. The difference even increases further downstream. In Boltigen, EB AG (2008) determined HQ_{30}, HQ_{100} and HQ_{300} as 145 m^3/s, 219

m^3/s and 238 m^3/s. The steps between the HQ_x are larger than the values here proposed even though Boltigen is next to the Oberwil RGS and therefore, the values are expected to concord.
Compared to the result from KH AG (2005), who proposed values of 182 m^3/s, 225 m^3/s and 260 m^3/s next to Erlenbach, the values of the here presented study are lower. Downwards of the Chirel, the opposite holds: the values of this study are higher than the values from KH AG (2005). Higher values could be due to the fact, that the extrapolation of the HQ_x values is only based on the RGS data in Latterbach, which is far away from the point of interest.

The comparison with the study of Wehren (2010) for the upper part of the Kander showed an interesting pattern. In the river section, the values of Wehren (2010) are similar to our HQ_{30} but lower for the HQ_{100} and HQ_{300}. Although Wehren (2010) had a similar approach to the presented study, he used the RGS data next to Kandersteg and next to Frutigen and could therefore proceed to an interpolation. This may explain these differences. At the RGS next to Hondrich, the values of Wehren (2010) are higher, which is probably due to a shorter period of data that Wehren (2010) was using for modelling.
Further downstream at the junction of the Simme and the Kander, the values of this master thesis are comparable to the study of Wehren and Weingartner (2007). The HQ_x evaluation of the study of Wehren and Weingartner (2007) is based on extreme value statistics. Their data input is the combined daily data of the RGS located at Hondrich and Latterbach, where this study also retrieved data from. Depending on the percentage flow of each river, three scenarios are developed by then. The range of the three scenarios for the HQ_{100} lies between 535 and 671 m^3/s. Our values fit within that broad range. They did not valuate the different scenarios.

Regarding the Lütschine, a study of Naef and Lehmann (2012) pointed at the complexity of this catchment. The run-off formation is influenced by many parameters. The spatial distribution of precipitation is heterogeneous due to topography. Snow and glacial melting magnify the discharge, and the storage capacity of some areas is rather high. Therefore, the study of Naef and Lehmann (2012) presented higher HQ_{30}, HQ_{100} and HQ_{300} values of 72 m^3/s, 87 m^3/s and 117 m^3/s next to Grund. That study suggests that the extrapolated values of our study may have been underestimated, because the RGS in Gsteig is located downstream of the Schwarze Lütschine. It supports the assumption that for the Schwarze Lütschine, this RGS data alone is insufficient for reliable extrapolation. This finding should be kept in mind for the attribution of weak points.

Regarding the Weisse and Vereinte Lütschine, the results from Naef and Lehmann (2012) correspond well to the results of this study. Naef and Lehmann (2012) found 48 m^3/s, 72 m^3/s and 82m^3/s for HQ_{30}, HQ_{100} and HQ_{300} for Stechelberg along the Weisse Lütschine. In Zweilütschinen Naef and Lehmann (2012) found 195 m^3/s, 232 m^3/s and 251 m^3/s for HQ_{30}, HQ_{100} and HQ_{300} along the Vereinte Lütschine. The HQ_{100} of the Vereinte Lütschine is an exception with rather different values, probably due to the integration of past flood events.

In summary, the results of this thesis are in agreement with the mentioned technical reports, where the approaches were mostly also based on an extrapolation. Differences in the outcome could mostly be explained by the additional information considered in the analysis of

other studies. The results of this study are not in agreement for the river Simme, where the deviation for some sections is high. Along the Simme, no tendency for a global under-or overestimation in relation to other studies was noticed . The advantage of this study is that the $HQ_{30,100,300}$ are calculated for each measured cross section along the rivers and not just for section next to the communities, i.e. target of primary interest.
This approach is judged adequate, since it is in broad agreement with other studies. Further it is less complex because it is only based on one variable: the catchment size. Moreover, large areas can be cover quite quickly. All in all, this method proved to be satisfactory for reaching the formulated aim.

3.4.2 Bank-full Discharge of the Cross Section

The results showed that each river has its own characteristics. The variability along the cross sections and between the rivers can be backtracked to the geometry of the riverbed and consequently, the differences in the heights of the bank sides. The results depicted that all the rivers exhibited at least in some parts a low channel capacity relative to other values of this river. This indicate the existence of weak points.

A further output of the results is that there were two forms of low channel capacity: on one hand a conglomeration of multiple cross sections with low capacity, and on the other hand single cross sections with a much lower capacity than the other cross sections nearby. The patches can then again be subdivided in two groups, one with a high internal variability and one with constant low values. Additionally, the results showed that the capacity increased together with the flow kilometres as expected. Exceptions to the latter were the Aare next to Bern and the second part of the Schwarze Lütschine.

Most of the time, the existence of one single low channel capacity, meaning a potential weak point, could be related to the topographic conditions or a wrong definition of the bank-full height (channel boundary). For example the Aare, next to kilometre 2 (Fig. 3.20) exhibited low channel capacity due to the topographic condition, while two of three low values along the upper part of the Kander (Fig. 3.22) were caused by a wrong definition of the bank-full height.
Evidently, the magnitude of the bank-full discharge depends on the dimension of the rivers. Therefore the Aare, Hasliaare and the lower part of the Kander had the highest channel capacity relative to the other rivers. The lowest channel capacity was modelled for the Simme, the Weisse und Schwarze Lütschine relative to the other rivers.

The homogeneous bank side heights and the constant channel capacity of some parts of the rivers are caused by the anthropogenic influence to correct the river and to protect against flood. The affected rivers are the Hasliaare (Fig. 3.19) along the whole river, the Aare Thun-Bern for some parts mostly near Thun and Bern (Fig. 3.20) and the Weisse Lütschine upstream of Lauterbrunnen and next to Zweilütschinen (Fig. 3.23). The Schwarze Lütschine was corrected in the upper part and near Zweilütschinen (Fig. 3.24), and the Vereinte Lütschine after the projected area (Fig. 3.25). The Simme is regulated in the section after Lenk and afterwards at single patches (Fig. 3.21), and the Kander (Fig. 3.22) has corrected sections along the whole river. The Kander and the Schwarze Lütschine showed also a rather high variation of the bank-full discharge from cross section to cross section in the constructed

section. Even tough the sections are corrected, the bank-full discharge was lower than in the other parts of the river.
High channel capacity relative to the other cross sections in the Simme, the Kander after the junction and the Weisse Lütschine after Lauterbrunnen caused by the gorge character of those river sections. For the Aare, the high channel capacities instead are may be caused by the inflow of the Chiese or the changing kst-coefficients next to the inflow.

In contrast to this study, all the technical reports considered predominantly populated areas, such as communities along the river. Further they often used 2D model with inundation areas considered. In contrast to the 1D simulation the water can go out of the river channel, where the focus is on the capacity of each cross section.

According to the report of Hunzinger, Zarn, and Bezzola (2008), the bank-full discharge of the Hasliaare for the first section from Meiringen to Brienzwiler is lower than 400 m^3/s for some cross sections.
For the part next to Brienzwiler, no comparison could be made. The low values found in this study were probably caused by the definition of the bank-full height. In comparison to the next cross section, the height of the left dam is much lower, but probably the measured width was to short. During the field survey, it became evident that there is also a narrowing of the river. The calculated values are plausible and this can be supported by the measured kst-coefficient for Brienzwiler by Vischer (1983), which is between 30-34 (one value for the whole channel).

Along the Aare, next to Bern the values were close to the values of EB AG et al. (2014), where the simulation is based on the 1D model MORMO calibrated with the flood event of 2005. EB AG et al. (2014) determined the channel capacity of the Aare as 420 m^3/s next to Dählhölzli and Marzilibad. This study showed much lower values, too low to be plausible. Probably the disagreement, is caused by the possibly wrong determined slope at the last cross section in the Basement simulation of this study, which have also a influence on the calibration process. Additionally, Aarewasser AG (2009) validated their model with the flood marks of 2005 with an input of a HQ_{100} 550m^3/s. Cross sections with a low bank-full discharge were identified two kilometres after the outflow of the lake of Thun (next to the RGS) and in Jaberg. Those points were also identified in this study. However, the potential weak points from Wichtrach to Münsigen and the one in Muri Bad were not found in the here presented model. A possible explanation for this could be the resolution of the measured cross sections used in this study, because there is no cross section next to the Muri Bad, and the distance between the cross sections is 200 m. Interestingly, after Münsigen, next to the Hunzigerbrücke, and between Belp and Muri, the potential weak points of the technical report are not only identified here, but they also agree in the magnitude of the capacity.

The Simme river is the longest of the analysed rivers and probably the most complex. Other studies examined only specific sections along the river including Lenk, St.Stephan, Boltigen and Diemtigen. No study considered the whole course of the river as this thesis did.
GEOTEST AG (2012) simulated the section Lenk with the model HEC-RAS that is based on cross sections of the risk prevention measurement campaign 2005. The estimation of the bank-full discharge of GEOTEST AG (2012) was between 50 m^3/s and 80 m^3/s from Sagisstrasse to Lischmatte, and up to the Schadaulibrücke, even lower. From Sagisstrasse to Lischmatte, the results of this study are slightly higher. Further downstream, our values

were lower, where GEOTEST AG (2012) predicted rising values. This is an interesting difference as both simulation were based on two kst-coefficients for the whole section. All in all, the two studies agree that for the whole section the channel capacity is low.
The upper stream part of St. Stephan was analysed by KH AG and KZ AG (2008) with the Software FLUMEN 2D. The overflowing occurs in Niderdorf on 75 m^3/s, similar to the result of this study. Further downstream, in the south of Matte, KH AG and KZ AG (2008) concluded that the capacity slightly increases. This concords with the results of this study (90 m^3/s).
Downstream of St. Stephan, the potential weak points are located in the north of Ried with a capacity between 120 m^3/s and 140 m^3/s according to the simulation of Mosimann (2015a) and KH AG and KZ AG (2008). The results are in a broader agreement with this study. At the end of a sharp S-curve upstream of Blankenburg, the presented study showed much lower values than Mosimann (2015a). The difference cannot be caused by the definition of the channel boundary.
For the region of Zweisimmen, the simulation in Basement again showed lower bank-full discharge values upstream and but higher values downstream of the kleine Simme inflow in comparison to Mosimann (2015a). He detected inundation by input discharge of 70 m^3/s (50 m^3/s in our study next to the RGS where we calibrated our model) for some points upstream, and downstream of 110 m^3/s (compared to 120 m^3/s in our study). The deviation of approximately 20 m^3/s at the upstream point in Zweisimmen is quite large. Because our model was calibrated close to there, we would not have expected such a deviation. The report of geo7 AG and KH AG (2004) calculated a deficit left side of the channel after the Kleine Simme inflow, next to the camping and next to Galgenbühl, for the first two by a capacity of 120 m^3/s and for the third of 150 m^3/s. These three points were modelled here, too, but the capacity of the last point was lower than at the second point. The simulation output of this study showed that the second cross section had its weak point on the right side. This could be explained by the definition of the bank-full height. The potential weak point next to the ARA in Grubenwald cannot be compared because there is no study considering this section.
For the section Weissenbach, the analysis of the EB AG (2008) report based on a simulation in HEC-RAS concluded that the channel capacity is below 175 m^3/s and that the capacity is lower in Weissenbach than in Reidenbach (EB AG, 2008; Mosimann, 2015a). These propositions were confirmed by this study. According to EB AG (2008), the river section in Boltigen had at least a capacity of 200 m^3/s and after Boltigen the bank-full discharge is around 215 m^3/s. The evaluated bank-full discharge for this study is lower with 160 m^3/s in front of Boltigen.
An analysis of the section between Boltigen and Erlenbach was not found in any of the reports probably because of the gorge character of the section. The results of this study showed low values. A reason for this could be that the foreland is not include in definition of the bank-full height of this study.
For Erlenbach, Mosimann (2015a) and KH AG (2005) found lower capacity values around the village. That outer part of the village, Blauweg, Au Allmi and Wilerau, exhibited a capacity of 180 m^3/s, while in the center, a capacity of 220 m^3/s was modelled. These potential weak points were also identified in the analysis of this study, but the values were lower. The lowest values were located in front of the barrier lake, in Au Allmi and Wilerau.
In Latterbach, the values of this study were lower than described in the report (KH AG,

2005), especially close to the barrier lake. This may be due to the fact that the lake is not considered in the simulations of this study.
To sum up, in terms of the Simme there is no clear trend of over- and underestimation of the channel capacity of this study with regard to the literature values. Rather, it differs between the section. Those differences may be caused by the division of the river for the calibration and the evaluated kst-coefficients in this study. Along the section Boltigen und Diemtigen, the agreement is higher. In conclusion, the 1D simulations did not lead to the same results as literature. However, the whole river could be simulated.

For the Kander, a comparison was conducted with HZP AG and EB AG (2007). They applied the REC-RAS 2D model over the course from Blausee to the outlet with a calibration as well as a validation. Therefore the results should be reliable. The possible weak points were located at Schwendi-Ey, Kien (approximately 170 m^3/s), where the values of this study were 70 m^3/s higher. Additionally, one in Kiene was only identified because the bank-full height was wrong determined there. The higher values in this study could be caused by the calibrated kst-coefficients downstream in Hondrich, which are high. Further downstream, the potential weak points are located between Reichenbach and Müelenen and next to Bad Heustrich, associated with values of 230 m^3/s to 300 m^3/s. These values are in similar range as the results of this study. The Kander exhibited no more potential weak points after the joining because it flows in a depression caused by the Kander tunnel (Mueller, 2009). In this study potential weak points appeared. They were determined by the definition of the bank-full height with no consideration about a potential of danger.

The course of the Schwarze Lütschine in the upper part next to Grund had a very low capacity along the whole part according to the technical report of MW AG (2014), which conducted a 1D simulation with HEC-RAS. The calculated capacity was between 70 m^3/s and 110 m^3/s. To compare, the lowest value of this study were slightly higher than the lower boundary of the technical report. As mentioned, no RGS data were available and the kst-coefficients were transferred from the Vereinte Lütschine. They are still similar to the used value (25) in the study of MW AG (2014). Downstream, only single potential weak points were evaluated in this study. Most of the times, they were caused by the definition of the bank-full height, without integrating the foreland. An exception of this is the one next to Zweilütschinen.

For the Weisse Lütschine around Lauterbrunnen GEOTEST AG and PORTA group (2014) showed a very similar pattern. Their simulation was run with HEC-RAS (2D) and the input discharge was 77 m^3/s. The inundation areas were found to be lie front of Loweli, the camping side and Äschmad. This study showed slightly lower values for the three potential weak points. According to FAN and KOHS (2015), a discharge of 48 m^3/s cannot pass below Matte and next to Lengwald. In this study, only the cross section below Matte showed a low channel capacity.

For the upper part of Vereinte Lütschine, where the protected area is located, no literature data was found. The potential weak points are probably again caused by the definition of the bank-full height. In this part of the river, floods are even intended for the purpose of nature preservation. IG Flussbau AG (2012) pointed out regions with low channel capacity with bank-full discharge of 100 m^3/s to 175 m^3/s along the agricultural zone Eyli, of 125 m^3/s to 150 m^3/s at the Gsteigwilerbrücke and along agricultural zone Flisou. This thesis

evaluated values in a similar range for the Gsteigwilerbrücke but not for the upper Eyli. Probably, due to the distribution of the cross sections along this river section, no cross section was measured at the narrow point. In Wilderswi, IG Flussbau AG (2012) calculated a capacity of around 300 m^3/s, much higher than the values of this study. Probably, this is again caused by the definition of the bank-full height. As the field survey indicated, high constructions were built to protect against floods along the river in the village. Thereby, it is not possible to have low channel capacity there.
Downstream of Wilderswil, next to RUAG, the capacity was again lower compared to the results of this thesis, with only 140 m^3/s to 190 m^3/s as compared to 200 m^3/s to 250 m^3/s. Along the last part in Bönigen, the calculated capacity by IG Flussbau AG (2012) was between 150 m^3/s and 220 m^3/s. The results of this study showed rather similar values for the upper part, and for the last part, the values are lower.

To sum up, the general pattern of the different rivers and their potential weak points could be identified with the method here applied. For most of the rivers, the pattern along the river was similar to what was found in literature. Mainly, along one river, small over- or underestimation as compared with the literature data was noticed. An exception occurs in the case of the Simme. It was rather intricate to detect a general pattern in the comparison between this study and the other conducted studies.

As explained, possible general reasons for the deviations between the values of this study and the others are: the definition of the bank-full height, the representativeness of the model as also geographical resolution and the calibration, that is, kst-coefficients.
The bank-full height determination is often responsible for the appearance of single low values.
The resolution of the river channel, depending on the number of measured cross sections in the model, could hold as a reason for the absence of some potential weak points. This possibly holds for the Vereinte Lütschine close to Eyli, the Muri Bad, the missing of the swells along the Kander and the barrier lake in Erlenbach and Latterbach. That is, not all important points (like a narrowing spot) along the rivers are represented in the model, and therefore, it is not possible to compare locations at some points. As showed in table 3.1, the resolution is different from river to river. The highest average resolution was achieved for the Kander and the Weisse Lütschine. As mentioned in section 3.2, it is recommended to keep the distance between the cross sections below 100 m. The average resolution of the here conducted analysis of the river sections can fulfil this recommendation. The Hasliaare with 220 m however poses an exception, but there the river bed is very homogeneous as explained.
The representation of the channel probably caused the low channel capacity at the end of most of the river sections as lakes are not included in the simulations. This is just a rough guess and its explanation lies outside of the scope of this study. Therefore the results of those cross sections have to be taken carefully.

Figure 3.18 in section 3.3.2.1 pointed at the difficulty to name the uncertainty of the calibrated kst-coefficient generally accepted for all the rivers. The effect of the kst-coefficients depend on the geometry (width and depth) and on the slope of the rivers. The change of the water level is different for each scaling up of the kst-coefficient (Fig. 3.18 left side). It illustrates that the increase of the kst-coefficient by 5 had a large influence on the water level in both cases (RGS Thun and RGS Zweilütschinen). Comparing the calibrated kst-coefficients

to other studies, they concorded rather well. The studies evaluated the following values: Schwarze Lütschine M = 18-25 (MW AG, 2014), Vereinte Lütschine M = 21.5-23.3 (measured values)(Vischer, 1983) and Hasliaare M = 30-34 (Vischer, 1983). In the models for the Simme, the used kst-coefficients for the Lenk were M = 25, 31, 25, and at St.Stephan, the coefficient was set to M = 30.
For the Kander, HZP AG and EB AG (2007) found the kst-coefficient to be 32 in the channel and 25-28 for the bank side. This values were also proposed to hold for the part of the Aare between Wichtrach and Münsigen. There, the calibrated values were probably the main reason for the deviations. One has to kept in mind that the calibrated values in the first place represent a kind of average condition along the river. The deviation of the values at the Aare between Wichtrach and Münsingen and the strongly deviating values along the Kander could be explained by the latter averaging of the conditions. Because the section Wichtrach-Münsigen is already at some parts renaturated, it exhibits other condition than those next to RGS Schönau or along the other parts (Fig. 3.41). All in all, the calibrated values in Bern, Schönau have to be questioned because the kst-coefficients were too high.

Figure 3.41: Aare: Wichtrach-Münsingen (left) and RGS Schönau (right)

The cross section where the calibration of the Kander was conducted is located in a complex morphological environment. This may have posed some problems for the implementation in Basement. There are three consecutive swells. This is difficult to represent in Basement (Fig. 3.42 left side). For a better representation, further cross sections were integrated. However, the river section of the site is heavily constructed not only at the bank side, but also at the channel. Therefore, the values here obtained are probably too high to represent the whole river (Fig. 3.42 right side). Additionally, there are a lot of swells along the Kander and mostly, they could not be represented in the model.

Figure 3.42: Kander upstreams (left) and downstream (right)

Considering the methodological approach to apply the calibrated values over the whole river or section, the results showed reasonable and plausible discharge values, except for some parts along the Kander and Aare Thun-Bern in comparison to other studies. Further the chosen kst-coefficients for the simulation were similar to the ones of other studies and the determination in the field. The deviation caused by the kst-coefficients varies from river to river and probably even from cross section to cross section. Therefore, deviation could not be generally explained. All in all, the methodological approach is straightforward and allows for large-scale analysis.

3.4.3 Weak Points

The results from the section 3.3.1 and section 3.3.2 are combined to yield the probability of flooding at potential weak points along the rivers. Thereby, weak points are identified. The results showed that most of the cross sections exhibiting lowest channel capacities were attributed with low return periods. An exception to that were the Kander and the upper part of the Lütschine, where the channel capacity was only at a few cross sections low enough to be attributed with a high probability of occurrence.

The field survey helped to classify the weak points within a certain range in terms of morphological conditions. Most of the cross sections with a low capacity are just at the edge of a curve, a narrowing of the river or at a steeper slope, where the flow accelerates mostly near bridges. Even though bridges can not be modelled in Basement, the effects at topography can be observed, if a cross section was measured next to the bridge.

The Hasliaare appeared as a river with a lot of weak points in the simulated results, and the probability of occurrence of the bank-full discharge was high for most of the cross sections. The upper part of the Simme and the surroundings of Erlenbach exhibited a lot of weak points with a high probability of occurrence even though both the parts of Hasliaare and Simme were already protected against flood by construction measure. The technical reports of these river sections do confirm the occurrence of those weak points.

For the Hasliaare, the values of this study are probably not valid anymore, because new constructions are under progress in the upper part. The results of the Simme have to be interpreted carefully because (as mentioned in section 3.4.2 and 3.4.1) it was very difficult to determine the bank-full discharge in comparison with the literature data. Upstream, the HQ_x here modelled was lower than in the consulted literature and after the inflow of the Chirel, it was higher. The lower values led to an attribution with higher return periods, that is to a weaker estimation of danger, and vice versa. The position of weak points however was in agreement with the other studies.

In section 3.4.2, it was concluded that the situation next to the calibration cross section was difficult to represent for the Kander because of the swells. Consequently, the calibration probably result in too high kst-coefficients and caused too high bank-full discharge values. The bank-full discharge was higher then in the consulted literature, and the return period is lower.

For the Schwarze Lütschine the calculated values for the HQ_x were lower compared to the estimated discharge value with the HQx_meso_CH tool and the results of Naef and Lehmann (2012). Consequently, the calculated channel capacity along Grund was attributed with an HQ_{100} according to Naef and Lehmann (2012). This differs from the analysis of this study, which for this part of the river did not identify danger of floods.

Provided that the results of the technical report are generally valid, the Aare Thun-Bern would exhibit more weak points than identified in this study, especially in the upper reaches and the lower course next to Bern. An explanation could be the higher expected values for the HQ_{100} of Aarewasser AG (2009). However note that the discharge values in Bern after Schönau in this study in contrast are to low.

It is remarkable that the protection aim of HQ_{100} along the populated areas is not hold along the Weisse Lütschine, the Aare in Thun and Bern and at some parts of the Simme according to the results of this study. However, the results showed that channel capacities with high frequencies of occurrence are located along unpopulated areas.

Despite the explained exceptions, the proposed approach of the extrapolation and simulations in Basement was able to produce results in agreement with other studies. It also managed to represent weak points and their associated return period along the main rivers of the Bernese Oberland in a broader agreement with the other studies.

3.5 Conclusion

This study aimed at assessing the weak points for floods and their associated return periods along the main rivers (Hasliaare, Aare Thun-Bern, Simme, Kander and Lütschine) of the Bernese Oberland. It was based on each single measured cross section. In contrast to past studies in the field of flood assessments and hydrodynamic modelling in Switzerland, focusing on small-scale catchments, this study applied a consistent approach to all the rivers on a large scale. Thereby, a comparison between different rivers was made possible.

First, the HQ_{30}, HQ_{100} and HQ_{300} were evaluated for each cross section based on the extrapolation or interpolation of the available HQ_{10}, HQ_{30}, HQ_{50}, HQ_{100} and HQ_{300} data next to a RGS. The discharge rate at a station was calculated and multiplied with the catchment size of the considered cross sections. Additionally, for the purpose of validation, the HQ_{30}, HQ_{100} and HQ_{300} were calculated with the methods of HQx_meso_CH and the PREVAH_regHQ for some chosen reference points.
Secondly, bank-full discharge representing the channel capacity was calculated by applying the 1D hydrodynamic model Basement to each river section. The advantage of using Basement instead of calculating the channel capacity for every cross section individually is that back water effects are included and different kst-coefficients are applicable to one cross section. The bank-full discharge was determined as the height where the associated water level reached the height of the manually pre-defined active range (channel boundary).The calibration of the model was conducted on the kst-coefficients. It was calibrated at the cross section next to the RGS, where the stage-discharge relation of a high discharge was available. The calibrated values were applied over the whole river. Lastly, the two parameter were combined to create a map indicating the weak points and their associated return period.

The results of the evaluation of the HQ_x for each cross section showed that the used method of extrapolation provided results in agreement with the method of HQx_meso_CH and the PREVAH_regHQ. The results of this method were more constant than the reference methods, since such a large study site was considered. The method is rather simple to apply because it considers only one variable, the catchment size. The magnitude and direction of the deviation of the approaches were different from river to river. One cause for these variable deviation pattern could be the position and the number of RGS along a river (the higher upstream and the higher in number, the better). Another cause could may ground in the limitation of the HQx_meso_CH tools and its methods. The output was in a broad agreement with other conducted studies, with some exceptions. Other studies mostly used an extrapolation and included additional information, but they were restricted to small study areas. It has to be kept in mind that there is no single true approach to this problem and that there are large uncertainties difficult to define.

For the determination of the bank-full discharges the variability along the cross sections and between the rivers could be backtracked to the geometry of the riverbed, namely the difference in the height and width of the bank sides. But, the appearance of low channel capacity is not only driven by the geometry but also by the resolution of the cross sections along the river. The model of each river could achieve results in broader line with other studies. Reasons for lower or higher values as compared to the literature may be the manually defined bank-full height (channel boundary), the resolution along the rivers (some important points

can be missing) and the calibration process. The disagreements between the here produced results and the literature differed from river to river and could not be generalized.

The output map locates the weak points attributed with the associated return period for the main rivers in the Bernese Oberland. Some already constructed areas are attributed with a low return period, and some populated areas are not protected against floods with a return period of 100 years.

The here chosen method might be of interest for the ongoing research. In contrast to current practice, this study evaluated the HQ_x along the whole river and not just along sections of interest (such as populated areas). Further, it has shown that this approach is applicable to whole watersheds and different rivers, something that was not practised in the studies here consulted, as they were concerned with a specific section of one river only. The outcome was a map of the Bernese Oberland showing the weak points of the whole area based on one single approach. It is thus not a conjunction of methodologically different approaches, but a study based on a universally applied method. One obvious advantage is that this facilitates the comparison between different rivers. It can be regarded as an extension to the today used approaches. In comparison to other approaches, here the whole river can be seen at once. Protective construction measures against floods can be evaluated in terms of newly occurring downstream weak points. In the herein used 1D simulation the water is kept in the river channel and no water leaves the system. In a 2D simulation the water leaves the system and inundates the surrounding, which means that the water overflows at the first weak point and is missing further downstream. This would be the naturally occurring phenomena that is not considered in this study. Therefore every potential weak point along a river can be identified. The time saving 1D simulation and the provided data by FOEN are advantages that allow for an easy application to other rivers. Thereby, a better comparison between other rivers and other regions may be rendered possible. It allows to start the analysis from large scale and than go in to detail based on the gained information of the large scale analysis. Furthermore, the comparison with results from the literature showed that the approach delivers reliable results.

However, the approach has a number of limitations that should be kept in mind when interpreting the results. First, HQ_x estimations have a very high uncertainty range, which could not be determined in this study. Secondly, the developed models in Basement were only calibrated and not validated because this reached beyond the scope of this study. Here, the comparison with results from literature had to serve as a plausibility test. Thirdly, the resolution of the rivers depended on the measured data, that is, not every important change was depicted, and the distances between the cross sections was variable. Further, the result are valid only for for the time of measurement of the cross sections. Also, there is an inherent weakness to the calibration itself, as no uncertainty range could be calculated. Lastly, the calibration over the whole river is an averaging of the morphological condition (kst-coefficient condition) along the whole river.

Considering the above outlined results and limitations, it is recommended to further investigate into the validation of the model. This may be done with existing high flood marks along some of the rivers in order to test the accuracy of the approach. In close relation to the latter point, the different possible calibration approaches should be tested. Thereby, a sensitivity analysis of the calibrations may be performed. An interesting topic to follow up

would be to track back the changes in the riverbed over the years, as with the cross section measurement campaign done iteratively over the years, historical data is available.

Chapter 4

Final Conclusion

This study aimed at improving hydrological understanding of the water flow in the two case study regions, Kenya and Switzerland, by applying hydrodynamic modeling to river flow. For both case studies, the hydrodynamic model Basement was the central tool used to satisfy both their specific aims. The Basechain model could be adapted to the peculiarities of the two case study and thereby, the research goals for both case studies could achieved despite of very different initial data requirements and initial knowledge of the hydrology of the two regions.

The results of the case study in the lower Ewaso Ng'iro Basin in Kenya showed that hydrodynamic modelling with 1D simulations in Basement could establish stage-discharge relations for the four river sites with a minimum of data collected during the field survey. It thereby provided basic and useful knowledge that permits to analyse the converted discharge from the measured water level and it permitted first calculation of the channel capacity based on the established rating curve functions. Fundamental question of hydrology, as 'how much water is approximately flowing and for how many days?' were in a first approach answered for the lower Ewaso Ng'iro Basin and its rivers. It may be an interesting approach to follow up for other rivers. However, one should keep in mind the geometric uncertainties caused by, in our case, the sandy river bed, which influence mainly the accuracy of the low flow measurements.

The case study in the Bernese Oberland intended to apply a hydrodynamic approach to evaluate the bank-full discharge for each measured cross section and to relate it to probabilities of flood events. Further, with the approach chosen, the channel capacity along a whole river could be taken into consideration, as opposed to analyses focussing on single sections. The weak points were identified by, methodologically speaking, a synergy of hydrodynamic modelling with hydrology knowledge. Basechain, a hydrodynamic model, could be applied to such a large study site, as a RGS monitoring network already exists and the cross section geometry along those rivers were already measured, that is because the hydrological condition of the area of interest was already known. Looking at the quality of the herewith produced results, it seems reasonable to aim at gaining knowledge of weak points along rivers with a similar data availability by the here proposed approach.

This study supports the statement of the developer of the Software Vetsch et al. (2015b) that it may be a useful tool for very different purposes. Some of the advantages Basement provides are, first, that the influence of one cross section to the other can be considered (back water effect), as compared to calculating the river flow individually for each cross section,

and secondly, that it is easier to implement more than one friction coefficient along one cross section.

The model for the second case study could be calibrated to a measured value of the discharge, as the availability of data was high for the Bernese Oberland. In contrast to that, for Kenya only a prediction of the river flow and channel capacity was possible. Even if the inquiries differed in their methodological progress from prediction to calibration and, eventually, validation, the Kenya case study being located at the first, the Swiss case study at the second grade, they could both make a first step into answering their respective questions. For Kenya, if water flows, knowledge of how much is to be expected and an idea of how high is the channel capacity is of great interest. Whilst for Switzerland, for high flows it is interesting to know where the river is likely to leave its bed. The here proposed result may be regarded as first steps in hydrodynamic modeling and understanding of the channel capacity of the river sites in the lower Ewaso Ng'iro Basin and as further steps towards more comprehensive understanding of weak points in the Bernese Oberland.

Appendix A

Field Survey

Field Sheet

Fieldsheet survey in the Ewaso Ng'rio Basin

site	coordinate	lattitude	longitude	Datum

Collimeter method

Point Aspect	horizontal distance		Staff reading			Elevation			Remark
	dumpy	tape	BS	Height of Instrument	FS	Ini RL	Adj	Adj RL	
Datum									

Figure A.1: Field sheet to apply the dumpy level method to the river sites

Table to Determined Roughness Coefficients

Gerinnetypen	k_{St} [$m^{1/3}/s$]
Erdkanäle	
Erdkanäle in festem Material, glatt	60
Erdkanäle in festem Sand mit etwas Ton oder Schotter	50
Erdkanäle mit Sohle aus Sand und Kies mit gepflasterten Böschungen	45–50
Erdkanäle aus Feinkies, etwa 10/20/30 mm	45
Erdkanäle aus mittlerem Kies, etwa 20/40/60 mm	40
Erdkanäle aus Grobkies, etwa 50/100/150 mm	35
Erdkanäle aus scholligem Lehm	30
Erdkanäle, mit groben Steinen angelegt	25–30
Erdkanäle aus Sand, Lehm oder Kies, stark bewachsen	20–25
Felskanäle	
Mittelgrober Felsausbruch	25–30
Felsausbruch bei sorgfältiger Sprengung	20–25
Sehr grober Felsausbruch, große Unregelmäßigkeiten	15–20
Gemauerte Kanäle	
Kanäle aus Ziegelmauerwerk, Ziegel, auch Klinker, gut gefugt	80
Bruchsteinmauerwerk	70–80
Kanäle aus Mauerwerk (normal)	60
Normales (gutes) Bruchsteinmauerwerk, behauene Steine	60
Grobes Bruchsteinmauerwerk, Steine nur grob behauen	50
Bruchsteinwände, gepflasterte Böschungen mit Sohle aus Sand und Kies	45–50
Betonkanäle	
Zementglattstrich	100
Beton bei Verwendung von Stahlschalung	90–100
Glattverputz	90–95
Beton geglättet	90
Gute Verschalung, glatter unversehrter Zementputz, glatter Beton	80–90
Beton bei Verwendung von Holzschalung, ohne Verputz	65–70
Stampfbeton mit glatter Oberfläche	60–65
Alter Beton, unebene Flächen	60
Betonschalen mit 150-200 kg Zement je m^3, je nach Alter u. Ausführung	50–60
Grobe Betonauskleidung	55
Ungleichmäßige Betonflächen	50
Holzgerinne	
Neue glatte Gerinne	95
Gehobelte, gut gefügte Bretter	90
Ungehobelte Bretter	80
Ältere Holzgerinne	65–70
Blechgerinne	
Glatte Rohre mit versenkten Nietköpfen	90–95
Neue gußeiserne Rohre	90
Genietete Rohre, Niete nicht versenkt, im Umfang mehrmals überlappt	65–70
Natürliche Wasserläufe	
Natürliche Flußbetten mit fester Sohle, ohne Unregelmäßigkeiten	40
Natürliche Flußbetten mit mäßigem Geschiebe	33–35
Natürliche Flußbetten, verkrautet	30–35
Natürliche Flußbetten mit Geröll und Unregelmäßigkeiten	30
Natürliche Flußbetten, stark geschiebeführend	28
Wildbäche mit grobem Geröll (kopfgroße Steine) bei ruhendem Geschiebe	25–28
Wildbäche mit grobem Geröll, bei in Bewegung befindlichem Geschiebe	19–22

Figure A.2: Strickler-Coefficient for applying the MSE according to Naudscher, 1987 (Uni Karlsruhe, 2016)

Appendix B

Cross Section Information

Hasliaare

Crosssection	Distance	Z_left_dam	Z_right_dam	Waterlevel	Discharge	Bank side	HQ30	HQ50	HQ100	HQ300	Category
370002	0	607.47	0	607.47	596	L	322.3	368.8	442.24	589.11	400
370003	247.74	605.11	0	605.11	504	L	322.44	368.97	442.44	589.38	300
370004	498.02	604.14	0	604.14	452	L	323.18	369.81	443.45	590.72	300
370005	585.32	0	604.19	604.2	670	R	323.21	369.85	443.49	590.78	400
370006	746.06	602.75	0	602.75	474	L	323.27	369.92	443.57	590.88	300
370007	994.19	601.43	0	601.44	382	L	323.57	370.26	443.99	591.44	100
370008	1245.58	0	600.06	600.06	370	R	323.62	370.32	444.06	591.54	50
370009	1303.79	0	601.53	601.53	1138	R	339.36	388.34	465.66	620.31	400
370010	1495.37	0	598.57	598.57	334	R	339.4	388.38	465.71	620.38	30
370011	1745.92	0	597.98	597.98	542	R	339.46	388.45	465.79	620.49	300
370012	1983.25	596.38	0	596.38	356	L	339.49	388.48	465.83	620.53	50
370013	2240.53	0	595.78	595.78	544	R	377.04	431.45	517.36	689.18	300
370014	2489.47	0	594.59	594.59	506	R	378.68	433.32	519.6	692.17	100
370015	2737.6	0	593.6	593.6	450	R	378.75	433.41	519.7	692.3	100
370016	2887.17	0	593.15	593.16	542	R	378.79	433.45	519.75	692.37	300
370017	2987.49	592.51	0	592.51	442	L	378.83	433.5	519.81	692.44	100
370018	3238.34	591.6	0	591.6	440	L	378.88	433.56	519.88	692.54	100
370019	3487.98	590.64	0	590.64	392	L	378.99	433.67	520.03	692.73	50
370020	3735.13	589.64	0	589.64	378	L	379.09	433.8	520.17	692.93	30
370021	3986.41	588.82	0	588.82	412	L	379.15	433.86	520.25	693.03	50
370022	4237	587.89	0	587.89	376	L	379.19	433.91	520.31	693.11	30
370023	4486.73	0	586.94	586.94	352	R	379.23	433.96	520.37	693.18	30
370024	4737.2	0	585.99	585.99	360	R	379.29	434.02	520.44	693.28	30
370025	4986.94	0	585	585	326	R	379.32	434.06	520.49	693.35	30
370026	5237.44	0	584.34	584.34	356	R	379.37	434.11	520.55	693.42	30
370027	5490.37	0	583.56	583.56	366	R	379.42	434.17	520.62	693.52	30
370028	5742.23	582.67	0	582.68	348	L	379.47	434.22	520.69	693.61	30
370029	5997.39	582.07	0	582.07	386	L	379.5	434.27	520.74	693.68	50
370030	6249.62	581.29	0	581.29	394	L	391.04	447.47	536.57	714.77	50
370031	6499.25	0	580.49	580.49	356	R	391.11	447.55	536.67	714.9	30
370032	6749.8	0	579.86	579.86	368	R	391.17	447.62	536.75	715.01	30
370033	6998.48	579.15	0	579.16	350	L	392.52	449.16	538.59	717.46	30
370034	7248.3	578.73	0	578.73	406	L	392.69	449.36	538.83	717.78	50
370035	7305.49	0	579.11	579.11	484	R	392.78	449.46	538.95	717.94	100
370036	7513.1	0	577.83	577.84	324	R	392.88	449.58	539.09	718.13	30
370037	7761.53	0	577.41	577.41	356	R	393.05	449.77	539.32	718.43	30
370038	8012.35	0	576.9	576.91	364	R	393.19	449.93	539.52	718.69	30
370039	8262.71	0	576.39	576.39	386	R	393.3	450.06	539.67	718.89	30
370040	8511.93	0	575.91	575.92	398	R	393.42	450.19	539.83	719.11	50
370041	8763.39	0	575.36	575.36	374	R	393.49	450.27	539.93	719.24	30
370042	9015.32	0	574.93	574.93	410	R	394.57	451.51	541.41	721.21	50
370043	9265.94	573.84	0	573.85	304	L	394.87	451.85	541.82	721.75	30
370044	9519.06	574.57	0	574.57	590	L	395	452	542	722	300
370045	9767.24	572.57	0	572.58	276	L	395.13	452.15	542.18	722.24	30
370046	10017.72	573.14	0	573.14	514	L	395.43	452.49	542.59	722.78	100
370047	10267.17	572.73	0	572.73	528	L	395.55	452.63	542.75	723	100
370048	10517.14	572.35	0	572.36	574	L	395.97	453.11	543.33	723.77	300
370049	10765.96	571.15	0	571.15	396	L	396.17	453.33	543.6	724.13	30
370050	11013.3	570.49	0	570.49	412	L	396.28	453.46	543.75	724.33	50
370051	11263.11	570.11	0	570.12	410	L	396.34	453.53	543.84	724.45	50
370052	11511.41	569.7	0	569.7	448	L	396.45	453.66	543.99	724.65	50
370053	11758.36	569.57	0	569.57	556	L	396.53	453.76	544.11	724.81	300
370054	12018.24	569.82	0	569.83	742	L	396.64	453.88	544.25	725	400

Crosssection	Distance	Z_left_dam	Z_right_dam	Waterlevel	Discharge	Bank side	HQ30	HQ50	HQ100	HQ300	Category
370055	12262.35	568.83	0	568.83	640	L	396.71	453.95	544.34	725.12	300
370056	12512.33	567.81	0	567.82	468	L	396.75	454	544.4	725.2	100
370057	12763.09	0	567.67	567.67	498	R	396.88	454.15	544.58	725.44	100
370058	12826.93	0	567.51	567.52	540	R	396.89	454.16	544.59	725.45	100
370059	12962.03	564.86	0	564.86	286	L	396.93	454.2	544.64	725.52	30

Table B.1: For each cross section along the Haasliaare: bank-full height and corresponding modelled bank-full discharge and side of overflow, estimated discharge for HQ_{10}, HQ_{30}, HQ_{50}, HQ_{100} and HQ_{300} and the associated return period for the modelled bank-full discharge.

Aare Thun-Bern

Crosssection	Distance	Z_left_dam	Z_right_dam	Waterlevel	Discharge	Bank side	HQ10	HQ30	HQ50	HQ100	HQ300	Category
370226	2740.69	552.95	0	552.96	640	L	380.93	424.93	443.92	470.92	511.92	400
370227	2931.68	552.95	0	552.96	716	L	380.97	424.96	443.96	470.96	511.96	400
370228	2969.23	552.88	0	552.88	704	L	380.97	424.97	443.97	470.96	511.96	400
370229	2992.02	552.65	0	552.65	668	L	380.97	424.97	443.97	470.97	511.96	400
370230	3010.99	552.86	0	552.87	736	L	380.97	424.97	443.97	470.97	511.96	400
370231	3040.09	0	554.35	554.35	1112	R	380.98	424.98	443.98	470.98	511.98	400
370232	3104.11	552.37	0	552.37	670	L	380.99	424.99	443.99	470.99	511.99	400
370233	3303.61	552.58	0	552.58	756	L	381	425	444	471	512	400
370234	3499.42	550.84	0	550.85	488	L	381.01	425.01	444.01	471.01	512.01	300
370235	3689.06	551.87	0	551.87	724	L	381.13	425.14	444.15	471.16	512.17	400
370236	3714.39	550.43	0	550.44	466	L	381.13	425.15	444.16	471.17	512.17	100
370237	3787.94	550.35	0	550.35	462	L	381.14	425.16	444.17	471.17	512.18	100
370238	3795.54	550.39	0	550.39	488	L	381.14	425.16	444.17	471.17	512.18	300
370239	3820.73	550.54	0	550.55	534	L	381.14	425.16	444.17	471.18	512.19	400
370240	3845.19	550.48	0	550.48	522	L	381.15	425.16	444.17	471.18	512.19	400
370241	3874.57	550.43	0	550.44	522	L	381.15	425.16	444.17	471.18	512.19	400
370242	3882.63	550.26	0	550.27	492	L	381.21	425.24	444.25	471.26	512.28	300
370243	3910.3	549.96	0	549.96	444	L	381.21	425.24	444.25	471.26	512.28	50
370244	3976.92	0	553.55	553.55	1420	R	381.22	425.24	444.26	471.27	512.29	400
370245	4110.82	0	554.23	554.23	1728	R	381.23	425.25	444.27	471.28	512.29	400
370246	4133.22	554.56	0	554.56	1934	L	381.4	425.45	444.48	471.5	512.53	400
370247	4305.24	553.42	0	553.42	1570	L	381.41	425.46	444.48	471.51	512.53	400
370248	4504.24	553.13	0	553.13	1702	L	381.71	425.79	444.84	471.87	512.92	400
370249	4576.29	553.04	0	553.04	1706	L	381.71	425.8	444.84	471.88	512.93	400
370250	4627.41	0	552.39	552.39	1518	R	393.11	438.52	458.32	485.94	527.77	400
370251	4708.46	0	551.89	551.89	1504	R	393.13	438.54	458.34	485.96	527.79	400
370252	4907.66	0	550.9	550.9	1242	R	393.15	438.57	458.37	485.99	527.83	400
370253	5106.71	0	551.16	551.16	1528	R	393.17	438.59	458.39	486.01	527.85	400
370254	5306.56	550.53	0	550.53	1480	L	393.22	438.64	458.45	486.07	527.91	400
370255	5449.62	547.09	0	547.09	518	L	393.22	438.65	458.45	486.08	527.92	300
370256	5502.29	549.92	0	549.92	1448	L	393.5	438.95	458.77	486.41	528.27	400
370257	5577.74	549.73	0	549.73	1362	L	393.5	438.96	458.78	486.42	528.28	400
370258	5708.4	549.34	0	549.34	1360	L	393.5	438.96	458.78	486.42	528.28	400
370259	5911.63	548.24	0	548.24	1100	L	393.52	438.98	458.8	486.44	528.3	400
370260	5978.63	547.89	0	547.89	1024	L	393.54	439	458.82	486.47	528.33	400
370261	6048	547.64	0	547.65	970	L	393.55	439.01	458.84	486.48	528.35	400
370262	6110.25	547.9	0	547.9	1132	L	393.55	439.02	458.84	486.48	528.35	400
370263	6314.91	0	547.15	547.15	992	R	393.56	439.03	458.86	486.5	528.36	400
370264	6511.15	0	546.46	546.46	918	R	393.57	439.04	458.86	486.51	528.37	400
370265	6715.79	546.23	0	546.23	1016	L	393.71	439.19	459.02	486.67	528.55	400
370266	6918.74	0	545.63	545.63	988	R	393.72	439.2	459.03	486.68	528.56	400
370267	7123.34	0	545.1	545.1	1018	R	394.07	439.59	459.45	487.12	529.02	400
370268	7328.67	0	544.25	544.25	1046	R	394.09	439.61	459.47	487.14	529.04	400
370269	7529.58	0	543.66	543.67	1016	R	394.09	439.62	459.48	487.15	529.05	400
370270	7736.79	0	542.68	542.68	850	R	394.1	439.63	459.49	487.16	529.06	400
370271	7758.63	0	542.49	542.49	882	R	394.1	439.63	459.49	487.16	529.06	400
370272	7813.9	0	542.97	542.97	1024	R	394.1	439.63	459.49	487.16	529.07	400
370273	7927.98	0	542.14	542.15	760	R	394.11	439.64	459.5	487.17	529.07	400
370274	8131.73	0	541.88	541.88	774	R	394.12	439.65	459.51	487.18	529.08	400
370275	8331.13	541.43	0	541.43	776	L	394.2	439.74	459.6	487.28	529.19	400
370276	8536.98	0	540.74	540.74	692	R	394.26	439.81	459.68	487.36	529.27	400
370277	8765.76	0	540.35	540.35	788	R	401.11	447.45	467.78	495.8	538.18	400
370278	8974.55	0	539.7	539.7	756	L	401.12	447.46	467.79	495.81	538.19	400

Crosssection	Distance	Z_left_dam	Z_right_dam	Waterlevel	Discharge	Bank side	HQ10	HQ30	HQ50	HQ100	HQ300	Category
370279	9184.46	0	538.46	538.46	516	R	401.15	447.5	467.83	495.85	538.23	300
370280	9382.43	0	538.81	538.81	718	L	401.22	447.58	467.91	495.94	538.32	400
370281	9585.79	0	537.91	537.91	678	R	405.97	452.88	473.53	501.8	544.5	400
370282	9805.07	0	537.73	537.74	662	R	406.05	452.97	473.62	501.9	544.61	400
370283	10006.22	0	537.12	537.12	620	R	406.07	452.99	473.65	501.92	544.63	400
370284	10203.2	536.17	0	536.17	470	L	406.09	453.02	473.67	501.95	544.66	50
370285	10402.26	536.13	0	536.14	624	L	406.17	453.11	473.77	502.05	544.77	400
370286	10608.29	535.65	0	535.65	590	L	406.2	453.14	473.8	502.08	544.8	400
370287	10696.68	0	535.04	535.04	496	L	406.27	453.21	473.88	502.16	544.89	100
370288	10806.62	0	535.37	535.37	1090	R	406.27	453.22	473.89	502.17	544.9	400
370289	10984.56	535.34	0	535.34	1412	L	415.15	463.13	484.39	513.12	556.43	400
370290	11184.09	534.23	0	534.23	1034	L	415.16	463.15	484.41	513.13	556.45	400
370291	11375.1	533.68	0	533.68	974	L	415.26	463.25	484.52	513.25	556.58	400
370292	11578.97	532.7	0	532.7	818	L	415.31	463.31	484.58	513.31	556.64	400
370293	11774.1	532.26	0	532.26	688	L	415.32	463.32	484.6	513.33	556.66	400
370294	11977.8	0	532.63	532.63	986	R	415.34	463.34	484.61	513.35	556.68	400
370295	12176.26	532.32	0	532.32	1056	L	415.38	463.39	484.66	513.4	556.73	400
370296	12374.66	532.13	0	532.13	1222	L	415.48	463.5	484.78	513.53	556.86	400
370297	12574.99	531.5	0	531.5	1134	L	415.49	463.51	484.79	513.54	556.88	400
370298	12739.25	0	532.97	532.97	1680	R	415.51	463.54	484.82	513.57	556.91	400
370299	12767.45	0	531.5	531.5	1532	R	415.52	463.54	484.83	513.57	556.91	400
370300	12826.98	530.92	0	530.92	1198	L	415.53	463.56	484.84	513.59	556.93	400
370301	12970.61	530.87	0	530.87	1558	L	415.54	463.57	484.86	513.6	556.95	400
370302	13169.3	529.31	0	529.31	700	L	415.55	463.58	484.87	513.62	556.96	400
370303	13362.06	529.24	0	529.24	854	L	415.56	463.6	484.88	513.63	556.98	400
370304	13576.97	0	529.45	529.45	1138	R	415.59	463.62	484.91	513.66	557.01	400
370305	13782.11	528.21	0	528.21	794	L	415.65	463.69	484.99	513.74	557.09	400
370306	13979.67	0	529.07	529.07	1376	R	415.7	463.74	485.04	513.79	557.15	400
370307	14184.57	0	528.03	528.03	1174	R	415.77	463.83	485.13	513.89	557.25	400
370308	14391.74	0	528.43	528.43	1262	R	415.8	463.86	485.16	513.92	557.28	400
370309	14585.3	527.69	0	527.69	1052	L	415.83	463.89	485.2	513.96	557.32	400
370310	14783.92	526.88	0	526.88	830	L	415.86	463.92	485.23	513.99	557.36	400
370311	14980.38	0	526.03	526.03	658	L	415.86	463.93	485.24	514	557.37	400
370312	15177.94	0	526.68	526.68	1472	L	415.9	463.97	485.28	514.05	557.41	400
370313	15380.47	0	0	0	0	L	415.93	464	485.31	514.08	557.45	30
370314	15580.17	0	526.07	526.07	1602	R	415.94	464.01	485.33	514.09	557.46	400
370315	15784.1	0	525.6	525.6	1278	R	416.02	464.1	485.42	514.19	557.57	400
370316	15982.32	525	0	525	1170	L	416.02	464.11	485.43	514.2	557.57	400
370317	16182.42	0	524.82	524.82	1266	R	416.05	464.13	485.45	514.23	557.6	400
370318	16385.33	0	524.34	524.34	1118	R	416.06	464.14	485.47	514.24	557.62	400
370319	16588.82	0	523.89	523.89	908	L	416.08	464.17	485.5	514.27	557.65	400
370320	16625.31	0	523.78	523.78	1446	L	416.32	464.44	485.77	514.56	557.95	400
370321	16791.02	0	523.37	523.37	1550	R	416.32	464.44	485.78	514.57	557.96	400
370322	16960.24	522.41	0	522.41	876	L	416.34	464.46	485.8	514.59	557.98	400
370323	17155.33	522.61	0	522.61	1398	L	416.36	464.48	485.82	514.61	558	400
370324	17361.23	522.65	0	522.65	1072	L	416.36	464.49	485.83	514.62	558.01	400
370325	17551.81	522.32	0	522.32	1036	L	416.37	464.5	485.84	514.63	558.02	400
370326	17754.65	0	521.33	521.33	910	R	416.38	464.51	485.85	514.64	558.03	400
370327	17853.19	0	521.22	521.22	776	R	416.38	464.51	485.85	514.64	558.04	400
370328	17952.81	0	521.3	521.3	872	R	416.39	464.52	485.86	514.65	558.05	400
370329	18053.6	0	520.89	520.89	1114	R	416.39	464.52	485.86	514.65	558.05	400
370330	18154.4	0	520.48	520.48	1214	L	416.39	464.52	485.86	514.65	558.05	400
370331	18256.04	0	520.09	520.09	630	R	416.4	464.53	485.87	514.66	558.06	400
370332	18358.35	0	520.09	520.09	702	R	416.4	464.53	485.87	514.66	558.06	400
370333	18459.9	0	519.66	519.66	648	R	416.4	464.53	485.88	514.67	558.07	400
370334	18561.6	0	519.64	519.64	664	R	416.41	464.54	485.88	514.67	558.07	400
370335	18664.59	0	519.6	519.6	780	R	416.42	464.55	485.89	514.68	558.08	400
370336	18766.1	0	519.53	519.53	814	R	416.42	464.56	485.9	514.69	558.09	400

Crosssection	Distance	Z_left_dam	Z_right_dam	Waterlevel	Discharge	Bank side	HQ10	HQ30	HQ50	HQ100	HQ300	Category
370337	18868.24	0	519.78	519.78	970	R	416.43	464.56	485.9	514.7	558.1	400
370338	18970.71	0	518.4	518.4	494	R	416.43	464.56	485.91	514.7	558.1	100
370339	19071.83	0	517.72	517.73	322	R	416.44	464.57	485.91	514.71	558.11	30
370340	19170.32	0	518.56	518.57	546	R	416.44	464.57	485.92	514.71	558.11	300
370341	19233.57	0	518.98	518.98	754	R	416.44	464.58	485.92	514.71	558.12	400
370342	19279.32	519.58	0	519.58	1286	L	416.44	464.58	485.93	514.72	558.12	400
370343	19383.99	0	518.6	518.6	974	L	416.45	464.58	485.93	514.72	558.12	400
370344	19595.97	0	518.09	518.09	800	R	416.45	464.59	485.93	514.73	558.13	400
370345	19799.84	0	517.62	517.62	810	R	416.46	464.59	485.94	514.73	558.14	400
370346	20001.82	0	517.23	517.23	648	R	416.46	464.6	485.95	514.74	558.14	400
370347	20204.78	0	517.31	517.31	902	R	416.47	464.6	485.95	514.74	558.15	400
370348	20408.99	0	517.06	517.06	1034	R	416.47	464.61	485.96	514.75	558.15	400
370349	20611.63	0	516.7	516.7	1184	R	416.48	464.61	485.96	514.76	558.16	400
370350	20814.72	0	516.45	516.45	1094	R	416.48	464.62	485.97	514.77	558.17	400
370351	21015.45	0	516.16	516.16	1082	R	416.49	464.63	485.98	514.77	558.18	400
370352	21219.83	0	515.1	515.1	674	L	421.94	470.71	492.43	521.49	565.25	400
370353	21428.75	0	514.54	514.55	834	L	421.94	470.72	492.43	521.5	565.26	400
370354	21633.48	0	514.66	514.66	824	R	421.95	470.72	492.44	521.5	565.27	400
370355	21835.39	0	515.1	515.1	972	R	421.95	470.73	492.44	521.51	565.27	400
370356	22046.48	0	513.71	513.71	522	R	421.99	470.78	492.49	521.56	565.33	300
370357	22244.72	0	513.33	513.33	538	R	422.01	470.79	492.51	521.58	565.34	300
370358	22445.7	0	513.48	513.48	704	R	422.02	470.8	492.52	521.59	565.36	400
370359	22642.5	0	513.23	513.23	996	R	422.03	470.82	492.54	521.61	565.38	400
370360	22841.83	0	512.59	512.6	764	R	422.04	470.83	492.55	521.62	565.39	400
370361	23036.46	0	512.48	512.48	946	R	422.05	470.84	492.56	521.63	565.41	400
370362	23250.2	0	511.76	511.76	592	L	422.08	470.88	492.6	521.67	565.45	400
370363	23448.1	0	511.58	511.58	620	R	422.12	470.91	492.64	521.71	565.49	400
370364	23630.52	0	512.46	512.46	1008	R	422.15	470.95	492.68	521.75	565.53	400
370365	23662.12	0	511.18	511.18	884	L	422.18	470.98	492.71	521.79	565.57	400
370366	23862.49	0	510.67	510.67	806	L	422.21	471.02	492.75	521.83	565.61	400
370367	24064.96	0	510.66	510.66	766	R	422.24	471.06	492.79	521.87	565.65	400
370368	24267.26	0	510.24	510.24	812	R	422.28	471.09	492.83	521.91	565.7	400
370369	24471.68	0	509.99	509.99	840	R	422.31	471.13	492.87	521.95	565.74	400
370370	24671.54	510.37	0	510.37	1134	L	422.34	471.16	492.9	521.99	565.78	400
370371	24874.62	0	510.04	510.04	970	R	422.37	471.2	492.94	522.03	565.82	400
370372	25084.54	0	509.7	509.7	890	R	422.4	471.23	492.98	522.07	565.86	400
370373	25312.34	509.45	0	509.45	1122	L	422.44	471.27	493.02	522.11	565.9	400
370374	25524.92	508.95	0	508.95	816	L	422.47	471.31	493.06	522.15	565.95	400
370375	25730.65	0	508.76	508.76	996	R	422.5	471.34	493.09	522.19	565.99	400
370376	25895.36	508.35	0	508.35	920	L	423.32	472.25	494.06	523.19	567.05	400
370377	26125.89	0	508.33	508.33	970	R	440.2	491.1	514.05	544.01	588.96	400
370378	26332.45	0	507.64	507.64	864	R	440.25	491.17	514.12	544.08	589.03	400
370379	26521.43	0	507.26	507.26	758	R	440.31	491.23	514.18	544.15	589.11	400
370380	26725.77	506.99	0	507	820	L	440.32	491.24	514.19	544.16	589.11	400
370381	26927.86	0	506.82	506.82	888	R	440.33	491.25	514.2	544.17	589.13	400
370382	27130.58	0	506.37	506.37	740	R	440.42	491.35	514.31	544.28	589.24	400
370383	27322.14	0	506.14	506.14	680	R	440.51	491.45	514.42	544.39	589.36	400
370384	27509.07	0	505.72	505.72	624	R	440.85	491.83	514.82	544.81	589.8	400
370385	27720.7	0	505.6	505.61	678	R	440.86	491.85	514.84	544.83	589.82	400
370386	27931.68	504.83	0	504.84	548	L	440.9	491.89	514.89	544.88	589.87	300
370387	28130.78	0	504.8	504.8	548	R	440.95	491.95	514.94	544.94	589.94	300
370388	28256.43	0	504.72	504.73	548	R	440.96	491.95	514.95	544.95	589.94	300
370389	28322.64	0	504.45	504.46	500	R	440.97	491.97	514.97	544.97	589.97	50
370390	28529.43	0	504.09	504.1	446	R	441	492	515	545	590	30
370391	28730.83	0	504.28	504.29	488	R	441.05	492.06	515.06	545.07	590.07	30
370392	28772.6	0	506.38	506.39	824	R	441.11	492.12	515.12	545.13	590.14	400
370393	28777.56	506.4	0	506.41	826	L	441.16	492.18	515.19	545.2	590.21	400
370394	28866.23	503.88	0	503.89	428	L	441.21	492.24	515.25	545.26	590.27	30

Crosssection	Distance	Z_left_dam	Z_right_dam	Waterlevel	Discharge	Bank side	HQ10	HQ30	HQ50	HQ100	HQ300	Category
370395	29046.83	503.67	0	503.68	402	L	441.26	492.29	515.31	545.33	590.34	30
370396	29231.74	0	503.37	503.37	362	R	441.32	492.35	515.37	545.39	590.41	30
370397	29427.88	502.58	0	502.58	268	L	441.37	492.41	515.44	545.46	590.48	30
370398	29601.71	502.29	0	502.3	238	L	443.8	495.13	518.32	548.45	593.63	30
370399	29803.74	501.93	0	501.98	220	L	443.84	495.17	518.37	548.5	593.69	30
370400	29947.23	502.56	0	502.57	266	L	443.86	495.19	518.38	548.52	593.71	30
370401	29982.77	501.9	0	502	220	L	443.86	495.19	518.38	548.52	593.71	30
370402	30105.17	0	502.06	502.14	222	R	443.86	495.2	518.39	548.53	593.71	30
370403	30216.96	0	501.28	501.3	178	R	443.87	495.2	518.39	548.53	593.72	30

Table B.2: For each cross section along the Aare Thun-Bern: bank-full height and corresponding modelled bank-full discharge and side of overflow, estimated discharge for HQ_{10}, HQ_{30}, HQ_{50}, HQ_{100} and HQ_{300} and the associated return period for the modelled bank-full discharge.

Simme

Crosssection	Distance	Z_left_dam	Z_right_dam	Waterlevel	Discharge	Bank side	HQ10	HQ30	HQ50	HQ100	HQ300	Category
439001	0.00	1064.60	0.00	1064.61	440	L	73.21	82.26	85.82	90.64	96.94	400
439002	89.81	1063.16	0.00	1063.17	598	L	74.57	84.11	87.90	93.07	99.94	400
439003	133.89	1059.69	0.00	1059.69	140	L	74.58	84.12	87.91	93.08	99.96	400
439004	189.59	0.00	1061.07	1061.09	536	R	74.59	84.13	87.92	93.10	99.97	400
439005	290.52	1057.18	0.00	1057.19	364	L	77.69	88.36	92.70	98.70	106.93	400
439006	371.60	1056.62	0.00	1056.62	1150	L	77.69	88.36	92.71	98.70	106.93	400
439007	477.43	1052.09	0.00	1052.09	384	L	78.48	89.44	93.93	100.15	108.73	400
439008	579.74	0.00	1048.73	1048.74	130	R	78.50	89.46	93.96	100.17	108.77	400
439009	600.77	0.00	1048.85	1048.86	166	R	78.50	89.47	93.96	100.18	108.78	400
439010	683.21	0.00	1047.92	1047.95	138	R	78.77	89.83	94.38	100.66	109.38	400
439011	779.94	0.00	1046.11	1046.11	136	R	78.79	89.86	94.40	100.70	109.42	400
439012	884.44	0.00	1044.35	1044.36	110	R	79.01	90.16	94.75	101.11	109.94	400
439013	987.99	0.00	1043.36	1043.39	154	R	79.03	90.19	94.78	101.14	109.97	400
439014	1081.51	1041.51	0.00	1041.52	114	L	79.06	90.23	94.83	101.20	110.05	400
439015	1123.72	0.00	1041.00	1041.01	114	R	79.07	90.25	94.85	101.22	110.08	400
439016	1174.74	1040.33	0.00	1040.35	96	L	79.09	90.27	94.87	101.25	110.12	100
439017	1275.82	1038.93	0.00	1038.97	90	L	79.12	90.31	94.92	101.30	110.18	30
439018	1374.05	1037.51	0.00	1037.55	70	L	79.16	90.38	94.99	101.39	110.29	30
439019	1476.74	1036.24	0.00	1036.26	72	L	79.22	90.46	95.08	101.50	110.42	30
439020	1582.06	1035.07	0.00	1035.08	60	L	79.29	90.55	95.19	101.63	110.59	30
439021	1684.69	1033.97	0.00	1034.00	70	L	79.33	90.60	95.25	101.69	110.67	30
439022	1784.47	1032.72	0.00	1032.80	82	L	79.34	90.62	95.27	101.72	110.70	30
439023	1884.88	1031.88	0.00	1031.91	100	L	79.35	90.63	95.27	101.72	110.71	100
439024	1985.06	1030.80	0.00	1030.81	82	L	79.35	90.63	95.28	101.73	110.72	30
439025	2070.66	0.00	1030.23	1030.24	66	R	79.35	90.63	95.28	101.73	110.72	30
439026	2174.35	0.00	1029.16	1029.18	90	R	79.53	90.88	95.56	102.06	111.13	30
439027	2275.44	0.00	1028.15	1028.16	46	R	79.68	91.09	95.80	102.34	111.48	30
439028	2374.22	1027.43	0.00	1027.45	60	L	79.69	91.10	95.82	102.37	111.51	30
439029	2475.55	0.00	1026.76	1026.77	74	R	79.72	91.14	95.86	102.41	111.57	30
439030	2577.09	0.00	1025.81	1025.82	62	R	79.79	91.24	95.98	102.55	111.74	30
439031	2680.50	1024.73	0.00	1024.75	54	L	79.80	91.25	95.99	102.56	111.76	30
439032	2778.63	1024.14	0.00	1024.15	56	L	79.83	91.29	96.03	102.61	111.82	30
439033	2874.43	1023.29	0.00	1023.33	52	L	79.85	91.32	96.07	102.66	111.88	30
439034	2981.74	1022.74	0.00	1022.75	64	L	79.87	91.35	96.10	102.69	111.92	30
439035	3011.90	0.00	1022.83	1022.84	70	R	79.88	91.37	96.11	102.71	111.95	30
439036	3078.07	1021.90	0.00	1021.93	66	L	79.90	91.38	96.14	102.74	111.98	30
439037	3183.18	0.00	1021.11	1021.12	54	R	79.92	91.41	96.17	102.77	112.02	30
439038	3288.83	0.00	1020.27	1020.28	62	R	79.93	91.43	96.18	102.80	112.05	30
439039	3389.32	1019.41	0.00	1019.46	58	L	79.94	91.44	96.19	102.81	112.07	30
439040	3493.53	1018.50	0.00	1018.52	50	L	79.94	91.44	96.20	102.82	112.08	30
439041	3595.54	1017.93	0.00	1017.95	82	L	79.95	91.46	96.22	102.84	112.11	30
439042	3702.93	0.00	1016.92	1016.95	62	R	79.96	91.47	96.23	102.85	112.12	30
439043	3787.64	0.00	1016.57	1016.60	92	R	79.96	91.48	96.24	102.86	112.14	50
439044	3876.15	0.00	1015.74	1015.75	82	R	79.97	91.49	96.25	102.88	112.16	30
439045	3973.17	0.00	1015.80	1015.82	116	R	79.98	91.49	96.26	102.89	112.17	400
439046	4030.13	0.00	1015.14	1015.15	112	R	81.29	93.30	98.32	105.31	115.22	300
439047	4071.93	1014.36	0.00	1014.36	136	L	81.29	93.30	98.32	105.31	115.22	400
439048	4180.76	1012.98	0.00	1012.98	82	L	82.68	95.22	100.50	107.90	118.48	30
439049	4288.23	1013.82	0.00	1013.83	424	L	82.70	95.25	100.54	107.94	118.53	400
439050	4375.83	0.00	1012.14	1012.15	266	R	82.72	95.28	100.57	107.98	118.58	400
439051	4478.92	1009.91	0.00	1009.93	90	L	82.74	95.31	100.60	108.02	118.63	30
439052	4575.28	1009.64	0.00	1009.65	118	L	82.75	95.32	100.62	108.04	118.65	300
439053	4677.28	1008.66	0.00	1008.69	96	L	82.76	95.33	100.63	108.05	118.67	50

Crosssection	Distance	Z_left_dam	Z_right_dam	Waterlevel	Discharge	Bank side	HQ10	HQ30	HQ50	HQ100	HQ300	Category
439054	4713.55	1008.80	0.00	1008.80	116	L	82.76	95.33	100.63	108.05	118.68	300
439055	4828.70	1007.56	0.00	1007.58	88	L	82.76	95.34	100.64	108.06	118.68	30
439056	4865.28	1006.70	0.00	1006.70	110	L	82.76	95.34	100.64	108.06	118.69	300
439057	4992.51	0.00	1005.97	1005.97	200	R	89.83	105.21	111.93	121.53	135.86	400
439058	5073.27	1004.43	0.00	1004.47	94	L	89.85	105.23	111.96	121.56	135.90	30
439059	5178.94	1003.65	0.00	1003.66	94	L	89.96	105.39	112.14	121.77	136.18	30
439060	5267.92	0.00	1002.94	1002.94	90	R	89.97	105.40	112.15	121.78	136.19	30
439061	5374.70	1001.64	0.00	1001.66	70	L	89.97	105.40	112.16	121.79	136.21	30
439062	5478.45	1000.85	0.00	1000.87	78	L	89.98	105.41	112.17	121.81	136.22	30
439063	5585.24	1000.15	0.00	1000.16	84	L	89.98	105.42	112.17	121.81	136.23	30
439064	5645.58	1000.00	0.00	1000.23	146	L	89.98	105.42	112.18	121.82	136.23	400
439065	5670.41	999.29	0.00	999.30	94	L	89.98	105.42	112.18	121.82	136.24	30
439066	5770.50	998.51	0.00	998.53	90	L	89.99	105.43	112.19	121.83	136.25	30
439067	5869.84	997.74	0.00	997.76	94	L	90.00	105.44	112.20	121.84	136.27	30
439068	5896.53	997.67	0.00	997.69	144	L	90.00	105.44	112.20	121.84	136.27	400
439069	5964.31	996.90	0.00	996.90	72	L	90.00	105.44	112.20	121.85	136.27	30
439070	6070.78	996.34	0.00	996.36	96	L	90.01	105.45	112.21	121.86	136.29	30
439071	6169.25	995.78	0.00	995.81	122	L	90.01	105.46	112.22	121.87	136.30	300
439072	6265.81	996.00	0.00	996.00	216	L	90.01	105.46	112.22	121.87	136.31	400
439073	6362.41	994.11	0.00	994.11	110	L	90.31	105.89	112.71	122.46	137.06	50
439074	6467.93	0.00	993.54	993.55	162	R	90.32	105.89	112.72	122.47	137.07	400
439075	6572.44	0.00	993.04	993.04	234	R	91.67	107.81	114.92	125.11	140.48	400
439076	6653.96	991.97	0.00	991.99	96	L	91.68	107.82	114.93	125.12	140.50	30
439077	6752.09	990.82	0.00	990.84	78	L	91.69	107.83	114.95	125.14	140.52	30
439078	6853.40	990.25	0.00	990.27	82	L	91.72	107.87	114.99	125.20	140.59	30
439079	6959.59	989.26	0.00	989.29	60	L	91.73	107.88	115.01	125.21	140.61	30
439080	6979.44	990.04	0.00	990.06	132	L	91.73	107.88	115.01	125.21	140.61	300
439081	7057.15	988.72	0.00	988.73	86	L	91.79	107.96	115.10	125.33	140.76	30
439082	7157.10	0.00	988.24	988.25	136	R	91.79	107.98	115.12	125.34	140.78	300
439083	7270.58	987.09	0.00	987.09	690	L	91.80	107.99	115.13	125.36	140.80	400
439084	7371.58	983.55	0.00	983.56	260	L	92.38	108.80	116.07	126.49	142.26	400
439085	7454.63	0.00	981.90	981.91	192	R	92.38	108.80	116.07	126.49	142.27	400
439086	7551.94	980.03	0.00	980.03	172	L	93.50	110.39	117.89	128.69	145.11	400
439087	7645.17	978.44	0.00	978.44	228	L	93.50	110.40	117.90	128.70	145.13	400
439088	7741.78	0.00	976.56	976.59	146	R	93.51	110.41	117.92	128.72	145.15	400
439089	7769.54	0.00	976.62	976.63	294	R	93.58	110.50	118.03	128.85	145.33	400
439090	7838.25	0.00	974.88	974.90	184	R	93.58	110.51	118.04	128.86	145.33	400
439091	7934.97	0.00	973.19	973.20	112	R	93.59	110.51	118.04	128.86	145.34	50
439092	8040.14	0.00	972.52	972.53	204	R	93.63	110.57	118.11	128.94	145.45	400
439093	8149.28	0.00	970.82	970.83	210	R	93.89	110.95	118.54	129.47	146.13	400
439094	8246.09	0.00	969.56	969.56	404	R	93.90	110.96	118.56	129.49	146.15	400
439095	8279.33	969.07	0.00	969.08	412	L	93.90	110.96	118.56	129.49	146.16	400
439096	8338.45	967.42	0.00	967.42	252	L	94.12	111.28	118.92	129.92	146.72	400
439097	8451.69	966.70	0.00	966.71	272	L	94.25	111.45	119.13	130.17	147.04	400
439098	8538.57	0.00	965.73	965.73	240	R	94.26	111.47	119.15	130.20	147.08	400
439099	8637.60	0.00	963.91	963.92	126	R	94.27	111.48	119.16	130.21	147.09	100
439100	8713.34	0.00	964.45	964.45	250	R	94.51	111.82	119.55	130.69	147.71	400
439101	8737.40	0.00	963.22	963.23	152	R	94.51	111.82	119.56	130.69	147.72	400
439102	8836.55	0.00	962.25	962.27	148	R	94.52	111.84	119.57	130.71	147.74	400
439103	8936.70	0.00	961.79	961.80	214	R	94.54	111.86	119.60	130.74	147.78	400
439104	9035.72	960.96	0.00	960.97	404	L	94.58	111.93	119.67	130.83	147.90	400
439105	9134.95	959.51	0.00	959.53	222	L	94.60	111.95	119.70	130.87	147.95	400
439106	9233.73	0.00	958.15	958.16	130	R	94.62	111.98	119.73	130.90	147.99	100
439107	9334.85	0.00	957.44	957.44	134	R	94.64	112.02	119.78	130.96	148.06	300
439108	9433.33	956.59	0.00	956.59	132	L	94.65	112.02	119.79	130.97	148.08	300
439109	9531.33	956.05	0.00	956.07	150	L	94.66	112.04	119.80	130.98	148.10	400
439110	9631.39	955.47	0.00	955.48	166	L	94.69	112.08	119.85	131.05	148.19	400
439111	9730.73	954.58	0.00	954.61	144	L	94.70	112.09	119.86	131.06	148.20	300

Crosssection	Distance	Z_left_dam	Z_right_dam	Waterlevel	Discharge	Bank side	HQ10	HQ30	HQ50	HQ100	HQ300	Category
439112	9831.20	953.83	0.00	953.85	156	L	94.73	112.14	119.92	131.13	148.29	400
439113	9930.81	953.18	0.00	953.20	144	L	94.73	112.15	119.92	131.13	148.30	300
439114	10030.12	952.27	0.00	952.29	134	L	95.03	112.57	120.42	131.73	149.07	300
439115	10131.20	951.72	0.00	951.73	152	L	95.12	112.70	120.56	131.91	149.30	400
439116	10229.25	951.15	0.00	951.16	160	L	95.13	112.72	120.58	131.93	149.33	400
439117	10289.19	950.97	0.00	950.98	152	L	95.14	112.72	120.59	131.93	149.34	400
439118	10327.59	949.87	0.00	949.88	164	L	95.14	112.72	120.59	131.94	149.34	400
439119	10435.97	0.00	948.34	948.36	56	R	95.14	112.72	120.59	131.94	149.35	30
439120	10533.55	947.73	0.00	947.76	50	L	95.14	112.72	120.59	131.94	149.35	30
439121	10630.83	947.30	0.00	947.31	94	L	95.18	112.77	120.65	132.01	149.44	30
439122	10718.34	0.00	946.44	946.46	88	R	95.19	112.79	120.67	132.03	149.46	30
439123	10815.97	0.00	945.96	945.98	106	R	95.21	112.82	120.70	132.07	149.52	30
439124	10919.63	945.40	0.00	945.42	104	L	95.31	112.96	120.87	132.28	149.78	30
439125	10951.07	0.00	945.80	945.82	198	R	95.31	112.96	120.87	132.28	149.79	400
439126	11021.74	944.17	0.00	944.18	108	L	97.61	116.26	124.68	136.88	155.80	30
439127	11122.23	0.00	943.15	943.16	74	R	97.62	116.26	124.69	136.89	155.82	30
439128	11222.41	942.81	0.00	942.83	104	L	97.64	116.29	124.71	136.93	155.86	30
439129	11321.70	0.00	942.06	942.07	110	R	97.64	116.29	124.72	136.93	155.87	30
439130	11422.15	0.00	940.96	940.98	88	R	98.05	116.88	125.40	137.76	156.95	30
439131	11522.93	0.00	940.23	940.23	78	R	98.05	116.88	125.41	137.77	156.96	30
439132	11622.43	0.00	939.79	939.80	130	R	98.07	116.91	125.44	137.81	157.01	100
439133	11729.89	938.63	0.00	938.65	94	L	98.09	116.93	125.46	137.83	157.05	30
439134	11831.35	938.33	0.00	938.34	122	L	98.13	116.99	125.53	137.91	157.15	50
439135	11915.82	0.00	936.98	937.02	56	R	98.14	117.00	125.55	137.94	157.18	30
439136	12019.82	937.05	0.00	937.06	122	L	98.16	117.03	125.58	137.98	157.24	50
439137	12099.43	937.34	0.00	937.35	270	L	98.20	117.10	125.66	138.07	157.36	400
439138	12120.61	938.59	0.00	938.60	380	L	98.21	117.10	125.66	138.07	157.36	400
439139	12205.46	935.60	0.00	935.61	90	L	98.21	117.11	125.67	138.08	157.38	30
439140	12317.09	935.17	0.00	935.18	132	L	98.25	117.17	125.73	138.16	157.48	100
439141	12426.16	934.55	0.00	934.56	144	L	98.32	117.27	125.85	138.30	157.67	300
439142	12532.89	0.00	932.67	932.70	48	R	98.37	117.34	125.93	138.41	157.80	30
439143	12628.51	932.49	0.00	932.52	68	L	98.38	117.36	125.95	138.43	157.83	30
439144	12716.58	0.00	931.96	931.98	78	R	98.42	117.41	126.02	138.51	157.94	30
439145	12812.18	931.60	0.00	931.61	98	L	98.44	117.43	126.04	138.54	157.98	30
439146	12926.70	0.00	931.05	931.06	88	R	98.52	117.55	126.17	138.70	158.18	30
439147	13002.69	0.00	930.85	930.86	92	R	98.52	117.55	126.18	138.70	158.19	30
439148	13102.57	0.00	930.16	930.18	118	R	98.60	117.67	126.32	138.87	158.41	50
439149	13203.62	929.19	0.00	929.21	76	L	98.60	117.67	126.32	138.87	158.42	30
439150	13302.79	928.50	0.00	928.51	104	L	98.60	117.67	126.32	138.88	158.42	30
439151	13402.32	927.88	0.00	927.88	280	L	105.26	127.28	137.49	152.49	176.42	400
439152	13554.35	0.00	925.45	925.46	120	R	105.34	127.40	137.63	152.66	176.65	30
439153	13702.71	925.21	0.00	925.23	166	L	105.35	127.41	137.65	152.68	176.68	300
439154	13855.08	0.00	923.84	923.85	170	R	105.35	127.42	137.66	152.70	176.70	300
439155	13933.32	0.00	923.48	923.50	190	R	105.72	127.95	138.28	153.45	177.71	400
439156	13982.07	0.00	922.80	922.81	150	R	105.72	127.95	138.28	153.46	177.71	100
439157	14137.67	0.00	921.63	921.64	154	R	105.73	127.97	138.30	153.48	177.73	300
439158	14287.56	0.00	920.41	920.42	160	R	105.73	127.97	138.30	153.48	177.75	300
439159	14437.44	919.67	0.00	919.67	192	L	106.98	129.80	140.43	156.09	181.23	400
439160	14485.17	919.83	0.00	920.05	268	L	106.99	129.80	140.44	156.10	181.23	400
439161	14547.86	918.12	0.00	918.13	126	L	106.99	129.80	140.44	156.10	181.23	30
439162	14673.94	917.11	0.00	917.12	150	L	106.99	129.81	140.45	156.11	181.25	100
439163	14972.40	0.00	914.78	914.78	550	R	107.39	130.39	141.13	156.95	182.37	400
439164	15115.34	915.13	0.00	915.14	672	L	107.40	130.41	141.15	156.97	182.40	400
439165	15271.24	913.11	0.00	913.12	404	L	107.45	130.48	141.23	157.07	182.54	400
439166	15420.38	0.00	913.23	913.24	420	R	107.46	130.49	141.24	157.09	182.56	400
439167	15459.72	912.90	0.00	912.90	402	L	107.46	130.49	141.24	157.09	182.56	400
439168	15549.08	0.00	909.70	909.71	142	R	107.48	130.51	141.27	157.13	182.61	100
439169	15598.14	0.00	910.40	910.42	222	R	107.48	130.52	141.28	157.14	182.62	400

Crosssection	Distance	Z_left_dam	Z_right_dam	Waterlevel	Discharge	Bank side	HQ10	HQ30	HQ50	HQ100	HQ300	Category
439170	15714.06	0.00	909.02	909.04	176	R	107.49	130.53	141.29	157.14	182.63	300
439171	15844.46	0.00	908.05	908.08	138	R	107.50	130.55	141.31	157.17	182.67	50
439172	15968.45	0.00	907.74	907.74	154	R	107.51	130.56	141.33	157.19	182.70	100
439173	16009.13	907.65	0.00	907.66	170	L	107.51	130.56	141.33	157.20	182.70	300
439174	16133.44	0.00	906.74	906.74	184	R	107.76	130.92	141.75	157.71	183.39	400
439175	16253.88	907.23	0.00	907.23	272	L	107.77	130.93	141.76	157.73	183.41	400
439176	16294.66	0.00	910.49	910.50	808	R	107.77	130.94	141.77	157.74	183.42	400
439177	16373.15	906.83	0.00	906.83	1338	L	107.77	130.94	141.77	157.74	183.43	400
439178	16495.46	0.00	901.19	901.19	840	R	107.97	131.23	142.11	158.15	183.97	400
439179	16581.99	0.00	898.00	898.00	1156	R	108.02	131.31	142.21	158.27	184.14	400
439180	16726.93	891.58	0.00	891.58	890	L	108.03	131.32	142.22	158.29	184.16	400
439181	16854.02	887.02	0.00	887.02	176	L	108.31	131.73	142.70	158.88	184.95	300
439182	17332.24	0.00	863.17	863.17	712	L	108.37	131.82	142.80	159.00	185.12	400
439183	17482.93	0.00	860.33	860.33	446	L	108.95	132.66	143.79	160.22	186.75	400
439184	17619.74	0.00	858.82	858.83	332	R	108.99	132.73	143.86	160.30	186.86	400
439185	17734.11	0.00	860.32	860.32	1594	L	109.00	132.74	143.87	160.32	186.89	400
439186	17841.37	857.61	0.00	857.61	1582	L	109.01	132.75	143.88	160.33	186.91	400
439187	17913.41	856.72	0.00	856.72	770	L	110.73	135.28	146.85	163.98	191.81	400
439188	18079.86	0.00	852.38	852.38	362	R	110.74	135.30	146.87	164.01	191.85	400
439189	18174.05	0.00	852.33	852.34	632	R	110.77	135.33	146.91	164.06	191.92	400
439190	18252.06	0.00	850.04	850.04	294	R	110.77	135.34	146.92	164.07	191.93	400
439191	18373.90	0.00	848.92	848.92	342	R	110.78	135.35	146.94	164.09	191.96	400
439192	18498.37	846.42	0.00	846.42	158	L	110.85	135.45	147.05	164.23	192.14	100
439193	18654.83	845.12	0.00	845.13	188	L	110.86	135.46	147.07	164.25	192.17	300
439194	18784.58	843.80	0.00	843.80	194	L	110.88	135.50	147.11	164.31	192.25	400
439195	18936.42	0.00	842.81	842.81	202	R	110.89	135.51	147.12	164.32	192.27	400
439196	19086.54	0.00	841.99	842.00	288	R	110.91	135.54	147.15	164.36	192.32	400
439197	19258.58	0.00	840.95	840.96	378	R	110.92	135.55	147.17	164.38	192.35	400
439198	19345.85	0.00	838.58	838.58	246	R	111.51	136.43	148.20	165.65	194.05	400
439199	19489.52	837.66	0.00	837.66	252	L	111.52	136.43	148.21	165.66	194.07	400
439200	19644.90	835.70	0.00	835.71	174	L	111.56	136.50	148.28	165.75	194.19	300
439201	19782.62	834.56	0.00	834.58	160	L	111.58	136.52	148.31	165.78	194.23	100
439202	19930.58	833.47	0.00	833.49	160	L	111.58	136.53	148.32	165.80	194.25	100
439203	20079.23	832.23	0.00	832.30	178	L	111.59	136.54	148.33	165.81	194.27	300
439204	20164.97	0.00	831.98	832.02	174	R	111.59	136.54	148.33	165.81	194.27	300
439205	20219.19	0.00	830.98	830.98	178	R	111.63	136.59	148.39	165.88	194.37	300
439206	20370.43	830.05	0.00	830.05	228	L	111.63	136.60	148.39	165.89	194.38	400
439207	20527.00	0.00	828.55	828.56	196	R	112.61	138.03	150.08	167.98	197.19	300
439208	20673.84	0.00	827.36	827.39	220	R	112.62	138.06	150.12	168.02	197.25	400
439209	20825.55	0.00	825.92	825.92	178	R	112.71	138.18	150.26	168.19	197.49	300
439210	20956.41	0.00	825.00	825.00	178	R	113.06	138.70	150.87	168.95	198.51	300
439211	21001.62	0.00	825.42	825.43	268	R	115.60	142.46	155.29	174.42	205.92	400
439212	21104.52	0.00	824.68	824.69	280	R	115.62	142.48	155.31	174.45	205.97	400
439213	21250.09	823.78	0.00	823.78	358	L	115.63	142.51	155.34	174.48	206.01	400
439214	21398.87	822.74	0.00	822.74	332	L	115.65	142.53	155.37	174.52	206.07	400
439215	21555.30	821.66	0.00	821.66	364	L	115.72	142.63	155.49	174.67	206.26	400
439216	21705.45	820.67	0.00	820.68	388	L	115.77	142.72	155.59	174.79	206.43	400
439217	21855.65	819.56	0.00	819.57	380	L	115.79	142.74	155.62	174.82	206.48	400
439218	22004.97	818.80	0.00	818.80	358	L	115.80	142.76	155.64	174.85	206.52	400
439219	22153.24	817.32	0.00	817.35	250	L	115.82	142.78	155.66	174.88	206.56	400
439220	22311.60	816.71	0.00	816.75	252	L	115.83	142.80	155.69	174.91	206.60	400
439221	22348.33	816.49	0.00	816.49	252	L	115.83	142.80	155.69	174.91	206.60	400
439222	22436.70	815.72	0.00	815.74	288	L	116.45	143.73	156.78	176.26	208.43	400
439223	22588.29	814.73	0.00	814.75	258	L	116.46	143.74	156.79	176.28	208.46	400
439224	22738.60	813.66	0.00	813.66	226	L	116.48	143.76	156.82	176.31	208.50	400
439225	22889.21	812.59	0.00	812.60	200	L	116.64	144.00	157.10	176.66	208.98	300
439226	23042.56	811.68	0.00	811.69	242	L	116.65	144.01	157.11	176.68	209.00	400
439227	23188.89	811.64	0.00	811.65	342	L	116.87	144.33	157.49	177.15	209.65	400

Crosssection	Distance	Z_left_dam	Z_right_dam	Waterlevel	Discharge	Bank side	HQ10	HQ30	HQ50	HQ100	HQ300	Category
439228	23334.88	0.00	809.66	809.68	192	R	116.91	144.40	157.57	177.25	209.77	300
439229	23486.55	0.00	808.68	808.74	172	R	117.02	144.57	157.77	177.50	210.12	100
439230	23636.32	0.00	807.72	807.72	158	R	117.03	144.59	157.79	177.52	210.15	100
439231	23697.18	0.00	808.97	808.98	336	R	117.04	144.59	157.80	177.53	210.16	400
439232	23766.94	0.00	806.97	807.00	170	R	117.10	144.68	157.91	177.67	210.35	100
439233	23913.37	0.00	806.12	806.12	226	R	117.12	144.72	157.95	177.71	210.41	400
439234	24052.19	0.00	804.90	804.91	318	R	117.15	144.76	158.00	177.78	210.50	400
439235	24206.36	0.00	803.98	803.99	188	R	117.19	144.81	158.06	177.85	210.60	300
439236	24363.83	803.70	0.00	803.70	638	L	117.20	144.84	158.09	177.89	210.65	400
439237	24477.93	803.85	0.00	803.85	590	L	117.27	144.94	158.20	178.03	210.85	400
439238	24636.27	0.00	801.18	801.18	198	R	117.28	144.95	158.22	178.05	210.87	300
439239	24780.98	0.00	799.59	799.60	258	R	117.29	144.96	158.23	178.07	210.90	400
439240	24921.44	0.00	798.13	798.13	130	R	117.32	145.01	158.29	178.14	210.99	30
439241	25065.55	0.00	800.28	800.28	464	R	117.33	145.03	158.31	178.17	211.03	400
439242	25234.86	0.00	799.03	799.04	354	R	117.36	145.06	158.36	178.22	211.10	400
439243	25311.60	799.45	0.00	799.46	514	L	117.36	145.07	158.36	178.23	211.11	400
439244	25394.23	797.72	0.00	797.72	1046	L	117.36	145.07	158.36	178.23	211.12	400
439245	25549.67	794.24	0.00	794.24	138	L	117.52	145.31	158.64	178.58	211.59	30
439246	25675.92	0.00	793.38	793.39	130	R	117.53	145.32	158.65	178.59	211.61	30
439247	25821.28	0.00	795.76	795.77	988	R	117.53	145.33	158.66	178.61	211.63	400
439248	25988.22	790.98	0.00	790.99	152	L	118.99	147.50	161.23	181.80	215.98	50
439249	26146.53	0.00	790.67	790.68	334	R	119.00	147.51	161.24	181.81	216.00	400
439250	26300.39	0.00	790.49	790.50	376	R	119.01	147.52	161.25	181.82	216.02	400
439251	26372.23	792.20	0.00	792.20	722	L	119.56	148.35	162.23	183.04	217.69	400
439252	26437.83	0.00	787.52	787.52	160	R	119.56	148.35	162.23	183.04	217.69	50
439253	26586.33	0.00	786.65	786.66	184	R	119.60	148.40	162.29	183.11	217.79	300
439254	26744.67	786.82	0.00	786.82	396	L	119.62	148.43	162.32	183.16	217.84	400
439255	26846.93	0.00	784.60	784.61	240	R	119.62	148.43	162.33	183.16	217.85	400
439256	26999.28	0.00	783.58	783.58	284	R	119.63	148.44	162.34	183.18	217.87	400
439257	27228.06	0.00	781.21	781.22	274	R	119.66	148.49	162.40	183.25	217.97	400
439258	27360.44	0.00	780.76	780.79	180	R	119.99	148.99	162.99	183.98	218.98	100
439259	27504.31	0.00	779.58	779.59	184	R	120.00	149.00	163.00	184.00	219.00	300
439260	27581.96	782.46	0.00	782.47	554	L	120.00	149.00	163.00	184.00	219.00	400
439261	27642.56	0.00	778.26	778.26	498	R	120.36	149.54	163.64	184.80	220.10	400
439262	27805.63	778.43	0.00	778.43	1568	L	120.38	149.57	163.67	184.83	220.14	400
439263	27949.49	776.98	0.00	776.98	1732	L	120.39	149.58	163.68	184.85	220.17	400
439264	28118.83	0.00	773.69	773.70	996	R	120.40	149.60	163.71	184.88	220.21	400
439265	28255.76	0.00	769.09	769.11	236	R	120.47	149.70	163.83	185.03	220.42	400
439266	28405.88	0.00	767.79	767.79	356	R	120.49	149.73	163.86	185.07	220.47	400
439267	28550.01	766.86	0.00	766.86	984	L	120.49	149.73	163.87	185.08	220.48	400
439268	28715.87	763.33	0.00	763.33	492	L	120.72	150.08	164.27	185.59	221.18	400
439269	28863.34	0.00	760.36	760.37	238	R	120.73	150.09	164.29	185.60	221.20	400
439270	28935.39	0.00	759.85	759.85	326	R	120.73	150.09	164.29	185.61	221.21	400
439271	29005.16	0.00	758.72	758.73	296	R	120.74	150.10	164.30	185.62	221.22	400
439272	29173.82	0.00	759.15	759.15	1126	L	120.75	150.12	164.33	185.66	221.27	400
439273	29323.18	0.00	758.70	758.70	1448	L	120.77	150.14	164.35	185.68	221.31	400
439274	29479.33	0.00	756.79	756.80	1204	L	120.79	150.18	164.39	185.74	221.38	400
439275	29628.26	0.00	754.87	754.87	782	R	120.80	150.19	164.40	185.75	221.40	400
439276	29758.96	753.82	0.00	753.82	642	L	120.82	150.22	164.44	185.80	221.46	400
439277	29913.36	0.00	749.37	749.38	192	R	120.83	150.25	164.47	185.84	221.52	300
439278	30044.27	748.13	0.00	748.13	226	L	120.84	150.25	164.48	185.85	221.53	400
439279	30194.73	748.72	0.00	748.73	394	L	120.85	150.27	164.50	185.87	221.57	400
439280	30347.68	748.27	0.00	748.27	602	L	121.07	150.59	164.88	186.34	222.22	400
439281	30495.02	746.98	0.00	746.99	598	L	121.11	150.66	164.96	186.45	222.36	400
439282	30632.71	0.00	744.45	744.46	388	R	121.12	150.67	164.97	186.46	222.37	400
439283	30802.67	741.33	0.00	741.33	274	L	121.12	150.68	164.98	186.47	222.39	400
439284	30949.47	740.31	0.00	740.31	332	L	121.13	150.68	164.99	186.48	222.40	400
439285	30982.06	741.03	0.00	741.03	638	L	121.13	150.68	164.99	186.48	222.40	400

Crosssection	Distance	Z_left_dam	Z_right_dam	Waterlevel	Discharge	Bank side	HQ10	HQ30	HQ50	HQ100	HQ300	Category
439286	31102.20	0.00	738.52	738.52	296	R	124.68	156.01	171.30	194.36	233.26	400
439287	31240.09	736.01	0.00	736.02	100	L	125.86	157.79	173.40	197.00	236.91	30
439288	31381.23	735.72	0.00	735.72	242	L	125.87	157.80	173.42	197.03	236.94	400
439289	31526.04	733.57	0.00	733.58	128	L	125.93	157.89	173.53	197.16	237.12	30
439290	31696.68	0.00	732.28	732.30	108	L	126.05	158.07	173.74	197.43	237.50	30
439291	31831.45	0.00	730.83	730.83	176	R	126.07	158.11	173.79	197.48	237.57	100
439292	31995.10	729.20	0.00	729.20	138	L	126.08	158.13	173.81	197.51	237.61	30
439293	32143.17	726.84	0.00	726.85	50	L	126.10	158.15	173.83	197.54	237.65	30
439294	32265.36	0.00	726.85	726.85	158	R	126.10	158.16	173.84	197.55	237.67	30
439295	32414.61	725.65	0.00	725.66	166	L	126.23	158.34	174.07	197.84	238.06	50
439296	32586.94	0.00	723.97	723.98	118	R	126.27	158.40	174.13	197.92	238.17	30
439297	32775.59	721.71	0.00	721.72	90	L	126.27	158.41	174.15	197.94	238.20	30
439298	32881.75	721.21	0.00	721.21	160	L	126.28	158.42	174.15	197.95	238.21	50
439299	33039.85	0.00	719.86	719.86	108	R	126.29	158.43	174.17	197.96	238.24	30
439300	33118.32	0.00	722.06	722.06	430	R	126.29	158.43	174.17	197.97	238.24	400
439301	33171.61	0.00	722.50	722.50	1108	R	127.14	159.72	175.70	199.89	240.90	400
439302	33370.35	0.00	717.05	717.06	118	R	127.29	159.95	175.97	200.23	241.38	30
439303	33619.88	0.00	714.97	714.98	190	R	127.32	159.99	176.02	200.28	241.45	100
439304	33800.02	712.92	0.00	712.93	118	L	127.38	160.08	176.13	200.43	241.65	30
439305	33931.24	711.78	0.00	711.79	94	L	127.39	160.09	176.14	200.44	241.67	30
439306	34138.25	0.00	710.55	710.55	148	R	127.42	160.14	176.20	200.51	241.77	30
439307	34259.29	0.00	709.90	709.91	182	R	127.51	160.28	176.37	200.73	242.07	100
439308	34403.40	710.62	0.00	710.62	458	L	127.52	160.29	176.38	200.74	242.08	400
439309	34558.99	707.13	0.00	707.14	174	L	127.70	160.57	176.71	201.16	242.67	50
439310	34685.62	0.00	706.10	706.10	88	R	127.75	160.64	176.79	201.26	242.80	30
439311	34910.05	704.71	0.00	704.71	118	L	127.79	160.70	176.87	201.35	242.93	30
439312	35052.87	703.66	0.00	703.67	186	L	127.79	160.70	176.87	201.35	242.94	100
439313	35185.51	0.00	702.82	702.83	230	R	127.80	160.71	176.88	201.36	242.95	300
439314	35253.03	702.38	0.00	702.39	160	L	127.80	160.71	176.88	201.37	242.96	30
439315	35328.02	701.91	0.00	701.91	166	L	127.91	160.89	177.09	201.63	243.32	50
439316	35470.27	0.00	700.22	700.24	76	R	127.94	160.93	177.14	201.69	243.41	30
439317	35648.95	0.00	699.66	699.67	236	R	128.25	161.40	177.69	202.39	244.38	300
439318	35823.68	697.69	0.00	697.69	206	L	128.32	161.51	177.82	202.55	244.61	300
439319	35976.77	0.00	696.48	696.48	308	R	128.33	161.52	177.84	202.57	244.63	400
439320	36111.40	0.00	697.48	697.48	480	R	128.34	161.54	177.86	202.60	244.67	400
439321	36260.49	0.00	693.92	693.93	240	R	128.36	161.57	177.89	202.64	244.73	300
439322	36415.86	0.00	693.33	693.34	298	R	128.47	161.72	178.08	202.88	245.06	400
439323	36559.23	0.00	692.03	692.03	216	R	128.62	161.95	178.36	203.22	245.54	300
439324	36715.94	690.47	0.00	690.48	210	L	128.63	161.97	178.38	203.25	245.58	300
439325	36865.48	691.97	0.00	691.98	684	L	128.64	161.98	178.39	203.26	245.59	400
439326	37005.88	691.56	0.00	691.57	648	L	129.30	162.98	179.58	204.76	247.68	400
439327	37152.68	0.00	688.82	688.83	344	R	129.35	163.06	179.68	204.88	247.85	400
439328	37253.63	689.52	0.00	689.53	554	L	129.37	163.09	179.71	204.93	247.91	400
439329	37345.62	0.00	686.54	686.55	230	R	129.38	163.10	179.72	204.94	247.92	300
439330	37434.22	0.00	685.80	685.80	154	R	129.39	163.12	179.74	204.97	247.97	30
439331	37520.78	0.00	685.10	685.11	142	R	129.42	163.16	179.79	205.03	248.06	30
439332	37610.28	0.00	684.92	684.92	150	R	129.43	163.18	179.81	205.05	248.09	30
439333	37707.98	0.00	684.31	684.33	138	R	129.43	163.19	179.82	205.07	248.11	30
439334	37808.72	0.00	683.77	683.78	164	R	129.44	163.20	179.83	205.08	248.12	50
439335	37878.74	686.62	0.00	686.62	616	L	129.50	163.28	179.94	205.21	248.30	400
439336	37906.50	683.74	0.00	683.75	238	L	129.50	163.28	179.94	205.21	248.30	300
439337	37957.02	683.79	0.00	683.80	580	L	129.50	163.29	179.94	205.22	248.31	400
439338	38005.97	0.00	683.79	683.79	920	R	129.50	163.29	179.94	205.22	248.31	400
439339	38049.66	684.01	0.00	684.01	690	L	129.50	163.29	179.94	205.22	248.32	400
439340	38091.78	0.00	683.93	683.94	752	R	129.50	163.29	179.95	205.22	248.32	400
439341	38224.55	681.72	0.00	681.73	422	L	156.11	187.63	202.64	223.66	257.43	400
439342	38288.75	680.46	0.00	680.46	272	L	157.90	189.78	204.97	226.22	260.38	400
439343	38370.19	680.56	0.00	680.57	346	L	157.91	189.79	204.98	226.23	260.39	400

Crosssection	Distance	Z_left_dam	Z_right_dam	Waterlevel	Discharge	Bank side	HQ10	HQ30	HQ50	HQ100	HQ300	Category
439344	38391.22	680.66	0.00	680.67	414	L	157.91	189.79	204.98	226.23	260.39	400
439345	38478.90	679.26	0.00	679.27	290	L	157.91	189.80	204.98	226.24	260.40	400
439346	38577.12	678.71	0.00	678.71	282	L	158.05	189.96	205.16	226.44	260.63	400
439347	38677.83	678.08	0.00	678.08	274	L	158.06	189.98	205.18	226.46	260.65	400
439348	38809.27	677.58	0.00	677.59	298	L	158.08	190.00	205.20	226.48	260.69	400
439349	38893.92	0.00	675.51	675.52	124	R	158.68	190.72	205.97	227.33	261.66	30
439350	38924.42	0.00	675.35	675.37	124	R	158.69	190.73	205.99	227.35	261.68	30
439351	38952.96	0.00	675.28	675.29	144	R	158.69	190.73	205.99	227.35	261.69	30
439352	38992.44	675.60	0.00	675.61	190	L	158.69	190.74	205.99	227.36	261.69	30
439353	39087.06	675.10	0.00	675.10	194	L	158.73	190.78	206.05	227.42	261.76	50
439354	39179.16	0.00	674.83	674.84	248	R	158.79	190.85	206.12	227.49	261.84	300
439355	39283.75	0.00	674.05	674.06	208	R	158.80	190.87	206.14	227.51	261.87	100
439356	39385.49	673.15	0.00	673.15	128	L	158.82	190.89	206.17	227.55	261.91	30
439357	39493.61	0.00	671.74	671.75	86	R	158.85	190.92	206.20	227.58	261.95	30
439358	39594.81	0.00	671.85	671.86	142	R	158.87	190.94	206.22	227.61	261.98	30
439359	39703.11	672.12	0.00	672.12	498	L	158.89	190.97	206.25	227.64	262.01	400
439360	39801.53	0.00	672.64	672.64	684	R	158.91	190.99	206.27	227.67	262.04	400
439361	39901.14	670.76	0.00	670.77	290	L	159.09	191.21	206.51	227.92	262.34	400
439362	40017.10	0.00	669.20	669.20	150	R	159.11	191.24	206.53	227.95	262.37	30
439363	40114.69	0.00	669.77	669.77	348	R	159.16	191.30	206.60	228.03	262.46	400
439364	40228.55	0.00	668.61	668.62	274	R	206.81	248.57	268.45	296.29	341.04	100
439365	40307.55	0.00	668.04	668.04	382	R	207.95	249.94	269.94	297.93	342.92	400
439366	40358.66	0.00	667.01	667.01	302	R	207.99	249.99	269.99	297.99	342.99	300
439367	40402.98	0.00	666.26	666.26	318	R	208.00	250.00	270.00	298.00	343.00	300
439368	40510.47	0.00	664.98	664.99	420	R	208.01	250.01	270.01	298.01	343.01	400
439369	40612.08	0.00	664.21	664.21	814	R	209.61	251.93	272.09	300.30	345.65	400
439370	40703.28	0.00	663.11	663.11	700	R	209.62	251.95	272.11	300.32	345.67	400
439371	40797.46	661.59	0.00	661.59	668	L	209.64	251.97	272.13	300.35	345.70	400
439372	40921.93	0.00	659.77	659.77	576	R	209.70	252.04	272.21	300.43	345.80	400
439373	41019.29	657.60	0.00	657.60	248	L	209.71	252.05	272.22	300.45	345.82	30
439374	41117.49	657.76	0.00	657.76	642	L	209.79	252.15	272.32	300.56	345.95	400
439375	41217.39	0.00	656.30	656.30	590	R	209.81	252.17	272.35	300.59	345.98	400
439376	41319.11	0.00	655.62	655.62	634	R	209.93	252.32	272.51	300.77	346.18	400
439377	41414.51	0.00	654.56	654.57	796	R	209.96	252.36	272.54	300.81	346.23	400
439378	41508.38	653.02	0.00	653.02	670	L	209.98	252.37	272.56	300.83	346.26	400
439379	41609.51	652.17	0.00	652.17	716	L	210.01	252.42	272.61	300.88	346.31	400
439380	41707.16	651.40	0.00	651.41	634	L	210.02	252.43	272.63	300.90	346.34	400
439381	41808.44	649.21	0.00	649.21	494	L	210.03	252.44	272.64	300.91	346.35	400
439382	41908.21	0.00	647.92	647.92	378	R	210.07	252.48	272.68	300.96	346.41	400
439383	42010.23	0.00	647.14	647.15	440	R	210.07	252.49	272.69	300.97	346.41	400
439384	42090.53	0.00	646.34	646.35	402	R	210.08	252.50	272.70	300.98	346.43	400
439385	42108.76	0.00	646.22	646.22	398	R	210.08	252.50	272.70	300.98	346.43	400
439386	42138.21	645.79	0.00	645.79	430	L	210.10	252.52	272.72	301.01	346.46	400
439387	42208.90	0.00	644.16	644.16	220	R	210.10	252.53	272.73	301.01	346.47	30
439388	42308.90	643.81	0.00	643.82	382	L	210.21	252.65	272.87	301.16	346.64	400
439389	42407.22	642.30	0.00	642.30	268	L	210.29	252.75	272.97	301.28	346.77	50
439390	42506.96	641.19	0.00	641.19	244	L	210.30	252.77	272.99	301.30	346.80	30
439391	42605.96	640.54	0.00	640.55	282	L	210.35	252.83	273.05	301.37	346.88	100
439392	42708.25	639.58	0.00	639.59	264	L	210.36	252.83	273.06	301.38	346.89	50
439393	42804.64	638.58	0.00	638.59	270	L	214.04	257.26	277.84	306.65	352.96	50
439394	42912.60	0.00	637.14	637.14	144	R	215.14	258.58	279.27	308.23	354.78	30
439395	43011.64	636.91	0.00	636.91	264	L	215.18	258.63	279.32	308.28	354.84	50
439396	43109.12	635.67	0.00	635.68	206	L	215.19	258.64	279.33	308.30	354.85	30
439397	43210.63	634.88	0.00	634.89	198	L	215.19	258.65	279.34	308.31	354.86	30
439398	43311.37	633.61	0.00	633.62	132	L	215.20	258.65	279.34	308.31	354.87	30
439399	43410.19	0.00	634.34	634.34	378	R	215.45	258.96	279.67	308.68	355.29	400
439400	43508.27	0.00	633.43	633.44	306	R	215.57	259.10	279.83	308.85	355.49	100
439401	43622.18	631.76	0.00	631.76	146	L	215.59	259.13	279.86	308.88	355.52	30

Crosssection	Distance	Z_left_dam	Z_right_dam	Waterlevel	Discharge	Bank side	HQ10	HQ30	HQ50	HQ100	HQ300	Category
439402	43682.14	631.28	0.00	631.29	132	L	215.62	259.15	279.89	308.91	355.56	30
439403	43743.08	630.38	0.00	630.40	56	L	215.62	259.15	279.89	308.91	355.56	30

Table B.3: For each cross section along the Simme: bank-full height and corresponding modelled bank-full discharge and side of overflow, estimated discharge for HQ_{10}, HQ_{30}, HQ_{50}, HQ_{100} and HQ_{300} and the associated return period for the modelled bank-full discharge.

Kander

Crosssection	Distance	Z_left_dam	Z_right_dam	Waterlevel	Discharge	Bank side	HQ10	HQ30	HQ50	HQ100	HQ300	Category
430001	0.00	0.00	754.57	754.57	484	R	128.65	162.51	180.11	207.20	257.30	400
430002	42.78	755.05	0.00	755.05	762	L	128.67	162.54	180.14	207.23	257.35	400
430003	52.30	0.00	753.52	753.52	1264	R	128.67	162.54	180.14	207.23	257.35	400
430004	105.13	752.43	0.00	752.43	670	L	128.69	162.56	180.17	207.26	257.38	400
430005	209.24	0.00	750.89	750.89	542	R	128.73	162.61	180.23	207.33	257.47	400
430006	308.63	749.94	0.00	749.94	530	L	128.86	162.77	180.41	207.53	257.72	400
430007	354.93	749.86	0.00	749.87	698	L	128.86	162.78	180.41	207.54	257.73	400
430008	406.79	746.99	0.00	746.99	970	L	129.33	163.36	181.06	208.29	258.66	400
430009	467.09	0.00	0.00	0.00	0	L	129.33	163.37	181.07	208.30	258.67	400
430010	531.31	745.94	0.00	746.18	1778	L	132.16	166.94	185.02	212.85	264.32	400
430011	600.08	0.00	744.99	745.00	1298	R	132.17	166.96	185.04	212.87	264.35	400
430012	656.55	744.45	0.00	744.46	988	L	132.24	167.04	185.14	212.98	264.48	400
430013	714.80	742.47	0.00	742.48	658	L	132.24	167.05	185.14	212.98	264.49	400
430014	754.61	741.74	0.00	741.76	544	L	132.25	167.05	185.15	212.99	264.50	400
430015	794.21	741.24	0.00	741.24	450	L	132.26	167.06	185.16	213.00	264.51	400
430016	843.93	740.38	0.00	740.39	298	L	132.28	167.09	185.19	213.04	264.55	400
430017	892.79	0.00	740.00	740.01	272	R	132.33	167.15	185.26	213.12	264.66	400
430018	940.92	0.00	739.71	739.71	316	R	132.46	167.32	185.45	213.33	264.92	400
430019	994.60	739.00	0.00	739.01	356	L	132.47	167.33	185.46	213.34	264.94	400
430020	1022.70	0.00	738.32	738.32	308	R	132.60	167.49	185.63	213.55	265.19	400
430021	1094.30	0.00	737.51	737.52	326	R	132.61	167.51	185.66	213.58	265.23	400
430022	1192.42	0.00	736.60	736.61	336	R	132.75	167.68	185.85	213.79	265.49	400
430023	1290.60	0.00	735.56	735.57	300	R	132.78	167.72	185.89	213.85	265.56	400
430024	1335.39	735.98	0.00	735.99	502	L	132.78	167.73	185.90	213.85	265.56	400
430025	1347.31	0.00	734.03	734.03	628	R	134.42	169.79	188.19	216.49	268.84	400
430026	1362.73	731.02	0.00	731.53	60	L	134.42	169.79	188.19	216.49	268.84	30
430027	1490.32	0.00	732.72	732.72	676	R	134.45	169.83	188.23	216.53	268.90	400
430028	1589.69	0.00	731.06	731.06	404	R	134.45	169.83	188.23	216.54	268.90	400
430029	1689.33	729.92	0.00	729.93	382	L	135.03	170.57	189.04	217.47	270.06	400
430030	1790.02	728.97	0.00	728.98	424	L	135.04	170.58	189.06	217.49	270.08	400
430031	1890.53	0.00	727.93	727.93	360	R	135.18	170.76	189.26	217.72	270.37	400
430032	1939.21	0.00	727.32	727.34	306	R	135.18	170.76	189.26	217.72	270.37	400
430033	1958.65	0.00	727.15	727.16	374	R	135.19	170.77	189.27	217.73	270.38	400
430034	1990.88	0.00	726.75	726.75	476	R	135.19	170.77	189.27	217.73	270.38	400
430035	2059.27	0.00	725.95	725.96	328	R	135.30	170.91	189.42	217.91	270.60	400
430036	2122.61	0.00	725.24	725.24	352	R	135.31	170.92	189.43	217.92	270.62	400
430037	2131.92	0.00	725.22	725.22	658	R	135.31	170.92	189.43	217.92	270.62	400
430038	2191.34	724.42	0.00	724.43	484	L	135.35	170.96	189.48	217.98	270.69	400
430039	2215.08	720.31	0.00	720.31	84	L	135.35	170.96	189.48	217.98	270.69	30
430040	2283.26	0.00	721.30	721.31	690	R	135.40	171.03	189.56	218.07	270.80	400
430041	2379.28	720.52	0.00	720.52	696	L	135.45	171.10	189.64	218.15	270.91	400
430042	2480.37	719.39	0.00	719.39	638	L	135.48	171.14	189.68	218.20	270.97	400
430043	2588.14	718.24	0.00	718.24	598	L	135.55	171.22	189.77	218.30	271.10	400
430044	2599.95	717.08	0.00	717.08	1128	L	135.55	171.22	189.77	218.30	271.10	400
430045	2680.32	715.69	0.00	715.69	476	L	135.57	171.24	189.79	218.33	271.13	400
430046	2781.18	714.51	0.00	714.51	378	L	135.92	171.69	190.29	218.91	271.85	400
430047	2848.40	0.00	714.55	714.55	602	R	135.93	171.71	190.31	218.92	271.87	400
430048	2977.40	712.54	0.00	712.54	616	L	170.99	215.99	239.39	275.38	341.98	400
430049	3078.65	0.00	712.24	712.24	474	R	171.00	216.00	239.40	275.40	342.00	400
430050	3172.63	0.00	711.58	711.58	514	R	171.03	216.04	239.44	275.45	342.06	400
430051	3276.68	0.00	711.55	711.55	738	R	171.12	216.15	239.57	275.59	342.24	400
430052	3389.35	0.00	709.78	709.78	558	R	171.14	216.17	239.59	275.62	342.27	400
430053	3454.37	0.00	708.69	708.69	618	R	171.22	216.28	239.71	275.75	342.44	400

Crosssection	Distance	Z_left_dam	Z_right_dam	Waterlevel	Discharge	Bank side	HQ10	HQ30	HQ50	HQ100	HQ300	Category
430054	3574.88	0.00	706.54	706.54	630	R	172.70	218.14	241.77	278.13	345.39	400
430055	3673.18	0.00	706.20	706.21	852	R	172.73	218.19	241.82	278.19	345.46	400
430056	3768.80	704.80	0.00	704.80	830	L	172.74	218.20	241.84	278.21	345.48	400
430057	3871.57	703.08	0.00	703.08	414	L	172.81	218.29	241.94	278.32	345.62	400
430058	3966.86	702.26	0.00	702.27	498	L	172.82	218.30	241.94	278.33	345.63	400
430059	4065.99	701.12	0.00	701.12	470	L	175.79	222.05	246.11	283.12	351.59	400
430060	4166.83	700.65	0.00	700.65	564	L	175.80	222.06	246.11	283.12	351.59	400
430061	4186.62	701.07	0.00	701.07	702	L	175.80	222.06	246.12	283.13	351.59	400
430062	4267.77	699.17	0.00	699.17	434	L	175.80	222.06	246.12	283.13	351.60	400
430063	4366.72	697.68	0.00	697.68	294	L	175.80	222.07	246.12	283.13	351.60	300
430064	4467.20	697.34	0.00	697.35	344	L	175.94	222.24	246.31	283.35	351.87	300
430065	4567.63	696.62	0.00	696.63	406	L	175.94	222.24	246.31	283.35	351.88	400
430066	4667.51	695.87	0.00	695.88	364	L	175.96	222.26	246.34	283.38	351.92	400
430067	4768.72	694.78	0.00	694.78	308	L	176.09	222.43	246.53	283.60	352.19	300
430068	4863.67	693.35	0.00	693.36	202	L	176.12	222.47	246.57	283.64	352.24	30
430069	4963.82	692.96	0.00	692.98	244	L	176.16	222.52	246.62	283.71	352.32	50
430070	5062.71	692.36	0.00	692.37	320	L	176.23	222.61	246.72	283.83	352.46	300
430071	5161.58	691.77	0.00	691.77	372	L	176.25	222.63	246.75	283.85	352.50	400
430072	5260.36	0.00	690.84	690.85	360	R	177.08	223.68	247.92	285.20	354.17	400
430073	5360.38	0.00	689.95	689.96	398	L	177.10	223.71	247.94	285.23	354.20	400
430074	5447.67	689.96	0.00	689.96	552	L	186.55	235.65	261.18	300.45	373.11	400
430075	5507.49	690.72	0.00	690.73	1034	L	186.56	235.65	261.18	300.46	373.11	400
430076	5561.69	688.86	0.00	688.86	604	L	186.63	235.75	261.29	300.58	373.27	400
430077	5661.43	0.00	688.13	688.14	602	R	186.91	236.10	261.68	301.03	373.82	400
430078	5761.56	0.00	687.22	687.23	528	R	186.93	236.12	261.70	301.06	373.86	400
430079	5786.88	0.00	687.11	687.12	732	R	186.93	236.13	261.71	301.06	373.87	400
430080	5857.20	683.46	0.00	683.46	762	L	186.95	236.15	261.73	301.09	373.90	400
430081	5955.76	682.54	0.00	682.54	704	L	186.96	236.15	261.74	301.10	373.91	400
430082	6056.68	681.19	0.00	681.19	536	L	186.97	236.17	261.76	301.12	373.94	400
430083	6155.33	680.10	0.00	680.10	408	L	187.31	236.60	262.23	301.67	374.62	400
430084	6252.34	678.98	0.00	678.98	302	L	187.35	236.65	262.28	301.73	374.69	300
430085	6347.91	678.14	0.00	678.14	310	L	187.35	236.65	262.29	301.73	374.70	300
430086	6449.33	677.34	0.00	677.34	472	L	187.35	236.65	262.29	301.73	374.70	400
430087	6548.01	676.52	0.00	676.52	282	L	187.65	237.03	262.71	302.22	375.30	100
430088	6646.65	675.97	0.00	675.98	300	L	187.74	237.15	262.84	302.36	375.48	100
430089	6749.98	674.89	0.00	674.90	260	L	187.80	237.23	262.92	302.46	375.61	50
430090	6849.19	674.08	0.00	674.09	284	L	187.83	237.25	262.96	302.50	375.65	100
430091	6948.10	673.32	0.00	673.32	290	L	187.92	237.37	263.09	302.65	375.84	100
430092	7093.43	673.49	0.00	673.49	700	L	188.18	237.70	263.45	303.07	376.36	400
430093	7103.90	668.46	0.00	669.15	60	L	188.18	237.70	263.45	303.07	376.36	30
430094	7144.44	0.00	671.19	671.19	2028	L	188.26	237.80	263.56	303.20	376.52	400
430095	7247.22	668.70	0.00	668.70	318	L	188.30	237.85	263.62	303.26	376.60	300
430096	7352.24	0.00	668.25	668.25	554	R	188.31	237.87	263.64	303.28	376.63	400
430097	7454.62	0.00	666.98	666.99	338	R	188.32	237.88	263.65	303.30	376.65	300
430098	7554.47	666.29	0.00	666.30	386	L	188.36	237.93	263.70	303.35	376.72	400
430099	7750.78	665.60	0.00	665.61	610	L	188.91	238.63	264.48	304.25	377.82	400
430100	7849.00	664.39	0.00	664.39	702	L	188.94	238.66	264.51	304.29	377.88	400
430101	7959.21	0.00	664.92	664.92	1218	R	188.95	238.67	264.53	304.31	377.90	400
430102	8053.73	0.00	663.44	663.44	844	L	189.33	239.16	265.07	304.93	378.67	400
430103	8176.36	0.00	662.03	662.03	714	R	189.41	239.26	265.18	305.05	378.82	400
430104	8189.13	0.00	661.73	661.73	1192	L	189.41	239.26	265.18	305.05	378.82	400
430105	8202.61	0.00	661.50	661.50	1574	L	189.41	239.26	265.18	305.05	378.82	400
430106	8250.16	0.00	0.00	0.00	0	L	189.43	239.28	265.20	305.08	378.86	400
430107	8348.87	0.00	658.07	658.07	1732	L	189.44	239.29	265.22	305.10	378.88	400
430108	8370.94	0.00	656.81	656.81	982	R	189.44	239.29	265.22	305.10	378.88	400
430109	8381.65	0.00	655.72	655.72	1490	L	189.44	239.29	265.22	305.10	378.88	400
430110	8439.71	0.00	0.00	0.00	0	L	189.84	239.80	265.78	305.74	379.68	400
430111	8545.35	0.00	0.00	0.00	0	L	189.88	239.85	265.84	305.81	379.76	400

Crosssection	Distance	Z_left_dam	Z_right_dam	Waterlevel	Discharge	Bank side	HQ10	HQ30	HQ50	HQ100	HQ300	Category
430112	8647.13	0.00	651.68	651.68	686	R	189.91	239.89	265.88	305.86	379.82	400
430113	8745.95	652.22	0.00	652.22	830	L	189.95	239.94	265.93	305.92	379.90	400
430114	8848.41	650.91	0.00	650.92	534	L	189.98	239.97	265.97	305.96	379.96	400
430114.5	8916.41	650.06	0.00	650.07	438	L	189.99	239.99	265.99	305.98	379.98	400
430115.5	8931.79	0.00	649.96	649.97	588	R	190.00	240.00	266.00	306.00	380.00	400
430115	8932.29	0.00	650.01	650.02	1058	R	190.00	240.00	266.00	306.00	380.00	400
430116.5	8945.15	648.59	0.00	648.59	574	L	190.00	240.00	266.00	306.00	380.00	400
430116	8945.65	648.61	0.00	648.62	826	L	190.00	240.00	266.00	306.00	380.00	400
430117	8959.01	0.00	647.63	647.63	986	R	190.00	240.00	266.00	306.00	380.00	400
430118	8979.08	647.12	0.00	647.13	980	L	190.01	240.02	266.02	306.02	380.03	400
430119	9051.35	0.00	646.46	646.46	926	L	190.02	240.02	266.02	306.03	380.03	400
430120	9128.82	645.25	0.00	645.25	730	L	190.02	240.03	266.03	306.03	380.04	400
430121	9148.00	643.86	0.00	643.86	1890	L	190.25	240.32	266.35	306.41	380.50	400
430122	9242.27	642.15	0.00	642.15	892	L	190.26	240.33	266.36	306.42	380.52	400
430123	9332.97	641.47	0.00	641.47	686	L	190.28	240.35	266.39	306.45	380.56	400
430124	9345.80	639.96	0.00	639.96	626	L	190.28	240.35	266.39	306.45	380.56	400
430125	9359.16	639.05	0.00	639.05	708	L	190.29	240.36	266.40	306.46	380.57	400
430126	9444.39	0.00	638.55	638.55	1804	R	190.30	240.38	266.42	306.49	380.60	400
430127	9539.90	637.31	0.00	637.31	882	L	190.41	240.52	266.57	306.66	380.82	400
430128	9622.97	0.00	636.41	636.41	682	R	190.42	240.53	266.59	306.68	380.84	400
430129	9633.56	631.88	0.00	631.88	250	L	190.42	240.53	266.59	306.68	380.84	50
430130	9685.24	0.00	633.70	633.70	756	R	190.43	240.55	266.61	306.70	380.86	400
430131	9846.59	0.00	630.87	630.87	1812	L	190.49	240.62	266.68	306.78	380.97	400
430132	10051.74	627.44	0.00	627.44	1914	L	190.53	240.67	266.75	306.86	381.07	400
430133	10151.84	624.83	0.00	624.83	618	L	190.56	240.70	266.78	306.89	381.11	400
430134	10242.87	624.02	0.00	624.02	676	L	190.57	240.72	266.79	306.91	381.13	400
430135	10272.21	623.85	0.00	623.85	1114	L	190.59	240.75	266.83	306.95	381.19	400
430136	10317.58	624.52	0.00	624.52	2022	L	190.59	240.75	266.83	306.95	381.19	400
430137	10332.48	0.00	0.00	0.00	0	L	190.59	240.75	266.83	306.96	381.19	400
430138	10354.63	0.00	0.00	0.00	0	L	190.60	240.76	266.84	306.96	381.20	400
430139	10378.31	0.00	0.00	0.00	0	L	190.60	240.76	266.84	306.96	381.20	400
430140	10404.35	0.00	0.00	0.00	0	L	190.60	240.76	266.84	306.96	381.20	400
430141	10554.78	620.16	0.00	620.16	850	L	190.61	240.77	266.85	306.98	381.21	400
430142	10630.57	621.84	0.00	621.84	1928	L	190.61	240.78	266.86	306.99	381.23	400
430143	10749.97	0.00	617.96	617.97	662	L	190.68	240.86	266.95	307.09	381.36	400
430144	10851.35	0.00	617.41	617.41	994	L	190.71	240.89	266.99	307.14	381.42	400
430145	10971.82	617.95	0.00	617.95	1606	L	190.73	240.93	267.03	307.18	381.47	400
430146	11024.67	0.00	0.00	0.00	0	L	190.74	240.93	267.03	307.19	381.48	400
430147	11076.75	0.00	0.00	0.00	0	L	190.75	240.94	267.04	307.20	381.49	400
430148	11105.86	0.00	0.00	0.00	0	L	190.75	240.94	267.04	307.20	381.49	400
430149	11155.95	0.00	612.85	612.85	1408	L	190.75	240.95	267.05	307.21	381.51	400
430150	11355.33	611.41	0.00	611.41	1014	L	190.81	241.03	267.14	307.31	381.63	400
430151	11558.00	0.00	608.11	608.12	236	R	190.89	241.13	267.25	307.44	381.79	30
430152	11599.41	0.00	608.58	608.58	452	R	190.90	241.13	267.25	307.44	381.79	400
430153	11611.66	608.08	0.00	608.08	818	L	190.90	241.14	267.27	307.46	381.81	400
430154	11623.51	607.95	0.00	607.95	1574	L	190.91	241.15	267.27	307.46	381.82	400
430155	11671.68	0.00	0.00	0.00	0	L	190.91	241.15	267.27	307.47	381.82	400
430156	11689.12	0.00	0.00	0.00	0	L	190.91	241.15	267.27	307.47	381.82	400
430157	11709.66	0.00	0.00	0.00	0	L	190.93	241.17	267.30	307.49	381.86	400
430158	11756.84	0.00	0.00	0.00	0	L	190.94	241.18	267.31	307.51	381.87	400
430159	11848.44	0.00	0.00	0.00	0	L	190.95	241.20	267.33	307.53	381.90	400
430160	11940.10	0.00	603.71	603.71	924	R	190.96	241.21	267.34	307.54	381.92	400
430161	12150.70	0.00	602.12	602.13	558	R	192.29	242.89	269.21	309.69	384.58	400
430162	12241.11	0.00	0.00	0.00	0	L	192.30	242.90	269.22	309.70	384.60	400
430163	12264.30	0.00	0.00	0.00	0	L	192.32	242.93	269.25	309.73	384.64	400
430164	12275.13	0.00	0.00	0.00	0	L	192.32	242.93	269.25	309.73	384.64	400
430165	12297.49	601.00	0.00	601.00	688	L	192.32	242.93	269.25	309.74	384.64	400
430166	12344.64	0.00	600.39	600.40	856	R	192.32	242.93	269.25	309.74	384.64	400

Crosssection	Distance	Z_left_dam	Z_right_dam	Waterlevel	Discharge	Bank side	HQ10	HQ30	HQ50	HQ100	HQ300	Category
430167	12358.32	0.00	600.70	600.70	1298	L	192.32	242.93	269.25	309.74	384.65	400
430168	12432.15	597.62	0.00	597.62	846	L	192.35	242.97	269.29	309.79	384.70	400
430169	12466.52	0.00	0.00	0.00	0	L	192.35	242.97	269.29	309.79	384.70	400
430170	12516.41	598.37	0.00	598.37	848	L	192.36	242.98	269.30	309.80	384.72	400
430171	12545.12	598.75	0.00	598.75	1362	L	192.38	243.00	269.33	309.83	384.75	400
430172	12734.48	0.00	597.44	597.44	800	R	192.42	243.05	269.38	309.89	384.83	400
430173	12827.59	0.00	595.09	595.10	470	L	192.43	243.07	269.40	309.91	384.86	400
430174	12940.44	0.00	0.00	0.00	0	L	192.44	243.08	269.42	309.93	384.88	400
430175	13022.81	0.00	0.00	0.00	0	L	192.46	243.10	269.44	309.96	384.91	400
430176	13152.84	0.00	594.23	594.23	1560	L	192.47	243.12	269.46	309.98	384.94	400
430177	13227.19	0.00	0.00	0.00	0	L	192.48	243.13	269.47	309.99	384.96	400
430178	13255.32	590.88	0.00	590.88	432	L	192.48	243.14	269.48	310.00	384.97	400
430179	13272.71	0.00	591.85	591.85	1888	L	192.48	243.14	269.48	310.00	384.97	400
430180	13337.37	0.00	589.82	589.82	822	R	192.49	243.14	269.48	310.00	384.97	400
430181	13355.72	0.00	588.94	588.94	1216	L	192.49	243.14	269.48	310.01	384.98	400
430182	13436.98	0.00	0.00	0.00	0	L	192.50	243.16	269.50	310.03	385.00	400
430183	13447.13	0.00	0.00	0.00	0	L	192.50	243.16	269.50	310.03	385.00	400
430184	13475.70	0.00	0.00	0.00	0	L	192.50	243.16	269.51	310.03	385.01	400
430185	13495.48	585.73	0.00	585.73	1366	L	192.50	243.16	269.51	310.03	385.01	400
430186	13515.67	583.64	0.00	583.64	446	L	420.81	531.55	589.14	677.73	841.62	30
430187	13535.87	0.00	586.71	587.04	1740	L	420.81	531.55	589.14	677.73	841.63	400
430188	13553.80	0.00	590.35	590.35	1704	L	420.82	531.56	589.15	677.74	841.64	400
430189	13575.41	0.00	587.10	587.10	978	R	420.82	531.57	589.15	677.75	841.65	400
430190	13596.19	0.00	585.25	585.25	678	R	420.82	531.57	589.15	677.75	841.65	300
430191	13616.22	0.00	585.10	585.10	866	R	420.83	531.58	589.16	677.76	841.66	400
430192	13637.05	586.40	0.00	586.40	1616	L	420.83	531.58	589.16	677.76	841.66	400
430193	13656.39	0.00	584.57	584.57	746	R	420.84	531.58	589.17	677.77	841.67	300
430194	13679.02	0.00	583.60	583.60	482	R	420.84	531.58	589.17	677.77	841.67	30
430195	13701.30	0.00	583.78	583.78	622	R	420.85	531.60	589.18	677.78	841.69	100
430196	13722.81	0.00	583.91	583.91	782	R	420.87	531.62	589.22	677.82	841.74	300
430197	13745.40	584.76	0.00	584.76	1546	L	420.87	531.62	589.22	677.82	841.74	400
430198	13848.43	0.00	0.00	0.00	0	L	420.89	531.65	589.25	677.86	841.78	400
430199	13948.73	0.00	583.22	583.22	1486	L	420.91	531.67	589.27	677.88	841.81	400
430200	14063.68	0.00	582.62	582.63	1828	L	420.95	531.73	589.33	677.95	841.90	400
430201	14142.71	0.00	582.11	582.12	1798	L	420.96	531.74	589.35	677.97	841.93	400
430202	14234.93	581.22	0.00	581.22	980	L	420.98	531.76	589.37	678.00	841.96	400
430203	14339.79	0.00	580.25	580.25	556	R	421.03	531.83	589.44	678.08	842.06	50
430204	14426.69	0.00	579.74	579.74	854	R	421.78	532.77	590.49	679.28	843.55	400
430205	14535.68	0.00	579.10	579.10	756	L	421.95	532.99	590.73	679.56	843.89	300
430206	14607.87	0.00	578.50	578.50	538	R	421.97	533.01	590.76	679.59	843.94	50
430207	14734.25	577.65	0.00	577.65	580	L	422.01	533.07	590.82	679.67	844.03	50
430208	14838.23	576.25	0.00	576.25	408	L	422.04	533.11	590.86	679.71	844.09	30
430209	14944.82	0.00	576.38	576.39	762	R	422.33	533.47	591.26	680.18	844.66	300
430210	14984.41	576.48	0.00	576.49	668	L	422.35	533.49	591.29	680.20	844.70	100
430211	15149.70	0.00	0.00	0.00	0	L	422.36	533.51	591.31	680.23	844.73	400
430212	15249.15	0.00	0.00	0.00	0	L	422.37	533.52	591.32	680.24	844.74	400
430213	15346.80	0.00	0.00	0.00	0	L	422.44	533.60	591.41	680.34	844.87	400
430214	15442.96	0.00	0.00	0.00	0	L	422.45	533.62	591.43	680.37	844.91	400
430215	15549.13	573.00	0.00	573.00	1664	L	422.48	533.66	591.47	680.42	844.96	400
430216	15649.18	0.00	570.81	570.81	636	L	422.49	533.67	591.48	680.43	844.98	100
430217	15762.71	0.00	570.32	570.32	802	L	422.49	533.68	591.49	680.44	844.99	300
430218	15836.15	0.00	0.00	0.00	0	L	422.50	533.69	591.50	680.45	845.01	400
430219	15887.69	0.00	573.73	573.74	1574	R	422.51	533.69	591.51	680.46	845.01	400
430220	15954.62	571.89	0.00	571.90	1270	L	422.51	533.70	591.52	680.47	845.02	400
430221	16036.23	0.00	0.00	0.00	0	L	422.52	533.71	591.53	680.48	845.04	400
430222	16101.69	0.00	0.00	0.00	0	L	422.53	533.73	591.55	680.50	845.06	400
430223	16299.01	0.00	0.00	0.00	0	L	422.57	533.77	591.59	680.56	845.13	400
430224	16383.04	0.00	0.00	0.00	0	L	422.58	533.78	591.61	680.57	845.16	400

Crosssection	Distance	Z_left_dam	Z_right_dam	Waterlevel	Discharge	Bank side	HQ10	HQ30	HQ50	HQ100	HQ300	Category
430225	16467.80	0.00	0.00	0.00	0	L	422.60	533.81	591.64	680.61	845.20	400
430226	16535.80	0.00	0.00	0.00	0	L	422.61	533.83	591.66	680.63	845.23	400
430227	16641.66	0.00	0.00	0.00	0	L	422.62	533.84	591.67	680.64	845.24	400
430228	16743.39	562.01	0.00	562.01	1234	L	422.64	533.87	591.70	680.68	845.29	400
430229	16843.45	0.00	560.44	560.44	680	R	422.66	533.88	591.72	680.70	845.31	100
430230	16928.23	558.98	0.00	558.98	530	L	422.84	534.12	591.98	681.00	845.69	30

Table B.4: For each cross section along the Kander: bank-full height and corresponding modelled bank-full discharge and side of overflow, estimated discharge for HQ_{10}, HQ_{30}, HQ_{50}, HQ_{100} and HQ_{300} and the associated return period for the modelled bank-full discharge

Weisse Lütschine

Crosssection	Distance	Z_left_dam	Z_right_dam	Waterlevel	Discharge	Bank side	HQ10	HQ30	HQ50	HQ100	HQ300	Category
502002	0.00	0.00	919.95	919.96	44.00	R	33.03	40.55	44.80	50.20	59.57	50
502003	14.28	919.74	0.00	919.74	206.00	L	33.03	40.55	44.80	50.20	59.57	400
502004	127.10	914.20	0.00	914.20	1194.00	L	33.04	40.56	44.82	50.21	59.59	400
502005	205.18	0.00	0.00	908.14	2000.00	L	33.06	40.59	44.85	50.25	59.63	400
502006	305.71	902.31	0.00	902.31	1560.00	L	33.07	40.60	44.86	50.26	59.65	400
502007	392.07	896.73	0.00	896.73	860.00	L	33.08	40.61	44.88	50.28	59.67	400
502008	567.73	890.71	0.00	890.71	750.00	L	47.12	57.21	62.86	70.14	82.82	400
502009	668.07	887.23	0.00	887.24	398.00	L	47.16	57.25	62.90	70.18	82.87	400
502010	767.21	884.14	0.00	884.15	314.00	L	47.96	58.20	63.92	71.31	84.18	400
502011	824.89	882.95	0.00	882.96	192.00	L	47.97	58.20	63.93	71.32	84.19	400
502012	864.41	880.53	0.00	880.56	62.00	L	47.99	58.23	63.96	71.35	84.22	50
502013	968.64	0.00	878.31	878.31	336.00	R	47.99	58.24	63.96	71.35	84.23	400
502014	1061.13	875.66	0.00	875.67	384.00	L	48.31	58.60	64.36	71.79	84.74	400
502015	1169.54	0.00	872.60	872.60	268.00	R	48.74	59.11	64.91	72.40	85.45	400
502016	1272.01	869.66	0.00	869.67	114.00	L	48.78	59.16	64.97	72.46	85.52	400
502017	1371.90	867.00	0.00	867.01	122.00	L	48.80	59.19	64.99	72.49	85.55	400
502018	1473.67	864.02	0.00	864.02	122.00	L	48.95	59.36	65.18	72.70	85.79	400
502019	1532.35	0.00	862.62	862.63	142.00	R	48.96	59.37	65.19	72.71	85.81	400
502020	1579.04	861.07	0.00	861.08	110.00	L	48.96	59.38	65.20	72.71	85.81	400
502021	1678.57	858.31	0.00	858.33	84.00	L	49.06	59.48	65.31	72.84	85.96	300
502022	1778.92	855.74	0.00	855.76	58.00	L	49.06	59.49	65.32	72.85	85.97	30
502023	1884.49	853.65	0.00	853.66	178.00	L	51.08	61.86	67.88	75.67	89.24	400
502024	1988.75	850.29	0.00	850.30	66.00	L	51.25	62.06	68.09	75.90	89.51	50
502025	2088.20	848.57	0.00	848.57	110.00	L	51.31	62.13	68.17	75.99	89.61	400
502026	2188.27	846.15	0.00	846.15	100.00	L	51.40	62.23	68.28	76.11	89.75	400
502027	2286.88	0.00	843.78	843.79	96.00	R	51.47	62.31	68.37	76.20	89.87	400
502028	2317.15	0.00	844.47	844.48	192.00	R	51.47	62.32	68.37	76.21	89.87	400
502029	2377.15	841.22	0.00	841.23	24.00	L	51.59	62.45	68.52	76.37	90.06	30
502030	2471.12	839.70	0.00	839.71	50.00	L	51.62	62.49	68.56	76.41	90.11	30
502031	2574.02	837.30	0.00	837.31	62.00	L	51.64	62.51	68.58	76.44	90.14	30
502032	2677.70	835.50	0.00	835.51	96.00	L	52.68	63.73	69.90	77.89	91.82	400
502033	2774.92	833.77	0.00	833.78	180.00	L	52.70	63.76	69.92	77.92	91.86	400
502034	2878.84	831.02	0.00	831.02	40.00	L	52.74	63.80	69.97	77.97	91.92	30
502035	2976.59	829.22	0.00	829.23	64.00	L	52.76	63.83	70.00	78.00	91.95	50
502036	3086.38	828.47	0.00	828.47	198.00	L	52.87	63.96	70.14	78.16	92.14	400
502037	3181.06	825.23	0.00	825.23	74.00	L	52.89	63.98	70.17	78.19	92.17	100
502038	3286.71	0.00	823.58	823.58	118.00	R	52.92	64.01	70.20	78.22	92.21	400
502039	3339.78	823.76	0.00	823.77	608.00	L	52.92	64.02	70.21	78.23	92.22	400
502040	3381.75	821.40	0.00	821.40	106.00	L	52.93	64.02	70.21	78.24	92.23	400
502041	3490.07	819.82	0.00	819.83	170.00	L	53.07	64.19	70.39	78.44	92.46	400
502042	3591.17	818.55	0.00	818.55	172.00	L	53.09	64.22	70.42	78.46	92.49	400
502043	3690.24	0.00	816.74	816.75	282.00	R	53.12	64.26	70.46	78.51	92.54	400
502044	3789.67	815.43	0.00	815.43	384.00	L	53.14	64.28	70.49	78.54	92.58	400
502045	3889.46	0.00	813.30	813.31	250.00	R	53.16	64.29	70.50	78.55	92.60	400
502046	3988.82	0.00	811.49	811.50	224.00	R	64.15	77.14	84.33	93.76	110.22	400
502047	4086.09	0.00	809.38	809.39	162.00	R	64.17	77.15	84.35	93.78	110.25	400
502048	4185.73	0.00	807.34	807.35	130.00	R	64.23	77.23	84.43	93.87	110.35	400
502049	4283.95	805.91	0.00	805.91	86.00	L	64.28	77.28	84.49	93.93	110.42	100
502050	4385.66	804.41	0.00	804.43	84.00	L	64.76	77.84	85.09	94.59	111.19	50
502051	4486.78	803.03	0.00	803.05	74.00	L	64.77	77.86	85.11	94.61	111.21	30
502052	4584.24	801.72	0.00	801.74	82.00	L	64.78	77.87	85.12	94.62	111.22	50
502053	4685.87	0.00	800.76	800.77	102.00	R	65.64	78.87	86.19	95.80	112.59	300
502054	4787.11	0.00	798.94	798.95	100.00	R	65.65	78.88	86.20	95.81	112.60	300

Crosssection	Distance	Z_left_dam	Z_right_dam	Waterlevel	Discharge	Bank side	HQ10	HQ30	HQ50	HQ100	HQ300	Category
502055	4840.74	0.00	799.43	799.43	288.00	R	66.08	79.38	86.74	96.40	113.28	400
502056	4911.06	0.00	797.33	797.34	110.00	R	66.09	79.39	86.75	96.42	113.30	300
502057	4981.83	0.00	796.96	796.97	150.00	R	66.12	79.43	86.79	96.46	113.35	400
502058	5074.04	795.00	0.00	795.03	70.00	L	66.13	79.44	86.81	96.48	113.37	30
502059	5175.78	793.55	0.00	793.58	64.00	L	66.14	79.46	86.82	96.50	113.39	30
502060	5283.46	0.00	792.77	792.78	106.00	R	66.28	79.61	86.99	96.68	113.60	300
502061	5382.81	0.00	791.32	791.34	90.00	R	66.29	79.62	87.00	96.69	113.62	100
502062	5464.28	790.40	0.00	790.40	98.00	L	66.29	79.62	87.01	96.70	113.62	300
502063	5481.91	0.00	790.09	790.10	90.00	R	66.29	79.63	87.01	96.70	113.62	100
502064	5582.16	0.00	788.61	788.62	68.00	R	68.22	81.87	89.41	99.34	116.68	30
502065	5681.76	0.00	787.40	787.43	70.00	R	68.22	81.87	89.42	99.35	116.69	30
502066	5785.01	0.00	787.05	787.05	132.00	R	68.25	81.91	89.46	99.39	116.74	400
502067	5833.98	0.00	785.70	785.72	108.00	R	68.26	81.91	89.46	99.40	116.74	300
502068	5936.55	0.00	784.58	784.58	144.00	R	68.30	81.97	89.52	99.46	116.82	400
502069	6026.69	0.00	786.03	786.03	548.00	R	68.42	82.10	89.67	99.62	117.00	400
502070	6140.58	781.16	0.00	781.17	170.00	L	68.67	82.39	89.98	99.96	117.40	400
502071	6224.82	0.00	780.74	780.74	512.00	R	69.94	83.87	91.56	101.70	119.41	400
502072	6319.24	0.00	779.22	779.23	764.00	R	69.96	83.90	91.59	101.73	119.45	400
502073	6449.03	0.00	0.00	0.00	0.00	L	70.76	84.82	92.59	102.82	120.71	400
502074	6536.10	0.00	0.00	775.62	2000.00	L	70.77	84.83	92.60	102.84	120.72	400
502075	6641.28	0.00	0.00	772.04	1924.00	L	70.78	84.85	92.62	102.86	120.75	400
502076	6742.39	0.00	765.18	765.18	546.00	R	71.83	86.07	93.92	104.29	122.40	400
502077	6822.33	0.00	762.54	762.55	456.00	R	71.84	86.07	93.93	104.30	122.41	400
502078	6846.53	0.00	762.55	762.55	678.00	R	72.90	87.31	95.26	105.75	124.09	400
502079	6947.66	758.28	0.00	758.28	1122.00	L	72.99	87.41	95.37	105.87	124.23	400
502080	7038.94	753.47	0.00	753.47	1576.00	L	73.08	87.52	95.48	106.00	124.37	400
502081	7142.45	0.00	751.13	751.13	1648.00	R	73.12	87.56	95.53	106.05	124.43	400
502082	7252.45	0.00	745.35	745.36	654.00	R	73.20	87.65	95.63	106.16	124.56	400
502083	7348.11	0.00	742.91	742.91	488.00	L	73.24	87.70	95.67	106.21	124.62	400
502084	7448.43	0.00	741.06	741.07	388.00	R	73.82	88.37	96.40	107.00	125.54	400
502085	7546.79	0.00	738.86	738.87	108.00	R	73.93	88.49	96.53	107.15	125.70	300
502086	7591.74	738.66	0.00	738.66	96.00	L	73.94	88.51	96.54	107.16	125.72	50
502087	7653.72	0.00	736.79	736.80	56.00	R	74.06	88.65	96.70	107.33	125.92	30
502088	7762.44	735.25	0.00	735.26	40.00	L	74.64	89.32	97.42	108.12	126.83	30
502089	7869.79	0.00	733.91	733.92	72.00	R	74.66	89.34	97.44	108.14	126.86	30
502090	7976.87	0.00	732.42	732.43	72.00	R	74.80	89.51	97.61	108.34	127.08	30
502091	8083.45	0.00	730.90	730.91	76.00	R	74.83	89.55	97.66	108.39	127.14	30
502092	8183.33	729.65	0.00	729.67	64.00	L	74.86	89.58	97.69	108.42	127.17	30
502093	8279.18	0.00	728.59	728.62	94.00	R	74.88	89.60	97.71	108.44	127.20	50
502094	8365.25	0.00	727.67	727.70	106.00	R	75.04	89.79	97.91	108.66	127.46	100
502095	8449.19	726.30	0.00	726.32	76.00	L	75.05	89.80	97.93	108.68	127.47	30
502096	8552.75	0.00	725.78	725.78	294.00	R	75.07	89.82	97.96	108.71	127.51	400
502097	8651.28	718.02	0.00	718.02	554.00	L	75.13	89.89	98.03	108.79	127.60	400
502098	8751.08	0.00	0.00	714.94	2000.00	L	75.16	89.92	98.06	108.82	127.64	400
502099	8862.45	0.00	0.00	708.17	2000.00	L	84.08	100.25	109.13	120.95	141.64	400
502100	8958.73	702.29	0.00	702.29	916.00	L	84.34	100.54	109.44	121.30	142.03	400
502101	9046.58	0.00	0.00	700.11	1926.00	L	84.38	100.59	109.49	121.35	142.09	400
502102	9159.37	0.00	694.15	694.15	1382.00	L	84.43	100.65	109.55	121.41	142.17	400
502103	9247.53	691.27	0.00	691.27	1650.00	L	84.46	100.68	109.59	121.46	142.22	400
502104	9336.53	686.38	0.00	686.38	1228.00	L	84.48	100.71	109.62	121.49	142.25	400
502105	9461.36	680.45	0.00	680.45	1660.00	L	84.51	100.74	109.66	121.53	142.30	400
502106	9551.18	676.34	0.00	676.34	968.00	L	84.89	101.18	110.12	122.04	142.89	400
502107	9688.22	672.28	0.00	672.28	970.00	L	84.95	101.25	110.20	122.12	142.99	400
502108	9766.18	0.00	670.01	670.01	486.00	R	84.95	101.25	110.20	122.13	142.99	400
502109	9851.28	0.00	668.11	668.12	496.00	R	85.06	101.37	110.33	122.26	143.15	400
502110	9924.31	666.68	0.00	666.68	660.00	L	85.21	101.55	110.52	122.48	143.40	400
502111	10015.24	664.97	0.00	664.97	632.00	L	85.30	101.65	110.62	122.59	143.53	400
502112	10094.20	0.00	662.04	662.05	328.00	R	85.31	101.66	110.64	122.61	143.55	400

Crosssection	Distance	Z_left_dam	Z_right_dam	Waterlevel	Discharge	Bank side	HQ10	HQ30	HQ50	HQ100	HQ300	Category
502113	10176.10	0.00	660.86	660.86	262.00	R	85.41	101.78	110.76	122.74	143.70	400
502114	10269.66	658.69	0.00	658.70	80.00	L	85.42	101.80	110.78	122.76	143.73	30
502115	10366.15	657.33	0.00	657.34	140.00	L	85.44	101.82	110.81	122.79	143.76	300
502116	10463.78	0.00	655.63	655.64	104.00	R	85.55	101.94	110.94	122.93	143.92	50
502117	10546.98	0.00	654.41	654.42	102.00	R	85.56	101.96	110.95	122.95	143.94	50
502118	10643.11	653.89	0.00	653.90	146.00	L	85.59	101.98	110.98	122.98	143.98	400
502119	10749.46	651.94	0.00	651.96	80.00	L	85.60	102.00	111.00	123.00	144.00	30
502120	10844.92	0.00	650.67	650.68	74.00	R	85.63	102.04	111.04	123.04	144.05	30
502121	10947.50	649.66	0.00	649.66	114.00	L	85.67	102.08	111.09	123.09	144.11	100
502122	11049.47	0.00	648.65	648.67	140.00	R	85.68	102.09	111.10	123.11	144.12	300

Table B.5: For each cross section along the Weisse Lütschine: bank-full height and corresponding modelled bank-full discharge and side of overflow, estimated discharge for HQ_{10}, HQ_{30}, HQ_{50}, HQ_{100} and HQ_{300} and the associated return period for the modelled bank-full discharge.

Schwarze Lütschine

Crosssection	Distance	Z_left_dam	Z_right_dam	Waterlevel	Discharge	Bank side	HQ10	HQ30	HQ50	HQ100	HQ300	Category
501001	0.00	962.35	0.00	962.36	232	L	23.13	26.98	29.05	31.94	37.03	400
501002	100.21	0.00	960.61	960.61	808	R	42.95	50.11	53.94	59.31	68.77	400
501003	198.12	0.00	957.86	957.87	190	R	42.97	50.14	53.97	59.35	68.81	400
501004	298.85	955.90	0.00	955.90	262	L	42.99	50.16	53.99	59.37	68.84	400
501005	395.54	0.00	954.22	954.22	214	R	43.44	50.68	54.56	59.99	69.55	400
501006	510.57	952.15	0.00	952.17	146	L	43.45	50.69	54.57	60.00	69.57	400
501007	594.08	0.00	952.61	952.61	354	R	45.82	53.46	57.55	63.28	73.37	400
501008	701.23	951.29	0.00	951.29	308	L	45.86	53.50	57.59	63.32	73.42	400
501009	806.82	0.00	948.27	948.28	156	R	47.08	54.93	59.13	65.02	75.38	400
501010	884.34	0.00	947.93	947.93	222	R	47.10	54.95	59.16	65.05	75.42	400
501011	907.36	946.61	0.00	946.61	88	L	47.11	54.96	59.16	65.05	75.43	400
501012	1008.17	944.94	0.00	944.96	100	L	47.13	54.98	59.19	65.08	75.46	400
501013	1110.92	0.00	944.19	944.20	92	R	47.14	55.00	59.21	65.10	75.49	400
501014	1126.65	944.35	0.00	944.35	164	L	47.18	55.04	59.25	65.15	75.54	400
501015	1209.03	943.11	0.00	943.12	240	L	47.19	55.05	59.27	65.16	75.56	400
501016	1307.71	941.90	0.00	941.91	204	L	47.21	55.08	59.30	65.20	75.60	400
501017	1414.34	0.00	939.87	939.88	134	R	47.24	55.12	59.33	65.24	75.64	400
501018	1510.15	938.43	0.00	938.44	86	L	47.99	55.99	60.28	66.27	76.84	400
501019	1573.01	938.76	0.00	938.77	204	L	48.02	56.02	60.31	66.31	76.89	400
501020	1611.02	937.69	0.00	937.70	114	L	48.03	56.04	60.33	66.33	76.91	400
501021	1711.77	0.00	935.72	935.73	76	R	48.04	56.05	60.34	66.34	76.92	300
501022	1797.79	0.00	934.54	934.56	66	R	54.05	63.06	67.89	74.64	86.55	50
501023	1894.52	934.21	0.00	934.21	194	L	54.33	63.39	68.24	75.03	86.99	400
501024	1990.14	0.00	932.36	932.37	124	R	54.34	63.40	68.25	75.04	87.01	400
501025	2090.75	0.00	930.92	930.92	108	R	54.92	64.07	68.98	75.84	87.94	400
501026	2193.23	930.25	0.00	930.26	128	L	54.92	64.08	68.98	75.85	87.94	400
501027	2292.34	928.78	0.00	928.79	120	L	54.93	64.09	68.99	75.86	87.96	400
501028	2403.51	928.96	0.00	928.96	592	L	55.01	64.17	69.09	75.96	88.08	400
501029	2515.14	928.45	0.00	928.46	472	L	57.38	66.94	72.06	79.24	91.87	400
501030	2610.76	0.00	924.55	924.56	120	R	57.41	66.98	72.11	79.28	91.93	400
501031	2712.40	0.00	922.36	922.37	68	R	57.48	67.06	72.19	79.37	92.03	50
501032	2792.10	922.31	0.00	922.32	224	L	57.53	67.12	72.26	79.45	92.12	400
501033	2906.29	921.20	0.00	921.20	256	L	58.71	68.49	73.73	81.07	94.00	400
501034	3014.01	920.16	0.00	920.18	258	L	58.72	68.50	73.75	81.09	94.02	400
501035	3093.57	919.10	0.00	919.10	220	L	58.90	68.71	73.97	81.33	94.30	400
501036	3116.46	919.04	0.00	919.04	266	L	58.90	68.72	73.98	81.34	94.31	400
501037	3217.95	0.00	917.23	917.23	194	R	58.91	68.73	73.99	81.36	94.33	400
501038	3326.47	0.00	915.82	915.82	168	R	59.14	68.99	74.27	81.67	94.69	400
501039	3422.37	914.61	0.00	914.61	216	L	59.16	69.02	74.30	81.70	94.73	400
501040	3521.77	913.79	0.00	913.80	280	L	59.18	69.04	74.32	81.72	94.75	400
501041	3625.02	911.49	0.00	911.50	156	L	64.15	74.84	80.57	88.58	102.71	400
501042	3715.40	909.96	0.00	909.97	96	L	64.20	74.90	80.63	88.65	102.79	300
501043	3812.33	0.00	908.86	908.87	66	R	64.22	74.93	80.66	88.69	102.83	30
501044	3916.32	907.95	0.00	907.96	170	L	64.28	74.99	80.73	88.76	102.92	400
501045	4007.66	906.93	0.00	906.93	162	L	64.32	75.05	80.79	88.83	103.00	400
501046	4110.52	0.00	905.77	905.78	122	R	64.36	75.09	80.84	88.88	103.06	400
501047	4217.01	904.65	0.00	904.65	146	L	64.37	75.10	80.85	88.89	103.07	400
501048	4312.47	0.00	904.74	904.74	294	R	64.43	75.17	80.93	88.98	103.17	400
501049	4370.13	0.00	905.51	905.52	536	R	64.44	75.18	80.93	88.99	103.18	400
501050	4409.68	902.52	0.00	902.53	90	L	64.51	75.26	81.02	89.09	103.29	300
501051	4514.82	901.76	0.00	901.77	140	L	64.58	75.35	81.11	89.19	103.41	400
501052	4614.04	900.20	0.00	900.20	78	L	64.68	75.46	81.24	89.32	103.57	50
501053	4711.99	0.00	899.16	899.17	78	R	64.69	75.48	81.25	89.34	103.59	50

Crosssection	Distance	Z_left_dam	Z_right_dam	Waterlevel	Discharge	Bank side	HQ10	HQ30	HQ50	HQ100	HQ300	Category
501054	4810.62	0.00	898.30	898.30	108	R	66.32	77.38	83.30	91.59	106.20	400
501055	4915.08	897.23	0.00	897.23	94	L	66.42	77.49	83.42	91.72	106.35	300
501056	5020.98	896.33	0.00	896.35	94	L	66.50	77.59	83.52	91.84	106.48	300
501057	5116.72	895.63	0.00	895.66	100	L	66.51	77.60	83.54	91.85	106.50	300
501058	5213.39	894.26	0.00	894.26	72	L	66.58	77.68	83.62	91.95	106.61	30
501059	5297.40	893.64	0.00	893.65	106	L	66.91	78.06	84.04	92.40	107.14	300
501060	5390.63	893.48	0.00	893.49	492	L	67.15	78.34	84.34	92.73	107.52	400
501062	5527.50	0.00	891.79	891.79	794	L	67.19	78.39	84.39	92.78	107.58	400
501063	7302.82	0.00	0.00	0.00	0	L	70.18	81.87	88.14	96.91	112.37	400
501064	7389.88	723.96	0.00	723.96	1378	L	70.47	82.22	88.51	97.32	112.84	400
501065	7513.95	0.00	718.14	718.15	828	L	70.69	82.47	88.78	97.62	113.19	400
501066	7609.95	0.00	714.97	714.98	470	R	70.70	82.48	88.80	97.63	113.20	400
501067	7709.40	0.00	712.75	712.76	442	R	70.93	82.75	89.08	97.95	113.57	400
501068	7761.99	0.00	711.80	711.80	996	R	70.93	82.75	89.08	97.95	113.57	400
501069	7813.52	708.81	0.00	708.81	566	L	71.24	83.11	89.47	98.38	114.07	400
501070	7903.54	705.33	0.00	705.33	518	L	71.25	83.13	89.49	98.40	114.09	400
501071	8005.71	0.00	702.60	702.61	262	R	71.38	83.27	89.65	98.57	114.29	400
501072	8107.03	701.17	0.00	701.18	216	L	71.41	83.31	89.68	98.61	114.34	400
501073	8202.02	0.00	699.67	699.69	192	R	71.42	83.32	89.69	98.62	114.35	400
501074	8304.73	0.00	697.91	697.91	208	R	71.67	83.62	90.02	98.98	114.76	400
501075	8406.36	0.00	696.13	696.13	188	R	71.90	83.89	90.31	99.29	115.13	400
501076	8510.53	694.40	0.00	694.41	176	L	73.14	85.33	91.86	101.00	117.11	400
501077	8607.28	693.73	0.00	693.74	256	L	73.14	85.33	91.86	101.01	117.12	400
501078	8706.29	0.00	692.21	692.22	192	R	73.55	85.80	92.37	101.56	117.76	400
501079	8806.73	690.83	0.00	690.84	178	L	73.56	85.82	92.39	101.58	117.78	400
501080	8906.02	0.00	690.12	690.13	226	R	73.60	85.87	92.44	101.64	117.85	400
501081	9003.42	0.00	689.39	689.39	292	R	73.63	85.90	92.48	101.68	117.90	400
501082	9108.70	0.00	687.98	687.99	232	R	73.64	85.91	92.49	101.69	117.91	400
501083	9180.65	0.00	686.98	686.98	162	R	73.87	86.18	92.78	102.01	118.28	400
501084	9207.90	0.00	0.00	0.00	0	L	73.90	86.22	92.82	102.05	118.33	400
501085	9313.79	0.00	685.21	685.21	470	R	74.00	86.33	92.94	102.19	118.49	400
501086	9408.46	681.71	0.00	681.71	328	L	74.01	86.35	92.96	102.21	118.51	400
501087	9504.69	0.00	680.07	680.08	356	L	76.51	89.26	96.09	105.66	122.51	400
501088	9605.40	0.00	677.41	677.41	156	R	76.53	89.29	96.12	105.69	122.55	400
501089	9712.59	0.00	674.93	674.94	164	R	76.82	89.62	96.48	106.09	123.00	400
501090	9815.57	0.00	673.38	673.38	198	R	76.91	89.72	96.59	106.20	123.14	400
501091	9906.22	0.00	672.84	672.85	306	R	76.92	89.74	96.61	106.22	123.16	400
501092	10017.23	0.00	669.86	669.86	100	R	77.32	90.20	97.11	106.77	123.80	100
501093	10118.94	672.41	0.00	672.41	1174	L	77.73	90.68	97.62	107.34	124.46	400
501094	10249.30	0.00	665.55	665.56	142	R	77.75	90.71	97.65	107.37	124.49	400
501095	10339.81	0.00	664.22	664.23	112	R	77.88	90.86	97.81	107.55	124.70	300
501096	10434.45	0.00	663.09	663.10	80	R	77.91	90.89	97.85	107.58	124.74	30
501097	10533.76	662.42	0.00	662.44	114	L	78.09	91.11	98.08	107.84	125.04	300
501098	10631.40	0.00	661.33	661.33	88	R	78.33	91.38	98.38	108.17	125.42	30
501099	10735.08	660.93	0.00	660.96	136	L	78.34	91.39	98.39	108.18	125.43	400
501100	10829.38	0.00	659.99	660.00	154	R	78.42	91.48	98.49	108.29	125.56	400
501101	10925.45	0.00	659.02	659.03	110	R	78.46	91.54	98.54	108.35	125.63	300
501102	10970.91	0.00	658.19	658.20	96	R	78.46	91.54	98.54	108.35	125.63	50
501103	11067.82	0.00	656.80	656.81	58	R	78.59	91.68	98.70	108.52	125.83	30
501104	11131.12	656.80	0.00	656.83	100	L	78.62	91.73	98.75	108.58	125.89	100
501105	11233.16	0.00	656.12	656.13	126	R	78.89	92.03	99.08	108.94	126.31	300
501106	11325.00	0.00	655.19	655.20	128	R	78.91	92.06	99.10	108.97	126.35	400
501107	11420.23	0.00	654.08	654.10	88	R	78.93	92.08	99.13	109.00	126.38	30
501108	11520.16	0.00	654.12	654.13	164	R	78.95	92.11	99.16	109.03	126.42	400
501109	11549.92	0.00	654.10	654.11	224	R	78.95	92.11	99.16	109.03	126.42	400
501110	11627.21	0.00	652.06	652.08	62	R	79.03	92.20	99.25	109.13	126.54	30
501111	11727.20	651.22	0.00	651.24	50	L	79.10	92.29	99.35	109.24	126.66	30
501112	11825.69	650.33	0.00	650.35	44	L	79.14	92.33	99.40	109.29	126.72	30

Crosssection	Distance	Z_left_dam	Z_right_dam	Waterlevel	Discharge	Bank side	HQ10	HQ30	HQ50	HQ100	HQ300	Category
501113	11923.09	0.00	649.75	649.76	78	R	79.18	92.38	99.45	109.35	126.79	30
501114	12015.76	647.24	0.00	647.90	20	L	79.21	92.41	99.48	109.38	126.82	30
501115	12120.39	0.00	648.01	648.01	128	R	79.22	92.43	99.50	109.40	126.85	400

Table B.6: For each cross section along the Schwarze Lütschine: bank-full height and corresponding modelled bank-full discharge and side of overflow, estimated discharge for HQ_{10}, HQ_{30}, HQ_{50}, HQ_{100} and HQ_{300} and the associated return period for the modelled bank-full discharge.

Vereinte Lütschine

Crosssection	Distance	Z_left_dam	Z_right_dam	Waterlevel	Discharge	Bank side	HQ10	HQ30	HQ50	HQ100	HQ300	Category
500001	51.64	648.46	0.00	648.47	268	L	160.81	186.25	199.73	218.41	250.81	400
500002	145.96	647.22	0.00	647.23	152	L	160.82	186.26	199.74	218.42	250.83	30
500003	243.49	646.64	0.00	646.65	216	L	160.84	186.29	199.77	218.46	250.88	100
500004	332.36	0.00	645.96	645.96	282	R	160.89	186.36	199.85	218.55	251.00	400
500005	421.95	0.00	645.02	645.02	290	R	160.91	186.38	199.88	218.59	251.05	400
500006	514.10	0.00	644.06	644.06	204	R	160.92	186.40	199.90	218.62	251.09	100
500007	623.98	643.20	0.00	643.21	148	L	161.05	186.57	200.09	218.85	251.40	30
500008	734.41	642.34	0.00	642.34	288	L	161.12	186.67	200.20	218.98	251.58	400
500009	851.35	641.47	0.00	641.48	204	L	161.14	186.69	200.23	219.01	251.62	100
500010	958.25	640.96	0.00	640.96	192	L	161.45	187.11	200.72	219.60	252.40	50
500011	1058.54	639.73	0.00	639.73	94	L	161.46	187.13	200.74	219.63	252.44	30
500012	1144.46	641.67	0.00	641.67	1064	L	161.47	187.14	200.75	219.64	252.46	400
500013	1238.96	0.00	640.14	640.14	438	R	161.49	187.17	200.79	219.69	252.52	400
500014	1328.82	0.00	638.94	638.94	442	R	162.11	188.00	201.75	220.84	254.05	400
500016	1532.13	636.41	0.00	636.42	160	L	162.13	188.03	201.78	220.88	254.11	30
500017	1639.05	635.88	0.00	635.89	234	L	162.14	188.05	201.80	220.90	254.14	300
500018	1744.23	634.61	0.00	634.63	152	L	162.17	188.09	201.84	220.95	254.21	30
500019	1844.17	634.63	0.00	634.63	294	L	162.22	188.16	201.93	221.05	254.34	400
500020	1944.78	634.58	0.00	634.58	470	L	162.25	188.20	201.98	221.11	254.42	400
500021	2043.55	0.00	635.63	635.64	1038	R	162.29	188.25	202.03	221.18	254.50	400
500022	2132.13	0.00	0.00	635.63	0	L	162.31	188.27	202.06	221.21	254.55	400
500023	2243.27	0.00	0.00	635.08	0	L	162.39	188.38	202.19	221.37	254.76	400
500024	2348.81	0.00	0.00	629.34	0	L	162.40	188.40	202.20	221.39	254.79	400
500025	2427.22	0.00	0.00	624.14	0	L	162.42	188.42	202.23	221.42	254.83	400
500026	2527.56	0.00	0.00	621.64	0	L	162.64	188.72	202.58	221.84	255.39	400
500027	2627.72	0.00	613.83	618.97	1858	L	162.64	188.73	202.59	221.85	255.40	400
500028	2729.89	0.00	0.00	0.00	0	L	162.96	189.16	203.08	222.45	256.20	400
500029	2835.42	0.00	608.95	613.66	1738	L	162.99	189.20	203.13	222.51	256.28	400
500030	2947.06	0.00	604.60	604.60	624	R	163.01	189.23	203.16	222.54	256.32	400
500031	3038.55	0.00	602.82	602.82	440	R	163.13	189.38	203.34	222.76	256.61	400
500032	3128.59	601.06	0.00	601.06	272	L	163.21	189.50	203.47	222.92	256.82	400
500033	3257.92	599.14	0.00	599.14	300	L	163.38	189.72	203.73	223.23	257.25	400
500034	3350.55	598.81	0.00	598.81	620	L	163.42	189.77	203.79	223.30	257.34	400
500035	3436.58	598.24	0.00	598.25	476	L	163.42	189.78	203.80	223.32	257.36	400
500036	3543.89	595.83	0.00	595.84	138	L	163.43	189.79	203.82	223.33	257.38	30
500037	3642.61	0.00	595.10	595.12	136	R	163.44	189.81	203.83	223.35	257.41	30
500038	3735.46	0.00	594.69	594.69	192	R	163.44	189.81	203.84	223.36	257.42	50
500039	3836.44	593.97	0.00	593.99	164	L	163.45	189.82	203.85	223.37	257.43	30
500040	3938.20	593.35	0.00	593.35	172	L	163.51	189.91	203.95	223.49	257.59	30
500041	4037.31	592.93	0.00	592.94	184	L	163.52	189.92	203.96	223.50	257.61	30
500042	4131.76	592.39	0.00	592.40	218	L	163.64	190.08	204.15	223.74	257.92	100
500043	4221.76	0.00	591.86	591.87	208	R	163.65	190.10	204.17	223.75	257.95	100
500044	4317.69	0.00	590.63	590.63	170	R	167.92	195.89	210.87	231.84	268.78	30
500045	4383.44	592.64	0.00	592.64	590	L	167.92	195.90	210.88	231.85	268.80	400
500046	4528.13	589.12	0.00	589.13	170	L	167.94	195.92	210.91	231.89	268.85	30
500047	4632.84	590.61	0.00	590.62	414	L	167.97	195.96	210.95	231.94	268.92	400
500048	4726.83	0.00	588.53	588.54	214	R	167.97	195.96	210.96	231.95	268.93	100
500049	4828.07	0.00	586.86	586.88	140	R	168.00	196.00	211.00	232.00	269.00	30
500050	4929.60	0.00	588.56	588.57	370	R	168.01	196.01	211.01	232.01	269.02	400
500051	4962.09	0.00	590.58	590.59	822	R	168.01	196.01	211.01	232.01	269.02	400
500052	5025.89	0.00	586.89	586.89	346	R	168.05	196.07	211.08	232.10	269.13	400
500053	5121.25	0.00	586.40	586.41	272	R	168.06	196.08	211.09	232.11	269.15	400
500054	5223.25	586.28	0.00	586.28	338	L	168.06	196.09	211.10	232.12	269.16	400

Crosssection	Distance	Z_left_dam	Z_right_dam	Waterlevel	Discharge	Bank side	HQ10	HQ30	HQ50	HQ100	HQ300	Category
500055	5321.81	585.17	0.00	585.18	388	L	168.07	196.09	211.11	232.13	269.17	400
500056	5419.51	584.54	0.00	584.55	302	L	168.08	196.10	211.12	232.15	269.20	400
500057	5521.28	0.00	583.59	583.59	268	R	168.69	196.94	212.09	233.32	270.78	300
500058	5622.40	583.46	0.00	583.50	328	L	168.71	196.96	212.11	233.35	270.81	400
500059	5727.45	582.10	0.00	582.10	258	L	168.71	196.97	212.12	233.36	270.83	300
500060	5828.29	581.79	0.00	581.80	270	L	168.82	197.11	212.29	233.56	271.09	300
500061	5922.98	581.41	0.00	581.42	298	L	168.83	197.13	212.31	233.58	271.13	400
500062	6018.73	580.87	0.00	580.88	292	L	168.84	197.15	212.33	233.61	271.17	400
500063	6119.07	0.00	580.20	580.21	298	R	168.85	197.16	212.35	233.63	271.19	400
500064	6221.34	0.00	583.33	583.33	946	R	168.96	197.31	212.51	233.83	271.46	400
500065	6322.60	578.96	0.00	578.97	342	L	169.16	197.58	212.84	234.22	271.99	400
500066	6427.09	578.27	0.00	578.28	274	L	169.17	197.59	212.85	234.23	272.00	400
500067	6530.78	577.70	0.00	577.71	272	L	169.17	197.60	212.85	234.24	272.02	300
500068	6623.19	577.08	0.00	577.08	264	L	169.18	197.61	212.87	234.26	272.04	300
500069	6718.99	576.56	0.00	576.57	274	L	169.20	197.63	212.89	234.29	272.08	400
500070	6823.77	576.23	0.00	576.23	294	L	169.36	197.86	213.15	234.61	272.51	400
500071	6929.08	575.59	0.00	575.59	294	L	169.38	197.88	213.18	234.64	272.55	400
500072	7029.40	574.80	0.00	574.81	236	L	169.43	197.95	213.26	234.74	272.69	300
500073	7128.08	574.38	0.00	574.40	246	L	169.44	197.96	213.27	234.75	272.70	300
500074	7221.77	573.85	0.00	573.86	240	L	169.52	198.06	213.39	234.89	272.90	300
500075	7324.46	573.19	0.00	573.20	228	L	169.52	198.07	213.40	234.91	272.91	100
500076	7417.50	573.62	0.00	573.62	382	L	169.53	198.08	213.41	234.92	272.93	400
500077	7530.87	0.00	572.72	572.74	284	R	169.55	198.11	213.45	234.96	272.98	400
500078	7635.48	571.69	0.00	571.70	340	L	169.56	198.12	213.46	234.97	273.00	400
500079	7735.86	571.56	0.00	571.57	334	L	169.56	198.13	213.47	234.99	273.02	400
500080	7824.99	0.00	571.32	571.33	332	R	169.57	198.13	213.47	234.99	273.03	400
500081	7922.43	0.00	570.70	570.71	336	R	169.57	198.14	213.49	235.01	273.05	400
500082	8018.29	570.55	0.00	570.56	324	L	169.58	198.15	213.50	235.02	273.06	400
500083	8063.45	0.00	569.86	569.87	254	R	169.58	198.16	213.50	235.02	273.07	300
500084	8113.24	0.00	569.63	569.64	274	R	169.58	198.16	213.50	235.03	273.07	400
500085	8209.96	0.00	568.86	568.87	218	R	169.59	198.17	213.51	235.04	273.09	100
500086	8308.93	568.19	0.00	568.20	178	L	169.60	198.18	213.52	235.05	273.11	30
500087	8407.37	0.00	567.96	567.98	202	R	169.72	198.35	213.72	235.29	273.43	50
500088	8507.38	0.00	567.65	567.65	194	R	169.73	198.35	213.73	235.30	273.44	30
500089	8608.20	0.00	566.26	566.27	98	R	169.74	198.37	213.75	235.33	273.48	30
500090	8660.16	0.00	565.97	565.99	86	R	169.75	198.38	213.76	235.34	273.49	30

Table B.7: For each cross section along the Vereinte Lütschine: bank-full height and corresponding modelled bank-full discharge and side of overflow, estimated discharge for HQ_{10}, HQ_{30}, HQ_{50}, HQ_{100} and HQ_{300} and the associated return period for the modelled bank-full discharge.

Bibliography

Aarewasser AG (2009). *Nachhaltiger Hochwasserschutz Aare Thun Bern, Technischer Bericht mit Kostenschaetzung*.

Adrien, G. Nicolas (2004). *Computation Hydraulics and Hydrology: An Illustrated Dictionary*. Ed. by CRC Press.

Aeschbacher, J. (2003). "Development of water use and water-shortage in the Naro Moru Catchment (Upper Ewaso Ng'iro Basin, Kenya)". MA thesis. University of Bern.

Aeschbacher, J., H. Linger, and R. Weingartner (2005). "River Water Shortage in a Highland-Lowland System, a case study of the impacts of water abstraction in the Mount Kenya region". In: *Mountain Research and Development* 25, pp. 155–162.

Barben, M. (2001). "Beurteilung von Verfahren zur Abschaetzung seltener Hochwasserabfluesse in mesoskaligen Einzugsgebieten". PhD thesis. University of Bern.

Benito, G. et al. (2011). "Hydrological response of a dryland ephemeral river to southern African climatic variability during the last millennium". In: *Quaternary Research* 75, pp. 471–482.

Bosshart, U. (1997). "Measurement of river discharge for the SCRP Research Catchments. Soil Conservation Research Programme". In: *research Report 31*.

Boursicaud, R. Le. et al. (2015). *Gauging extreme floods on YouTube: Application of LSPIV to home movies fro the post-event determination of stream discharge*.

Braca, G. (2008). "Stage-discharge relations in open channels: practices and problems". In: *FORALPS Technical Report, Trento, Italy* 11, p. 24.

Brechtold, T. (2015). *Numerische Modellierung von Flussausweitungen*. VAW Mitteilungen 231, Versuchsanstalt Wasserbau, Hydrologie und Glaziologie.

Brunner, M. (2014). "Modeling the influence of spatial and temporal precipitation variability on the peak discharge of the Simme basin in the Bernese Oberland". MA thesis. University of Bern.

CDE (2014). *The water and land Resource Centre Project*. [02.04.2015]. CDE University of Bern. URL: `http://www.cde.unibe.ch/Pages/Project/6/43/The-Water-and-Land-Resource-Centre-Project.aspx`.

De Leeuw, J. et al. (2012). "Benefits of Riverine Water Discharge into the Lorian Swamp". In: *Water* 4(4), pp. 1009–1024.

Dobmann, J. (2009). "Hochwasserabschaetzung in kleinen Einzugsgebieten der Schweiz: Interpretations – und Praxishilfe". PhD thesis. University of Bern.

Drosg, M. (2006). *Der Umgang mit Unsicherheiten: Ein Leitfaden zur Fehleranalyse*. Fachultas Verlags- und Buchhandels AG.

EB AG (2008). *Technischer Bericht und Gefahrenkarte Boltigen*. Emch Berger AG.

EB AG et al. (2014). *Hochwasserschutz Aare Bern, Gebietsschutz Quartiere an der Aare*. Emch Berger AG, IUB Engieering und Flussbau AG.

FAN and KOHS (2015). *Empfehlung der Beurteilung der Gefahr der Ufererosion an Fliessgewaesser*. Fachleute Naturgefahren Schweiz FAN, Kommission fuer Hochwasserschutz KOHS des schweizer Wasserwirschaftsverbandes.

Fischerei BE (2016). [09.03.2016]. Volksdirektion Kanton Bern Fischerei. URL: http://www.vol.be.ch/vol/de/index/natur/fischerei/angelfischerei/pachtgewaesser.

FOEN (2015a). *Gewaesserinformationssystem der Schweiz (GEWISS)*. [01.11.2015]. URL: http://www.bafu.admin.ch/wasser/13462/13496/15009/index.html?lang=de.

– (2015b). *Hydrologische Daten und Vorhersagen*. [01.05.2016]. Federal Office for the Environment FOEN. URL: www.hydrodaten.admin.ch.

geo7 AG and KH AG (2004). *Technischer Bericht zur Gefahrenkarte Zweisimmen*. GEO7 AG and Kellerhals Haefeli AG.

Geomap (2016). [20.02.2016]. URL: https://map.geo.admin.ch.

GEOTEST AG (2012). *Technischer Bericht zur Gefahrenkarte Lenk*. GEOTEST AG.

GEOTEST AG and PORTA group (2014). *Technischer Bericht Hochwasserschutz Eyeltil, Lauterbrunnen Wasserbaubewilligung*. GEOTEST AG and PORTA group.

Gichuki, F., H. Linger, and G. Schwilch (1998). "Knowledge about Highland-Lowland interactions: The Role of a Natural Resource Information System". In: *Eastern and southern Africa Geographic Journal* 8, p. 5.

Gichuki, F. et al. (1998). "Scarce Water: Exploring Resource Availability, Use and Improved Management". In: *Eastern and southern Africa Geographic Journal* 8.special number.

Gorden, N. et al. (2004). *Stream Hydrology, Introduction for Ecologists*. second. Wiley.

Hauer, R. F. and G.A. Lamberti (2006). *Methods in stream ecology*. Elsevier.

Hunzinger, L., B. Zarn, and G.R. Bezzola (2008). *Beurteilung der Wirkung von Schutzmassnahmen gegen Naturgefahren als Grundlage fuer ihre Beruecksichtigung in der Raumplanung, Teil F: Fluesse*. Nationale Plattform Naturgefahren PLANAT.

HZP AG and EB AG (2007). *Gewaesserentwicklungskonzept GEKa Modul Umwelt, Fachbericht Teilprojekt Fluss-Morphologie und Wasserbau (FluMoKa)*. Hunziker Zarn Partner AG and Emch Berger AG.

IG Flussbau AG (2012). *Technischer Bericht Hochwasserschutz Boedeli Luetschine*. IG Flussbau AG, SAH and Wyss.

IUCN (2015). *Ewaso Ngiro North River Basin*. [05.05.2015]. International Union for Conservation of Nature. URL: http://www.iucn.org/wisp/our_projects_in_wisp/cocoon_initiative_kenya/overview_of_the_four_basins/ewaso_ngiro_north_river_basin/.

KH AG (2005). *Technischer Bericht zur Gefahrenkarte Erlenbach*. Kellerhals Haefeli AG.

KH AG and KZ AG (2008). *Technischer Bericht zur Gefahrenkarte St.Stephan*. Kellerhals Haefeli AG and Kissling Zbinden AG.

Kiteme, B. et al. (1998). "A Highland-Lowland System under Transitional Pressure: A Spatio-Temporal Analysis". In: *Eastern and Southern Africa Geographic Journal* 8, p. 45.

Kiteme, B. et al. (2007). "Land use transformation and global change: The Case of Mount Kenya". In: *Proceedings of the Launching Workshop for the Global Change Research Network in African Mountains*.

Kiteme, B.P. et al. (2008). "Dimensions of global changes in African Mountains: The example of Mount Kenya". In: *Magazine of the international Human Dimensions Programme on global environmental change* Issue 2, pp. 18 –22.

Klauser, H. (2004). "Hochwasserrelevante Darstellung von mesoskaligen Einzugsgebieten in der Schweiz - Entwicklung der Software HQx_meso_CH". PhD thesis. University of Bern.

Le Coz, J (2012). "A literature review of methods for estimating the uncertainty associated with stage-discharge relations". In: *WMO Rep. PO6a*.

Liniger, H. (2015). *Personal communication*.

Liniger, H., R. Weingartner, and M Grosjean (1998). "Mountains of the world, Water Towers for the 21st Century - A Contributaion to Global Freshwater Management". In: *Mountain Agenda*.

Liniger, H. et al. (2005). "Assessing and managing scarce tropical mountain water resources, the case of Mount Kenya and the semiarid upper Ewaso Ngiro Basin". In: *Mountain Research and Development* 25, pp. 163–173.

Liniger, H. et al. (2014). "Concept for monitoring of water availability and use at Lower Ewaso Ngiro Basin: Merti Aquifer and Loran Swamps". In:

MacMillan, L. and H. Liniger (2005). "Monitoring and modelling for the sustainable management of water resources in tropical mountain basins - the Mount Kenya example". In: *Huber, U.M., Reasoner, M.A., Bugmann, H. (Eds.): Global Change and Mountain Regions*.

MobiliarLab (2015). *Flagship-Projekt "M-AARE"*. [05.08.2015]. University of Bern. URL: http://mobiliarlab.unibe.ch/content/projekte/flagship_projekt_m_aare/index_ger.html.

Mosimann, M. (2015a). "Erhebung der regionalen Hochwasservulnerabilitaet im Simmental". MA thesis. University of Bern.

– (2015b). *R code: manual determination of the bank-full height*. kindly made available by M. Mosimann.

Mueller, W. (2009). *Gesamtprojekt Kander.2050, Gewaesserentwicklungskonzept GEKa, Technischer Bericht*. Fischereininspektorat and Flussbau AG SAH.

MW AG (2014). *Technischer Bericht, Wasserbaubewilligung Hochwasserschutz Grindelwald Grund Schwarze Luetschine*.

Naef, F. and C. Lehmann (2012). *Massgebende Hochwasser der Luetschine, Study*.

Notter, B. (2003). "Rainfall-Runoff Modelling of meso-scale catchments in the upper Ewaso Ngiro Basin". MA thesis. University of Bern.

Notter, B. et al. (2012). "Modelling water provision as an ecoystem service in large East African river basin". In: *Hydrol. Earth Syst.Sci* 16, pp. 69–86.

Rousselot, P., D. Vetsch, and R. Faeh (2012). "Numerische Fliessgewaessermoderllierung". In: *Merkblatt Sammlung Wasserbau und Oekologie*.

Schmocker, J. (2013). "Long-term precipitation trends and rainy season performance in view of climate change in the Mt. Kenya region". MA thesis. University of Bern.

Schwanbeck, J. (2016). *R-code: prepare shape file for HQx_meso_CH*. kindly made available by J. Schwanbeck.

Spreafico, S. et al. (2003). *Hochwasserabschaetzung in schweizerischen Einzugsgebieten*. Vol. Beriche des BWG, Serie Wasser. 4. Bundesamt fuer Wasser und Geologie.

Suter, H. (2014). "Hydrological Studies in a Meso-Scale Ethiopian Catchment". MA thesis. Universitiy of Berne.

Sutter, A. (2012). "Impact of different land management on the hydrology of two catchments on the south-eastern slopes of Mount Kenya and the eastern slopes of the Aberdare Mountains". MA thesis. University of Bern.

Swisstopo (2016). *LK25, DEM, Vektor25, Swissimage 25*. [30.10.2015]. Bundesamt fuer Landestopographie. URL: www.swisstopo.admin.ch.

Uni Karlsruhe (2016). *Gerinnestroemung*. [01.05.2016]. URL: www.hydro.ifh.uni-karlsruhe.de.

Unsinn, B. (2008). "Anwendung des Programms Basement zur numerischen Berechnung von Gerinnestroemungen mit Geschiebetransport". MA thesis. Technische Universitaet Muenchen.

Vetsch, D. et al. (2015a). *System Manuals of BASEMENT, Reference Manual*. Laboratory of Hydraulics, Glaciology and Hydrology (VAW), ETH Zurich.

– (2015b). *System Manuals of BASEMENT, Version 2.5*. Laboratory of Hydraulics, Glaciology and Hydrology (VAW), ETH Zurich.

Vischer, D. (1983). *Berechnung des Normalabflusses in Gerinnen mit einfachen und gegliederten Querschnitten*. VAW Mitteilungen Versuchsanstalt Wasserbau, Hydrologie und Glaziologie.

Viviroli, D. and R. Weingartner (2012). *prozessbasierte Hochwasserabschaetzung fuer mesoskalige Einzugsgebiete: Grundlagen und Interpretationshilfe zum Verfahren PREVAH-regHQ*. Ed. by Beitraege zur Hydrologie der Schweiz. Schweizerischen Gesellschaft fuer Hydrologie und Limnologie (SGHL) und der schweizerischen Hydrologischen Kommission (CH)y.

Viviroli, D. et al. (2009). "Continous simulation for flood estimation in ungauged mesoscale catchments of Switzerland, Part 2: Parameter regionalisation and flood estimation results". In: *Journal of Hydrology*.

Walther, J. et al. (2012). "Flaechenhafte Bestimmung von Hochwasserspenden, Schlussbericht 2010". In: *Schriftenreihe, Heft 3*.

Wehren, B. (2010). "Die Hydrologie der Kander - gestern, heute, morgen. Analyse und Modellierung der Hochwasser und ihrer raum - zeitlichen Dynamik". PhD thesis. University of Bern.

Wehren, B. and R. Weingartner (2007). *Kander2050 Teil M1.1 Hydrologie: Hochwasserabschaetzung fuer Ausgewaehlte Teileinzugsgebiete der Kander*. Projektbericht Kanton Bern.

Wiesmann, U. et al. (2000). "Mitigating conflicts over scarce water resources in the Highland-Lowland system of Mount Kenya". In: *Mountain Research and Development* 20, pp. 10–15.

Wiliams, G.P (1978). "Bank-full discharge of Rivers". In: *Water resource research* 14.6, pp. 1141 –1155.

WMO (2009). *Guide to Hydrological Practices*. 6th ed. Vol. 1. Geneve: Chairperson, Publication Board, World Meteorlogical Organization (WMO).

– (2010). *Manual on Stream Gauging - VOLUME 2, Computation of discharge*. Ed. by Geneva.

– (2013). "Integrated flood Management tools series, flood mapping". In: Integrated Flood Management Tools Series.20.

Zgraggen, S. (2009). "Hochwasserverhaeltnisse in kleinen Teileinzugsgebieten der Kander". MA thesis. University of Bern.

Declaration

under Art. 28 Para. 2 RSL 05

Last, first name: Huser, Danielle

Matriculation number: 09-059-601

Programme: Master in climate science

Bachelor ☐ Master☒ Dissertation ☐

Thesis title:
River Conveyance Analysis in a Data Sparse and a Data Rich Region: Case Studies in Kenya and Switzerland

Thesis supervisor: Prof. Dr. Rolf Weingartner

I hereby declare that this submission is my own work and that, to the best of my knowledge and belief, it contains no material previously published or written by another person, except where due acknowledgement has been made in the text. In accordance with academic rules and ethical conduct, I have fully cited and referenced all material and results that are not original to this work. I am well aware of the fact that, on the basis of Article 36 Paragraph 1 Letter o of the University Law of 5 September 1996, the Senate is entitled to deny the title awarded on the basis of this work if proven otherwise. I grant inspection of my thesis.

Bern, 25.07.2016